Some dynamical problems in micropolar elasticity

Singh Dilbag

SOME DYNAMICAL PROBLEMS IN MICROPOLAR ELASTICITY

A THESIS

Submitted to the

FACULTY OF SCIENCE

PANJAB UNIVERSITY, CHANDIGARH

for the degree of

DOCTOR OF PHILOSOPHY

2008

DILBAG SINGH

DEPARTMENT OF MATHEMATICS

PANJAB UNIVERSITY, CHANDIGARH - 160 014

INDIA

Acknowledgements

It gives me immense pleasure to thank my respected supervisor Dr. Sushil Kumar Tomar, Professor, Department of Mathematics, Panjab University, Chandigarh, who not only suggested the interesting problems of this thesis but also helped in numerous ways to take it to completion. I gratefully acknowledge his academic guidance, stimulating discussions, unfailing support and nurturing in me a desire to know more and thus paving the way to a future research.

I am highly obliged to Dr. Madhu Raka, Professor and Chairperson, Department of Mathematics, Panjab University, Chandigarh for providing the necessary facilities during the course of my research work. I am also highly obliged to Dr. Vikas Bist, Reader, Department of Mathematics, Chandigarh for providing his own computer to me, which was a great help for me to explore the things in off hours.

I deeply acknowledge for financial assistance by Council of Scientific and Industrial Research, New Delhi, India in the form of Senior Research Fellowship.

I am thankful to all staff members of the Department of Mathematics, Panjab University for their co-operation and assistance in the completion of this thesis.

Finally, I express my deepest gratitude to my parents, my brother and friend Amita Kumari for their unconditional support in all spheres of my life.

Date:

Place: Chandigarh *Dilbag Singh*

Contents

Chapter 1

Introduction

1.1 Microcontinuum theories

Classical theory of elasticity deals with those materials, in which the material is considered as a continuum in mathematical sense. In such continuum, we neglect the molecular structure of the material and its points are regarded as material particles, i.e., the material particles are simply the geometrical points. In three dimensional Euclidean space, the continuous distribution of particles is characterized by a scalar quantity, called density of the material. The deformation of the body is characterized by the displacement vector and the transmission of loads across a surface element is uniquely determined by a force, called stress vector. Thus, the deformation of the body is described in terms of symmetric tensors of stress and strain. Within the elastic limits, some materials, e.g., steel, aluminium, concrete etc are found to exhibit results fairly coinciding with those of experimentally observed. However, in some materials, e.g., fibrous, polymers, asphalts, remarkable discrepancies are observed between the experimental results and those obtained using classical elasticity. These discrepancies are mainly because of the dominance of atomic structures of the material neglected in classical elasticity. These discrepancies are clearly noticed in case of dynamical problems of elastic vibrations involving high frequencies and short wavelengths, i.e., ultrasonic waves. When the wavelength is of the same order of magnitude as the average dimension of the microelements, the intrinsic motion of the microelements of a volume element with respect to the center of mass of the volume element, can affect the response remarkably. The influence of microstructure becomes more important in

the case of vibrations of granular and multimolecular bodies, where new types of waves appear, not encountered in classical theory of elasticity.

Voigt (1887) was the first who tried to correct these shortcomings of classical elasticity by taking into account the assumption that interaction between the two parts through an area element inside the body is transmitted not only by a force vector but also by a moment vector giving rise to a 'couple stress theory'. This assumption led to the fact that not only the force stresses but also the couple stresses acting on the faces of an elementary parallelepiped are asymmetric in nature. The complete theory of asymmetric elasticity was developed by Cosserat and Cosserat (1909), which was non-linear in the beginning. They assumed that each material point of a three dimensional continuum is associated with a 'rigid triad' and during the process of deformation, it can rotate independently, in addition to the displacement. This is how, the concept of rotation of a point was introduced in the continuum. The assumption of these additional degrees of freedom of rotation at each material point led to the consequence of the asymmetry of strain and stress tensors. This very idea of Cosserat brothers provided a good continuum modelization for molecular lattices, in which a group of particles (atoms, molecules) bounded by important cohesive forces forms a rigid system subjected to rotational motion.

In spite of novelty of the idea, the Cosserat brothers' work did not catch sufficient attention of the then researchers and the theory remained dormant during their lifetime. May be because the theory was non-linear in nature and its presentation as a unified theory incorporating mechanics, optics and electrodynamics. After a gap of about fifty years, Cosserats theory drew attention of researchers and several Cosserat - type theories were developed independently, e.g., Gunther (1958), Grioli (1960), Rajagopal (1960), Aero and Kuvshinskii (1960), Mindlin and Tiersten (1962), Toupin (1962), Eringen (1962), Koiter (1964), Palmov (1964), Nowacki (1974), among several others. In all these theories, the kinematic variable corresponding to rotation of a point is taken into account, but not as an independent variable like in Cosserats theory. Of course, these theories were similar to Cosserats theory, but were called by name, e.g., Toupin's theory was called 'Cosserat theory with constrained motion', Koiter's theory was called 'Couple stress theory', Eringen's theory was called 'Indeterminate couple stress theory', Nowacki's theory was called 'Cosserat pseudo-continuum theory' etc. In Nowacki's theory, the micro-rotation vector $\boldsymbol{\phi}$ is fully described by the displacement

vector $\mathbf{u}$ through the formula $\boldsymbol{\phi} = \frac{1}{2}\nabla \times \mathbf{u}$. Later, the general Cosserat continuum theory acquired the name of 'micropolar continuum theory' following Eringen (1966a), in which the micro-rotation vector is taken independent of displacement vector. Eringen and Suhubi (1964) and Suhubi and Eringen (1964) developed a non-linear theory for 'micro-elasticity', in which intrinsic motions of the microelements were taken into account. This theory is basically the generalization of 'Indeterminate couple stress theory' and 'Cosserat theory' in the sense that in this theory the skew-symmetric part of the stress tensor, the symmetric part of the couple stress tensor and the spin inertia are fully covered.

A further generalization of the continuum with microstructure leads to micromorphic continuum (Eringen 1964b). Micromorphic continuum treats a material body as a continuous collection of a large number of deformable particles, with each particle possessing finite size and inner structure. Using assumptions such as infinitesimal deformation and slow motion, micromorphic theory can be reduced to Mindlin's microstructure theory (1964). When the microstructure of the material is considered rigid, it becomes the Eringen's micropolar theory (1966a). Assuming a constant microinertia, Eringen's micropolar theory is identical to the Cosserats theory (1909). Eliminating the distinction of macromotion of the particle and the micromotion of its inner structure, it becomes couple stress theory (Mindlin and Tiersten, 1962; Toupin, 1962). Moreover, when the particle reduces to a mass point, all theories reduce to classical or ordinary continuum mechanics. The theory developed by other researchers in that time are found to be in close contact with the theory of 'microelasticity'. The connections between various theories of microcontinua has been nicely presented by Eringen (1999). Eringen (1966a, 1990) developed the theories of 'micropolar continua' and 'microstretch continua', which are special cases of the theory of 'micromorphic continua' earlier developed by Eringen and his coworker (1964). Thus, the Eringen's **'3M'** theories (Micromorphic, Microstretch, Micropolar) are the generalization of the classical theory of elasticity. As said earlier, in classical continuum, each particle of a continuum is represented by a geometrical point and can have three degrees of freedom of translation during the process of deformation. While in micromorphic continuum, each particle is itself a continuum of small extent, which can further deform during the process of deformation of the whole continuum. Thus, a micromorphic body or microcontinuum can be thought of a continuous collection of deformable point particles. At

each point of a micromorphic body, in addition to the translational degrees of freedom, it has deformable directors giving extra degrees of freedom. Thus, in polar continuum mechanics, each material point carries its own deformable microstructure. The deformation of a particle in a micromorphic continuum is composed of 'classical macrodeformation' and 'microdeformation' (micro-rotation of directors and microstretch of directors). During the process of deformation of a Microstrech continuum, each point can undergo micro-rotation and microstretch (breathing micro-motion) without microshearing (breathing micro-rotation). Note that 'breathing micro-motion' is responsible for expansion or contraction of the particle, while 'breathing micro-rotation' is responsible for changing the shape of the particle. Thus in microstretch bodies, there are seven degrees of freedom given by three of translation, three of micro-rotation and one of stretch. In microstretch continuum, the directors at a typical point are orthogonal and they are allowed to breath in their directions, in addition to rotation. Micropolar continuum is again a special case of microstretch continuum, in which microstretch is absent and the deformation of a micropolar continuum is characterized by six degrees of freedom, namely, three of translation and three of micro-rotation. In micropolar continuum, the directors are orthonormal and rigid, consequently, the micro-motion is only a rigid body rotation with respect to an axis, in addition to motion at macroscale. Note that in classical theory of elasticity, there is no concept of directors. The relation between these continuum can be ascribed through Figure 1.1.

Eringen's theory of polar elasticity keeps importance because of its applications in many physical substances, e.g., material particles having rigid directors, chopped fiber composites, platelet composites, aluminium epoxy, liquid crystal with side chains, a large class of substances like liquid crystals with rigid molecules, rigid suspensions, animal blood with rigid cells, foams, porous materials, bones, magnetic fluids, clouds with dust, concrete with sand and muddy fluids are examples of micropolar materials; polymers with flexible molecules, animal lungs, bubbly fluids, polluted air, springy suspension, mixtures with breathing elements, porous media, lattices with base, fish colonies that live in ground are examples of microstretch materials; animal blood with deformable cells and turbulent fluids with flexible vortices are best examples of micromorphic continua.

Grot (1969) extended Eringen's theory of micromorphic materials and developed a theory of thermodynamics of elastic materials with microstructure whose microele-

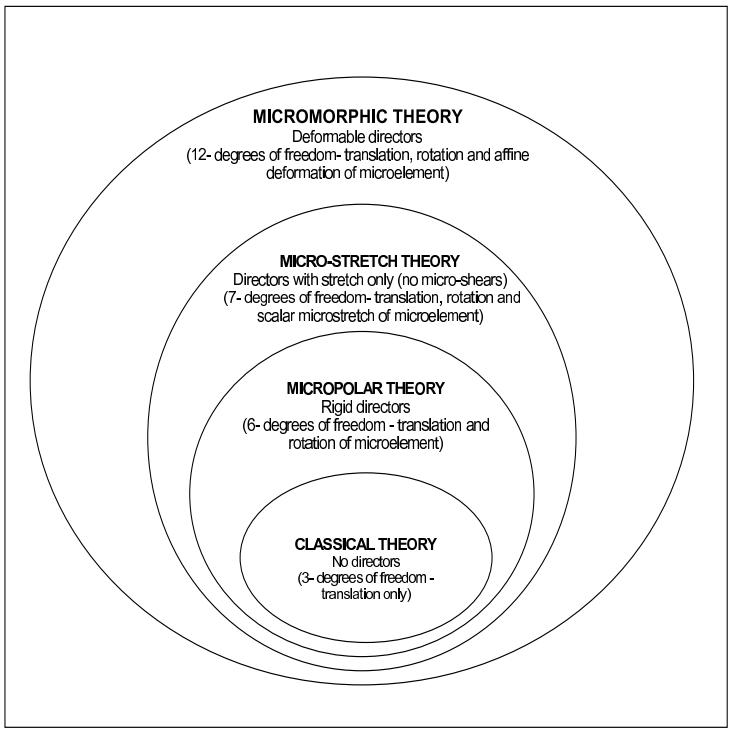

Figure 1.1: Sub-classes of Eringen's Micromorphic continua.

ments, in addition to microdeformations, possess microtemperatures. He applied modified Clausius-Duhem inequality to include microtemperatures, and the first order moment of the energy equations are added to the usual balance laws of a micromorphic continuum. Recently, a linear theory of Eringen's microstretch elastic materials has been extended by Iesan (2007) by incorporating microtemperatures at microelements, but neglected microrotational effects. In Iesan's theory, the material particles possess microtemperatures, in addition to classical displacement and temperature fields and they can stretch and contract independently of their translation. He called his theory as the theory of microstretch thermoelastic bodies with microtemperatures. Eringen (2003b) extended his theory of micromorphic continuum to include electromagnetic phenomena and called it as micromorphic electromagnetic theory and discussed wave propagation. The theory of microstretch materials has also been extended by Eringen (2004) himself to include electric and magnetic effects and named it as 'electromagnetic theory of microstretch elasticity'.

1.1.1 Deformation and microdeformation

Consider a material point P of a continuum B contained in a volume V bounded by a surface S in its undeformed state and located at position $(X_1,\ X_2,\ X_3)$ with respect to a rectangular frame of reference. If the body is allowed to move and deform under some external loads, it will occupy a region B' of volume V' and having surface S'. Referred to the same rectangular frame of reference, let the new position of the material point P be $(x_1,\ x_2,\ x_3)$. Under the assumptions of indestructibility and impenetrability of matter, each material point in the undeformed body B will occupy a unique position in the deformed body B'. Conversely, each point in B' can be traced back to a unique point in B. Thus, the deformation of the body at time t may be described by a one-one and onto mapping as follows

$$x_k = x_k(X_1,\ X_2,\ X_3,\ t), \qquad k = 1,\ 2,\ 3 \tag{1.1}$$

and its inverse motion

$$X_K = X_K(x_1,\ x_2,\ x_3,\ t), \qquad K = 1,\ 2,\ 3. \tag{1.2}$$

We assume that equation (1.2) is a unique inverse of equation (1.1) for all the points contained in the body except possibly at some singular surfaces, lines and points. For this to be valid, the three functions $x_k(X_1,\ X_2,\ X_3,\ t)$ must possess continuous partial derivatives with respect to $X_1,\ X_2$, and X_3 for all times, and the Jacobian

$$J \equiv \det \frac{\partial x_k}{\partial X_K} = \begin{vmatrix} \partial x_1/\partial X_1 & \partial x_1/\partial X_2 & \partial x_1/\partial X_3 \\ \partial x_2/\partial X_1 & \partial x_2/\partial X_2 & \partial x_2/\partial X_3 \\ \partial x_3/\partial X_1 & \partial x_3/\partial X_2 & \partial x_3/\partial X_3 \end{vmatrix}, \tag{1.3}$$

must not vanish. We define the deformation gradients $x_{k,K}$ and $X_{K,k}$ given by the following partial derivatives

$$x_{k,K} \equiv \partial x_k/\partial X_K, \qquad X_{K,k} \equiv \partial X_K/\partial x_k, \tag{1.4}$$

In the granular and fibrous structured bodies, if the physical phenomenon under study has a certain characteristic length (such as wavelength), comparable with the size of grains in the body, then the microstructure of the material becomes important and

it must be taken into account while studying the problems of deformation. For such bodies, classical continuum mechanics must be modified by incorporating the effect of granular structure of the medium. To account the microstructure of the continuum, we shall consider the material point of the continuum as a continuum of small extent, which itself undergo deformation under the action of applied forces. We may call this deformable material point as 'macroelement'. Let this macroelement has volume $\triangle V$, density ρ and enclosed within the surface $\triangle S$ in the undeformed state of the body. With reference to certain fixed Cartesian system, let the position vector of the center of mass of the macroelement P having volume $\triangle V$ be denoted by $\mathbf{X}$. Suppose the element P (i.e, $\triangle V + \triangle S$) contains N discrete micromaterial elements called 'microelements', $\triangle V^{(\alpha)} + \triangle S^{(\alpha)}$, $(\alpha = 1,\ 2, ..., N)$, each with a mass density ρ^{α}. As the macroelements are constructed by microelements, therefore, $\sum_{\alpha=1}^{N} \rho^{\alpha} \triangle V^{(\alpha)} = \rho \triangle V$. The position vector of α^{th} microelement positioned at Q may be expressed as

$$\mathbf{X}^{(\alpha)} = \mathbf{X} + \mathbf{\Xi}^{(\alpha)}, \tag{1.5}$$

where $\mathbf{\Xi}^{(\alpha)}$ is the position vector of α^{th} microelement relative to the center of mass of the macroelement. Upon the deformation of the body, the macroelement P (i.e., $\triangle V + \triangle S$) goes into new macroelement p (i.e., $\triangle v + \triangle s$) with the microelement displaced with respect to its center of mass. Because of the relative change in the positions of the microelements, the microelement Q goes to a new position q with respect to center of mass of p (see Figure 1.2).

The final position of the α^{th} particle will therefore be

$$\mathbf{x}^{(\alpha)} = \mathbf{x} + \boldsymbol{\xi}^{(\alpha)} \quad \text{or} \quad x_k^{(\alpha)} = x_k + \xi_k^{(\alpha)}, \tag{1.6}$$

where $\mathbf{x}$ is the position vector of the center of mass of macroelement p having volume $\triangle v$ and $\boldsymbol{\xi}^{\alpha}$ is the relative position vector of the point q in the deformed state. The motion of the center of the mass of P having volume $\triangle V$ is expressed by equation (1.1) as

$$\mathbf{x} = \mathbf{x}(\mathbf{X}, t) \quad \text{or} \quad x_k = x_k(X_K, t), \tag{1.7}$$

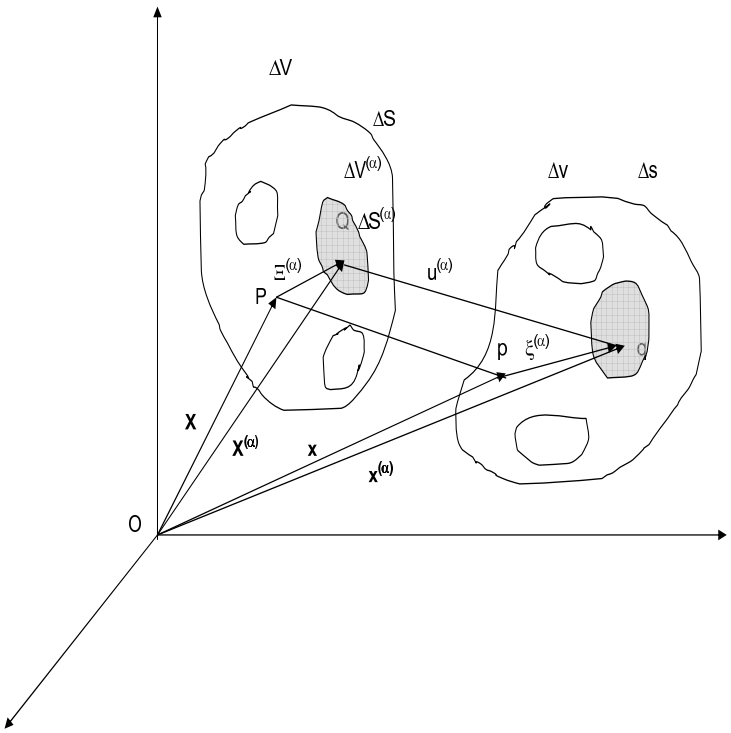

Figure 1.2: Deformation of microvolume.

The relative position vector $\boldsymbol{\xi}^{(\alpha)}$, however, depends not only on $\mathbf{X}$ and t but also on $\boldsymbol{\Xi}^{(\alpha)}$, i.e.,

$$\boldsymbol{\xi}^{(\alpha)} = \boldsymbol{\xi}^{(\alpha)}(\mathbf{X}, \boldsymbol{\Xi}^{(\alpha)}, t) \quad \text{or} \quad \xi_k^{(\alpha)} = \xi_k^{(\alpha)}(X_K, \Xi_K^{(\alpha)}, t), \tag{1.8}$$

Note that the transformation given by (1.7) is called 'macromotion' and the transformation given by (1.8) is called 'micromotion'.

Since the material particles are of infinitesimally small size as compared to macroscopic scale of the body, and assuming that $\boldsymbol{\xi}^{(\alpha)}$ is analytical function of $\boldsymbol{\Xi}^{(\alpha)}$, therefore expanding $\boldsymbol{\xi}^{(\alpha)}(\mathbf{X}, \boldsymbol{\Xi}^{(\alpha)}, t)$ by means of McLaurin's series in terms of $\Xi_1^\alpha, \Xi_2^\alpha$ and Ξ_3^α (retaining linear terms only for sufficiently small $|\boldsymbol{\Xi}^\alpha|$) as,

$$\boldsymbol{\xi}^{(\alpha)} = \boldsymbol{\xi}^{(\alpha)}(\mathbf{X}, 0, t) + \boldsymbol{\chi}_1(\mathbf{X},\ t)\Xi_1^{(\alpha)} + \boldsymbol{\chi}_2(\mathbf{X},\ t)\Xi_2^{(\alpha)} + \boldsymbol{\chi}_3(\mathbf{X},\ t)\Xi_3^{(\alpha)}, \qquad \alpha = 1,\ 2, ...,\ N$$

Since $\mathbf{X}$ is taken to be the centroid of particle P, therefore $\boldsymbol{\xi}^{(\alpha)}(\mathbf{X}, 0, t) = 0$ and the above equation can be written as

$$\boldsymbol{\xi}^{(\alpha)} = \boldsymbol{\chi}_K(\mathbf{X},\ t)\Xi_K^{(\alpha)} \quad \text{or} \quad \xi_k^{(\alpha)} = \chi_{kK}(\mathbf{X},\ t)\Xi_K^{(\alpha)}, \tag{1.9}$$

where $\boldsymbol{\chi}_K(\mathbf{X},\ t) = \left[\dfrac{\partial \boldsymbol{\xi}^\alpha}{\partial \Xi_K^\alpha}\right]_{\Xi_K^\alpha=0}$ and summation convention is taken over repeated indices. Equation (1.9) defines the homogeneous (or affine) deformation of macroelement $\triangle V$. *Thus the material points in* $\triangle v + \triangle s$ *undergo a homogeneous deformation about the center of mass.*

A material is called a micromorphic continuum if its motions are characterized by (1.7) and (1.9). In order to determine these motions, one will need to determine three scalar functions $x_k(\mathbf{X}, \mathbf{t})$ and three vector functions $\boldsymbol{\chi}_K(\mathbf{X}, \mathbf{t})$, (equivalently nine scalar functions χ_{kK}). Using (1.9), equation (1.6) can be written in coordinate form as

$$x_k^{(\alpha)} = x_k(\mathbf{X},\ t) + \chi_{kK}(\mathbf{X},\ t)\Xi_K^{(\alpha)}, \qquad k,\ K = 1,\ 2,\ 3 \tag{1.10}$$

Thus, the spatial position $x_k^{(\alpha)}$ of the α^{th} material point, requires 12 functions (three due to $x_k(\mathbf{X},\ t)$ and nine due to $\chi_{kK}(\mathbf{X},\ t)$).

We assume that the 'macro' and 'micro' motions given by (1.7) and (1.9) are continuous and possess continuous partial derivatives with respect to X_K and t, and they are invertible uniquely, i.e., the inverse motions are defined by

$$\mathbf{X} = \mathbf{X}(\mathbf{x}, t) \quad \text{or} \quad X_K = X_K(x_k, t), \tag{1.11}$$

$$\boldsymbol{\Xi}^{(\alpha)} = \mathfrak{S}_k(\mathbf{x}, t)\xi_k^{(\alpha)} \quad \text{or} \quad \Xi_K^{(\alpha)} = \Im_{Kk}(x_k, t)\xi_k^{(\alpha)}, \tag{1.12}$$

Here, the second order tensors χ_{kK} and $\Im_{Kk}$ are called 'microdeformation' and 'inverse microdeformation' tensors, respectively. These are the deformable directors. Upon deformation, the three independent directors $\mathfrak{S}_K$ goes to three independent directors $\boldsymbol{\chi}_k$, as follows

$$\chi_K = \chi_{kK}(\mathbf{X}, t)\hat{\mathbf{i}}_k, \qquad \Im_k = \Im_{Kk}(\mathbf{x}, t)\hat{\mathbf{I}}_K, \tag{1.13}$$

where $\hat{\mathbf{I}}_K$ and $\hat{\mathbf{i}}_k$ are, respectively, the unit base vectors for the material coordinates X_K and the spatial coordinates x_k. Note that the existence of solutions of (1.7) and (1.9) requires that

$$J = det(x_{k,K}) = \frac{1}{6}\epsilon_{KLM}\epsilon_{klm}x_{k,K}x_{l,L}x_{m,M} \quad \text{and} \quad j = det(\chi_{kK}) = \frac{1}{6}\epsilon_{KLM}\epsilon_{klm}\chi_{kK}\chi_{lL}\chi_{mM}$$

must be positive in some neighborhood of $\mathbf{X}$ during the time interval under consideration. Here J represents the macrovolume change with macrodeformation and j represents the microvolume change with microdeformation. The notations ϵ_{klm} and ϵ_{KLM} are the well known permutation symbols. Inserting (1.9) and (1.12) into (1.5) and (1.6), the motion and the inverse motion of a material point in a microelement are expressed by

$$\mathbf{x}^{(\alpha)} = \mathbf{x}(\mathbf{X}, t) + \boldsymbol{\chi}_K(\mathbf{X}, t)\Xi_K^{(\alpha)} \qquad \text{or} \qquad x_k^{(\alpha)} = x_k(\mathbf{X}, t) + \chi_{kK}(\mathbf{X}, t)\Xi_K^{(\alpha)}, \quad (1.14)$$

$$\mathbf{X}^{(\alpha)} = \mathbf{X}(\mathbf{x}, t) + \mathfrak{S}_k(\mathbf{x}, t)\xi_k^{(\alpha)} \qquad \text{or} \qquad X_K^{(\alpha)} = X_K(\mathbf{x}, t) + \Im_{Kk}(\mathbf{x}, t)\xi_k^{(\alpha)}. \quad (1.15)$$

Using (1.12) and (1.9), we obtain

$$(\delta_{kl} - \chi_{kK}\Im_{Kl})\xi_l^{(\alpha)} = 0, \qquad (\delta_{KL} - \chi_{kK}\Im_{Lk})\Xi_K^{(\alpha)} = 0. \quad (1.16)$$

It follows that the microdeformation tensors satisfy the following relations

$$\chi_{kK}\Im_{Kl} = \delta_{kl}, \qquad \chi_{kK}\Im_{Lk} = \delta_{KL}, \quad (1.17)$$

where δ_{kl} and δ_{KL} are the Kronecker deltas. Moreover, the deformation gradients $x_{k,K}$ and $X_{K,l}$ defined earlier also satisfy the following relations

$$x_{k,K}X_{K,l} = \delta_{kl}, \qquad x_{k,K}X_{L,k} = \delta_{KL}. \quad (1.18)$$

We see that whenever either set $(x_k,\ \chi_{kK})$ or $(X_K,\ \Im_{Kk})$ is known, the other set can be obtained by solving the linear equations in (1.17) and (1.18) for $X_{K,k}$ and $\Im_{Kk}$. On solving, one may obtain

$$X_{K,k} = \frac{1}{2J}\epsilon_{KLM}\epsilon_{klm}x_{l,L}x_{m,M} \quad (1.19)$$

and

$$\Im_{Kk} = \frac{1}{2j}\epsilon_{KLM}\epsilon_{klm}\chi_{lL}\chi_{mM}. \quad (1.20)$$

In our study, we assume that the mass of the microelement and mass of the macroelement are conserved. Eringen and Suhubi (1964) and Suhubi and Eringen (1964) have shown that
(i) during the motion defined by (1.14) under the assumption (1.9), carries the center of gravity of $\triangle V + \triangle S$ to the center of gravity of $\triangle v + \triangle s$ and a necessary and sufficient condition for conservation of mass is $\dfrac{D(\rho dv)}{Dt} = 0$, where $\dfrac{D}{Dt}$ is the material derivative and ρ is the average mass density of $\triangle v$.
(ii) the center of momentum and inertia of $\triangle v$ coincides with its center.
In this thesis, we are concerned with microstretch and micropolar elasticity, which are particular cases of micromorphic theory. As said earlier, in microstretch theory, in addition to translation there is microrotation of macroelement with scalar microstretch while micropolar theory admits only rigid microrotations of the microvolume elements about the center of mass of the volume element in addition to translation.

Suppose we write χ_{kK} in matrix form as $\boldsymbol{\chi}$, then this matrix can be decomposed as a product of two matrices, one of which is orthogonal and other is symmetric in nature [Eringen, 1980, pp-46],

$$\boldsymbol{\chi} = \mathbf{ru} = \mathbf{vr} \tag{1.21}$$

The matrix $\mathbf{r}$ is orthogonal (i.e., $\mid det(\mathbf{r}) \mid$=1) and represents the microrotation tensor, while the matrices $\mathbf{u}$ and $\mathbf{v}$ are symmetric (i.e., $\mathbf{u}^T = \mathbf{u}$ and $\mathbf{v}^T = \mathbf{v}$) in nature and represent the right and left stretch tensors of microdeformation, respectively. Pre-multiplying and post-multiplying the equation (1.21) by $\boldsymbol{\chi}^T$, we obtain

$$\boldsymbol{\chi}^T\boldsymbol{\chi} = (\mathbf{ru})^T(\mathbf{ru}) = \mathbf{u}^T(\mathbf{r}^T\mathbf{r})\mathbf{u} = \mathbf{u}^T\mathbf{Iu} = \mathbf{u}^2,$$

$$\boldsymbol{\chi}\boldsymbol{\chi}^T = (\mathbf{vr})(\mathbf{vr})^T = \mathbf{v}(\mathbf{rr}^T)\mathbf{v}^T = \mathbf{vIv}^T = \mathbf{v}^2.$$

When $\mathbf{u}^2 = \mathbf{v}^2 = \mathbf{I}$, the identity matrix, we see that $\boldsymbol{\chi}^T\boldsymbol{\chi} = \boldsymbol{\chi}\boldsymbol{\chi}^T = \mathbf{I}$. Then $\boldsymbol{\chi}^T = \boldsymbol{\chi}^{-1} \equiv \mathfrak{S}$ and hence $\mathfrak{S}\boldsymbol{\chi} = \boldsymbol{\chi}\mathfrak{S} = \mathbf{I}$. Besides microstretch tensors $\mathbf{u}$ and $\mathbf{v}$, there exist other microstretch tensors arising from the gradients of $\boldsymbol{\chi}$. Taking derivative of (1.21) with respect to X_K, we have

$$\boldsymbol{\chi}_{,K} = \mathbf{r}_{,K}\mathbf{u} + \mathbf{ru}_{,K} = \mathbf{v}_{,K}\mathbf{r} + \mathbf{vr}_{,K}. \tag{1.22}$$

It is easy to prove that if $\mathbf{u}^2 = \mathbf{v}^2 = \mathbf{I}$ then $\mathbf{u} = \mathbf{v} = \mathbf{I}$, therefore $\mathbf{u}_{,K} = \mathbf{v}_{,K} = 0$ and from (1.22), we have

$$\boldsymbol{\chi}_{,K} = \mathbf{r}_{,K}\mathbf{I} = \mathbf{Ir}_{,K}.$$

Hence microdeformation gradient is equal to microrotation gradient. From (1.21), we have

$$\boldsymbol{\chi} = \mathbf{r} \quad \text{and} \quad \mathbf{u}^2 = \mathbf{v}^2 = \mathbf{I}. \tag{1.23}$$

We see that the matrices $\mathbf{u}$ and $\mathbf{v}$ representing the right and left stretches are constant, therefore the directors associated at each microelement are fixed, i.e., they are rigid. In this case, the micromorphic continua is reduced to micropolar continua. Also, it is clear that for micropolar continua, the matrix $\boldsymbol{\chi}$ is nothing but represents the microrotation tensor. We also note that

$$j^2 = (\det \chi_{kK})^2 = (\det \boldsymbol{\chi})^2 = (\det \mathbf{r})^2 = 1, \qquad \Rightarrow j = 1 \quad (\text{as } \ j > 0). \tag{1.24}$$

So, in micropolar continua, the micromotion is just a rigid body rotation.
A micromorphic continuum is said to be microstretch continuum, if the deformable directions in the deformed and undeformed states are related as

$$\Im_{Kk} = \frac{1}{j^2}\chi_{kK}. \tag{1.25}$$

Multiplying equation (1.25) with χ_{lK} and χ_{kL} and using (1.17), we obtain

$$\chi_{kK}\chi_{lK} = j^2\Im_{Kk}\chi_{lK} = j^2\delta_{kl} \qquad \text{and} \qquad \chi_{kK}\chi_{kL} = j^2\Im_{Kk}\chi_{kL} = j^2\delta_{KL} \tag{1.26}$$

Similarly, we can obtain

$$\Im_{Kk}\Im_{Kl} = \frac{1}{j^2}\delta_{kl} \qquad \text{and} \qquad \Im_{Kk}\Im_{Lk} = \frac{1}{j^2}\delta_{KL}. \tag{1.27}$$

Expressions in (1.26) and (1.27) show that the directors are orthogonal in the deformed and undeformed states of the microelement. Moreover, the quantity j is non-negative, therefore the micromotion would not contain microshear and the directors can undergo rotations and stretches. Hence, in microstretch continuum, the deformation contains only microrotation and microstretch without microshearing, in addition to translation of classical elasticity. Note that when $j = 1$ (case of micropolar continua), then from (1.26) one can obtain

$$\chi_{kK}\chi_{lK} = \delta_{kl} \qquad \text{and} \qquad \chi_{kK}\chi_{kL} = \delta_{KL}.$$

We see that the *orthogonal directors* in micropolar continua becomes *orthonormal*.

These expressions also indicate that the directors of micropolar continuum are rigid.

1.1.2 Strain and microstrain tensors

The differential line element in the deformed body is calculated through equation (1.14) by taking total derivative as

$$d\mathbf{x}^{(\alpha)} = (\mathbf{x}_{,K} + \boldsymbol{\chi}_{L,K}\Xi_L^{(\alpha)})dX_K + \boldsymbol{\chi}_K d\Xi_K^{(\alpha)}, \tag{1.28}$$

where the suffix followed by a comma denotes partial differentiation as earlier. The square of the arc length is obtained as (dropping the superscript α on Ξ_K and $d\Xi_K$)

$$(ds^{(\alpha)})^2 = d\mathbf{x}^{(\alpha)} \cdot d\mathbf{x}^{(\alpha)} = (C_{KL} + 2\Gamma_{KLM}\Xi_M + \chi_{kM,K}\chi_{kN,L}\Xi_M\Xi_N)dX_K dX_L$$

$$+2(\Psi_{KL} + \chi_{kL}\chi_{kM,K}\Xi_M)dX_K d\Xi_L + \chi_{kK}\chi_{kL}d\Xi_K d\Xi_L, \tag{1.29}$$

where

$$C_{KL}(\mathbf{X},t) \equiv x_{k,K}x_{k,L}, \quad \Psi_{KL}(\mathbf{X},t) \equiv x_{k,K}\chi_{kL}, \quad \Gamma_{KLM}(\mathbf{X},t) \equiv x_{k,K}\chi_{kL,M}. \tag{1.30}$$

The symmetric tensor C_{KL} is the classical Green deformation tensor (see Chandrasekharaiah and Debnath (1994), pp-188). The appearance of tensors Ψ_{KL} and Γ_{KLM} is new in the microstructure continuum. They are called microdeformation tensors and were introduced by Eringen and Suhubi (1964) and Suhubi and Eringen (1964).

Introducing the displacement vector $\mathbf{u}^{(\alpha)}$ (see Figure 1.2) as the vector that extends from $\mathbf{X}^{(\alpha)}$ to $\mathbf{x}^{(\alpha)}$, we write

$$\mathbf{u}^{(\alpha)} = \mathbf{x} - \mathbf{X} + \boldsymbol{\xi} - \boldsymbol{\Xi} = \mathbf{u} + \boldsymbol{\xi} - \boldsymbol{\Xi}, \tag{1.31}$$

where $\mathbf{u} = \mathbf{x} - \mathbf{X}$ is the classical displacement vector, the components of which in terms of X_K and x_k are, respectively,

$$U_K \equiv \mathbf{u} \cdot \hat{\mathbf{I}}_K = (x_k\hat{\mathbf{i}}_k - X_K\hat{\mathbf{I}}_K) \cdot \hat{\mathbf{I}}_K = x_k\delta_{kK} - X_K, \tag{1.32}$$

$$u_k \equiv \mathbf{u} \cdot \hat{\mathbf{i}}_k = (x_k\hat{\mathbf{i}}_k - X_K\hat{\mathbf{I}}_K) \cdot \hat{\mathbf{i}}_k = x_k - X_K\delta_{Kk}, \tag{1.33}$$

where $\delta_{kK} \equiv \delta_{Kk} \equiv \hat{\mathbf{i}}_k \cdot \hat{\mathbf{I}}_K$. Differentiating partially the equation (1.32) with respect to X_K and equation (1.33) with respect to x_k, we get

$$x_{k,K} = (\delta_{LK} + U_{L,K})\delta_{kL} \qquad \text{and} \qquad X_{K,k} = (\delta_{lk} - u_{l,k})\delta_{Kl}. \tag{1.34}$$

Analogously, Eringen (1968) introduced the microdisplacement tensors $\Phi_{LK}(\mathbf{X}, t)$ and $\phi_{lk}(\mathbf{x}, t)$ as follows

$$\chi_{kK} = (\delta_{LK} + \Phi_{LK})\delta_{kL} \quad \text{and} \quad \Im_{Kk} = (\delta_{lk} - \phi_{lk})\delta_{Kl}. \tag{1.35}$$

Using equations (1.9), (1.32), (1.33) and (1.35) into equation (1.31), we have

$$\begin{aligned}
\mathbf{u}^{(\alpha)} &= U_K\hat{\mathbf{I}}_K + (\xi_k\delta_{kK} - \Xi_K)\hat{\mathbf{I}}_K = U_K\hat{\mathbf{I}}_K + (\chi_{kL}\Xi_L\delta_{kK} - \Xi_K)\hat{\mathbf{I}}_K, \\
&= U_K\hat{\mathbf{I}}_K + ((\delta_{NL} + \Phi_{NL})\delta_{kN}\Xi_L\delta_{kK} - \Xi_K)\hat{\mathbf{I}}_K, \\
&= U_K\hat{\mathbf{I}}_K + (\delta_{NL}\delta_{kN}\Xi_L\delta_{kK} + \Phi_{NL}\delta_{kN}\Xi_L\delta_{kK} - \Xi_K)\hat{\mathbf{I}}_K, \\
&= U_K\hat{\mathbf{I}}_K + (\delta_{Lk}\Xi_L\delta_{kK} + \Phi_{NL}\delta_{NK}\Xi_L - \Xi_K)\hat{\mathbf{I}}_K, \\
&= U_K\hat{\mathbf{I}}_K + (\delta_{LK}\Xi_L + \Phi_{KL}\Xi_L - \Xi_K)\hat{\mathbf{I}}_K, \\
&= U_K\hat{\mathbf{I}}_K + (\Xi_K + \Phi_{KL}\Xi_L - \Xi_K)\hat{\mathbf{I}}_K, \\
&= (U_K + \Phi_{KL}\Xi_L)\mathbf{I}_K.
\end{aligned} \tag{1.36}$$

Similarly, using equations (1.12), (1.32), (1.33) and (1.35) into equation (1.31), we have

$$\begin{aligned}
\mathbf{u}^{(\alpha)} &= u_k\hat{\mathbf{i}}_k + (\xi_k - \Xi_K\delta_{Kk})\hat{\mathbf{i}}_k = u_k\hat{\mathbf{i}}_k + (\xi_k - \Im_{Kl}\xi_l\delta_{Kk})\hat{\mathbf{i}}_k, \\
&= u_k\hat{\mathbf{i}}_k + (\xi_k - (\delta_{nl} - \phi_{nl})\delta_{Kn}\xi_l\delta_{Kk})\hat{\mathbf{i}}_k, \\
&= u_k\hat{\mathbf{i}}_k + (\xi_k - \delta_{nl}\delta_{Kn}\xi_l\delta_{Kk} + \phi_{nl}\delta_{Kn}\xi_l\delta_{Kk})\hat{\mathbf{i}}_k, \\
&= u_k\hat{\mathbf{i}}_k + (\xi_k - \delta_{Kl}\xi_l\delta_{Kk} + \phi_{nl}\xi_l\delta_{nk})\hat{\mathbf{i}}_k, \\
&= u_k\hat{\mathbf{i}}_k + (\xi_k - \delta_{lk}\xi_l + \phi_{kl}\xi_l)\hat{\mathbf{i}}_k, \\
&= (u_k + \phi_{kl}\xi_l)\hat{\mathbf{i}}_k.
\end{aligned} \tag{1.37}$$

On substituting equations $(1.34)_1$ and $(1.35)_1$ into equations (1.30), we can easily obtain

$$C_{KL} = \delta_{KL} + U_{K,L} + U_{L,K} + U_{M,K}U_{M,L}, \tag{1.38}$$

$$\Psi_{KL} = \delta_{KL} + \Phi_{KL} + U_{L,K} + U_{M,K}\Phi_{ML}, \tag{1.39}$$

$$\Gamma_{KLM} = \Phi_{KL,M} + U_{N,K}\Phi_{NL,M}. \tag{1.40}$$

So far, all these expressions are exact. For a linear theory, one assumes that the product terms are negligible so that

$$C_{KL} \approx \delta_{KL} + U_{K,L} + U_{L,K}, \quad \Psi_{KL} \approx \delta_{KL} + \Phi_{KL} + U_{L,K}, \quad \Gamma_{KLM} \approx \Phi_{KL,M}. \tag{1.41}$$

In this thesis, we shall deal with the linear theory, so we do not distinguish between material and spatial representation. Therefore, under linear theory, the material strain tensor E_{KL} is defined as

$$E_{KL} \equiv \frac{1}{2}(C_{KL} - \delta_{KL}) = \frac{1}{2}(U_{K,L} + U_{L,K}), \tag{1.42}$$

and the material microstrain tensors ε_{KL} and Γ_{KLM} are defined as

$$\varepsilon_{KL} \equiv \Psi_{KL} - \delta_{KL} = \Phi_{KL} + U_{L,K}, \qquad \Gamma_{KLM} \equiv \Phi_{KL,M}. \tag{1.43}$$

Following the same procedure, we introduce the spatial strain tensor, e_{kl}, and spatial microstrain tensors, ϵ_{kl} and γ_{klm} as

$$e_{kl} \equiv \frac{1}{2}(u_{k,l} + u_{l,k}), \quad \epsilon_{kl} \equiv \phi_{kl} + u_{l,k}, \quad \gamma_{klm} \equiv -\phi_{kl,m}. \tag{1.44}$$

We see that when the above tensors in equation (1.44) are known, we can calculate the changes in arc length and angles during deformation.

Now, we see that the difference between the squares of arc length in the deformed and undeformed body follows from equation (1.29) and the use of equation (1.35) and equations (1.42)-(1.43):

$$(ds^{(\alpha)})^2 - (dS^{(\alpha)})^2 \approx 2(E_{KL} + \Gamma_{KML}\Xi_M)dX_K dX_L + 2(\varepsilon_{KL} + \Gamma_{LMK}\Xi_M)dX_K d\Xi_L$$

$$+(\varepsilon_{KL}+\varepsilon_{LK}-2E_{KL})d\Xi_K d\Xi_L. \tag{1.45}$$

Note that for classical elasticity, only the first term on the right side involving E_{KL} survives. It can also be seen from equation (1.45) that when E_{KL}, ε_{KL}, and Γ_{KLM} are zero, then there is no change in the arc length after a deformation. So, in such a situation, the body is said to undergo a rigid motion.

1.1.3 Micropolar strains and rotations

We now consider a special class of micromorphic materials, called micropolar materials, in which the state of the microdeformation can be described by a local rigid motion of the microelements. Mathematically, this specialization under the assumption of linear theory is obtained by setting that the microdisplacement tensor is skew-symmetric, that is,

$$\Phi_{KL}=-\Phi_{LK}, \tag{1.46}$$

or in the spatial notation, $\phi_{kl}=-\phi_{lk}$. In three-dimensional space, every skew-symmetric, second order tensor Φ_{KL} can be expressed by an axial vector Φ_K (i.e., $\mathbf{\Phi}$) defined by

$$\Phi_K=\frac{1}{2}\epsilon_{KLM}\Phi_{ML}. \tag{1.47}$$

Equation (1.47) is a compact expression of

$$\Phi_1=\Phi_{32},\quad \Phi_2=\Phi_{13},\quad \Phi_3=\Phi_{21}.$$

Multiplying equation (1.47) with ϵ_{KLN} and using the identity $\epsilon_{KLN}\epsilon_{KLM}=2\delta_{NM}$, one can obtain the expression for Φ_{KL} as

$$\Phi_{KL}=-\epsilon_{KLM}\Phi_M. \tag{1.48}$$

Substituting this into equation $(1.35)_1$, we obtain

$$\chi_{kK}=(\delta_{LK}-\epsilon_{KLM}\Phi_M)\delta_{kL}=\delta_{LK}\delta_{kL}-\epsilon_{LKM}\Phi_M\delta_{kL}=\delta_{kK}-\epsilon_{kKM}\Phi_M. \tag{1.49}$$

The rotation tensor in the classical theory is given by

$$R_{KL} = \frac{1}{2}(U_{K,L} - U_{L,K}), \tag{1.50}$$

which is skew-symmetric second order tensor, i.e., $R_{KL} = -R_{LK}$, hence by the same argument as above, R_{KL} can be expressed by an axial vector R_K (i.e., $\mathbf{R}$) analogous to equations (1.47) and (1.48) as

$$R_K = \frac{1}{2}\epsilon_{KLM}R_{ML} = \frac{1}{2}\epsilon_{KLM}U_{M,L}, \quad R_{KL} = -\epsilon_{KLM}R_M. \tag{1.51}$$

From equations (1.42) (1.50) and $(1.51)_2$, we have

$$E_{KL} = \frac{1}{2}(U_{K,L} + U_{L,K}),$$

$$\Leftrightarrow E_{KL} + R_{KL} = \frac{1}{2}(U_{K,L} + U_{L,K}) + \frac{1}{2}(U_{K,L} - U_{L,K}),$$

$$\Leftrightarrow U_{K,L} = E_{KL} + R_{KL} = E_{KL} - \epsilon_{KLM}R_M. \tag{1.52}$$

Substituting equations (1.52) and (1.48) into equation (1.43), we get

$$\varepsilon_{KL} = -\epsilon_{KLM}\Phi_M + E_{LK} - \epsilon_{LKM}R_M = E_{KL} + \epsilon_{KLM}(R_M - \Phi_M) \tag{1.53}$$

and

$$\Gamma_{KLM} = -\epsilon_{KLN}\Phi_{N,M}. \tag{1.54}$$

We observe that if $R_M = \Phi_M$, then $\varepsilon_{KL} = E_{KL}$ and $\Gamma_{KLM} = R_{KL,M}$, then the microstrains are no longer independent of the classical strain and rotations. But, in micropolar theory, the classical rotation R_K is different from the microrotations. Thus, in micropolar theory, six functions are to be determined; namely, $U_K(\mathbf{X}, t)$ and $\Phi_K(\mathbf{X}, t)$.

Now, we shall obtain the spatial position of the α^{th} point $\mathbf{x}^{(\alpha)}$ through equations (1.31), (1.36), and (1.48). Substituting (1.48) into (1.36), we have

$$\mathbf{u}^{(\alpha)} = (U_K - \epsilon_{KLM}\Phi_M\Xi_L)\hat{\mathbf{I}}_K = (U_K + \epsilon_{MLK}\Phi_M\Xi_L)\hat{\mathbf{I}}_K = \mathbf{U} + \boldsymbol{\Phi} \times \boldsymbol{\Xi}$$

$$= \mathbf{u} - \boldsymbol{\Phi} \times \boldsymbol{\Xi}, \qquad \text{as} \qquad \mathbf{U} = \mathbf{x} - \mathbf{X} = \mathbf{u}.$$

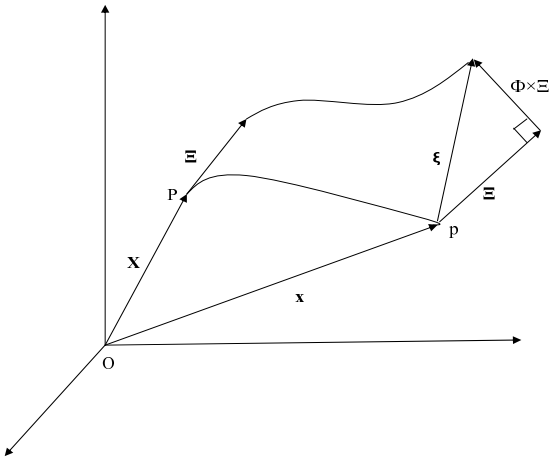

Figure 1.3: Microrotation.

The displacement vector $\mathbf{u}^{(\alpha)}$ is the difference of $\mathbf{X}^{(\alpha)}$ to $\mathbf{x}^{(\alpha)}$, therefore

$$\mathbf{u}^{(\alpha)} = \mathbf{x}^{(\alpha)} - \mathbf{X}^{(\alpha)} \qquad \Rightarrow \qquad \mathbf{x}^{(\alpha)} = \mathbf{u}^{(\alpha)} + \mathbf{X}^{(\alpha)}.$$

Since $\mathbf{X}^{(\alpha)} = \mathbf{X} + \boldsymbol{\Xi}$, then from the above expressions, we have

$$\mathbf{x}^{(\alpha)} = \mathbf{X} + \boldsymbol{\Xi} + \mathbf{u} - \boldsymbol{\Xi} \times \boldsymbol{\Phi}. \tag{1.55}$$

But

$$\mathbf{x}^{(\alpha)} = \mathbf{x} + \boldsymbol{\xi} = (\mathbf{X} + \mathbf{u}) + \boldsymbol{\xi}. \tag{1.56}$$

Therefore, from (1.55) and (1.56) we obtain

$$\boldsymbol{\xi} = \boldsymbol{\Xi} - \boldsymbol{\Xi} \times \boldsymbol{\Phi}. \tag{1.57}$$

The position of α^{th} particle given by $\mathbf{x}^{(\alpha)}$ in (1.56) has been expressed so as to make the meaning of $\boldsymbol{\xi}$ geometrically clear. Here the vector $\boldsymbol{\Phi}$ represents the angular rotation of a microelement about the center of mass of the deformed macrovolume element and $\boldsymbol{\xi}$ is the moment arm from this centroid (see Figure 1.3). Accordingly, the expression in (1.57) shows that, aside from a rigid body translation, the relative position $\boldsymbol{\Xi}$ of a material point after deformation is obtained by translating $\boldsymbol{\Xi}$ parallel to itself to the center of mass $\mathbf{x}$ of the deformed macrovolume element and then rotating it in

accordance with $\boldsymbol{\Xi} \times \boldsymbol{\Phi}$. Similarly, we can also have

$$\boldsymbol{\Xi} = \boldsymbol{\xi} + \boldsymbol{\xi} \times \boldsymbol{\phi}, \tag{1.58}$$

where $\boldsymbol{\phi} \simeq \boldsymbol{\Phi}$ is the spatial microrotation vector. Complete dual of equations (1.46)-(1.55) can be easily obtained and are given by

$$\phi_k = \frac{1}{2}\epsilon_{klm}\phi_{ml}, \qquad \phi_{kl} = -\epsilon_{klm}\phi_m, \tag{1.59}$$

$$\Im_{Kl} = \delta_{Kl} + \epsilon_{Klm}\phi_m, \tag{1.60}$$

$$r_k = \frac{1}{2}\epsilon_{klm}r_{ml}, \qquad r_{kl} = -\epsilon_{klm}r_m, \qquad r_k = \frac{1}{2}\epsilon_{klm}u_{m,l}, \tag{1.61}$$

$$u_{k,l} = e_{kl} - \epsilon_{klm}r_m, \tag{1.62}$$

$$\epsilon_{kl} = e_{kl} + \epsilon_{klm}(r_m - \phi_m), \tag{1.63}$$

$$\gamma_{klm} = \epsilon_{kln}\phi_{n,m}, \tag{1.64}$$

$$\mathbf{X}^{(\alpha)} = \mathbf{x} + \boldsymbol{\xi} - \mathbf{u} + \boldsymbol{\xi} \times \boldsymbol{\phi}. \tag{1.65}$$

From (1.55), we can have

$$d\mathbf{x}^{(\alpha)} = d\mathbf{X} + d\boldsymbol{\Xi} + d\mathbf{u} - d\boldsymbol{\Xi} \times \boldsymbol{\Phi} - \boldsymbol{\Xi} \times d\boldsymbol{\Phi}$$

$$= d\mathbf{X} + d\boldsymbol{\Xi} + \mathbf{u}_{,K}dX_K - d\boldsymbol{\Xi} \times \boldsymbol{\Phi} - \boldsymbol{\Xi} \times \boldsymbol{\Phi}_{,K}dX_K. \tag{1.66}$$

Using equations (1.51) and (1.52), we get

$$\mathbf{u}_{,K}dX_K = U_{L,K}dX_K\hat{\mathbf{I}}_L = E_{LK}dX_K\hat{\mathbf{I}}_L + R_{LK}dX_K\hat{\mathbf{I}}_L = E_{KL}dX_K\hat{\mathbf{I}}_L - d\mathbf{X} \times \mathbf{R}. \tag{1.67}$$

Similarly, using equation (1.54), we obtain

$$\boldsymbol{\Xi} \times \boldsymbol{\Phi}_{,N} dX_N = \epsilon_{KLM} \Xi_L \Phi_{M,N} dX_N \hat{\mathbf{I}}_K = -\Gamma_{KLN} \Xi_L dX_N \hat{\mathbf{I}}_K. \tag{1.68}$$

Introducing the following notation (for convenience) $\Gamma_{KM} \equiv \Gamma_{KLM} \Xi_L$, so that

$$\boldsymbol{\Xi} \times \boldsymbol{\Phi}_{,N} dX_N = -\Gamma_{KM} dX_N \hat{\mathbf{I}}_K = -\Gamma_{(KM)} dX_M \hat{\mathbf{I}}_K - \Gamma_{[KM]} dX_M \hat{\mathbf{I}}_K, \tag{1.69}$$

where indices in parentheses(and square brackets) indicate the symmetric (and anti-symmetric) parts of Γ_{KM}. Further introducing new microrotation vector $\boldsymbol{\Gamma}$ as $\Gamma_{[KL]} = -\epsilon_{KLM} \Gamma_M$ (where $\Gamma_K \equiv \frac{1}{2} \epsilon_{KLM} \Gamma_{ML}$), equation (1.69) can be written as

$$\boldsymbol{\Xi} \times \boldsymbol{\Phi}_{,N} dX_N = -\Gamma_{(KM)} dX_M \hat{\mathbf{I}}_K + \epsilon_{KLM} \Gamma_M dX_M \hat{\mathbf{I}}_K. \tag{1.70}$$

Substituting (1.67) and (1.69) into equation (1.66), we rearrange it as

$$d\mathbf{x}^{(\alpha)} = d\mathbf{X} + d\boldsymbol{\Xi} - (d\mathbf{X} \times \boldsymbol{R} + d\boldsymbol{\Xi} \times \boldsymbol{\Phi} + d\mathbf{X} \times \boldsymbol{\Gamma}) + (E_{KL} + \Gamma_{(KL)}) dX_K \hat{\mathbf{I}}_L,$$

$$= d\mathbf{X} + d\boldsymbol{\Xi} - [d\mathbf{X} \times (\boldsymbol{R} + \boldsymbol{\Gamma}) + d\boldsymbol{\Xi} \times \boldsymbol{\Phi}] + (E_{KL} + \Gamma_{(KL)}) dX_K \hat{\mathbf{I}}_L. \tag{1.71}$$

Equation (1.71) reveals that the deformation of the vector $d\mathbf{X}^{(\alpha)} \equiv d\mathbf{X} + d\boldsymbol{\Xi}$ may be achieved by the following three operations:
I. A rigid translation of $d\mathbf{X} + d\boldsymbol{\Xi}$ from the material centroid $\mathbf{X}$ to the spatial centroid $\mathbf{x}$.
II. Rigid rotations of $d\mathbf{X}$ and $d\boldsymbol{\Xi}$ by the amounts $d\mathbf{X} \times (\mathbf{R} + \boldsymbol{\Gamma})$ and $d\boldsymbol{\Xi} \times \boldsymbol{\Phi}$, respectively.
III. Finally, stretch represented by the strains E_{KL} and $\Gamma_{(KL)}$ in equation (1.71).
The expressions of Γ_K can be simplified as

$$\Gamma_K = \frac{1}{2} \epsilon_{KLM} \Gamma_{ML} = \frac{1}{2} \epsilon_{KLM} \Gamma_{MNL} \Xi_N = -\frac{1}{2} \epsilon_{KLM} \epsilon_{MNP} \Phi_{P,L} \Xi_N = -\frac{1}{2} \epsilon_{KLM} \epsilon_{NPM} \Phi_{P,L} \Xi_N,$$

$$= -\frac{1}{2} (\delta_{KN} \delta_{LP} - \delta_{KP} \delta_{LN}) \Phi_{P,L} \Xi_N = -\frac{1}{2} (\delta_{KN} \delta_{LP} \Phi_{P,L} \Xi_N - \delta_{KP} \delta_{LN} \Phi_{P,L} \Xi_N),$$

$$= -\frac{1}{2} (\delta_{KN} \Phi_{L,L} \Xi_N - \delta_{LN} \Phi_{K,L} \Xi_N) = -\frac{1}{2} (\Phi_{L,L} \Xi_K - \Phi_{K,L} \Xi_L),$$

$$= \frac{1}{2} (-\Phi_{L,L} \Xi_K + \Phi_{K,L} \Xi_L), \tag{1.72}$$

where the identity $\epsilon_{ijk}\epsilon_{pqk} = \delta_{ip}\delta_{jq} - \delta_{iq}\delta_{jp}$ has been used.

We can also write (1.71) as

$$d\xi = d\mathbf{x}^{(\alpha)} - d\mathbf{x} = d\boldsymbol{\Xi} - d\mathbf{X} \times \boldsymbol{\Gamma} - d\boldsymbol{\Xi} \times \boldsymbol{\Phi} - \Gamma_{(KL)} dX_K \hat{\mathbf{I}}_L. \tag{1.73}$$

In this form, we see that the difference between the deformation of $d\mathbf{X}^{(\alpha)}$ and that of $d\mathbf{X}$ of which the latter is known to us from the classical theory. This difference, therefore, is the result of the composition of a minirotation of $d\mathbf{X}$, a microrotation of $d\Xi$, and the ministraining of $d\mathbf{X}$ characterized by $\Gamma_{(KL)}$. The terminology of a minirotation is being used for $\boldsymbol{\Gamma}$ and ministraining for $\Gamma_{(KL)}$. Of course, $\mathbf{R}$ is the classical rotation for which we use the terminology 'macrorotation'.

Following the same procedure, we can have the dual of equation (1.55) is in the spatial representation as

$$\mathbf{X}^{(\alpha)} = \mathbf{x} + \boldsymbol{\xi} - \mathbf{u} + \boldsymbol{\xi} \times \boldsymbol{\phi}. \tag{1.74}$$

From this, in the same way as in the case of equation (1.71), we obtain

$$d\mathbf{X}^{(\alpha)} = d\mathbf{x} + d\boldsymbol{\xi} + (d\mathbf{x} \times \mathbf{r} + d\boldsymbol{\xi} \times \boldsymbol{\phi} - d\mathbf{x} \times \boldsymbol{\gamma}) - (e_{kl} - \gamma_{(kl)}) dx_k \hat{\mathbf{i}}_l, \tag{1.75}$$

where $\mathbf{r}$ is the spatial macrorotation vector defined by equation (1.61) and e_{kl} is the spatial macrostrain tensor. The spatial minirotation vector $\boldsymbol{\gamma}$ is given by

$$\gamma_k = \frac{1}{2}\epsilon_{klm}\gamma_{ml} = \frac{1}{2}(\phi_{l,l}\xi_k - \phi_{k,l}\xi_l) \quad \text{and} \quad \gamma_{km} \equiv \gamma_{klm}\xi_l = \epsilon_{kln}\phi_{n,m}\xi_l. \tag{1.76}$$

1.1.4 Useful definitions and relations

The velocity vector $\mathbf{v}$ and the acceleration vector $\mathbf{a}$ of a macroelement material point are defined as

$$\mathbf{v} = \dot{\mathbf{x}}(\mathbf{X}, t) \quad \text{or} \quad v_k = \dot{x}_k, \quad \text{and} \quad \mathbf{a} = \dot{\mathbf{v}} \quad \text{or} \quad a_k = \dot{v}_k.$$

Taking temporal derivative of relation (1.9) and using (1.12), we obtain

$$\dot{\boldsymbol{\xi}} = \boldsymbol{\nu}_k(\mathbf{x}, t)\xi_k \quad \text{or} \quad \dot{\xi}_k = \nu_{kl}\xi_l.$$

where $\boldsymbol{\nu}_k(\mathbf{x}, t) = \dot{\boldsymbol{\chi}}_K(\mathbf{X}, t)\Im_{Kk}(\mathbf{x}, t)$ (or $\nu_{lk} = \dot{\chi}_{lK}\Im_{Kk}$) and is called *gyration vector* (or gyration tensor). We now introduce an axial vector ν_k as $\nu_k = \frac{1}{2}\epsilon_{klm}\nu_{ml}$ and

$\nu_{kl} = -\epsilon_{klm}\nu_m$, which is called *microgyration vector*. It can be seen that

$$\ddot{\boldsymbol{\xi}} = \dot{\boldsymbol{\nu}}_k\xi_k + \boldsymbol{\nu}_k\dot{\xi}_k = \dot{\boldsymbol{\nu}}_k\xi_k + \boldsymbol{\nu}_k\nu_{kl}\xi_l = \boldsymbol{\alpha}_k(\mathbf{x},t)\xi_k,$$

where

$$\boldsymbol{\alpha}_k(\mathbf{x},t) = \dot{\boldsymbol{\nu}}_k + \boldsymbol{\nu}_m\nu_{mk} \qquad \text{or} \qquad \alpha_{lk} = \dot{\nu}_{lk} + \nu_{lm}\nu_{mk}.$$

The tensor α_{lk} is called *spin tensor*. Taking time derivative of (1.17) one obtains $\dot{\chi}_{kK}\Im_{Lk} + \chi_{kK}\dot{\Im}_{Lk} = 0$. Also, the material derivatives of χ_{kK} and $\Im_{Kk}$ are given by $\dot{\chi}_{kK} = \nu_{kl}\chi_{lK}$ and $\dot{\Im}_{Kk} = -\nu_{lk}\Im_{Kl}$. With the help of (1.49) and (1.60), the gyration tensor ν_{kl} can be written as

$$\nu_{kl} = -\epsilon_{klM}\dot{\Phi}_M + \epsilon_{kKM}\epsilon_{Klm}\dot{\Phi}_M\phi_m.$$

For linear theory of micropolar elasticity, we can write (Eringen 1968)

$$\nu_{kl} \simeq -\epsilon_{klm}\dot{\phi}_m \quad (\text{as } \dot{\Phi}_M = \dot{\phi}_m) \qquad \Rightarrow \qquad \nu_k = \dot{\phi}_k.$$

Introducing the microinertia tensor i_{kl} defined as follows (see Eringen, 1999)

$$i_{kl} = \int_{\triangle v} \rho'\xi_k\xi_l dv' =< \xi_k\xi_l > \quad \text{or} \quad \rho i_{kl}\triangle v = \sum_{\alpha} \rho^{(\alpha)}\xi_k\xi_l\triangle v^{(\alpha)}.$$

We also adopt the following decomposition as $i_{kl} = \frac{1}{2}j_{mm}\delta_{kl} - j_{kl}$ and $j_{kl} = i_{mm}\delta_{kl} - i_{kl}$. Here $i_{mm} = \frac{1}{2}j_{mm} =$ constant.

1.1.5 Stresses-Force stress and Couple stress

When an elastic body is subjected to external loads, the body is said to be under deformation if the relative positions of its particles gets altered. The external loads may be of two kinds: *Body loads* and *Surface loads*. A load which acts on the entire mass of the body is called body load. Gravitational force and magnetic force are the examples of body load. These forces are non-contact forces. A load which acts across a surface, is called surface load. Stress force and pressure force are the examples of surface load. These forces are contact forces. Internal stresses in a deformed body arises due to the application of external loads. To explain the concept of stresses in a micropolar body, we consider a small macrovolume, $v + s$ (volume v and surface s), fully contained in the body. At a point $\mathbf{x}$ of s, the effect of the remainder of the body is equivalent to the surface force per unit area, $\boldsymbol{\tau}_{(\mathbf{n})}$, called the *force stress vector*, and

the couple per unit area, $\mathbf{m_{(n)}}$, called the *couple stress vector*. These stresses depend on the position $\mathbf{x}$, time t and orientation of the surface s at $\mathbf{x}$, which is described by the exterior normal vector $\mathbf{n}$ to s at $\mathbf{x}$. In tensor notations, the force stress and couple stress tensors are denoted by τ_{kl} and m_{kl} respectively, while the body force and body couple tensors are denoted respectively by f_k per unit mass and l_k per unit mass.

In a micromorphic body, a third order tensor m_{klm} replaces m_{kl} and a second order tensor l_{kl} replaces l_k given by (see Eringen and Suhubi, 1964 and Suhubi and Eringen, 1964)

$$m_{klm} =< \tau'_{kl}\xi_m >_2, \qquad l_{kl} =< f'_k\xi_l >, \tag{1.77}$$

Here $<>_2$ represents the surface mean and $<>$ denotes the volume average. The primed quantities refer to the microelement contained in a particle. These quantities are restricted by 'Principle of Energy Balance' postulated for the entire body. This principle states that *the time rate of the sum of the kinetic energy (K_e) and internal energy (ϵ) is equal to the work done by all loads acting on the body per unit time,* that is,

$$\frac{d}{dt}\int_{V-\sigma}\rho K_E dv = \int_{\partial V-\sigma}(\tau_{kl}v_l + m_{klm}\nu_{lm} + q_k)da_k + \int_{V-\sigma}\rho(f_k v_k + l_{kl}\nu_{kl} + h)dv. \tag{1.78}$$

Here, $K_E = \epsilon + K_e$ and ρ is the average density. On the right hand side, under the surface integral, the three terms, respectively, represent the stress energy, the energy of stress moments, and the heat energy per unit time, and under the volume integral, the three terms, denote respectively, the energy of the body force, the energy of body moments, and the heat input per unit time. The volume and surface integrals exclude the line and surface intersections of the discontinuity surface σ which may be sweeping the body with its own velocity $\mathbf{u}$ (see Figure 1.4).

This is denoted by

$$V - \sigma \equiv V - V \cap \sigma, \qquad \partial V - \sigma \equiv \partial V - \partial V \cap \sigma. \tag{1.79}$$

Note that the internal energy density ϵ is postulated to exist. The kinetic energy K_e, per unit mass, defined by

$$K_e \equiv \frac{1}{2} < (\dot{\mathbf{x}} + \dot{\boldsymbol{\xi}}) \cdot (\dot{\mathbf{x}} + \dot{\boldsymbol{\xi}}) > \tag{1.80}$$

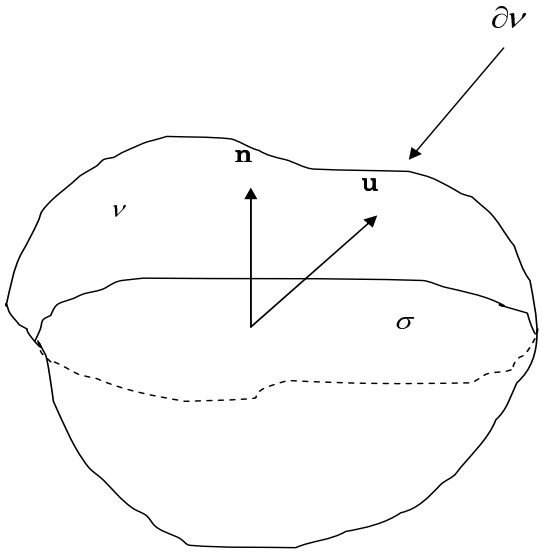

Figure 1.4: Discontinuity surface.

turns out to be

$$K_e = \frac{1}{2}\mathbf{v}\cdot\mathbf{v} + \frac{1}{2}i_{kl}\nu_{mk}\nu_{ml}. \tag{1.81}$$

We note that the energy balance law (1.78) differs from classical counterpart only in the terms involving m_{klm} and l_{kl}. The origin of these terms may be explained by a physical picture. Consider a macrosurface δa (see Figure 1.5) on the surface of the body with exterior unit normal $\mathbf{n}$. The work per unit time of a stress vector $\boldsymbol{\tau}'_k$ acting at a microsurface element da'_k with unit normal $\mathbf{n}'$, upon integration over $\triangle a$ gives the energy due to tractions on $\triangle a$. For the stress vector, we have, $\boldsymbol{\tau}'_k = \tau'_{kl}\hat{\mathbf{i}}_l$, where τ'_{kl} is the microstress tensor. The energy due to the force $\boldsymbol{\tau}'_k$ is then given by

$$\int_{\Delta a}\tau'_{kl}(v_l + \dot{\xi}_l)da'_k = \int_{\Delta a}\tau'_{kl}v_l da'_k + \int_{\Delta a}\tau'_{kl}\nu_{lm}\xi_m da'_k = (\tau_{kl}v_l + m_{klm}\nu_{lm})\triangle a_k, \tag{1.82}$$

where the *stress tensor* τ_{kl} and *stress moment tensor* m_{klm} are defined in the limit as $\triangle a \to 0$

$$\tau_{kl}\triangle a_k = \int_{\triangle a_k}\tau'_{kl}da'_k, \qquad m_{klm}\triangle a_k = \int_{\triangle a_k}\tau'_{kl}\xi_m da'_k, \tag{1.83}$$

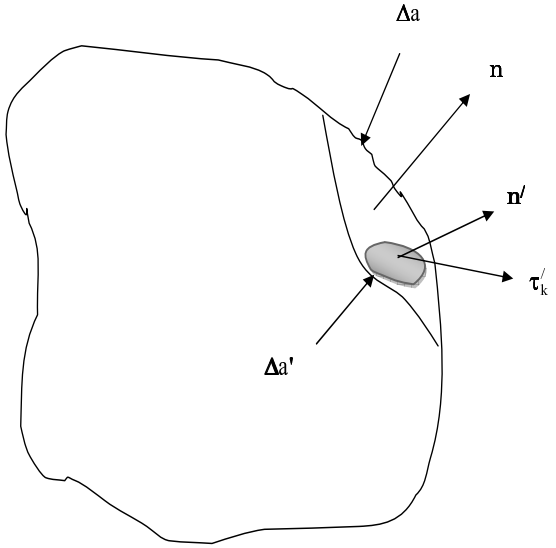

Figure 1.5: Traction at microsurface element.

in accordance with (1.77). The presence of the term involving $l_{kl}\nu_{kl}$ in (1.78) is similarly obtained by the volume average

$$\int_{\triangle v} \rho' f'_k (v_k + \dot{\xi}_k) dv' = (\rho f_k v_k + \rho l_{kl}\nu_{kl}) \triangle v, \tag{1.84}$$

where l_{kl} is defined in the limit as $\triangle v \to 0$

$$\rho l_{kl} \triangle v \equiv \int_{\triangle v} \rho' f'_k \xi_l dv'. \tag{1.85}$$

For microstretch continua, we decompose m_{klm} into a microstretch vector m_k and a couple stress tensor m_{kl} ; and decomposing l_{kl} into body microstretch force density l and body couple density l_k as

$$m_{klm} = \frac{1}{3} m_k \delta_{lm} - \frac{1}{2} \epsilon_{lmr} m_{kr}, \qquad l_{kl} = \frac{1}{3} l \delta_{kl} - \frac{1}{2} \epsilon_{klr} l_r, \tag{1.86}$$

and using $\nu_{kl} = \nu\delta_{kl} - \epsilon_{klm}\nu_m$, where ν represents the uniform microstretch (a breathing motion) and ν_k represents the rigid microrotation in a microstretch continuum (see Eringen, 1999), (1.78) takes the form

$$\frac{d}{dt} \int_{V-\sigma} \rho(\epsilon + K_e) dv = \int_{\partial V - \sigma} (\tau_{kl} v_l + m_{kl}\nu_l + m_k \nu + q_k) da_k$$

$$+\int_{V-\sigma}\rho(f_k v_k + l\nu + l_k\nu_k + h)dv. \tag{1.87}$$

For micropolar continua, the energy balance law can be written directly from (1.87) by substituting $\nu = 0$, $m_k = 0$ and $l = 0$.

Next, we shall show that the force stress and couple stress vectors on opposite sides of the same surface at a given point in micropolar continua are equal in magnitude and opposite in sign. For this, we consider a small tetrahedron with three faces s_k taken as the coordinate surfaces and the fourth face s_n being a part of the surface of the body (see Figure 1.6).

The equation of 'balance of momentum' *which states that the time rate of change of momentum is equal to the sum of all forces acting on a body*, applied to the tetrahedron is given by

$$\frac{d}{dt}\int_v \rho\mathbf{v}dv = \oint_{s_n}\boldsymbol{\tau}_{(\mathbf{n})}\cdot d\mathbf{a} + \oint_{s_k}(-\boldsymbol{\tau}_k)\cdot d\mathbf{a}_k + \int_v \rho\mathbf{f}dv, \tag{1.88}$$

where ρ is the mass density, $\mathbf{v}$ is the velocity and $\mathbf{f}$ is the body force. The force $\boldsymbol{\tau}_{(\mathbf{n})}$ is the surface traction per unit area acting on the surface s_n with an outward directed normal $\mathbf{n}$ and the forces $\boldsymbol{\tau}_k$ are the surface tractions per unit area acting on the surfaces s_k with an outward directed normals $\hat{\mathbf{i}}_k$. The right hand side of equation (1.88) gives the vector sum of the surface and body forces. Using the mean value theorem to estimate the volume and surface integrals, we write

$$\frac{d}{dt}(\rho^*\mathbf{v}^*\triangle v) = \boldsymbol{\tau}^*_{(\mathbf{n})}\triangle a - \boldsymbol{\tau}^*_k\triangle a_k + \rho f^*\triangle v, \tag{1.89}$$

where the quantities marked with asterisks are the values of those without asterisks at some points of $v+s$. The volume of tetrahedron is denoted by $\triangle v$ and its surface areas by $\triangle a_k$ and $\triangle a$. Since the mass is conserved, we get $\dfrac{d}{dt}(\rho dv) = 0$. Now dividing the equation (1.89) by $\triangle a$ and letting $\triangle a$ and $\triangle v \to 0$, we see that $\triangle v/\triangle a \to 0$ and we obtain

$$\boldsymbol{\tau}_{(\mathbf{n})}da = \boldsymbol{\tau}_k da_k. \tag{1.90}$$

Now da_k is the projection of vector area $d\mathbf{a}$ on the coordinate plane $x_k = 0$. Hence $da_k = d\mathbf{a}\cdot\hat{\mathbf{i}}_k = da\ (\mathbf{n}\cdot\hat{\mathbf{i}}_k) = n_k da$. Substituting this into (1.90), we get

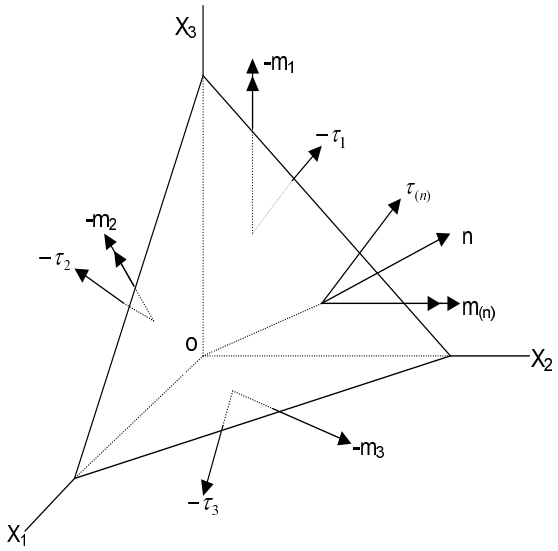

Figure 1.6: A tetrahedron with surface loads.

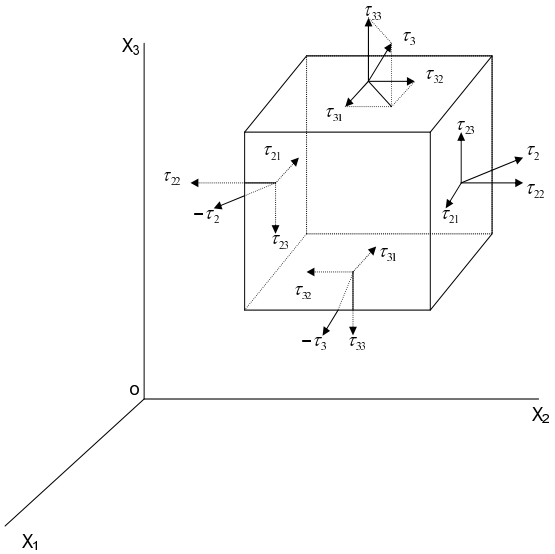

Figure 1.7: Stress tensor.

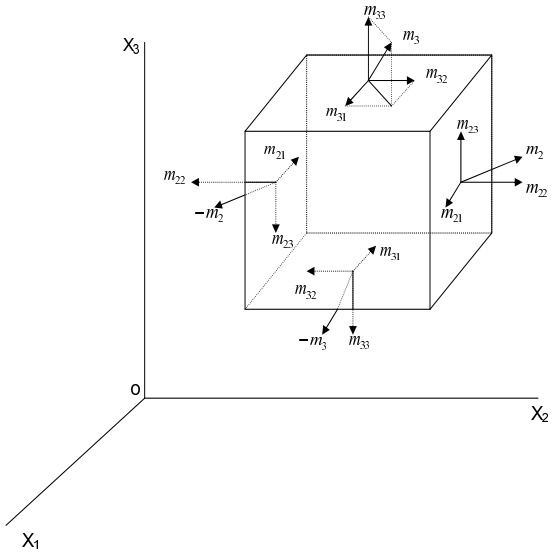

Figure 1.8: Couple stress tensor.

$$\boldsymbol{\tau}_{(\mathbf{n})} = \boldsymbol{\tau}_k n_k, \tag{1.91}$$

where $\boldsymbol{\tau}_k$ is independent of $\mathbf{n}$. Thus, the stress vector $\boldsymbol{\tau}_{(\mathbf{n})}$ is a linear function of $\mathbf{n}$. It is clear from (1.91) that

$$\boldsymbol{\tau}_{(-\mathbf{n})} = -\boldsymbol{\tau}_{(\mathbf{n})}, \tag{1.92}$$

which proves that the stress vectors on the opposite sides of the same surface at a given point are equal in magnitude and opposite in sign.
Similarly, using 'principle of balance of moment of momentum' *which states that the time rate of change of moment of momentum about a point is equal to the sum of all couples and the moments of all forces about that point*, gives

$$\mathbf{m}_{(\mathbf{n})} = \mathbf{m}_k n_k, \qquad \mathbf{m}_{(-\mathbf{n})} = -\mathbf{m}_{(\mathbf{n})}. \tag{1.93}$$

To define the stress tensor τ_{kl} and couple stress tensor m_{kl}, we decompose the tensors $\boldsymbol{\tau}_k$ and $\mathbf{m}_k$ as

$$\boldsymbol{\tau}_k = \tau_{kl}\hat{\mathbf{i}}_l, \qquad \mathbf{m}_k = m_{kl}\hat{\mathbf{i}}_l. \tag{1.94}$$

Thus, τ_{kl} is the l^{th} components of the stress vector $\boldsymbol{\tau}_k$ which acts on the surface $x_k =$ constant and m_{kl} is the l^{th} components of the couple stress vector which acts on the same surface. The positive directions of τ_{kl} and those of m_{kl} are shown on Figures 1.7

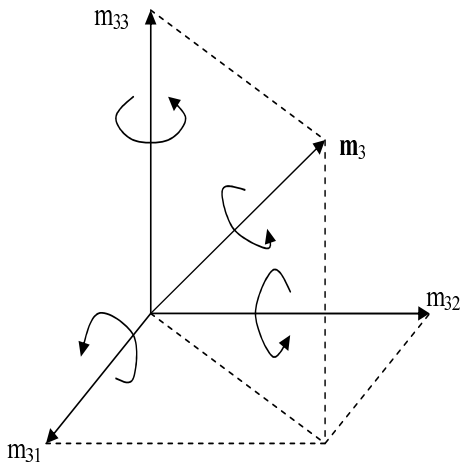

Figure 1.9: Directions of couple stress.

and 1.8. Equations (1.91), $(1.93)_1$ and (1.94), it follows that

$$\boldsymbol{\tau}_{(\mathbf{n})} = \tau_{kl} n_k \hat{\mathbf{i}}_l, \qquad \mathbf{m}_{(\mathbf{n})} = m_{kl} n_k \hat{\mathbf{i}}_l. \tag{1.95}$$

It is thus clear that the couple stress vectors have a sign convention identical with that of the stress vectors. The plane of each couple is perpendicular to the couple vector, and the direction is as described by the right-hand screw rule (see Figure 1.9).

1.1.6 Stress-strain relations in micropolar elasticity

In micropolar continuum, the constitutive dependent variables are stress tensor τ_{kl}, couple stress tensor m_{kl},, heat vector q_k, Helmholtz free energy ψ, and the entropy η. Eringen (1968) proposed the following set of constitutive equations given by

$$\tau_{kl} = F_{kl}(\epsilon_{rs}, \phi_{r,s}, \theta), \quad m_{kl} = M_{kl}(\epsilon_{rs}, \phi_{r,s}, \theta), \quad q_k = G_k(\epsilon_{rs}, \phi_{r,s}, \theta),$$

$$\psi = \Psi(\epsilon_{rs}, \phi_{r,s}, \theta), \quad \eta = N(\epsilon_{rs}, \phi_{r,s}, \theta) \tag{1.96}$$

where ϵ_{rs} and $\phi_{r,s}$ are given by (1.63) and (1.64) respectively and θ is the temperature. The above equations are legitimate for linear homogeneous materials, whether isotropic or not. For nonlinear isotropic materials, they are acceptable in form. However, since we are employing the infinitesimal strain measures, a nonlinear constitutive theory, in terms of linear strain measures, would be inconsistent.

The constitutive equations (1.96) must be consistent with second law of thermody-

namics, as expressed by

$$\rho\overline{\gamma} \equiv -(\rho/\theta)(\dot{\psi} - \eta\dot{\theta}) + (1/\theta)\tau_{kl}\upsilon_{l,k} - (1/\theta)\epsilon_{kmn}\tau_{mn}\nu_k$$

$$+(1/\theta)m_{lk}\nu_{k,l} + (1/\theta^2)q_k\theta_{,k} \geq 0. \tag{1.97}$$

Thus, on substituting equation (1.96) into equation (1.97), we have

$$-\frac{\rho}{\theta}(\frac{\partial\Psi}{\partial\epsilon_{kl}}\dot{\epsilon}_{kl} + \frac{\partial\Psi}{\partial\phi_{k,l}}\dot{\phi}_{k,l} + \frac{\partial\Psi}{\partial\theta}\dot{\theta} + \eta\dot{\theta})$$

$$+(1/\theta)\tau_{kl}\dot{\epsilon}_{kl} + (1/\theta)m_{kl}\dot{\phi}_{l,k} + (1/\theta^2)q_k\theta_{,k} \geq 0. \tag{1.98}$$

Consistent with the linear theory, we write

$$\frac{D}{Dt}(\phi_{k,l}) = \dot{\phi}_{k,l}, \qquad \dot{\epsilon}_{kl} \simeq \upsilon_{l,k} - \epsilon_{klm}\nu_m. \tag{1.99}$$

The inequality equation (1.98), is postulated to be valid for all independent processes. Here, the quantities $\dot{\epsilon}_{kl},\ \dot{\phi}_{k,l},\ \dot{\theta}$ and $\theta_{,k}$ can be varied independently. Since this inequality is linear in all these variables, we must set the coefficients of these variables equal to zero. Hence

$$\tau_{kl} = \rho\partial\Psi/\partial\epsilon_{kl}, \quad m_{kl} = \rho\partial\Psi/\partial\phi_{l,k}, \quad q_k = 0, \quad \eta = -\partial\Psi/\partial\theta. \tag{1.100}$$

We therefore see that, *for a micropolar elastic solid, the stress, couple stress and entropy density are derivable from a potential, and the heat vector vanishes.* Since we did not consider the temperature gradient, we have no heat conduction. Nevertheless, the free energy Ψ and, consequently, the material moduli will depend on the temperature θ. Since all terms in equation (1.98) vanish, we have the entropy production density $\overline{\gamma}$ also vanishing. Thus, the micropolar elastic solid is in *thermal equilibrium.*

Here we are concerned with the linear theory, we therefore consider a polynomial for Ψ which is second degree in the strain measures ϵ_{kl} and $\phi_{k,l}$, i.e.,

$$\rho\Psi = A_0 + A_{kl}\epsilon_{kl} + \frac{1}{2}A_{klmn}\epsilon_{kl}\epsilon_{mn} + B_{kl}\phi_{k,l} + \frac{1}{2}B_{klmn}\phi_{k,l}\phi_{m,n} + C_{klmn}\epsilon_{kl}\phi_{m,n}, \tag{1.101}$$

where $A_0,\ A_{kl},\ A_{klmn},\ B_{kl}, ...$ are functions of θ only. Since ϕ_k is an axial vector on a reflection of the spatial axes, the fourth and the last terms change sign while the other

terms do not. For the function Ψ to be invariant, $B_{kl} = 0$ and $C_{klmn} = 0$. We further note the following symmetry conditions which are clear from various summations in equation (1.101) (on interchanging k with m and l with n)

$$A_{klmn} = A_{mnkl}, \qquad B_{klmn} = B_{mnkl}. \tag{1.102}$$

This shows that, for the most general micropolar anisotropic elastic solid, the number of distinct components for A_{klmn} and B_{mnkl} is 45 each. In addition, we have nine A_{kl} terms which give rise to an initial stress in the undeformed state of the body.

On substituting equation (1.101) into equations $(1.100)_1$ and $(1.100)_2$, we obtain

$$\tau_{kl} = A_{kl} + A_{klmn}\epsilon_{mn}, \qquad m_{kl} = B_{lkmn}\phi_{m,n}. \tag{1.103}$$

These are the linear forms of the stress and couple stress constitutive equations for anisotropic micropolar elastic solids. when the initial stress is zero, we must also have $A_{kl} = 0$. Thus, for the micropolar solid which is free from initial stress, we have

$$\tau_{kl} = A_{klmn}\epsilon_{mn}, \qquad m_{kl} = B_{lkmn}\phi_{m,n}. \tag{1.104}$$

Various material symmetry conditions place further restrictions on the constitutive coefficients A_{klmn} and B_{lkmn}. These restrictions are found in the same manner as in classical elasticity. Here, we obtain the case of isotropic solids. If the body is isotropic with respect to both the stress and couple stress, we call it isotropic. In this case, the constitutive coefficients must be isotropic tensors. For second and fourth order isotropic tensors, we have the most general forms

$$A_{klmn} = \lambda\delta_{kl}\delta_{mn} + (\mu + K)\delta_{km}\delta_{ln} + \mu\delta_{kn}\delta_{lm}, \tag{1.105}$$

$$B_{klmn} = \alpha\delta_{kl}\delta_{mn} + \beta\delta_{kn}\delta_{lm} + \gamma\delta_{km}\delta_{ln}, \tag{1.106}$$

where $\lambda, \mu, K, \alpha, \beta$ and γ are elastic moduli, which are functions of θ only. In this case, equations in (1.104) can be written as

$$\tau_{kl} = \lambda\epsilon_{rr}\delta_{kl} + (\mu + K)\epsilon_{kl} + \mu\epsilon_{lk}, \qquad m_{kl} = \alpha\phi_{r,r}\delta_{kl} + \beta\phi_{k,l} + \gamma\phi_{l,k}. \tag{1.107}$$

Using (1.63), the alternative form of first relation in (1.107) can be written as

$$\tau_{kl} = \lambda e_{rr}\delta_{kl} + (2\mu + K)e_{kl} + K\epsilon_{klm}(r_m - \phi_m), \tag{1.108}$$

Free energy, in this case is given by

$$\rho\Psi = \frac{1}{2}[\lambda e_{kk}e_{ll} + (2\mu + K)e_{kl}e_{kl}] + K(r_k - \phi_k)(r_k - \phi_k)$$

$$+\frac{1}{2}(\alpha\phi_{k,k}\phi_{l,l} + \beta\phi_{k,l}\phi_{l,k} + \gamma\phi_{k,l}\phi_{k,l}). \tag{1.109}$$

We note the difference between isotropic micropolar elasticity and classical elasticity by the presence of four extra elastic moduli; namely, $K,\ \alpha,\ \beta$ and γ. When these are set equal to zero, equations $(107)_2$, (1.108)-(1.109) revert to Hooke's law of the linear isotropic elastic solid.

The stability of materials requires that the stored elastic energy should be nonnegative. This condition is also essential for the uniqueness of the solutions. This requirement places certain restrictions on the micropolar elastic moduli. Eringen (1966a) provided these conditions: *The necessary and sufficient conditions for the internal energy to be nonnegative are*

$$0 \leq 3\lambda + 2\mu + K,\ 0 \leq 2\mu + K,\ 0 \leq K,\ 0 \leq 3\alpha + \beta + \gamma,\ -\gamma \leq \beta \leq \gamma,\ 0 \leq \gamma.$$

1.2 Equations of motion of micropolar elasticity

To derive the equations of small deformation in micropolar elasticity, we use the *principle of balance of momentum* and *principle of moment of momentum* which are expressed respectively as

$$\int_{v'} \rho\mathbf{a}dv = \oint_{s'} \boldsymbol{\tau}_{(\mathbf{n})}da + \int_{v'} \rho\mathbf{f}dv, \tag{1.110}$$

$$\int_{v'} (\mathbf{x} \times \rho\mathbf{a} + \rho\dot{\boldsymbol{\sigma}})dv = \oint_{s'} (\mathbf{x} \times \boldsymbol{\tau}_{(\mathbf{n})} + \mathbf{m}_{(\mathbf{n})})da + \int_{v'} \rho(\boldsymbol{l} + \mathbf{x} \times \mathbf{f})dv, \tag{1.111}$$

where $\boldsymbol{l}$ is the body couple density and other symbols are defined earlier. Here s' and v' are the small internal portion $v + s$ of the body. The quantity $\boldsymbol{\sigma}$ is the intrinsic spin

and it is defined by

$$\rho\boldsymbol{\sigma}\triangle v = \sum_{\alpha} \rho^{(\alpha)}\boldsymbol{\xi} \times (\boldsymbol{\nu} \times \boldsymbol{\xi})\triangle v^{(\alpha)}.$$

Expanding the vector triple product and writing in component form, we have

$$\rho\triangle v\sigma_k = \sum_{\alpha} \rho^{(\alpha)}\epsilon_{klm}\xi_l\epsilon_{mLM}\nu_L\xi_M\triangle v^{(\alpha)},$$

$$= \sum_{\alpha} \rho^{(\alpha)}(\delta_{kL}\delta_{lM} - \delta_{kM}\delta_{lL})\xi_l\nu_L\xi_M\triangle v^{(\alpha)} = \sum_{\alpha} \rho^{(\alpha)}(\delta_{kL}\xi_M\xi_M - \xi_k\xi_L)\nu_L\triangle v^{(\alpha)},$$

$$= \sum_{\alpha} \rho^{(\alpha)}\delta_{kL}\xi_M\xi_M\nu_L\triangle v^{(\alpha)} - \sum_{\alpha} \rho^{(\alpha)}\xi_k\xi_L\nu_L\triangle v^{(\alpha)} = \rho j_{kL}\nu_L\triangle v,$$

where the definition, $\rho i_{kl}\triangle v = \sum_{\alpha} \rho^{(\alpha)}\xi_k\xi_l\triangle v^{(\alpha)}$ and the relation $j_{kL} = \delta_{kL}i_{MM} - i_{kL}$ have been used. Thus, we have $\sigma_l = j_{kl}\nu_k$. Substituting equations (1.91) and $(1.93)_1$ into (1.110) and (1.111), we obtain

$$\int_v \rho\mathbf{a}dv = \oint_s \boldsymbol{\tau}_k n_k da + \int_v \rho\mathbf{f}dv, \tag{1.112}$$

$$\int_v \rho(\mathbf{x} \times \mathbf{a} + \dot{\boldsymbol{\sigma}})dv = \oint_s (\mathbf{x} \times \boldsymbol{\tau}_k + \mathbf{m}_k)n_k da + \int_v \rho(\boldsymbol{l} + \mathbf{x} \times \mathbf{f})dv. \tag{1.113}$$

Employing the following Green - Gauss theorem,

$$\oint_s \mathbf{g}_k n_k da = \int_v \mathbf{g}_{k,k}dv, \tag{1.114}$$

into equations (1.112) and (1.113), we get

$$\int_v [\boldsymbol{\tau}_{k,k} + \rho(\mathbf{f} - \mathbf{a})]dv = 0, \tag{1.115}$$

$$\int_v [\mathbf{m}_{k,k} + \hat{\mathbf{i}}_k \times \boldsymbol{\tau}_k - \rho(\boldsymbol{l} - \dot{\boldsymbol{\sigma}})]dv + \int_v \mathbf{x} \times [\boldsymbol{\tau}_{k,k} + \rho(\mathbf{f} - \mathbf{a})]dv = 0. \tag{1.116}$$

For these equations to be valid for any arbitrary volume v in the body, the necessary and sufficient conditions are the vanishing of the integrands, hence we obtain

$$\boldsymbol{\tau}_{k,k} + \rho(\mathbf{f} - \dot{\mathbf{v}}) = 0, \tag{1.117}$$

$$\mathbf{m}_{k,k} + \hat{\mathbf{i}}_k \times \boldsymbol{\tau}_k + \rho(\boldsymbol{l} - \ddot{\boldsymbol{\sigma}}) = 0, \tag{1.118}$$

or in components form, we can write

$$\tau_{lk,l} + \rho(f_k - \dot{v}_k) = 0, \tag{1.119}$$

$$m_{lk,l} + \epsilon_{kmn}\tau_{mn} + \rho(l_k - \ddot{\sigma}_k) = 0. \tag{1.120}$$

Substituting (1.107) into equations (1.119) and (1.120), we get

$$(\lambda + \mu)u_{l,lk} + (\mu + K)u_{k,ll} + K\epsilon_{klm}\phi_{m,l} + \rho(f_k - \ddot{u}_k) = 0, \tag{1.121}$$

$$(\alpha + \beta)\phi_{l,lk} + \gamma\phi_{k,ll} + K\epsilon_{klm}u_{m,l} - 2K\phi_k + \rho(l_k - j\ddot{\phi}_k) = 0, \tag{1.122}$$

where we have taken $j_{kl} = j\delta_{kl}$ for the microscopic solid. These are the field equations of linear micropolar elasticity. In the linear theory, the accelerations $\ddot{u}_k$ and $\ddot{\phi}_k$ are calculated by their approximate expressions $\ddot{u}_k \simeq \partial^2 u_k/\partial t^2$ and $\ddot{\phi}_k \simeq \partial^2\phi_k/\partial t^2$. The vectorial form of these equations can be written as

$$(\lambda + 2\mu + K)\nabla\nabla\cdot\mathbf{u} - (\mu + K)\nabla\times\nabla\times\mathbf{u} + K\nabla\times\boldsymbol{\phi} + \rho(\mathbf{f} - \ddot{\mathbf{u}}) = 0, \tag{1.123}$$

$$(\alpha + \beta + \gamma)\nabla\nabla\cdot\boldsymbol{\phi} - \gamma\nabla\times\nabla\times\boldsymbol{\phi} + K\nabla\times\mathbf{u} - 2K\boldsymbol{\phi} + \rho(\boldsymbol{l} - j\ddot{\boldsymbol{\phi}}) = 0. \tag{1.124}$$

The equations of motion and constitutive relations in a linear homogeneous and isotropic micropolar elastic solid medium can be extended to microstretch medium. In the absence of body forces and body couple densities, the extended equations of motion are given by (Eringen (1999), pp: 254-255)

$$(c_1^2 + c_3^2)\nabla(\nabla\cdot\mathbf{u}) - (c_2^2 + c_3^2)\nabla\times(\nabla\times\mathbf{u}) + c_3^2\nabla\times\boldsymbol{\phi} + \bar{\lambda_0}\nabla\psi = \ddot{\mathbf{u}}, \tag{1.125}$$

$$(c_4^2 + c_5^2)\nabla(\nabla\cdot\boldsymbol{\phi}) - c_4^2\nabla\times(\nabla\times\boldsymbol{\phi}) + \omega_0^2\nabla\times\ \mathbf{u} - 2\omega_0^2\boldsymbol{\phi} = \ddot{\boldsymbol{\phi}}, \tag{1.126}$$

$$c_6^2\nabla^2\psi - c_7^2\psi - c_8^2\nabla\cdot\mathbf{u} = \ddot{\psi}, \tag{1.127}$$

where $c_1^2 = (\lambda + 2\mu)/\rho$, $c_2^2 = \mu/\rho$, $c_3^2 = K/\rho$, $c_4^2 = \gamma/\rho j$, $c_5^2 = (\alpha + \beta)/\rho j$, $\omega_0^2 = c_3^2/j$, $c_6^2 = 2\alpha_0/\rho j$, $c_7^2 = 2\lambda_1/3\rho j$, $c_8^2 = 2\lambda_0/3\rho j$, $\bar{\lambda}_0 = \lambda_0/\rho$; λ_0, λ_1 and α_0 are microstretch constants and ψ is the scalar microstretch.
The extended constitutive relations are given by

$$\tau_{kl} = \lambda u_{r,r}\delta_{kl} + \mu(u_{k,l} + u_{l,k}) + K(u_{l,k} - \varepsilon_{klr}\phi_r) + \lambda_0\psi\delta_{kl}, \tag{1.128}$$

$$m_{kl} = \alpha\phi_{r,r}\delta_{kl} + \beta\phi_{k,l} + \gamma\phi_{l,k}, \tag{1.129}$$

$$m_k = \alpha_0\psi_{,k}, \tag{1.130}$$

where m_k is the microstretch tensor and other symbols are defined earlier.

1.3 Literature review

The problems of elastic wave propagation and their reflection and transmission from boundary surfaces/interfaces is of keen interest since long. These problems have been studied by many researchers by taking different models and have appeared in the open literature. The basic concepts of classical elasticity, wave propagation in elastic media and their reflection/ refraction from boundary surfaces can be found in several books, e.g., Sokolnikoff (1956), Love (1911), Brekhoviskikh (1960), Achenbach (1973), Ewing et al. (1957), Ben-Menahem and Singh (1981), Bullen and Bolt (1985), Udias (1999), Pujol (2003), Graff (1991) including several others. There are two types of waves that can propagate in a homogeneous isotropic elastic medium: One is longitudinal in nature and other is transverse. Longitudinal wave is called P-wave and transverse wave is called S-wave in seismology. These are body waves and can travel into the deep of the medium. Besides these body waves, there occurs surface waves, which can travel near the boundary surface of a medium and goes on diminishing with the distance away from the boundary surface. There are three types of surface waves: Rayleigh wave, Love wave and Stoneley wave. The literature related to these waves is available frequently in several books on the pertinent topic of research. In nature, there exist some continuum whose microstructure play very important role and it can not be disregarded during investigation of problems related to wave propagations. Due to their significant microstructural properties, the results obtained by the application of classical elasticity are found to disagree with the experimental ones. In this way, the classical theory of

elasticity is inadequate to explain all phenomena of microstructure of a continuum. As explained earlier, several non-classical polar theories were developed to explain the behavior of these microstructural bodies. One of them is the well established theory of micropolar elasticity due to Eringen. In this section, we shall confine ourselves to the works of wave propagation in micropolar and microstretch theories.

Parfitt and Eringen (1969) have investigated the possibility of plane wave propagation in an infinite micropolar elastic solid medium and proved that there can exist four plane waves. These waves are given as follows
i) A longitudinal displacement wave propagating with phase speed

$$v_1 = \sqrt{(\lambda + 2\mu + K)/\rho},$$

ii) A longitudinal microrotational wave propagating with phase speed

$$v_2 = \sqrt{(\alpha + \beta + \gamma)/\rho j + 2\omega_0^2/k^2}, \qquad (\omega_0 = K/\rho j),$$

iii) Two sets of coupled transverse waves (each consists of a transverse displacement coupled with a transverse microrotational) propagating at phase speeds,

$$v_3 = \{(1/2a)[-b + (b^2 - 4ac)^{1/2}]\}^{1/2}$$

and

$$v_4 = \{(1/2a)[-b - (b^2 - 4ac)^{1/2}]\}^{1/2},$$

where $a = 1-2\omega_0^2/\omega^2$, $b = -[c_4^2+c_2^2(1-2\omega_0^2/\omega^2)+c_3^2(1-\omega_0^2/\omega^2)]$ and $c = c_4^2(c_2^2+c_3^2)$. The waves propagating with speeds v_2 and v_3 can exist only when the frequency ω is greater than $\sqrt{2}\omega_0$, otherwise they degenerate into distance decaying sinusoidal vibrations. The longitudinal displacement wave is similar to the longitudinal wave of classical elasticity and actually reduces to that in the limiting case. The appearance of longitudinal microrotational and coupled transverse waves is new and arise due to the microstructure of the medium. They showed that the longitudinal micro-rotational waves and the two sets of coupled waves are dispersive in nature. They have also presented the formulae for amplitude ratios of various reflected waves when these waves are made incident obliquely at a mechanically stress free plane boundary of a micropolar elastic half-space. Several limiting cases are also discussed. Ariman (1972) discussed the problem of reflection of plane longitudinal displacement wave from a fixed flat boundary of a micropolar elastic half-space. He showed that there exist three reflected waves (a longitudinal displacement wave and two coupled transverse waves) as compared with the

two waves of classical elasticity. Smith (1967) investigated the propagation of surfaces of discontinuity of the derivatives of the macro and micro-displacements. He found that a surface of discontinuity of the partial derivatives of macro displacement $\mathbf{u}$ travels with normal velocity $\sqrt{(\lambda+2\mu)/\rho}$ or $\sqrt{(\mu+K)/\rho}$, while that of microdisplacement $\boldsymbol{\phi}$ travels with a normal velocity $\sqrt{(\alpha+\beta+\gamma)/\rho j}$, when $\nabla\cdot\boldsymbol{\phi}=0$ and with velocity $\sqrt{\beta/\rho j}$, when $\nabla\times\boldsymbol{\phi}=0$. He also discussed the modes of macro and micro-vibrations of the solid cylinder and solid sphere. McCarthy and Eringen (1969) derived the propagation condition of waves in micropolar viscoelastic solids by defining a wave to be a propagating surface, across which some kinematical variable suffers discontinuity. They have also derived the expressions for the speeds of propagation of macro and micro shock waves of longitudinal and transverse nature. It is found that the possible speeds of macro shock waves are determined solely by the macro relaxation functions, while the speeds of micro shock waves are determined solely by the micro relaxation functions. They also studied the growth of shock waves and the coupling between the discontinuities in the macroscopic and microscopic fields. Maugin (1974) extended the work of McCarthy and Eringen (1969) to the propagation of acceleration waves. He derived the conditions of propagation of acceleration waves in a simple micropolar media and in a linear micropolar viscoelastic media. Musgrave (1988) derived the field equations for arbitrary anisotropic micropolar elasticity and discussed the stress wave propagation in three types of orthorhombic micropolar medium. He found that at high frequency, the decoupling of equations of motion is possible, which gives two sets of equations corresponding to quasi-translational and spin wave displacements. Recently, Singh (2007) studied the propagation of plane waves in orthotropic micropolar elastic solid and found that the phase speeds of the waves depend on their angle of propagation similar to the classical anisotropic elastic solids. He also obtained the reflection coefficients of these waves from a stress free boundary and depicted their behavior against the angle of propagation. Propagation of acceleration waves in micropolar elastic media is investigated by Eremeyev (2005). He derived the condition of existence of an acceleration waves and showed that it is equivalent to the requirement of a strong ellipticity of equilibrium equations likewise in classical elasticity. Parameshwaran and Koh (1973) investigated the propagation of plane waves in a micro-isotropic, microelastic solid and found that there exist twelve waves propagating with real phase speeds. Out of the twelve waves, eleven are dispersive and one is non-dispersive in nature. These may be classified into two sets: one set of four longitudinal waves and two identical sets of transverse waves, each consisting of four waves. The non-dispersive wave and two coupled transverse waves propagate at all frequencies, while the other two coupled

transverse waves and the remaining seven uncoupled waves propagate only at frequencies higher than certain cut-off frequency. Twiss and Eringen (1971, 1972) derived the micromorphic and micropolar balance equations and entropy production inequalities for a mixtures of any number of chemically non-reacting constituents. They discussed the plane wave propagation in a linear, isotropic, micropolar two constituent mixture with restricted coupling. They showed that there exist longitudinal and transverse microrotational waves, in addition to longitudinal and transverse displacement waves of classical theory. The two displacement waves are found to be dispersive, while the two transverse waves are complexly coupled.

Tomar and Gogna (1992) discussed the problem of reflection and refraction of a longitudinal microrotational wave at an interface between two micropolar elastic media in welded contact and obtained the expressions of reflection and refraction coefficients. The problems of reflection and refraction of a longitudinal wave and a coupled wave at an interface between two dissimilar micropolar elastic solids are also discussed in detail by Tomar and Gogna (1995a, b). These problems of Tomar and Gogna are basically the extensions of the three specific problems earlier studied by Parfitt and Eringen (1969), to cover the transmission phenomena through the plane interface. They used potential method and Snell's law to derive the amplitude ratios of various reflected and transmitted waves. They found that these coefficients depend on the angle of incidence, elastic properties of the half-spaces and frequency of the incident wave. Tomar and Kumar (1995) obtained the reflection and refraction coefficients at the interface between a homogeneous liquid half space and a micropolar solid half-space, when a longitudinal displacement wave is impinging obliquely at the interface after propagating through the micropolar solid half-space. Later, Tomar and Kumar (1999b) discussed the corresponding problem when the longitudinal displacement wave becomes incidence at the liquid / micropolar half-space after propagating through the liquid half-space. The reflection and transmission of elastic waves (longitudinal/ coupled wave) at viscous liquid/ micropolar elastic solid interface was discussed by Kumar and Tomar (2001). They studied the effect of viscosity on various amplitude ratios. Kumar and Singh (1997) investigated the problem of reflection and transmission of elastic waves at a loosely bonded interface between an elastic and a micropolar elastic solids. They computed these coefficients against the angle of incidence at different values of bonding parameters. Recently, Hsia and Cheng (2006) presented reflection and transmission phenomena due to an incident longitudinal plane wave at a plane interface between a uniform elastic medium and a micropolar elastic medium. They presented two sets of boundary conditions: one set contains a boundary condition of vanishing the micro-

rotation at the interface, while the other set contains a boundary condition of vanishing of couple stress at the interface, in addition to the four usual boundary conditions of classical elasticity corresponding to the continuity of force stresses and displacements. The solution of these two sets of boundary conditions are discussed in a separate paper by Hsia et al. (2006), where they presented energy partitioning of various reflected and transmitted waves and showed that the energy ratios not only depend on the angle of incidence but also on the micro-inertia of the micropolar half-space, in addition that there is a remarkable distinction between the two sets of possible boundary conditions. They discovered that only four material moduli are required for full description of the wave propagation and presented normalized power densities of the wave fields versus angle of incidence corresponding to each set of boundary conditions for a particular model. Later, Hsia et al. (2007) investigated the propagation of transverse wave and reflection and transmission of incident $SV/\ SH$ waves from a plane interface between elastic $-$ micropolar porous solids in perfect contact. Singh and Kumar (1998a, b) studied a problem of reflection and refraction of micropolar elastic waves at a loosely bonded interface between a viscoelastic solid and a micropolar elastic solid. They discussed the effect of looseness of the interface on various transmitted waves. Later, Singh (2002a) considered the reflection and refraction coefficients of elastic waves at a loosely bonded interface between two distinct micropolar viscoelastic solid half-spaces. He showed that the coefficients depend on the bonding parameter of the interface and studied the effect of viscoelasticity on them. Recently, Singh and Kumar (2007) studied a problem of reflection and refraction of elastic waves at a welded contact interface between a viscoelastic solid and a micropolar elastic solid. They considered the incidence of longitudinal micro-rotational wave propagating through the micropolar medium and the incidence of $SH-$ wave propagating through the viscoelastic medium. Tomar et al. (1998) discussed the propagation of plane waves in an infinite micropolar elastic medium with stretch and studied the reflections of these waves from the free plane surface of a micropolar elastic half-space with stretch. Kumar and Singh (2000) extended their problem to the interface between a linear viscoelastic half-space and a micropolar elastic half-space with stretch, when a plane $P/\ SV-$ wave after propagating through the viscoelastic half-space becomes incident at the interface. Singh (2000b) also covered the case of reflection and transmission of waves at the interface between liquid half-space and micropolar viscoelastic solid with stretch. Kumar and Deswal (2000) studied the reflection of micropolar elastic waves from the free surface of a liquid saturated micropolar elastic half-space. They have also derived the wave-velocity equation of Rayleigh waves in a micropolar liquid-saturated poroelastic

half-space. Yang and Hsia (1998) discussed the propagation, reflection and transmission of an incident acoustic plane wave (from the liquid half-space) at the fluid − micropolar interface and discussed the normalized power densities. Kumar and Barak (2007) studied a problem of reflection and transmission at an interface between a homogeneous liquid half space and a micropolar liquid saturated porous half-space, when longitudinal waves (fast/slow) and coupled transverse waves are made incident at the interface. They studied the micropolarity and porosity effects on the coefficients corresponding to various reflected and transmitted waves.

Reflection of plane elastic waves from the boundary surface of a micropolar generalized thermoelastic solid half-space in the context of Green-Lindsay (G-L) and Lord-Shulman (L-S) theories was studied by Singh and Kumar (1998d). They obtained the reflection coefficients of various reflected waves and showed that the effect of thermoelastic coupling coefficient is more in G-L theory as compared to L-S theory. Kumar (2000) extended the problem of Singh and Kumar (1998d) to the micropolar viscoelastic generalized thermoelastic solid. Singh (2000a) studied the reflection and refraction of plane sound wave at an interface between a liquid half-space and a micropolar generalized thermoelastic solid half-space. He also compared the amplitude ratios obtained in the corresponding problem without thermal effects. Singh (2001b) investigated the problem of reflection and refraction of micropolar thermoelastic waves at a thermally conducting liquid half-space and a micropolar generalized thermoelastic solid half-space. He found that the amplitude ratios for various reflected and transmitted waves in G-L theory are different from those in L-S theory. This is how he explained the effect of second thermal relaxation time on the amplitude ratios. Singh (2002d) studied the reflection of thermo-viscoelastic plane waves from the free plane boundary surface in the presence of magnetic field. Frequency equation of Rayleigh surface wave propagation in a micropolar thermoelastic medium without energy dissipation has been investigated by Kumar and Deswal (2002b). Song et al. (2006a) obtained the reflection and transmission coefficients at the interface of two different magneto-thermoviscoelastic micropolar solids in context of three different theories of thermoelasticity. Song et al. (2006b) studied the problem of reflection and refraction of magneto-thermoviscoelastic waves at the interface between two micropolar viscoelastic media when a uniform magnetic field permeates the media using micropolar generalized thermoviscoelastic theories. They obtained the expressions of reflection and refraction coefficients for dilatational and rotational waves and found that these coefficients depend upon the angle of incidence. They also found that the viscosity plays a significant role, while magnetic field has a salient influence on reflection and refraction coefficients.

Othman and Song (2007) discussed the reflection and refraction of a plane harmonic wave at the interface between two micropolar thermoviscoelastic media without energy dissipation and obtained the amplitude ratios corresponding to the reflected and refracted waves. Kumar and Partap (2007) derived secular equations corresponding to axisymmetric free vibrations in an infinite homogeneous isotropic micropolar thermoelastic plate without energy dissipation, when the faces of plate are stress free and when they are rigidly fixed. They studied the micropolar and thermal effects on the phase velocity and derived the amplitudes of displacement components, microrotation and temperature distribution in symmetric and skew symmetric modes.

Singh and Kumar (1998c) extended their problem (Singh and Kumar, 1998d) to include stretch. They considered the case of incident longitudinal displacement, incident coupled waves and incident longitudinal microstretch waves and studied the thermal and stretch effects on various reflected waves. Singh and Kumar (1998e) discussed wave propagation in a generalized thermo-microstretch elastic solid and studied the problem of reflection of incident plane waves from the free surface of a generalized thermo-microstretch half space. This problem was later extended to liquid/ microstretch interface in the presence of temperature/magnetic fields by Singh (2001a, 2002c). Plane wave propagation and their reflection from a free surface of a microstretch elastic solid is investigated by Singh (2002b). He studied the effect of microstretch property on various reflected waves. Tomar and Garg (2005) investigated the wave propagation and their reflection and transmission through a plane interface between two different microstretch elastic solid half-spaces in perfect contact. It is shown that there exist five waves in a linear homogeneous isotropic microstretch elastic solid, one of them travel independently, while other waves are two sets of two coupled waves. It is also shown that these waves travel with different velocities, three of which disappear below a critical frequency. Amplitude ratios and energy ratios of various reflected and transmitted waves are presented when a set of coupled longitudinal waves and a set of coupled transverse waves is made incident. Recently, Kumar and Rupinder (2008) studied the reflection and deformation in magneto-thermo-microstretch elastic solid.

Willson (1972) discussed the fundamental vibrations of a long circular cylinder made up of micropolar material. He derived the dispersion equation and discovered that torsional type surface waves may propagate independently of waves of extension. The dispersion relation of these waves were earlier discovered by Smith (1970), but in a complicated form. Rao (1988) studied the micropolar effect on the longitudinal wave propagating in an elastic layer and derived the frequency equation corresponding to Rayleigh-Lamb wave propagation. He found that the longitudinal wave propagates

in the layer with an extra velocity, which arises due to micropolarity of the layer. He observed that even modes are anti-symmetric and odd modes are symmetric unlike in classical elasticity. The results obtained are compared with the corresponding results of classical elasticity. Rayleigh type surface waves propagating on the surface in the azimuthal direction of an elastic circular cylinder of a micropolar elastic material is studied by Rao and Reddy (1993). Tajuddin (1995) studied the propagation of Stoneley waves at an unbonded interface between two micropolar elastic half-spaces. He derived the condition of propagation when the solids are Poission solids and have the material properties close to each other. Kumar and Singh (1996) studied the Rayleigh-Lamb waves and Rayleigh surface waves in a micropolar generalized thermoelastic body with stretch. Deswal et al. (2000) studied the effect of micropolarity and viscosity on dispersion curves on the surface waves in cylindrical bore filled with viscous liquid and hosted in micropolar media. Kumar and Deswal (2002a) obtained the frequency equation for the propagation of Stoneley type waves along the surface of a cylindrical bore filled with viscous liquid and embedded in a microstretch elastic medium. Nowacki and Nowacki (1969) discussed the propagation of monochromatic elastic waves in an infinite micropolar elastic plate. They obtained the symmetric and anti-symmetric vibrations by deriving the corresponding characteristic equations and approximated them for wavelengths small compared to plate thickness. They also showed that Love waves are possible in a micropolar elastic half-space in addition to the usual Rayleigh waves. Bera(1973) investigated the propagation of monochromatic waves in an initially stressed infinite micropolar elastic plate and reduced the result of Nowacki and Nowacki (1969) by neglecting initial stress. Tomar (2002) investigated the wave propagation in a micropolar elastic plate bordered with layers of homogeneous inviscid liquid. Tomar (2005) has also investigated the frequency equation of Rayleigh−Lamb waves in a micropolar elastic plate with voids. He found that both symmetric and antisymmetric modes of vibrations are dispersive and attenuated. The presence of voids has negligible effect on the dispersion curves, however attenuation coefficient is significantly influenced.

Kumar and Deswal (2006) studied wave propagation in micropolar elastic medium with voids. They studied three different problems. One is on the propagation of waves in a micropolar elastic layer with voids immersed in an infinite liquid, second is on the reflection of longitudinal and coupled waves at the free surface of micropolar elastic half-space with voids and third is on Rayleigh wave propagation. They derived the frequency equations corresponding to symmetric and anti-symmetric modes in the micropolar elastic layer with voids and studied the effect of voids and micropolarity

on dispersion curves. They also computed the reflection coefficients for a particular model and compared with classical case. Tomar and Singh (2006) discussed the propagation of plane waves in an infinite micropolar porous elastic medium and studied the problem of reflection of a plane longitudinal displacement wave and coupled waves from a plane free surface and obtained the expressions of amplitude and energy ratios. Recently, Singh and Tomar (2007) discussed the plane wave propagation in a linear, homogeneous, and isotropic micropolar porous elastic solid rotating with a uniform angular velocity. They showed the existence of three longitudinal waves and two sets of coupled transverse waves. They observed that out of the three longitudinal waves, one is a longitudinal microrotational wave, the second is a longitudinal displacement wave and the third is a longitudinal void volume fractional wave carrying a change in the void volume and showed that the rotation of the body does influence the phase speed, energy loss, and decay coefficient, in general. Propagation of shear surface wave along the interface of a liquid half-space and a micropolar solid half-space is investigated by Yerofeyev and Soldatov (1999) and determined the phase speed and attenuation. They found that these surface waves are almost non-dispersive unlike the corresponding problem in classical elasticity. Midya (2004) discussed the propagation of SH-type surface waves in homogeneous isotropic elastic media consisting of a layer of finite thickness lying over a half-space when either the layer or the half-space or both are micropolar and observed that a new type of surface wave is arising in all cases due to the micropolarity of one or both the media. Recently, Midya et al. (2007, 2008) studied a problem of diffraction of normally incident P and SH-waves by a line crack in micropolar medium. He obtained stress intensity factor for limitly low and high frequencies by taking small coupling parameter.

1.4 Plan of thesis

In this thesis, we have investigated some interesting dynamical problems in microstructural continuum using Eringen's polar theory. These problems are pertaining to surface waves in a microstretch plate, Stoneley waves at an interface between two different microstretch half-spaces, surface waves in a micropolar cylindrical borehole filled with micropolar fluid, reflection and transmission of elastic waves at a liquid/solid half-space and reflection of elastic waves from a micropolar mixture porous half-space. There are six chapters, including a list of references given in the end of this thesis.

Chapter 1 is on Introduction, in which the development of microcontinuum theories, derivations of basic equations and constitutive relations for micropolar elastic

solid and an exhaustive review on the works done by various researchers in the field of wave propagation in microcontinuum are presented.

Chapter 2 is on the propagation of Rayleigh−Lamb waves in an infinite plate of finite thickness and composed of microstretch elastic material. The top and bottom of the plate are cladded with finite layers of a homogeneous and inviscid liquid (non-micropolar and non-microstretch). There exist two sets of boundary conditions at solid/liquid interface and corresponding frequency equations are derived for symmetric and antisymmetric modes of propagation for Rayleigh Lamb wave propagation. Numerical computations are performed for a specific model to compute the phase velocity and attenuation coefficient for different values of wavenumber, for both symmetric and antisymmetric vibrations. Results of some earlier workers have been deduced as special cases at the end of the chapter.

In Chapter 3, we derived frequency equations for Stoneley wave propagation at unbonded and bonded interfaces between two dissimilar microstretch elastic half-spaces. Numerical treatment to the problem is dealt in detail. The results of earlier workers have been derived as particular cases of the present problem, and some other interesting particular cases have also been discussed in this chapter.

In Chapter 4, the possibility of plane wave propagation in a micropolar fluid of infinite extent has been explored. The reflection and transmission of longitudinal elastic waves at a plane interface between a homogeneous micropolar fluid half-space and a micropolar solid half-space has also been investigated. The expressions of energy ratios have been obtained in explicit form. Frequency equation for the Stoneley wave at micropolar solid/fluid interface has also been derived in the form of sixth-order determinantal expression, which is found in full agreement with the corresponding result of inviscid liquid/elastic solid interface. Numerical computations have been performed for a specific model. The dispersion curves and attenuation of the existed waves in micropolar fluid have been computed and depicted graphically. The variations of various amplitudes and energy ratios are also shown against the angle of incidence. Results of some earlier workers have been deduced from the present formulation at the end of this chapter.

In Chapter 5, the micropolar mixture theory of porous media developed by Eringen (2003a) is employed to explore the possible propagation of waves in this continuum. A problem of reflection of coupled longitudinal waves from a free boundary surface of a half-space consisting the mixture of a micropolar elastic solid and Newtonian liquid, is investigated. The expressions of phase velocity, various amplitude and energy ratios and surface responses are calculated and computed numerically for a specific model.

All the numerical results computed are depicted graphically.

In Chapter 6, we derived the dispersion equation for the propagation of surface waves in a cylindrical borehole filled with a micropolar viscous fluid and hosted in an infinite micropolar elastic solid medium. The effects of fluid viscosity, micropolarity of the fluid and radius of the borehole on the dispersion curves are noticed and depicted graphically.

A list of references mentioned at various places in the entire thesis, has been given at the end of this thesis.

List of publications

1. Rayleigh-Lamb waves in a microstretch elastic plate cladded with liquid layers, Dilbag Singh and S. K. Tomar, *Journal of Sound and Vibrations*, 302(1-2), 313-331 (2007).

2. Propagation of Stoneley waves at an interface between two microstretch elastic half-spaces, S. K. Tomar and Dilbag Singh, *Journal of Vibration and Control*, 12(9), 995-1009 (2006)[Erratum, *Journal of Vibration and Control*, 13(12), 1835-1836 (2007)].

3. Longitudinal waves at a micropolar fluid/solid interface, Dilbag Singh and S. K. Tomar, *International Journal of Solids and Structures*, 45(1), 225-244 (2008).

4. Wave propagation in micropolar mixture of porous media, Dilbag Singh and S. K. Tomar, *International Journal of Engineering Science*, 44(18-19), 1304-1323 (2006).

5. Waves in a cylindrical borehole filled with micropolar fluid, Dilbag Singh and S. K. Tomar, *Journal of Applied Physics*, 103(12), (2008).

Chapter 2

Rayleigh-Lamb waves in a microstretch elastic plate cladded with liquid layers[1]

2.1 Introduction

Lamb (1917) was the first to investigate the problem of wave propagation in an elastic plate of uniform material. Since then the term 'Lamb wave' has been used to refer to an elastic disturbance propagating in a solid plate with free boundaries. When a plate of finite thickness is bordered with homogeneous liquid half-spaces on both sides then some part of the Lamb wave energy in the plate radiates into the liquid, while most of the energy still remains in the solid. The density and viscosity sensing with Lamb waves is based on the principle that the presence of liquid in contact with a solid plate changes the velocity and amplitude of the Lamb waves in the plate with free boundaries. Wu and Zhu (1992) and Zhu and Wu (1995) studied the propagation of Lamb waves in an elastic plate when both sides of the plate are bordered with liquid layers. Sharma et al. (2003) analyzed the propagation of thermoelastic waves in a homogeneous, transversely isotropic, thermally conducting plate bordered with layers of inviscid liquid or with inviscid liquid half-spaced on both sides, in the context of coupled theory of thermoelasticity. Sharma and Pathania (2003), Sharma et al. (2004),

[1] ***Journal of Sound and Vibration,* 302(1-2)**, 313-331(2007).

Sharma and Pathania (2004) and Sharma and Pal (2004) discussed various problems of propagation of thermoelastic waves in a plate bordered with layers of inviscid liquid in the context of generalized theories of thermoelasticity. Tomar (2002) derived the frequency equations for wave propagation in a micropolar plate of finite thickness and bordered with layers of homogeneous inviscid liquid. In this chapter, we have discussed the propagation of Rayleigh-Lamb waves in a plate of homogeneous and isotropic microstretch elastic material cladded with layers of homogeneous, inviscid and nonpolar liquid. The field equations and constitutive relations for microstretch elastic material developed by Eringen are employed for mathematical analysis. The frequency equations corresponding to symmetric and antisymmetric modes of vibrations of the plate are obtained. These frequency equations are discussed for some limiting cases and some known results of earlier authors have been reduced. Phase velocity and attenuation coefficient are also computed for a specific model and the effect of microstretch is noticed on them.

2.2 Formulation of problem

We consider a plate of finite thickness $'2d'$ and composed of microstretch elastic solid material. The plate is assumed to be of infinite extent in the $x-y$ plane, whose top

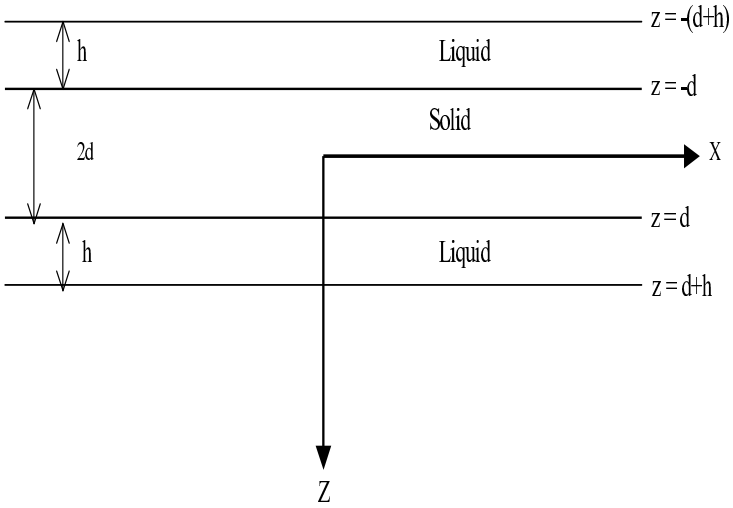

Figure 2.1: Geometry of the problem

and bottom faces are bordered with layers of a homogeneous inviscid liquid of thickness $'h'$. The $x-y$ plane is taken to coincide with the middle plane of the plate and the

z-axis is taken normal to it along the thickness of the plate. The complete geometry of the problem is shown in Figure 2.1.

The equations of motion and constitutive relations in a linear homogeneous and isotropic microstretch elastic solid medium, in the absence of body force and body couple densities, are given in Chapter-1 through equations (1.125) -(1.130). We shall discuss a two-dimensional problem in $x-z$ plane, so we take the following components of displacement vector, microrotation vector and scalar microstretch respectively

$$\mathbf{u} = (u(x,z),\ 0,\ w(x,z))\,, \qquad \boldsymbol{\phi} = (0,\ \phi(x,z),\ 0)\,, \qquad \psi = \psi(x,z).$$

With these considerations and introducing potentials L and M such that

$$u = \frac{\partial L}{\partial x} + \frac{\partial M}{\partial z}, \qquad w = \frac{\partial L}{\partial z} - \frac{\partial M}{\partial x},$$

into equations (1.125) - (1.27), we obtain

$$(\lambda + 2\mu + K)\nabla^2 L + \lambda_0 \psi = \rho \frac{\partial^2 L}{\partial t^2}, \tag{2.1}$$

$$(\mu + K)\nabla^2 M - K\phi = \rho \frac{\partial^2 M}{\partial t^2}, \tag{2.2}$$

$$\gamma \nabla^2 \phi + K\nabla^2 M - 2K\phi = \rho j \frac{\partial^2 \phi}{\partial t^2}, \tag{2.3}$$

$$6\alpha_0 \nabla^2 \psi - 2\lambda_0 \nabla^2 L - 2\lambda_1 \psi = 3\rho j \frac{\partial^2 \psi}{\partial t^2}. \tag{2.4}$$

We see that the equations (2.1) and (2.4) are coupled in the potential L and microstretch ψ, while the equations (2.2) and (2.3) are coupled in the potential M and micro-rotation ϕ. To find out the time harmonic solution of these equations, we assume the form of $L,\ M,\ \phi$ and ψ as follows

$$\{L,\ M,\ \phi,\ \psi\}(x,z,t) = \{\bar{L},\ \bar{M},\ \bar{\phi},\ \bar{\psi}\}(x,z)\exp\{-\imath\omega t\}, \tag{2.5}$$

where ω is angular frequency, which is related to the wavenumber ξ and phase velocity c through the relation $\omega = \xi c$. Substituting (2.5) into equations (2.1)-(2.4), we obtain

$$(\lambda + 2\mu + K)\nabla^2 \bar{L} + \lambda_0 \bar{\psi} = -\rho\omega^2 \bar{L}, \tag{2.6}$$

$$(\mu + K)\nabla^2 \bar{M} - K\bar{\phi} = -\rho\omega^2 \bar{M}, \tag{2.7}$$

$$\gamma\nabla^2 \bar{\phi} + K\nabla^2 \bar{M} - 2K\bar{\phi} = -\rho j\omega^2 \bar{\phi}, \tag{2.8}$$

$$6\alpha_0 \nabla^2 \bar{\psi} - 2\lambda_0 \nabla^2 \bar{L} - 2\lambda_1 \bar{\psi} = -3\rho j\omega^2 \bar{\psi}. \tag{2.9}$$

Again, we can see that the equations (2.6) and (2.9) are coupled in $\bar{L}$ and $\bar{\psi}$, while the equations (2.7) and (2.8) are coupled in $\bar{M}$ and $\bar{\phi}$. By elimination procedure, it can be seen that these potentials satisfy the following equations

$$\left[\nabla^4 + \ell_1 \nabla^2 + \ell_2\right](\bar{\psi}, \bar{L}) = 0, \tag{2.10}$$

$$\left[\nabla^4 + \ell_3 \nabla^2 + \ell_4\right](\bar{\phi}, \bar{M}) = 0, \tag{2.11}$$

where

$$\ell_1 = \left(\frac{3\rho j\omega^2 - 2\lambda_1}{6\alpha_0} + \frac{3\alpha_0\rho\omega^2 + \lambda_0^2}{3\alpha_0(\lambda + 2\mu + K)}\right), \qquad \ell_2 = \frac{\rho\omega^2(3\rho j\omega^2 - 2\lambda_1)}{6\alpha_0(\lambda + 2\mu + K)},$$

$$\ell_3 = \left(\frac{\rho j\omega^2 - 2K}{\gamma} + \frac{\gamma\rho\omega^2 + K^2}{\gamma(\mu + K)}\right), \qquad \ell_4 = \frac{\rho K\omega^2}{\gamma(\mu + K)}\left(\frac{\rho j\omega^2}{K} - 2\right).$$

The solutions of equations (2.10) and (2.11) for the waves propagating along positive $x-$ direction can be worked out easily and finally the time harmonic solutions of equations (2.1)-(2.4) can be written as

$$L = (A\sinh Rz + B\cosh Rz + C\sinh Sz + D\cosh Sz)e^{\imath(\xi x - \omega t)}, \tag{2.12}$$

$$\psi = a(A\sinh Rz + B\cosh Rz) + b(C\sinh Sz + D\cosh Sz)e^{\imath(\xi x - \omega t)}, \tag{2.13}$$

$$M = (E\sinh Pz + F\cosh Pz + G\sinh Qz + H\cosh Qz)e^{\imath(\xi x-\omega t)}, \tag{2.14}$$

$$\phi = c'(E\sinh Pz + F\cosh Pz) + d'(G\sinh Qz + H\cosh Qz)e^{\imath(\xi x-\omega t)}, \tag{2.15}$$

where the quantities $a,\ b,\ c'$ and d' are coupling constants and their expressions can be obtained by substituting equations (2.12)-(2.15) into equations (2.1) and (2.2) as

$$a = -\{(c_1^2 + c_3^2)(-\xi^2 + R^2) + \omega^2\}/\bar{\lambda}_0, \quad b = -\{(c_1^2 + c_3^2)(-\xi^2 + S^2) + \omega^2\}/\bar{\lambda}_0,$$

$$c' = \{(c_2^2 + c_3^2)(-\xi^2 + P^2) + \omega^2\}/c_3^2, \quad d' = \{(c_2^2 + c_3^2)(-\xi^2 + Q^2) + \omega^2\}/c_3^2,$$

and the expressions of $R,\ S,\ P$ and Q are given by

$$R^2, S^2 = \xi^2 - \frac{1}{2}\left[\ell_1 \pm \sqrt{\ell_1^2 - 4\ell_2}\right], \qquad P^2, Q^2 = \xi^2 - \frac{1}{2}\left[\ell_3 \pm \sqrt{\ell_3^2 - 4\ell_4}\right].$$

The expressions of R^2 and P^2 are taken with ' $+$ ' sign and expressions of S^2 and Q^2 are taken with ' $-$ ' sign.

The equation of motion in liquid medium is given by

$$\nabla^2\Psi = \frac{1}{c_L^2}\frac{\partial^2\Psi}{\partial t^2}, \tag{2.16}$$

where Ψ is the displacement potential and $c_L = \sqrt{\lambda_L/\rho_L}$ is the velocity of sound in liquid, λ_L and ρ_L being the bulk modulus and density of the liquid respectively.
Denoting the displacement potential function by ϕ_{L_1} and ϕ_{L_2} in the top and bottom layers of the liquid respectively, the normal component of displacement w_{L_i} and pressure p are given by

$$w_{L_i} = \frac{\partial\phi_{L_i}}{\partial z}, \quad p = \rho_L\omega^2\phi_{L_i}. \tag{2.17}$$

($i = 1$ for the liquid in top layer and $i = 2$ for the liquid in bottom layer).
The time harmonic solutions of equation (2.16) for the waves propagating along $x-$ direction in the top and bottom liquid layers are given by (see Wu and Zhu, 1992)

$$\phi_{L_1} = F_1\sin\{T[z - (d + h)]\}e^{\imath(\xi x-\omega t)} \quad \text{for} \quad [d \le z \le (d + h)], \tag{2.18}$$

$$\phi_{L_2} = F_2 \sin\{T[z + (d + h)]\} e^{\imath(\xi x - \omega t)} \quad \text{for} \quad [-(d + h) \leq z \leq -d], \tag{2.19}$$

where F_1 and F_2 are unknown, $T^2 = K_L^2 - \xi^2$ and $K_L = \omega/c_L$. To derive the frequency equation for Rayleigh-Lamb waves in the plate considered, we shall use the following boundary conditions at the solid-liquid interfaces.

2.3 Boundary conditions

The relevant boundary conditions at the solid/liquid interface will be the continuity of displacement and stresses. Corresponding to the continuity of normal component of stress at the interface, the normal stress of the solid must be equal to the pressure of the liquid layer. However, shear stress of solid should be equal to zero at the interface as the inviscid liquid can not support shear stress. Also, as one can not protect the flow of an inviscid liquid over a solid, the continuity condition can not be put on the displacement component along $x-$ axis, however normal component of displacement must be continuous at liquid $-$ solid interface. Mathematically, these boundary conditions can be expressed as

$$\tau_{zx} = 0, \quad \tau_{zz} = -p \qquad \text{and} \qquad w = w_L. \tag{2.20}$$

These equations constitute the three boundary conditions. However, to solve a boundary value problem at the interface of interest, we need two more conditions. The balance of moment of momentum across the interface of two microstretch elastic solids requires the continuity of normal component of couple stress and continuity of microstretch vector. In the present instance, we have the interface between a microstretch elastic solid and an inviscid liquid. Since our liquid neither exhibit micropolarity nor microstretch property, therefore, at liquid $-$ solid interface couple stress and microstretch tensor must vanish. These conditions can be written as

$$m_{zy} = 0 \qquad \text{and} \qquad m_z = 0. \tag{2.21}$$

These two equations constitute the remaining two boundary conditions we need.
The boundary conditions on the displacement fields are purely kinematic, so the boundary conditions on microrotation and microstretch cannot be ruled out. We see that

other set of boundary conditions are also possible for the present case. These are the vanishing of microrotation and microstretch of the solid at liquid − solid interface as our liquid can not support both (however, one can consider such a liquid in which both microrotation and microstretch are non-null). Therefore, one can use the following boundary conditions in place of those given in (2.21)

$$\phi = 0 \quad \text{and} \quad \psi = 0. \tag{2.22}$$

Thus, we see that there are two sets of boundary conditions at the solid-liquid interfaces. These two sets of boundary conditions to be satisfied at the solid-liquid interfaces $z = \pm d$ are given by

Set I: $\tau_{zx} = 0, \quad m_{zy} = 0, \quad m_z = 0, \quad \tau_{zz} = -p, \quad w = w_L.$

Set II: $\tau_{zx} = 0, \quad \phi = 0, \quad \psi = 0, \quad \tau_{zz} = -p, \quad w = w_L.$

Using equations (2.12) - (2.15), (2.17)-(2.19) and relevant quantities from (1.128) - (1.130) into the boundary conditions given in Set-I, we obtain the following ten homogeneous equations in ten unknown, namely A, B, C, D, E, F, G, H, F_1 and F_2, given by

$$[-\lambda\xi^2 + (\lambda + 2\mu + K)R^2 + \lambda_0 a](A\sinh Rd + B\cosh Rd) + [-\lambda\xi^2 + (\lambda + 2\mu + K)S^2 + \lambda_0 b]$$

$$\times(C\sinh Sd + D\cosh Sd) - P(2\mu + K)\imath\xi(E\cosh Pd + F\sinh Pd) - Q(2\mu + K)\imath\xi$$

$$\times(G\cosh Qd + H\sinh Qd) - \rho_L\omega^2 F_1 \sin Th = 0, \tag{2.23}$$

$$[-\lambda\xi^2 + (\lambda + 2\mu + K)R^2 + \lambda_0 a](-A\sinh Rd + B\cosh Rd) + [-\lambda\xi^2 + (\lambda + 2\mu + K)S^2 + \lambda_0 b]$$

$$\times(-C\sinh Sd + D\cosh Sd) - P(2\mu + K)\imath\xi(E\cosh Pd - F\sinh Pd) - Q(2\mu + K)\imath\xi$$

$$\times(G\cosh Qd - H\sinh Qd) + \rho_L\omega^2 F_2 \sin Th = 0, \tag{2.24}$$

$$R(2\mu + K)\imath\xi[A\cosh Rd + B\sinh Rd] + S(2\mu + K)\imath\xi[C\cosh Sd + D\sinh Sd]$$

$$+[\mu\xi^2 + (\mu + K)P^2 - Kc'](E\sinh Pd + F\cosh Pd) + [\mu\xi^2 + (\mu + K)Q^2 - Kd']$$

$$\times(G\sinh Qd + H\cosh Qd) = 0, \tag{2.25}$$

$$R(2\mu+K)\imath\xi[A\cosh Rd - B\sinh Rd] + S(2\mu+K)\imath\xi[C\cosh Sd - D\sinh Sd]$$
$$+[\mu\xi^2 + (\mu+K)P^2 - Kc'](-E\sinh Pd + F\cosh Pd) + [\mu\xi^2 + (\mu+K)Q^2 - Kd']$$
$$\times(-G\sinh Qd + H\cosh Qd) = 0, \tag{2.26}$$

$$Pc'(E\cosh Pd + F\sinh Pd) + Qd'(G\cosh Qd + H\sinh Qd) = 0, \tag{2.27}$$

$$Pc'(E\cosh Pd - F\sinh Pd) + Qd'(G\cosh Qd - H\sinh Qd) = 0, \tag{2.28}$$

$$R(A\cosh Rd + B\sinh Rd) + S(C\cosh Sd + D\sinh Sd)$$
$$-\imath\xi(E\sinh Pd + F\cosh Pd + G\sinh Qd + H\cosh Qd) - TF_1\cos Th = 0, \tag{2.29}$$

$$R(A\cosh Rd - B\sinh Rd) + S(C\cosh Sd - D\sinh Sd)$$
$$-\imath\xi(-E\sinh Pd + F\cosh Pd - G\sinh Qd + H\cosh Qd) - TF_2\cos Th = 0, \tag{2.30}$$

$$aR(A\cosh Rd + B\sinh Rd) + bS(C\cosh Sd + D\sinh Sd) = 0, \tag{2.31}$$

$$aR(A\cosh Rd - B\sinh Rd) + bS(C\cosh Sd - D\sinh Sd) = 0. \tag{2.32}$$

For non-trivial solution of these equations, the determinant of their coefficient matrix should vanish. For $T \neq 0$ and $Th \neq \dfrac{(2n-1)\pi}{2}$, $(n = 1, 2, ...)$, this determinantal equation leads to the following frequency equations for symmetric (with index '+1') and antisymmetric (with index '-1') modes of vibrations respectively

$$(aRM_2(\coth Sd)^{\pm1} - bSM_1(\coth Rd)^{\pm1})(Pc'N_2(\coth Pd)^{\pm1} - Qd'N_1(\coth Qd)^{\pm1})$$
$$-(b-a)(d'-c')\xi^2M_3^2RSPQ(\coth Qd\coth Pd)^{\pm1} = -RS(b-a)\frac{\rho_L\omega^2}{T}\tan Th$$

$$\times[\xi^2 M_3(Qd'(\coth Qd)^{\pm 1} - c'P(\coth Pd)^{\pm 1})$$

$$-(Qd'N_1(\coth Qd)^{\pm 1} - c'PN_2(\coth Pd)^{\pm 1})], \tag{2.33}$$

where

$$M_1 = -\lambda\xi^2 + (\lambda + 2\mu + K)R^2 + \lambda_0 a, \quad M_2 = -\lambda\xi^2 + (\lambda + 2\mu + K)S^2 + \lambda_0 b,$$

$$M_3 = (2\mu + K), \quad N_1 = \mu\xi^2 + (\mu + K)P^2 - Kc', \quad N_2 = \mu\xi^2 + (\mu + K)Q^2 - Kd'$$

It can be seen that equation (2.33) exhibit implicit functional relationship between phase velocity and wavenumber, therefore, the symmetric and antisymmetric modes of Rayleigh-Lamb waves are dispersive in nature. Moreover, the $'\tanh'$ and $'\coth'$ functions are multiple valued functions, therefore there exist infinite number of modes of propagation.

Similarly, using the boundary conditions given in Set -II, we obtain the following frequency equations for symmetric (with index '+1') and antisymmetric (with index '-1') modes of propagation of Rayleigh-Lamb waves respectively.

$$(aM_2 - bM_1)[aN_2(\coth Sd)^{\pm 1} - bN_1(\coth Rd)^{\pm 1}][M_3 d'(\tanh Pd)^{\pm 1} - M_4 c'(\tanh Qd)^{\pm 1}]$$

$$= \frac{\rho_L}{T}\omega^2 \tan Th[(aS(\coth Sd)^{\pm 1} - bR(\coth Rd)^{\pm 1})$$

$$\times(N_3 d' - N_4 c') - \imath\xi(aN_2(\coth Sd)^{\pm 1} - bN_1(\coth Rd)^{\pm 1})(c' - d')] \tag{2.34}$$

2.4 Limiting cases

2.4.1 Symmetric vibrations:

(a) For waves long compared with the thickness of the plate, the quantity ξd is small and therefore the quantities Rd, Sd, Pd, and Qd may be assumed small as long as c is finite. In this case, $\tanh x \to x$ and we obtain from equation (2.33) for symmetric (with index '+1') mode

$$(aR^2M_2 - bS^2M_1)(N_2c' - N_1d') - R^2S^2\xi^2M_3^2(b - a)(d' - c')$$

$$= R^2S^2(b-a)\frac{\rho_L\omega^2}{T}\tan Th[\xi^2M_3(d'-c')-(N_1d'-N_2c')]. \tag{2.35}$$

In the absence of liquid layers, i.e., when $\rho_L = 0$, the above equation (2.35) reduces to

$$(aR^2M_2 - bS^2M_1)(N_2c' - N_1d') - R^2S^2\xi^2M_3^2(b-a)(d'-c') = 0. \tag{2.36}$$

This is the frequency equation for symmetric modes of vibration in a microstretch elastic plate with free boundaries in the present case. If we further neglect the microstretch property from the plate, then we shall be left with the problem of Lamb wave propagation in a micropolar elastic plate with free boundaries. Thus, by putting $\lambda_0 = \alpha_0 = \lambda_1 = 0$ and $b/a = 0$, the equation (2.36) reduces to

$$[(2\mu+K)\xi^2 - \rho\omega^2][N_2c' - N_1d'] = \xi^2S'^2(2\mu+K)^2(c'-d'), \tag{2.37}$$

where

$$S' = \sqrt{\xi^2 - \frac{\rho\omega^2}{\lambda+2\mu+K}}.$$

This equation matches with the frequency equation as obtained by Nowacki and Nowacki (1969) for the relevant problem apart from notations.

Again, in the absence of micropolarity, i.e., when $K = d'/c' = 0$, we get from equation (2.37) after some simplification

$$c^2 = 4\beta^2\left(1 - \frac{\beta^2}{\alpha^2}\right) \tag{2.38}$$

where $\alpha^2 = (\lambda+2\mu)/\rho$ and $\beta^2 = \mu/\rho$. This equation exactly matches with Lamb (1917).

(b) For very short waves as compared with the thickness of the plate, the quantity ξd is large, therefore, the quantities Rd, Sd, Pd and Qd are large as long as c is finite and $\tanh x \to 1$. In this case, equation (2.33) for symmetric mode (with index '+1') reduces to

$$(aRM_2 - bSM_1)(Pc'N_2 - Qd'N_1) - RSPQ\xi^2M_3^2(b-a)(d'-c')$$

$$= -RS(b-a)\frac{\rho_L\omega^2}{T}\tan Th[\xi^2M_3^2(d'Q - Pc') - (d'QN_1 - Pc'N_2)]. \tag{2.39}$$

This is the frequency equation for Rayleigh waves in microstretch elastic half space with liquid layers.

If we neglect the liquid layers, then the problem reduces to Rayleigh waves in microstretch elastic half space. To obtain the Rayleigh wave equation in microstretch elastic half-space, we put $\rho_L = 0$ into equation (2.39), we have

$$(aRM_2 - bSM_1)(Pc'N_2 - Qd'N_1) = RSPQ\xi^2 M_3^2(b-a)(d'-c'). \tag{2.40}$$

Further, if we neglect the microstretch effect, then the problem reduces to Rayleigh waves in micropolar elastic half-space. Thus by putting $\lambda_0 = \alpha_0 = \lambda_1 = b/a = 0$ into equation (2.40), we get the following Rayleigh wave equation in micropolar half-space

$$M_2(Pc'N_2 - Qd'N_1) = -SPQ\xi^2 M_3^2(d'-c'). \tag{2.41}$$

This equation coincides with the Rayleigh wave frequency equation in a micropolar elastic half-space earlier obtained by De and Sengupta (1974).

Also, If we again neglect the micropolar effect, we shall obtain Rayleigh wave equation in a uniform elastic half space. By putting $K = d'/c' = 0$ into equation (2.41), we get

$$\left(2 - \frac{c^2}{\beta^2}\right)^2 = 4\left(1 - \frac{c^2}{\alpha^2}\right)^{1/2}\left(1 - \frac{c^2}{\beta^2}\right)^{1/2}, \tag{2.42}$$

which is a well known classical Rayleigh wave frequency equation in an elastic half space.

2.4.2 Antisymmetric vibrations:

(a) For waves long compared with the thickness of the plate, the quantity ξd is small, therefore, the quantities $Rd,\ Sd,\ Pd$ and Qd are small and we have $\tanh x \simeq x - \frac{x^3}{3}$. Using this into equation (2.33) for antisymmetric mode (with index '-1'), we obtain the following equation

$$(aM_2Y_1 - bM_1Y_2)(P^2c'N_2Z_1 - Q^2d'N_1Z_2) - P^2Q^2\xi^2M_3^2(b-a)(d'-c')Z_1Z_2$$

$$= -(b-a)\frac{\rho_L\omega^2}{Td}\tan Th[\xi^2M_3(Q^2d'Z_2 - P^2c'Z_1) - (Q^2d'N_1Z_2 - P^2c'N_2Z_1)], \tag{2.43}$$

where

$$Y_1 = 1 - (Sd)^2/3, \quad Y_2 = 1 - (Rd)^2/3, \quad Z_1 = 1 - (Pd)^2/3, \quad Z_2 = 1 - (Qd)^2/3.$$

If we neglect the liquid layer, then the above equation reduces to (by putting $\rho_L = 0$)

$$(aM_2Y_1 - bM_1Y_2)(P^2c'N_2Z_1 - Q^2d'N_1Z_2) = P^2Q^2\xi^2M_3^2(b-a)(d'-c')Z_1Z_2. \quad (2.44)$$

Further, if we neglect the microstretch effect from the plate, then the equation (2.44) reduces to the following after putting $\lambda_0 = \alpha_0 = \lambda_1 = 0$ and $b/a = 0$

$$M_2\left(1 - \frac{(Sd)^2}{3}\right)\left(\frac{c'N_2}{Q^2Z_2} - \frac{d'N_1}{P^2Z_1}\right) = \xi^2M_3^2(c'-d'), \quad (2.45)$$

where $M_2 = -\lambda\xi^2 + (\lambda + 2\mu + K)S^2$. This equation is same as obtained by Nowacki and Nowacki (1969) for the corresponding problem.
If we remove micropolar effect from the plate, then by putting $K = 0$ and $d'/c' = 0$, the equation (2.45) reduces to

$$c^2 = \frac{4}{3}(\xi d)^2\beta^2\left(1 - \frac{\beta^2}{\alpha^2}\right), \quad (2.46)$$

which coincides with the equation of classical elasticity for the relevant problem as given in Ewing et al. (1957).
(b) For very short waves compared with the thickness of the plate, the frequency equation (2.33) for antisymmetric (with index '-1') modes of vibrations can be reduced to equation (2.39), in a similar way as done in case of symmetric vibrations.

2.5 Special cases

(i) If we neglect the presence of liquid layers from both sides of the plate, then we shall be left with the problem of wave propagation in a microstretch plate with free faces. To do this, we shall put $\rho_L = 0$ into equation (2.33). The reduced frequency equations for symmetric (with index '+1') and antisymmeric (with index '-1') modes of vibrations are given by

$$[aRM_2(\coth Sd)^{\pm 1} - bSM_1(\coth Rd)^{\pm 1}][Pc'N_2(\coth Pd)^{\pm 1} - Qd'N_1(\coth Qd)^{\pm 1}]$$

$$-(b-a)(d'-c')\xi^2 M_3^2 RSPQ(\coth Qd \coth Pd)^{\pm 1} = 0, \tag{2.47}$$

(ii) When microstretch effect is neglected from the plate, we shall be left with the problem of Lamb wave propagation in micropolar plate bordered with liquid layers. In this case, we substitute $\lambda_0 = \lambda_1 = \alpha_0 = 0$ and $b/a = 0$ into equation (2.33) to obtain the following frequency equations for symmetric (with index '+1') and antisymmetric (with index '-1') modes

$$(\coth Sd)^{\pm 1}[-\lambda\xi^2 + (\lambda + 2\mu + K)S^2][(\mu\xi^2 + (\mu + K)P^2 - Kc')d'Q(\coth Qd)^{\pm 1}$$

$$-(\mu\xi^2+(\mu+K)Q^2-Kd')c'P(\coth Pd)^{\pm 1}]-\xi^2 PQS(2\mu+K)^2(d'-c')(\coth Qd \coth Pd)^{\pm 1}$$

$$= \rho_L\omega^2 \tan Th\left(\frac{S}{T}\right)[(\mu\xi^2 + (\mu + K)P^2 - Kc')Qd'(\coth Qd)^{\pm 1} - c'P[\mu\xi^2 + (\mu + K)Q^2$$

$$-Kd'](\coth Pd)^{\pm 1} - \xi^2(2\mu + K)[Pc'(\coth Pd)^{\pm 1} - Qd'(\coth Qd)^{\pm 1}]] \tag{2.48}$$

These equations exactly match with the equations (30) and (31) of Tomar (2002) apart from notations.

Further, if we neglect the presence of liquid layers, we shall be left with the problem of wave propagation in a micropolar plate with free boundaries. For this, putting $\rho_L = 0$ into equation (2.48), we obtain

$$(\coth Sd)^{\pm 1}[-\lambda\xi^2+(\lambda+2\mu+K)S^2][(\mu\xi^2+(\mu+K)P^2-Kc')d'Q(\coth Qd)^{\pm 1}-(\mu\xi^2+(\mu+K)Q^2$$

$$-Kd')c'P(\coth Pd)^{\pm 1}] - \xi^2 PQS(2\mu + K)^2(d' - c')(\coth Qd \coth Pd)^{\pm 1} = 0, \tag{2.49}$$

which is the frequency equation corresponding to symmetric (with index '+1') and antisymmetric (with index '-1') modes for Lamb wave propagation in a micropolar elastic plate with free boundaries.

(iii) When $h \to \infty$, then $\tan Th \to \imath$ and the equation (2.33) corresponding to symmetric (with index +1) and antisymmetric (with index -1) modes, reduces to

$$[aRM_2(\coth Sd)^{\pm 1} - bSM_1(\coth Rd)^{\pm 1}][Pc'N_2(\coth Pd)^{\pm 1} - Qd'N_1(\coth Qd)^{\pm 1}]$$

$$-(b-a)(d'-c')\xi^2 M_3^2 RSPQ(\coth Qd \coth Pd)^{\pm 1}$$

$$= -RS(b-a)\imath\frac{\rho_L\omega^2}{T}[\xi^2 M_3[Qd'(\coth Qd)^{\pm 1}$$

$$-c'P(\coth Pd)^{\pm 1}] - [Qd'N_1(\coth Qd)^{\pm 1} - c'PN_2(\coth Pd)^{\pm 1}]]. \tag{2.50}$$

Equation (2.50) is the dispersion equation for symmetric (with index '+1') and anti-symmetric (with index '-1') modes of leaky Lamb waves in a microstretch elastic plate bordered with identical inviscid liquid half-space on both sides.

(iv) When microstretch and micropolar effects are neglected from the plate, then by putting $K = \alpha_0 = \lambda_1 = \lambda_0 = 0$ and $b/a = 0$ and $d'/c' = 0$ into equation (2.33), we get the frequency equation corresponding to symmetric (with index '+1') and anti-symmetric (with index '-1') modes of Lamb wave propagation of classical elastic plate bordered with liquid layers, as

$$M_2N_2\,(\coth Sd \tanh Qd)^{\pm 1} - SQ\xi^2 M_3^2$$

$$= -S\frac{\rho_L\omega^2}{T}\tan Th\,(\tanh Qd)^{\pm 1}\,(\xi^2 M_3 - N_2). \tag{2.51}$$

These equations are the same as equations (5) and (6) of Wu and Zu (1992) for the corresponding problem, apart from notations.

(v) If we neglect the presence of liquid layers from the elastic plate of case (iv), we get the problem of Lamb wave propagation in classical elastic plate. By putting $\rho_L = 0$ in the frequency equation of case (iv), we obtain

$$M_2N_2\,(\coth Sd \tanh Qd)^{\pm 1} - SQ\xi^2 M_3^2 = 0, \tag{2.52}$$

which further reduces to the following well known equations corresponding to symmetric and antisymmetric modes, respectively

$$\left(2 - \frac{c^2}{c_2^2}\right)^2 \left(\frac{\tanh Qd}{\tanh Sd}\right)^{\pm 1} = 4\sqrt{\left(1 - \frac{c^2}{c_1^2}\right)\left(1 - \frac{c^2}{c_2^2}\right)}, \tag{2.53}$$

where $c_1^2 = (\lambda+2\mu)/\rho$ and $c_2^2 = \mu/\rho$. These equations exactly match with those obtained by Lamb (1917) in the classical case.

It can be verified that if we neglect the micropolar, microstretch and liquid layers from the problem, then equation (2.34) reduces to equation (2.53) for Lamb waves in elastic plate given by Lamb (1917).

2.6 Numerical results and discussions

Frequency equations for Rayleigh-Lamb waves are solved numerically for a particular model using functional iteration method. Following values of relevant elastic parameters have been taken.

Symbol	Value
λ	$7.583 \times 10^{11}\ dyne/cm^2$
μ	$6.334 \times 10^{11}\ dyne/cm^2$
K	$0.0149 \times 10^{11}\ dyne/cm^2$
λ_0	$0.773 \times 10^{11}\ dyne/cm^2$
λ_1	$0.030 \times 10^{11}\ dyne/cm^2$
α_0	$0.085 \times 10^{11}\ dyne$
γ	$2.89 \times 10^{11}\ dyne$
j	$0.000625\ cm^2$
ρ	$1.2\ gm/cm^3$
d	$1.5\ cm$
ρ_L	$1.1\ gm/cm^3$
λ_L	$0.245 \times 10^{11}\ dyne/cm^2$
h	$0.5\ cm$

We have computed the non-dimensional phase velocity (c/V), $(V = \sqrt{c_1^2 + c_3^2})$ at different values of non-dimensional wavenumber (ξd). The values of velocity ratio (c/V) are computed from frequency equation (2.33) obtained by using the boundary conditions given in Set-I and equation (2.34) obtained by using the boundary conditions given by Set-II for different values of wavenumber $'\xi d'$. For real values of wavenumber, the real values of phase velocity are found for microstretch plate bordered with liquid layers and micropolar plate bordered with liquid layers. It is found that in the case of microstretch plate with free boundaries and in case of micropolar plate with free boundaries, the waves are attenuated. The results obtained for symmetric mode (s-mode) and antisymmetric mode (a-mode) are depicted graphically through Figures

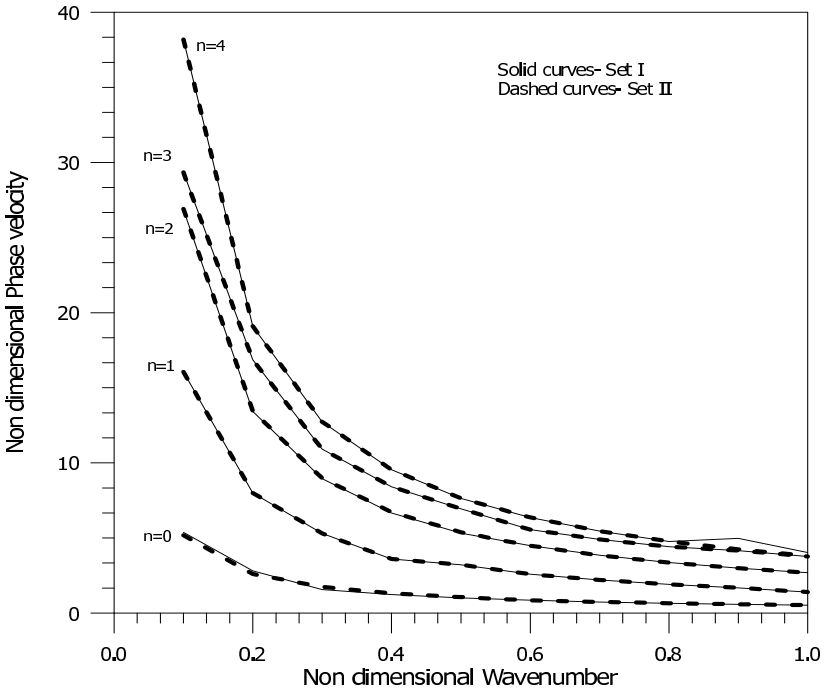

Figure 2.2: Comparison of symmetric modes of microstretch plate bordered with liquid layers for Set-I and for Set-II

2.2-2.18.

In Figure 2.2, we have depicted the dispersion curves corresponding to fundamental, first, second, third and fourth symmetric modes of Rayleigh-Lamb wave propagation of microstretch plate bordered with liquid layers obtained by using frequency equation due to Set-I and Set-II. It is clear from this figure that the dispersion curves for symmetric modes do not differ significantly. Thus we conclude that we can choose any one set of the boundary conditions mentioned earlier.

In Figure 2.3, we have depicted the dispersion curves for first five symmetric modes of vibrations for microstretch plate bordered with liquid layers and with free boundaries. For given real value of the wavenumber, the value of phase velocity is found real for microstretch plate bordered with liquid layers, while for microstretch plate with free boundaries, the value of phase velocity is found complex. In this figure, we have depicted the real part of phase velocity for both the curves. It is clear from the figure that the phase velocity for microstretch plate with free boundaries is greater than the phase velocity for microstretch plate bordered with liquid layers. We conclude that presence of liquid layers results in decrease the phase velocity of Rayleigh-Lamb wave propagation in the symmmetric modes.

In Figure 2.4, we have depicted the dispersion curves for first five symmetric modes

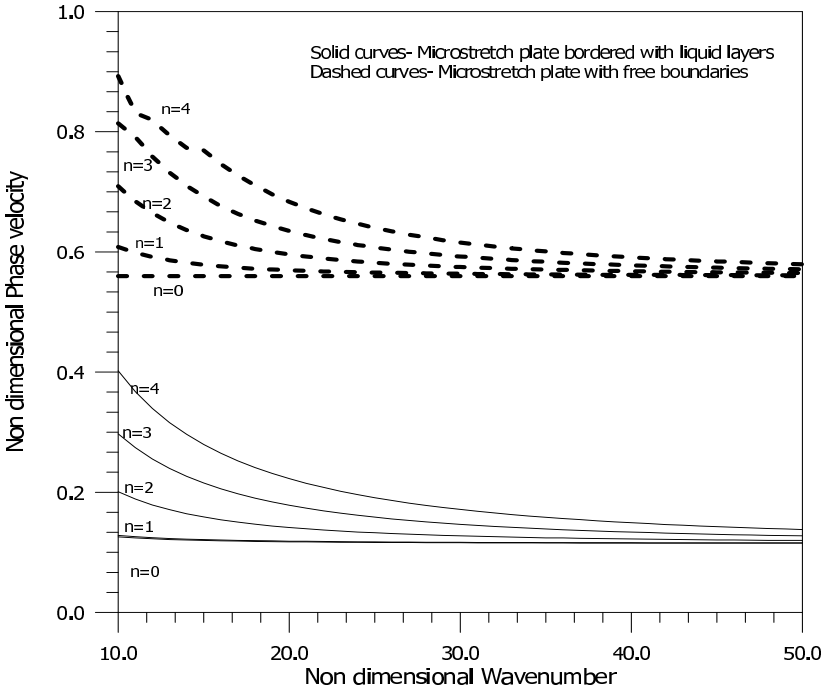

Figure 2.3: Comparison of real parts of symmetric modes of microstretch plate bordered with liquid layers and with free boundaries.

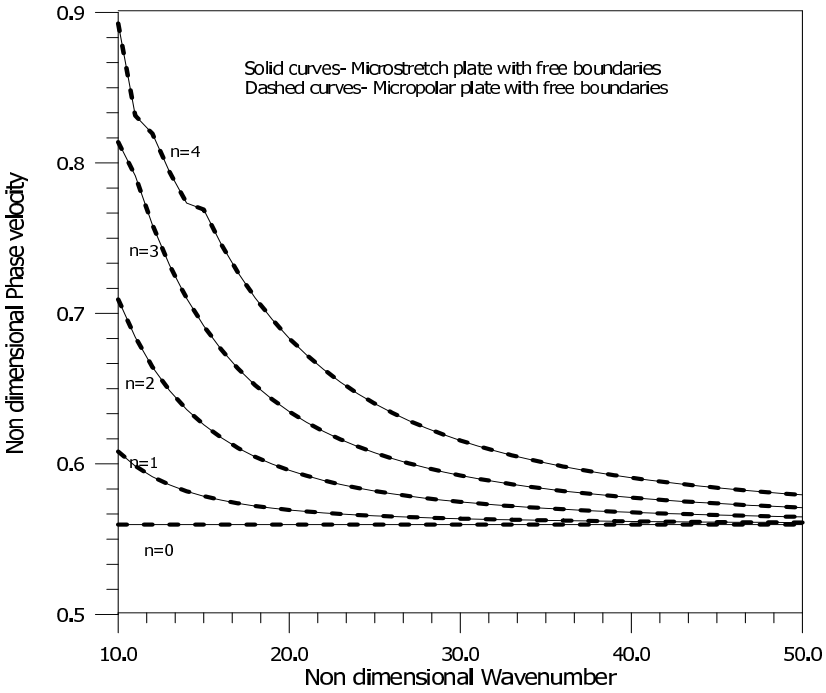

Figure 2.4: Comparison of real parts of symmetric modes of microstretch plate and micropolar plate with free boundaries.

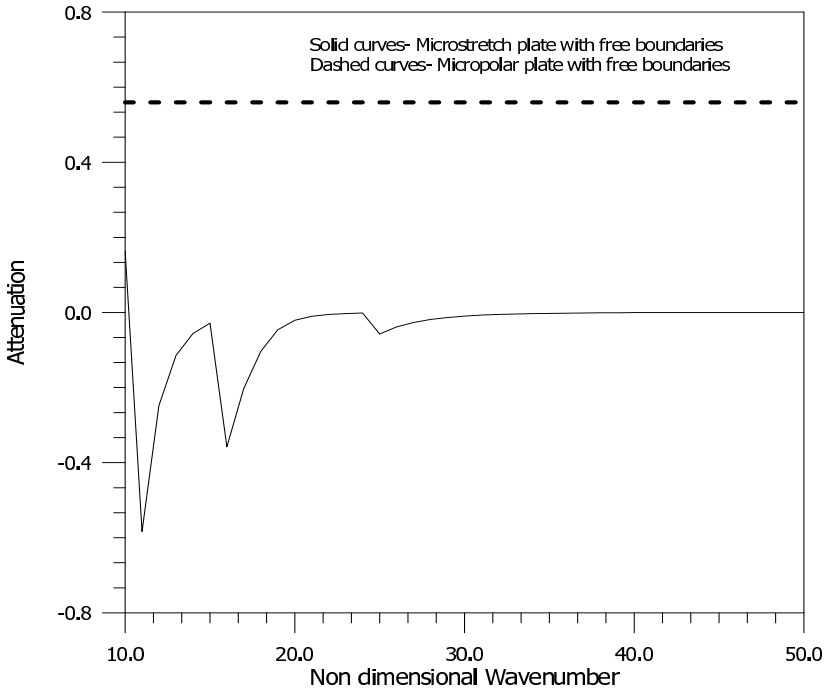

Figure 2.5: Comparison of attenuation in symmetric fundamental mode of microstretch plate and micropolar plate with free boundaries.

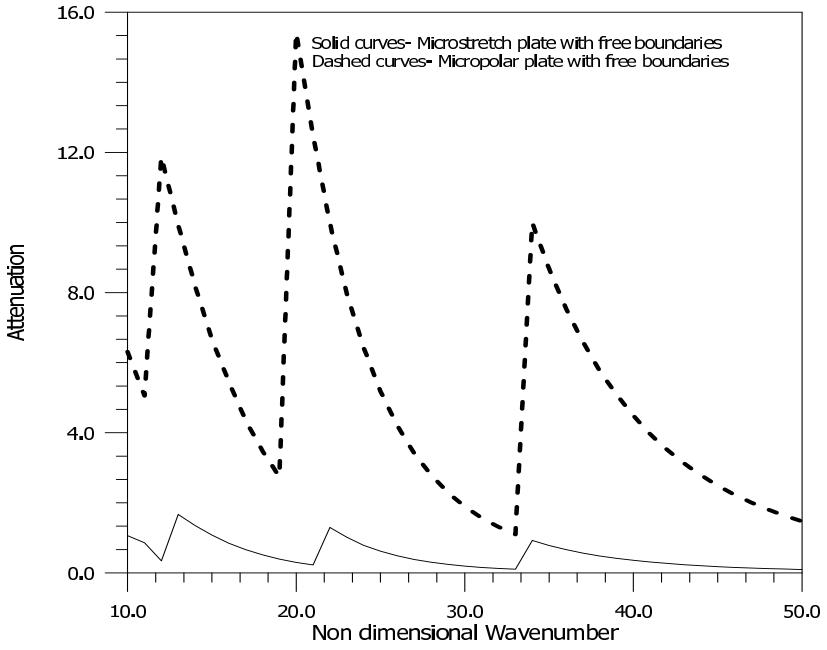

Figure 2.6: Comparison of attenuation in symmetric first mode of microstretch plate and micropolar plate with free boundaries.

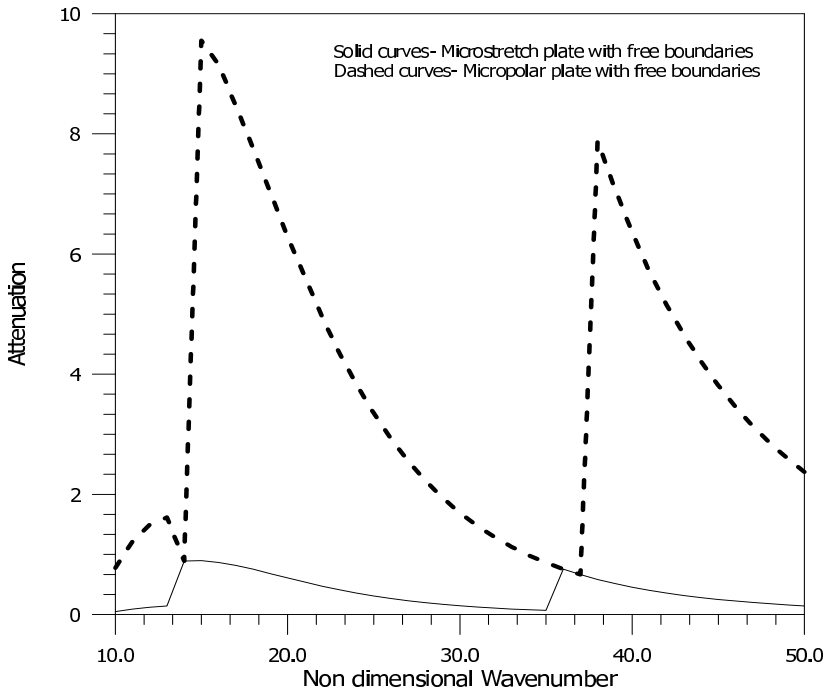

Figure 2.7: Comparison of attenuation in symmetric second mode of microstretch plate and micropolar plate with free boundaries.

of vibrations in microstretch plate and micropolar plate with free boundaries for real phase velocity. It is clear from the above figure that there is no significant difference between these two curves. Thus, no considerable effect of microstretch property is noticed on the symmetric modes of propagation.

Figures 2.5-2.9 depict the variation of attenuation coefficient for fundamental, first, second, third and fourth symmetric modes of microstretch plate and micropolar plate with free boundaries respectively. Curves for microstretch plate with free boundaries are represented by solid lines, while the curves for micropolar plate are represented by dotted lines. To plot the variation of attenuation coefficient, we have multiplied the original value by a factor of 10^6. It is clear that there is significant effect of microstretch property on the attenuation of the symmetric modes of propagation on dispersion curves. The presence of microstretch property results in decrease in attenuation of waves for symmetric modes.

Figure 2.10 depicts the dispersion curves from fundamental mode to fourth mode of antisymmetric modes of Rayleigh-Lamb wave propagation for microstretch plate bordered with liquid layers obtained by using equations due to Set-I and Set-II. It is concluded that for these two sets of boundary conditions, the curves are same. We

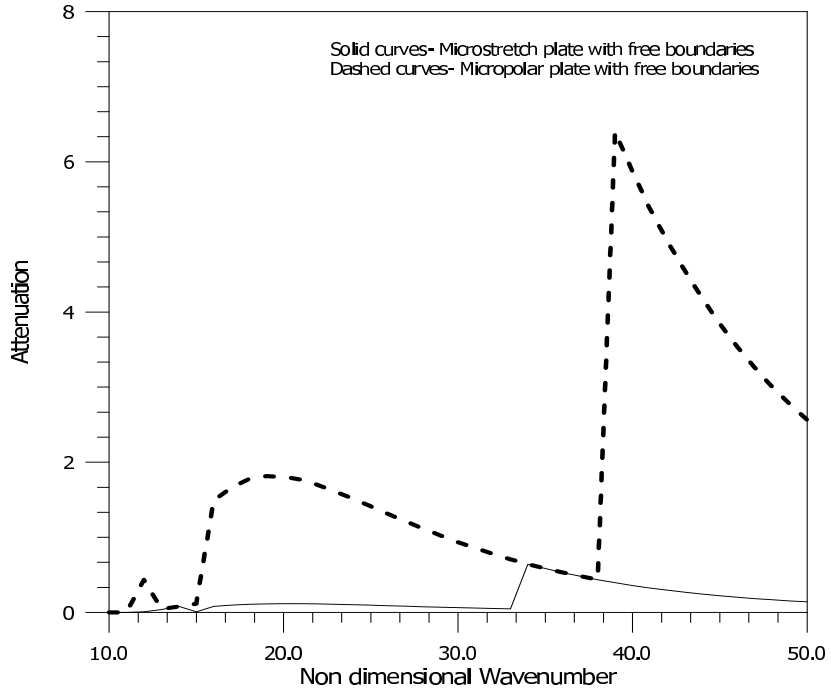

Figure 2.8: Comparison of attenuation in symmetric third mode of microstretch plate and micropolar plate with free boundaries.

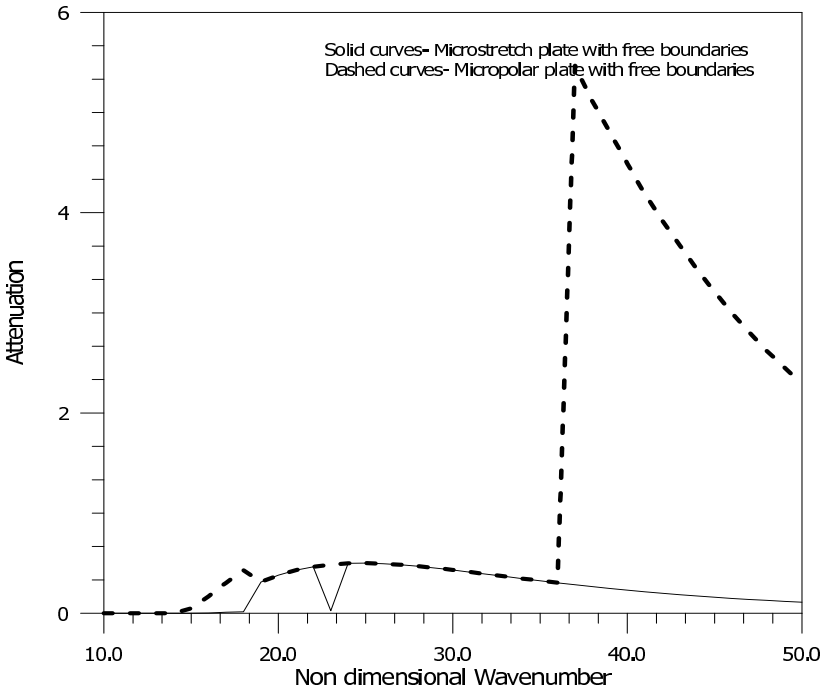

Figure 2.9: Comparison of Attenuation in Symmetric fourth mode of Microstretch plate and Micropolar plate with free boundaries.

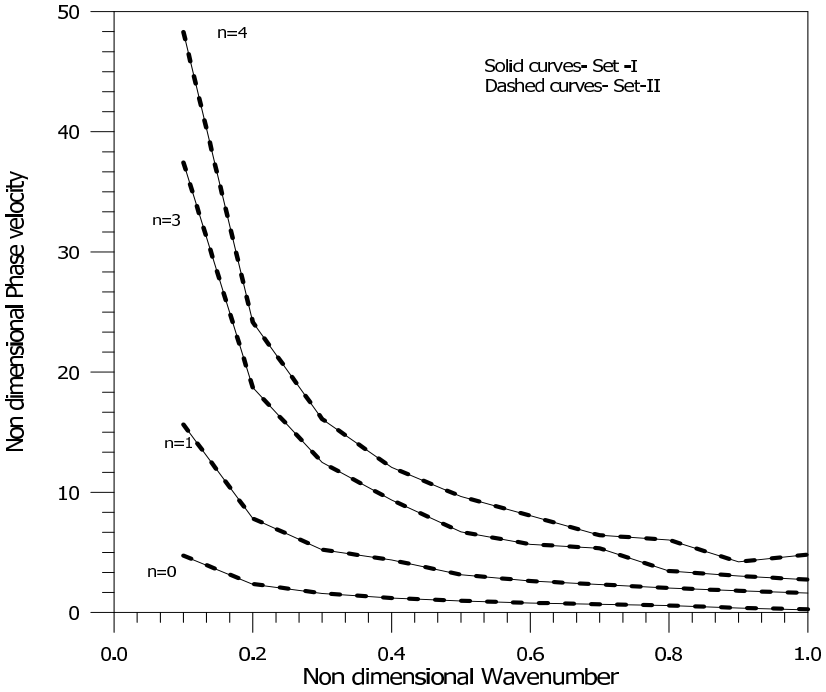

Figure 2.10: Comparison of antisymmetric modes of microstretch plate bordered with liquid layers for Set-I and for Set-II.

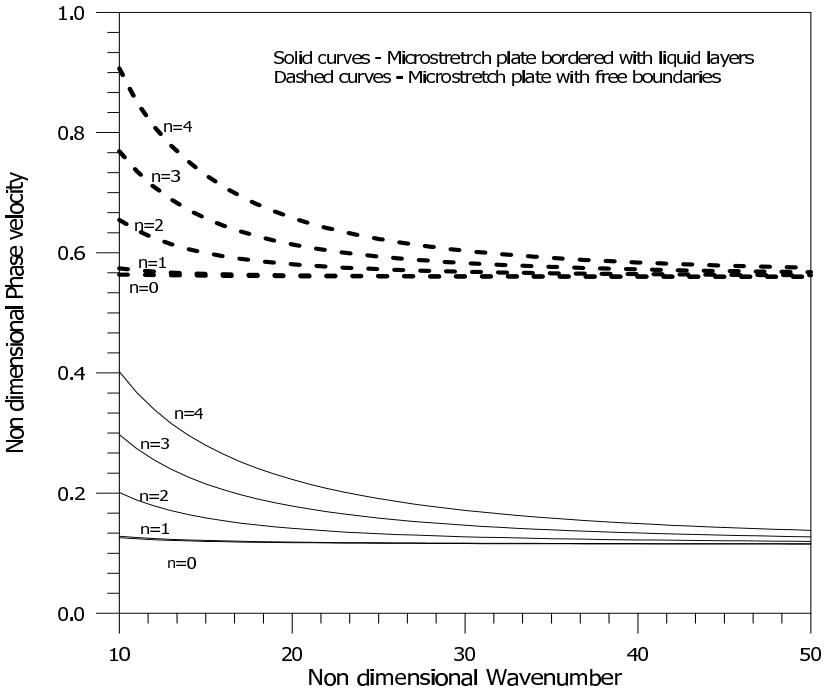

Figure 2.11: Comparison of antisymmetric modes of microstretch plate bordered with liquid layers and with free boundaries.

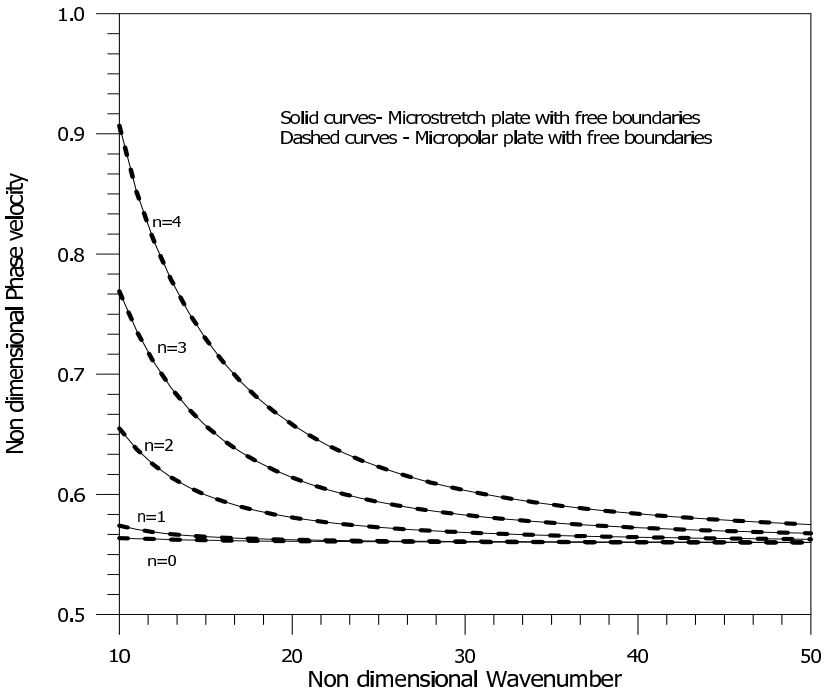

Figure 2.12: Comparison of real parts of antisymmetric modes of microstretch plate and micropolar plate with free boundaries.

conclude that there is no significant difference in the phase velocity of Lamb waves propagation for these two sets of boundary conditions in antisymmetric modes.

Figure 2.11, we have depicted the dispersion curves of fundamental to fourth modes of antisymmetric vibrations in microstretch plate bordered with and without liquid layers. It is found that non-dimensional phase velocity of microstretch plate with free boundaries is more than that for microstretch plate bordered with liquid layers in the antisymmetric modes of propagation.

Figure 2.12 depicts the dispersion curves for fundamental to fourth antisymmetric modes for microstretch plate and micropolar plate with free boundaries. It is noted that there is no significant difference between these two curves. Hence, we conclude that there is no effect of microstretch property on real part of the phase velocity for microstretch plate with free boundaries in antisymmetric modes.

Figures 2.13-2.17 depict the attenuation part of the phase velocity for fundamental to fourth antisymmetric modes of Rayleigh-Lamb wave propagation of microstretch plate and micropolar plate with free boundaries. Here, the solid curves and dotted curves correspond to microstretch plate and micropolar plate respectively. The attenuation coefficient is plotted after multiplying the original value of imaginary part of the phase

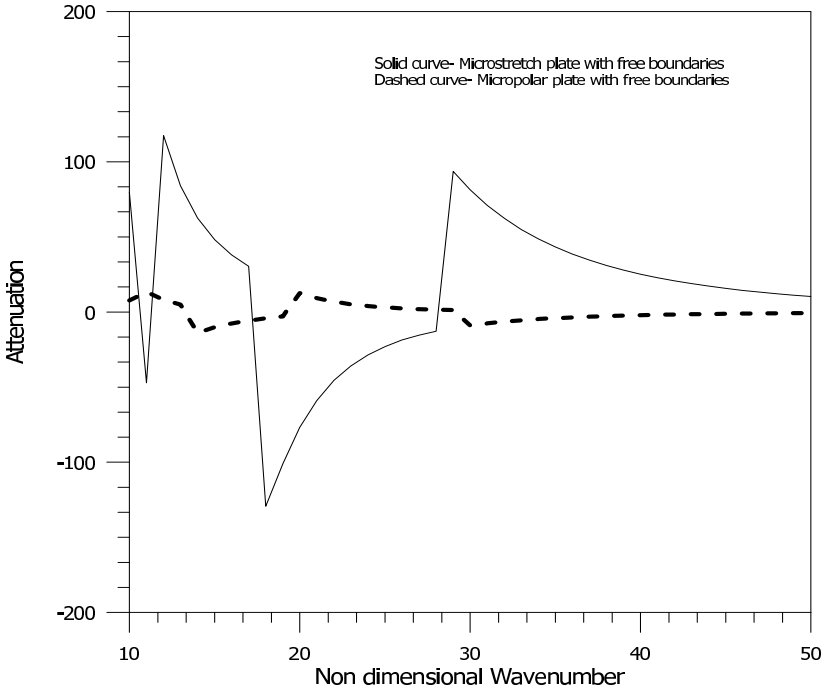

Figure 2.13: Comparison of attenuation in antisymmetric fundamental mode of microstretch plate and micropolar plate with free boundaries.

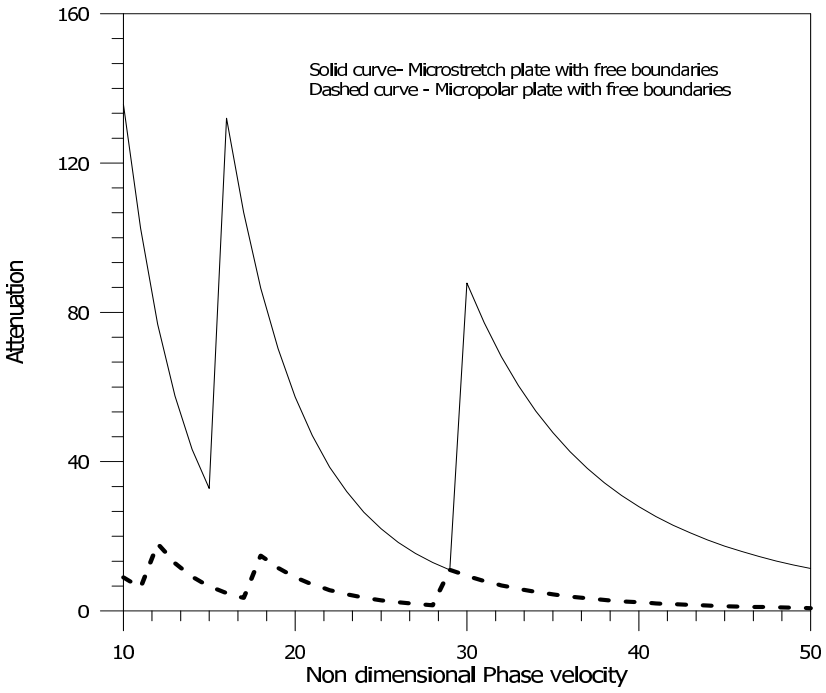

Figure 2.14: Comparison of attenuation in antisymmetric first mode of microstretch plate and micropolar plate with free boundaries.

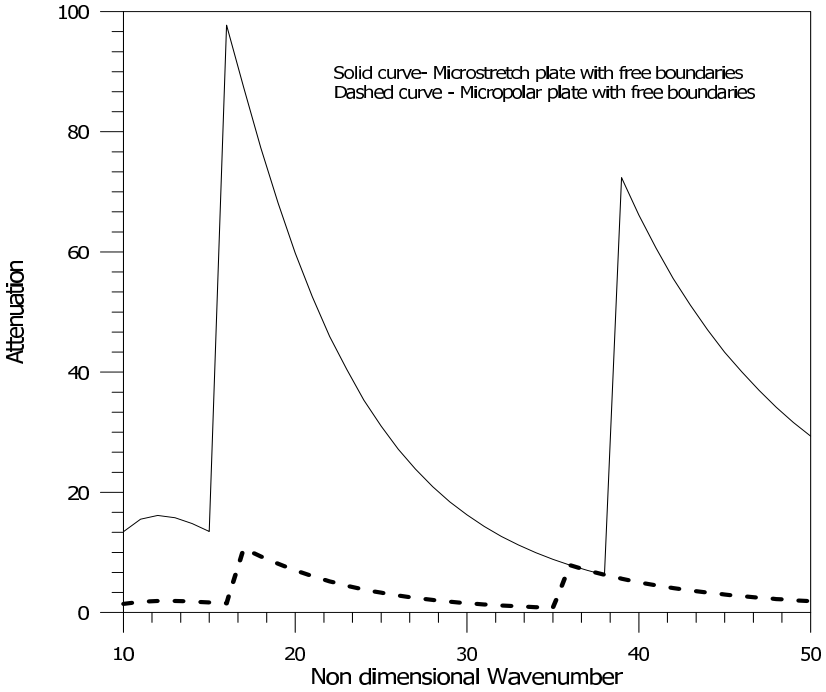

Figure 2.15: Comparison of attenuation in antisymmetric second mode of microstretch plate and micropolar plate with free boundaries.

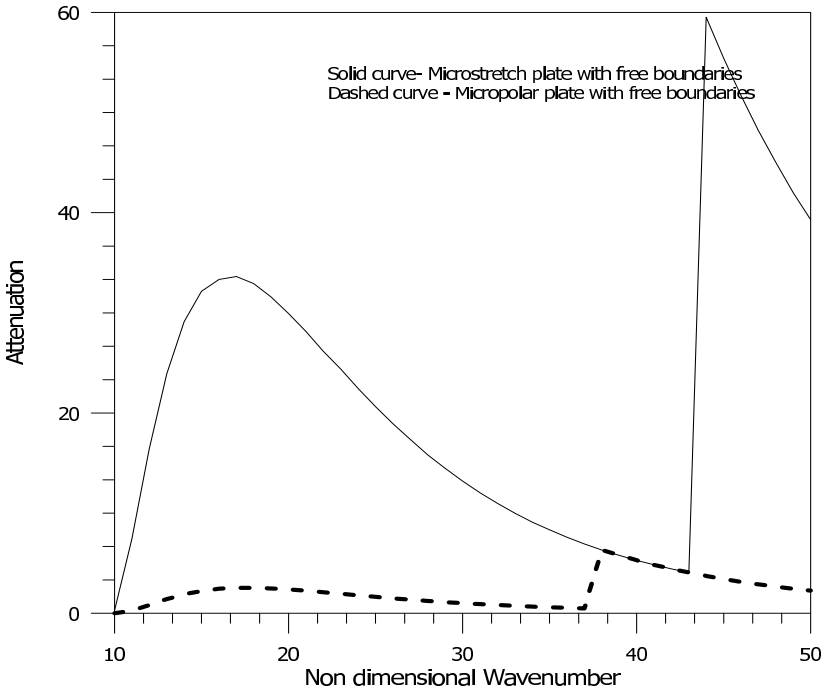

Figure 2.16: Comparison of attenuation in antisymmetric third mode of microstretch plate and micropolar plate with free boundaries.

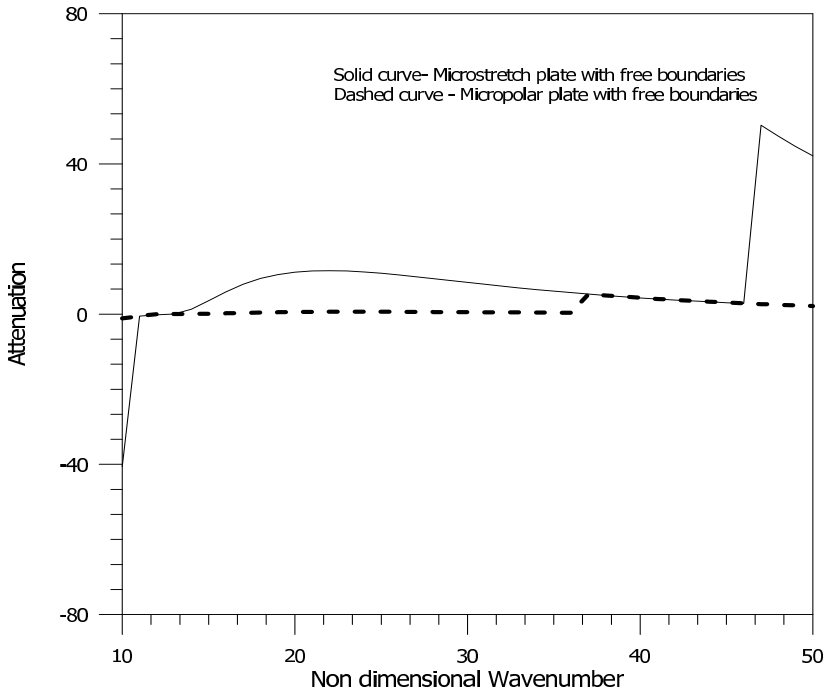

Figure 2.17: Comparison of attenuation in antisymmetric fourth mode of microstretch plate and micropolar plate with free boundaries.

velocity by a factor of 10^6. It is observed that attenuation is strongly affected by the presence of microstretch in antisymmmetric modes of propagation. Moreover, the presence of microstretch property results in increase in attenuation for all these five modes.

Figure 18 depicts the dispersion curves for fundamental symmetric mode at different thickness of liquid layers. We see that as the thickness of the liquid layers increases, the phase velocity for fundamental symmetric mode decreases.

2.7 Conclusions

In this Chapter, we have described the effect of microstretch property on the propagation of Rayleigh-Lamb waves in microstretch plate cladded with inviscid liquid layers. Two sets of boundary conditions at the interface of plate and liquid layers are possible. Dispersion equations for symmetric and antisymmetric modes are derived by employing both these sets of boundary conditions. We conclude that

(a) The choice on the boundary conditions at the interface of plate and liquid layers is arbitrary. Results obtained from both the sets of boundary conditions give same dispersion curves for Rayleigh-Lamb wave propagation in symmetric and antisymmetric

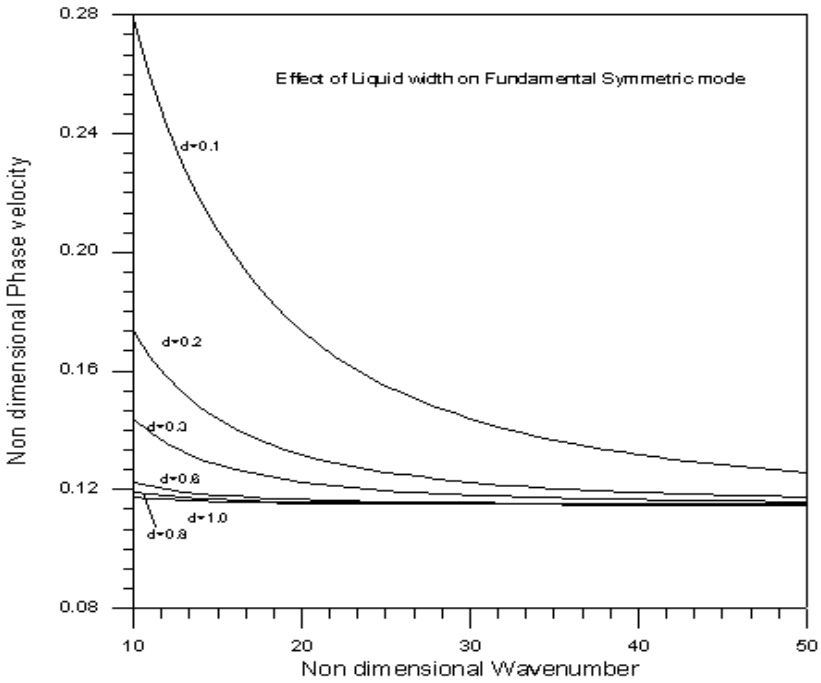

Figure 2.18: Comparison of Symmetric Fundamental mode at different width of cladded liquid layers.

modes.

(b) It is noted that the presence of cladded liquid layers in microstretch plate decreases the phase velocity for both symmetric and antisymmetric modes of Rayleigh-Lamb wave propagation. It is also observed that the frequency equations give real phase velocity for given real value of wavenumber when the plate is cladded with liquid layers, otherwise real values of non-dimensional wavenumber gives complex value of non-dimensional phase velocity. Thus, the waves are non-attenuated when plate is cladded with liquid layers, while waves are found to be attenuated when both faces of plate are free. This may be due to small values of microstretch parameters considered here.

(c) We also noticed that there is no significant effect of microstretch property on symmetric and antisymmetric modes of dispersion curves for real phase velocity on microstretch plate with free boundaries. The curves for real phase velocity for microstretch plate with free boundaries are same as the dispersion curves for real phase velocity of micropolar plate with free boundaries.

(d) The attenuation is found to be highly affected by the presence of microstretch property in the plate with free boundaries for both symmetric and antisymmetric modes.

Chapter 3

Propagation of Stoneley waves at an interface between two microstretch elastic half-spaces[2]

3.1 Introduction

Stoneley (1924) investigated the possible existence of waves, which are similar to surface waves and propagating along the plane interface between two distinct uniform elastic solid half-spaces in perfect contact and they are universally known by his name. Stoneley waves can propagate on interfaces between either two solid media or solid and liquid media. These waves are the harmonic waves and attenuate exponentially with distance normal to the interface in both the half-spaces, provided the range of the elastic constants of the two solids lie within some suitable limits. Stoneley obtained the frequency equation for propagation of these waves and showed that such interfacial waves can exist only if the velocity of distortional waves in the two half-spaces is approximately same. Since then a number of problems concerning the propagation of Stoneley waves along the solid − solid and fluid − solid boundary have been discussed by several researchers, e.g., Murty (1975a, b, 1976), Hsieh et al. (1991), Abbudi and Barnett (1990), Goda (1992), Tajuddin (1995), Ashour (1999), Abd-Alla (1999), Abd-Alla and Ahmed (2003) among several others. Murty (1975b) discussed the wave

[2] ***Journal of Vibration and Control,* 12(9)**, 995-1009(2006).

propagation at an unbonded interface between two elastic half-spaces. He derived the explicit condition for the existence of Stoneley waves when the two half-spaces are incompressible or Poisson solids whose elastic constants and material densities are nearly equal. Tajuddin (1995) studied the corresponding problem at unbonded interface between two micropolar elastic solid half-spaces. In the present chapter, we have investigated the propagation of Stoneley waves at an unbonded/bonded interface between two microstretch elastic solid half-spaces. Frequency equations for Stoneley wave propagation are derived. It is found that Stoneley waves are dispersive in microstretch medium and there is a significant effect of microstretch property on dispersion curve. The results of some earlier workers have been reduced as particular cases from the present formulation.

3.2 Formulation of problem

We consider two linear isotropic homogeneous microstretch elastic solid half spaces, namely, H_1 and H_2 with different elastic properties. Introducing the Cartesian axes such that the upper half-space H_2 occupies the region $-\infty < z \leq 0$ and the lower half space H_1 occupies the region $0 \leq z < \infty$. The $x-$ axis is taken along the plane of separation of half-spaces H_1 and H_2 and the z-axis is taken perpendicular to the plane of separation directed vertically downward into the lower half space H_1.

Now, considering the equations of motion for microstretch elastic medium given by (1.125) -(1.27) and adopting the procedure followed in Chapter-2 to solve these equations of motion, we can arrive at equations (2.10) and (2.11). The time harmonic solutions of these equations for the waves propagating along $x-$ direction, are given by

$$L = (Ae^{Rz} + Be^{-Rz} + Ce^{Sz} + De^{-Sz})e^{\iota(\xi x - \omega t)}, \tag{3.1}$$

$$\psi = \{a(Ae^{Rz} + Be^{-Rz}) + b(Ce^{Sz} + De^{-Sz})\}e^{\iota(\xi x - \omega t)}, \tag{3.2}$$

$$M = (Ee^{Pz} + Fe^{-Pz} + Ge^{Qz} + He^{-Qz})e^{\iota(\xi x - \omega t)}, \tag{3.3}$$

$$\phi = \{c'(Ee^{Pz} + Fe^{-Pz}) + d'(Ge^{Qz} + He^{-Qz})\}e^{\iota(\xi x - \omega t)}, \tag{3.4}$$

where the quantities $A,\ B,\ C,\ D,\ E,\ F,\ G$ and H are unknown and the expressions of the coupling parameters $a,\ b,\ c',\ d'$ and $R,\ S,\ P,\ Q$ are defined in Chapter-2, just after equation (2.15). The quantities with subscript 1 correspond to the half-space H_1 and the quantities with subscript 2 correspond to the half space H_2, i.e., the constants $\lambda_i,\ \mu_i$(Lame's parameters), $K_i,\ \gamma_i$(micropolar parameters), $\lambda_{0i},\ \lambda_{1i},\ \alpha_{0i}$ (microstretch parameters), j_i(micro-inertia) and ρ_i(densities) denote the material moduli in $H_i,\ (i = 1, 2)$. We will discuss Stoneley mode at bonded and unbonded interface between H_1 and H_2 half spaces.

In order to discuss Stoneley waves at the interface $z = 0$, we take the following appropriate solutions of equations (2.1)-(2.4). In the lower half space H_1, the expressions of relevant potentials are taken as

$$L_1 = (Be^{-R_1 z} + De^{-S_1 z})e^{\imath(\xi x - \omega t)}, \tag{3.5}$$

$$\psi_1 = \{a_1 Be^{-R_1 z} + b_1 De^{-S_1 z}\}e^{\imath(\xi x - \omega t)}, \tag{3.6}$$

$$M_1 = (Fe^{-P_1 z} + He^{-Q_1 z})e^{\imath(\xi x - \omega t)}, \tag{3.7}$$

$$\phi_1 = \{c_1' Fe^{-P_1 z} + d_1' He^{-Q_1 z}\}e^{\imath(\xi x - \omega t)}, \tag{3.8}$$

and in the upper half-space H_2, we shall take the expressions of relevant potentials as

$$L_2 = (Ae^{R_2 z} + Ce^{S_2 z})e^{\imath(\xi x - \omega t)}, \tag{3.9}$$

$$\psi_2 = \{a_2 Ae^{R_2 z} + b_2 Ce^{S_2 z}\}e^{\imath(\xi x - \omega t)}, \tag{3.10}$$

$$M_2 = (Ee^{P_2 z} + Ge^{Q_2 z})e^{\imath(\xi x - \omega t)}, \tag{3.11}$$

$$\phi_2 = \{c_2' Ee^{P_2 z} + d_2' Ge^{Q_2 z}\}e^{\imath(\xi x - \omega t)}, \tag{3.12}$$

where $Re(R_i, S_i, P_i, Q_i) > 0$. The expressions of the quantities $a_i,\ b_i,\ c_i',\ d_i',\ P_i,\ Q_i,\ R_i$ and S_i can be written from the expressions of quantities $a,\ b,\ c',\ d',\ P,\ Q,\ R$ and S given in Chapter-2. Their expressions can be written easily by inducting the subscript i appropriately, e.g., $a_i = -\{(\lambda_i + 2\mu_i + K_i)(-\xi^2 + R_i^2) + \rho_i\omega^2\}/\lambda_{0i}$, etc.

3.3 Boundary conditions

Followings are the appropriate boundary conditions at unbonded interface and at bonded interface between the half-space H_1 and the half-space H_2:
(A) At an unbonded interface, we assume that the interface is frictionless, so that shear traction is absent and shear displacement is discontinuous at the interface. Thus for an unbonded interface, there is continuity of normal component of the displacement vector and stress tensor, couple stress tensor, microrotation, scalar microstretch and microstretch tensor, while shear components of stress tensor vanish across the interface.
(B) At a bonded interface, we assume that both the half-spaces are in perfect contact. Thus, for a bonded interface, the components of displacement vector, microrotation vector, scalar microstretch, stress tensor, couple stress tensor and microstretch tensor at the interface should be continuous.
Mathematically, these boundary conditions at $z = 0$ can be expressed as

$$[\tau_{zz}]_1 = [\tau_{zz}]_2, \quad [m_{zy}]_1 = [m_{zy}]_2, \quad [m_z]_1 = [m_z]_2, \quad w_1 = w_2, \quad \psi_1 = \psi_2, \quad \phi_1 = \phi_2$$

and
$$\begin{cases} [\tau_{zx}]_1 = 0, \quad [\tau_{zx}]_2 = 0, & \text{for an unbonded interface,} \\ [\tau_{zx}]_1 = [\tau_{zx}]_2, \quad u_1 = u_2, & \text{for a bonded interface.} \end{cases}$$

From (1.128) - (1.130), the requisite components of stresses can be written as $(i = 1, 2)$

$$[\tau_{zz}]_i = \lambda_i \frac{\partial^2 L_i}{\partial x^2} + (\lambda_i + 2\mu_i + K_i)\frac{\partial^2 L_i}{\partial z^2} - (2\mu_i + K_i)\frac{\partial^2 M_i}{\partial x \partial z} + \lambda_{0i}\psi_i,$$

$$[\tau_{zx}]_i = (2\mu_i + K_i)\frac{\partial^2 L_i}{\partial x \partial z} - \mu_i \frac{\partial^2 M_i}{\partial x^2} + (\mu_i + K_i)\frac{\partial^2 M_i}{\partial z^2} - K_i\phi_i,$$

$$[m_{zy}]_i = \gamma_i \frac{\partial \phi_i}{\partial z}, \qquad [m_z]_i = \alpha_{0i}\frac{\partial \psi_i}{\partial z},$$

and using (3.5) - (3.12) into the above boundary conditions, one obtains eight homogeneous equations in eight unknowns, namely, A, B, C, D, E, F, G and H. For non-trivial solution of these equations, the determinant of the coefficient matrix should be equal to zero, that is,

$$|a_{ij}| = 0. \tag{3.13}$$

The non-vanishing entries of this determinantal equation are given by

$$a_{11} = \{-\lambda_2\xi^2+(\lambda_2+2\mu_2+K_2)R_2^2+\lambda_{02}a_2\},\ \ a_{12} = -\{-\lambda_1\xi^2+(\lambda_1+2\mu_1+K_1)R_1^2+\lambda_{01}a_1\},$$

$$a_{13} = \{-\lambda_2\xi^2+(\lambda_2+2\mu_2+K_2)S_2^2+\lambda_{02}b_2\},\ \ a_{14} = -\{-\lambda_1\xi^2+(\lambda_1+2\mu_1+K_1)S_1^2+\lambda_{01}b_1\},$$

$$a_{15} = -\imath\xi(2\mu_2 + K_2)P_2,\ \ a_{16} = -\imath\xi(2\mu_1 + K_1)P_1,\ \ a_{17} = -\imath\xi(2\mu_2 + K_2)Q_2,$$

$$a_{18} = -\imath\xi(2\mu_1 + K_1)Q_1,\ \ a_{25} = \gamma_2 c_2' P_2,\ \ a_{26} = \gamma_1 c_1' P_1,\ \ \ a_{27} = \gamma_2 d_2' Q_2,$$

$$a_{28} = \gamma_1 d_1' Q_1,\ \ a_{31} = \alpha_{02}a_2R_2,\ \ a_{32} = \alpha_{01}a_1R_1,\ \ a_{33} = \alpha_{02}b_2S_2,\ \ a_{34} = \alpha_{01}b_1S_1,$$

$$a_{41} = R_2,\ \ a_{42} = R_1,\ \ a_{43} = S_2,\ \ a_{44} = S_1,\ \ a_{45} = a_{47} = -\imath\xi,\ \ a_{46} = a_{48} = \imath\xi,$$

$$a_{51} = a_2,\ \ a_{52} = -a_1,\ \ a_{53} = b_2,\ \ a_{54} = -b_1,\ \ a_{65} = c_2',\ \ a_{66} = -c_1',\ \ a_{67} = d_2',\ \ a_{68} = -d_1',$$

the remaining entries for an unbonded interface are given by

$$a_{72} = -(2\mu_1 + K_1)\imath\xi R_1,\ \ a_{74} = -(2\mu_1 + K_1)\imath\xi S_1,\ \ a_{76} = \{\mu_1\xi^2 + (\mu_1 + K_1)P_1^2 - K_1c_1'\},$$

$$a_{78} = \{\mu_1\xi^2 + (\mu_1 + K_1)Q_1^2 - K_1d_1'\},\ \ a_{81} = (2\mu_2 + K_2)\imath\xi R_2,\ \ a_{83} = (2\mu_2 + K_2)\imath\xi S_2$$

$$a_{85} = \{\mu_2\xi^2 + (\mu_2 + K_2)P_2^2 - K_2c_2'\},\ \ a_{87} = \{\mu_2\xi^2 + (\mu_2 + K_2)Q_2^2 - K_2d_2'\},$$

while those for a bonded interface are given by

$$a_{71} = (2\mu_2+K_2)\imath\xi R_2,\ \ a_{72} = (2\mu_1+K_1)\imath\xi R_1,\ \ a_{73} = (2\mu_2+K_2)\imath\xi S_2,\ \ a_{74} = (2\mu_1+K_1)\imath\xi S_1,$$

$$a_{75} = \{\mu_2\xi^2 + (\mu_2 + K_2)P_2^2 - K_2c_2'\},\ \ a_{76} = -\{\mu_1\xi^2 + (\mu_1 + K_1)P_1^2 - K_1c_1'\},$$

$$a_{77} = \{\mu_2\xi^2 + (\mu_2 + K_2)Q_2^2 - K_2d_2'\},\ \ a_{78} = -\{\mu_1\xi^2 + (\mu_1 + K_1)Q_1^2 - K_1d_1'\},$$

$$a_{81} = a_{83} = \imath\xi,\ \ a_{82} = a_{84} = -\imath\xi,\ \ a_{85} = P_2,\ \ a_{86} = P_1,\ \ a_{87} = Q_2,\ \ a_{88} = Q_1.$$

Equation (3.13) represents the period equation for Stoneley wave propagation at unbonded/bonded interface between two dissimilar microstretch solid half-spaces. This equation is an implicit function of phase velocity and wavenumber. Hence, Stoneley waves are dispersive in nature. Analytically, no definite conclusion can be drawn regarding the behavior of phase velocity of Stoneley wave propagation and other characteristics from this equation. However, for very small values of parameters $\lambda_{01},\ \lambda_{02},\ K_1$ and K_2, a definite conclusion regarding phase velocity of Stoneley waves can be obtained. Neglecting the second and higher powers of the quantities $\lambda_{01},\ \lambda_{02},\ K_1$ and K_2, one can obtain (see Midya, 2004)

$$R_i = \sqrt{\xi^2 - \frac{3\rho_i j_i\omega^2 - 2\lambda_{1i}}{6\alpha_{0i}}},\quad S_i = \sqrt{\xi^2 - \frac{\rho_i\omega^2}{\lambda_i + 2\mu_i + K_i}},$$

$$P_i = \sqrt{\xi^2 - \frac{\rho_i j_i\omega^2 - 2K_i}{\gamma_i}},\quad Q_i = \sqrt{\xi^2 - \frac{\rho_i\omega^2}{\mu_i + K_i}},$$

and the entries a_{ij} reduce to

$$a_{11} = (2\mu_2 + K_2)\xi^2 - \rho_2\omega^2,\quad a_{12} = -\{(2\mu_1 + K_1)\xi^2 - \rho_1\omega^2\},\quad a_{13} = (2\mu_2 + K_2)\xi^2 - \rho_2\omega^2$$

$$a_{14} = -\{(2\mu_1 + K_1)\xi^2 - \rho_1\omega^2\},\quad a_{15} = -(2\mu_2 + K_2)\imath\xi P_2,\quad a_{16} = -(2\mu_1 + K_1)\imath\xi P_1,$$

$$a_{17} = -(2\mu_2 + K_2)\imath\xi Q_2,\quad a_{18} = -(2\mu_1 + K_1)\imath\xi Q_1,\quad a_{25} = \gamma_2 c_2' P_2,\quad a_{26} = \gamma_1 c_1' P_1,$$

$$a_{31} = \alpha_{02}a_2 R_2,\quad a_{32} = \alpha_{01}a_1 R_1,\quad a_{41} = R_2,\quad a_{42} = R_1,\quad a_{43} = S_2,\quad a_{44} = S_1,$$

$$a_{45} = a_{47} = -\imath\xi,\quad a_{46} = a_{48} = \imath\xi,\quad a_{51} = a_2,\quad a_{52} = -a_1,\quad a_{65} = c_2',\quad a_{66} = -c_1',$$

along with the following for an unbonded interface

$$a_{72} = -(2\mu_1 + K_1)\imath\xi\ R_1,\quad a_{74} = -(2\mu_1 + K_1)\imath\xi\ S_1,\quad a_{76} = (2\mu_1 + K_1)\xi^2 - \rho_1\omega^2,$$

$$a_{78} = (2\mu_1 + K_1)\xi^2 - \rho_1\omega^2,\quad a_{81} = (2\mu_2 + K_2)\imath\xi R_2,\quad a_{83} = (2\mu_2 + K_2)\imath\xi S_2,$$

$$a_{85} = (2\mu_2 + K_2)\xi^2 - \rho_2\omega^2,\quad a_{87} = (2\mu_2 + K_2)\xi^2 - \rho_2\omega^2,$$

while those for bonded interface

$$a_{71} = (2\mu_2+K_2)\imath\xi R_2,\ a_{72} = (2\mu_1+K_1)\imath\xi R_1,\ a_{73} = (2\mu_2+K_2)\imath\xi S_2,\ a_{74} = (2\mu_1+K_1)\imath\xi S_1,$$

$$a_{75} = (2\mu_2 + K_2)\xi^2 - \rho_2\omega^2, \quad a_{76} = -\{(2\mu_1 + K_1)\xi^2 - \rho_1\omega^2\}, \quad a_{77} = (2\mu_2 + K_2)\xi^2 - \rho_2\omega^2,$$

$$a_{78} = -\{(2\mu_1 + K_1)\xi^2 - \rho_1\omega^2\}, \quad a_{81} = a_{83} = \imath\xi, \quad a_{82} = a_{84} = -\imath\xi, \quad a_{85} = P_2,$$

$$a_{86} = P_1, \quad a_{87} = Q_2, \quad a_{88} = Q_1,$$

all other entries are zero.

Expanding the determinant in equation (3.13) for unbonded interface, the frequency equation of Stoneley wave yields

$$\alpha_{02}R_2 + \alpha_{01}R_1 = 0, \tag{3.14}$$

$$\gamma_2 P_2 + \gamma_1 P_1 = 0, \tag{3.15}$$

and

$$\rho_1\beta_1^4 Z_1(c)\left(1 - \frac{c^2}{\alpha_1^2 + \epsilon_1\beta_1^2}\right)^{-1/2} + \rho_2\beta_2^4 Z_2(c)\left(1 - \frac{c^2}{\alpha_2^2 + \epsilon_2\beta_2^2}\right)^{-1/2} = 0, \tag{3.16}$$

where

$$Z_i(c) = (2 + \epsilon_i)^2\left(1 - \frac{c^2}{(1 + \epsilon_i)\beta_i^2}\right)^{1/2}\left(1 - \frac{c^2}{\alpha_i^2 + \epsilon_i\beta_i^2}\right)^{1/2} - \left(2 + \epsilon_i - \frac{c^2}{\beta_i^2}\right)^2,$$

$$\alpha_i^2 = (\lambda_i + 2\mu_i)/\rho_i, \quad \beta_i^2 = \mu_i/\rho_i, \quad \epsilon_i = K_i/\mu_i,$$

α_i and β_i are the speeds of dilatational and shear waves respectively in medium H_i respectively. Equation (3.14) shows a new wave velocity, which is not observed in micropolar elasticity and purely depends on microstretch elastic constants. Hence, the waves related to these modes may be called as microstretch waves and refer to hypothetical medium wherein only microstretch may occur. Similarly, equation (3.15) shows a new wave velocity, which is not observed in classical elasticity and purely depends on micropolarity constants. Hence, the waves related to these modes correspond to micropolar waves and refer to hypothetical medium in which only rotation may occur.

Next, expanding the determinant in equation (3.13) for a bonded interface, the frequency equation of Stoneley waves between two microstretch elastic media yields

equations (3.14), (3.15) and

$$\begin{vmatrix} \rho_2\beta_2^2 M_2 & -\rho_1\beta_1^2 M_1 & -\rho_2\beta_2^2(2+\epsilon_2)N_2 & -\rho_1\beta_1^2(2+\epsilon_1)N_1 \\ M_4 & M_3 & -1 & 1 \\ \rho_2\beta_2^2(2+\epsilon_2)M_4 & \rho_1\beta_1^2(2+\epsilon_1)M_3 & -\rho_2\beta_2^2 M_2 & \rho_1\beta_1^2 M_1 \\ -1 & 1 & N_2 & N_1 \end{vmatrix} = 0, \quad (3.17)$$

where

$$M_i = \left(2+\epsilon_i - \frac{c^2}{\beta_i^2}\right), \ M_{i+2} = \left(1 - \frac{c^2}{\alpha_i^2+\epsilon_i\beta_i^2}\right)^{1/2}, \ N_i = \left(1 - \frac{c^2}{(1+\epsilon_i)\beta_i^2}\right)^{1/2}, \ (i=1,2).$$

The presence of equations (3.14) and (3.15) in both the cases indicates that the modes corresponding to microstretch and micropolar waves are independent of the bonded or unbonded nature of the interface.

3.4 Particular cases

(i) *Micropolar/Micropolar unbonded interface:* If we neglect microstretch effects from both the half-spaces then we shall be left with the problem of Stoneley waves at an interface between two dissimilar micropolar elastic solid half-spaces. In this limiting case, when the quantities $\lambda_{0i},\ \lambda_{1i}$ and α_{0i} approach to zero, we see that equation (3.14) is automatically satisfied and equations (3.15) and (3.16) represent the frequency equations for Stoneley waves at micropolar/micropolar unbonded interface. These equations are the same equations as obtained by Tajuddin (1995) for the relevant problem.

(ii) *Micropolar/Micropolar bonded interface:* It is easy to see that in the absence of microstretch parameters, equation (3.14) is automatically satisfied and equations (3.15) and (3.17) would represent the frequency equation for Stoneley waves at micropolar/micropolar bonded interface.

(iii) *Elastic/Elastic unbonded interface:* If microstretch and micropolarity effects are both neglected from both the half spaces then we shall be left with the problem of Stoneley wave propagation at an unbonded interface between two uniform elastic half-spaces. For this, making the quantities $\lambda_{0i},\ \lambda_{1i},\ \alpha_{0i},\ K_i$ and γ_i equal to zero, into the frequency equations (3.14)-(3.16), we see that equations (3.14) and (3.15) are automat-

ically satisfied, while equation (3.16) reduces to

$$\frac{\rho_1\beta_1^4}{\left(1-\dfrac{c^2}{\alpha_1^2}\right)^{1/2}}\overline{Z}_1(c)+\frac{\rho_2\beta_2^4}{\left(1-\dfrac{c^2}{\alpha_2^2}\right)^{1/2}}\overline{Z}_2(c)=0, \tag{3.18}$$

where

$$\overline{Z}_i(c)=\left(2-\frac{c^2}{\beta_i^2}\right)^2-4\left[1-\frac{c^2}{\beta_i^2}\right]^{1/2}\left[1-\frac{c^2}{\alpha_i^2}\right]^{1/2}, \quad (i=1,2).$$

Equation (3.18) matches exactly with equation (1) of Murty (1975b) for the relevant problem.

(iv) *Elastic/Elastic bonded interface:* Proceeding in a similar way as in case (iii), we can obtain the frequency equation for Stoneley waves at a bonded interface between two uniform elastic half-spaces given by

$$\begin{vmatrix} -\rho_2\left(c^2-2\beta_2^2\right) & \rho_1\left(c^2-2\beta_1^2\right) & 2\rho_2\beta_2^2\left(1-\frac{c^2}{\beta_2^2}\right)^{1/2} & -2\rho_1\beta_1^2\left(1-\frac{c^2}{\beta_1^2}\right)^{1/2} \\ \left(1-\frac{c^2}{\alpha_2^2}\right)^{1/2} & \left(1-\frac{c^2}{\alpha_1^2}\right)^{1/2} & 1 & 1 \\ 2\rho_2\beta_2^2\left(1-\frac{c^2}{\alpha_2^2}\right)^{1/2} & 2\rho_1\beta_1^2\left(1-\frac{c^2}{\alpha_1^2}\right)^{1/2} & \rho_2\beta_2^2\left(2-\frac{c^2}{\beta_2^2}\right) & \rho_1\beta_1^2\left(2-\frac{c^2}{\beta_1^2}\right) \\ -1 & 1 & -\left(1-\frac{c^2}{\beta_2^2}\right)^{1/2} & \left(1-\frac{c^2}{\beta_1^2}\right)^{1/2} \end{vmatrix}=0.$$

This equation exactly match with equation (23) of Stoneley (1924) for the relevant problem

(v)*Rayleigh waves in a microstretch elastic half-space:* If the upper half space is totally neglected, then we shall be left with the problem of Rayleigh wave propagation at the free boundary surface of a microstretch elastic solid half space. In this case, the relevant boundary conditions would be $[\tau_{zz}]_1=[\tau_{zx}]_1=[m_{zy}]_1=[m_z]_1=0$ at the interface $z=0$. Using the requisite quantities and expressions in these boundary conditions, we shall obtain four homogeneous equations in four unknowns. The condition for non-trivial solution of these unknowns would yield

$$b_{31}(b_{12}b_{23}-b_{13}b_{22})-b_{32}(b_{11}b_{23}-b_{13}b_{21})=0, \tag{3.19}$$

where $b_{11}=-(2\mu_1+K_1)\xi P_1$, $b_{12}=-(2\mu_1+K_1)\xi Q_1$, $b_{13}=[(2\mu_1+K_1)\xi^2-\rho_1\omega^2](1-\frac{b_1S_1}{a_1R_1})$, $b_{21}=(2\mu_1+K_1)\xi^2-\rho_1\omega^2=b_{22}$, $b_{23}=-S_1(2\mu_1+K_1)\xi(1-\frac{b_1}{a_1})$, $b_{31}=\gamma_1c_1'P_1$, $b_{32}=\gamma_1d_1'Q_1$ and P_1, R_1, Q_1 and S_1 are those defined in equations (3.5)-(3.8).

Equation (3.19) represents the frequency equation for Rayleigh wave propagation at free boundary of a microstretch half-space. This equation is the same equation as given in Eringen (1999) (see equation (6.6.20) pp: 264 by replacing λ_1 with $\lambda_1/3$ and λ_0 with $\lambda_0/3$, as there is difference in notations)

(vi) *Rayleigh waves in a micropolar half-space:* If we neglect the microstretch effect in case (v), we shall be left with the problem of Rayleigh wave propagation at free surface of a micropolar elastic half-space. Thus, putting $\lambda_{11} = \lambda_{01} = \alpha_{01} = 0$, we see that equation (3.19) reduces to

$$(c_1'P_1 - d_1'Q_1)[(2\mu_1 + K_1)\xi^2 - \rho_1\omega^2]^2 - P_1Q_1S_1(2\mu_1 + K_1)^2\xi^2(c_1' - d_1') = 0. \quad (3.20)$$

where now

$$S_1^2 = \xi^2 - \frac{\rho_1\omega^2}{\lambda_1 + 2\mu_1 + K_1}$$

and P_1 and Q_1 are the same as defined in equations (3.5)-(3.8). Equation (3.20) is the frequency equation for Rayleigh wave propagation at free surface of a micropolar half-space. This equation coincides with equation [(5.16.6) pp: 179)] given in Eringen (1999) for the relevant problem.

3.5 Numerical results and discussions

In order to solve the frequency equations numerically, we have taken a particular model and *Bisection method* is employed through FORTRAN program. The following values of relevant elastic parameters have been taken. In the elastic half-space H_1:

Symbol	Value
λ_1	$7.583 \times 10^{11} dyne/cm^2$
μ_1	$6.334 \times 10^{11}\ dyne/cm^2$
K_1	$0.0149 \times 10^{11}\ dyne/cm^2$
λ_{01}	$0.034 \times 10^{11}\ dyne/cm^2$
λ_{11}	$0.035 \times 10^{11}\ dyne/cm^2$
α_{01}	$0.035 \times 10^{11}\ dyne$
γ_1	$0.289 \times 10^{11}\ dyne$
j_1	$0.00625\ cm^2$
ρ_1	$1.2\ gm/cm^3$

In the elastic half-space H_2:

Symbol	Value
λ_2	$6.653 \times 10^{11} dyne/cm^2$
μ_2	$5.823 \times 10^{11}\ dyne/cm^2$
K_2	$0.0140 \times 10^{11}\ dyne/cm^2$
λ_{02}	$0.032 \times 10^{11}\ dyne/cm^2$
λ_{12}	$0.032 \times 10^{11}\ dyne/cm^2$
α_{02}	$0.034 \times 10^{11}\ dyne$
γ_2	$0.267 \times 10^{11}\ dyne$
j_2	$0.00515\ cm^2$
ρ_2	$1.1\ gm/cm^3$

We have solved the frequency equation (3.13) for Stoneley waves at an unbonded interface for different values of non-dimensional wavenumber ξd, where d is an entity having dimension of length. We have also solved the frequency equations (3.19) and (3.20) to obtain the dispersion curves for Rayleigh waves at the free boundary of a microstretch solid half-space and at the free boundary of a micropolar solid half-space, respectively using the above values of relevant elastic parameters given for half-space H_1. It is found that both Stoneley and Rayleigh waves are dispersive in nature for certain initial range of parameter ξd.

Figure 3.1 depicts the variation of non-dimensional phase velocity c/V ($V = \sqrt{c_1^2 + c_3^2}$) versus ξd. The solid curves refer to the dispersion curves for Stoneley waves and the dotted curves refer to the dispersion curves of Rayleigh waves. It can be noticed from this figure that the phase velocity of Stoneley waves at an unbonded microstretch/microstretch interface is increasing in the range $0.1 < \xi d \leq 2.0$, beyond which it remains almost constant, that is, independent of wavenumber. However, the phase velocity of Stoneley waves at an unbonded micropolar/micropolar interface first increases with ξd in the range $0 < \xi d \leq 0.36$ and then decreases with ξd in the range $0.36 < \xi d \leq 2.0$, thereafter, it also remains almost constant. We also note that the dispersion curve for Rayleigh waves at free surface of microstretch elastic half-space behaves like the dispersion curve of Stoneley waves at an unbonded microstretch/microstretch interface. Similarly, the dispersion curve of Rayleigh waves at free surface of a micropolar elastic half-space behaves like the dispersion curve of Stone-

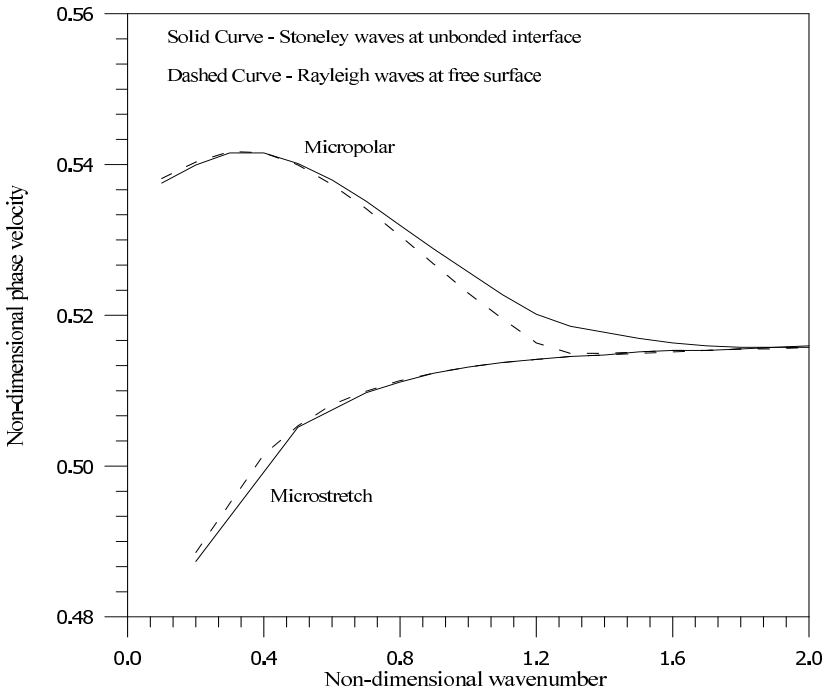

Figure 3.1: Dispersion curves for Stoneley and Rayleigh waves.

ley waves at an unbonded micropolar/micropolar interface. Thus, we conclude that the Stoneley waves are dispersive at an unbonded microstetch/microstretch and at an unbonded micropolar/micropolar interface only for small values of wavenumber. For higher values of wavenumber, both Stoneley and Rayleigh waves are almost constant and hence almost non-dispersive. It can be seen that there is significant difference in the dispersion curves for Stoneley wave propagation at an unbonded micropolar/micropolar interface and that of at an unbonded microstretch/microstretch interface in the range $0.1 < \xi d \leq 2.0$. This difference is due to the microstretch property of the half-spaces, which is responsible for lowering the phase velocity of Stoneley wave in this range of ξd. A similar conclusion can be inferred about the Rayleigh wave dispersion curve.

Figure 3.2 depicts the effect of the microstretch parameters λ_{0i} on the dispersion curves of Stoneley wave at an unbonded interface between microstretch/microstretch elastic half-spaces. We observe that as the values of these parameters increase, the phase velocity of Stoneley wave decreases in a certain initial range of non-dimensional wavenumber. Curves I to IV indicate the dispersion curves of Stoneley wave propagation at $\lambda_{0i} = 0.01$, $\lambda_{0i} = 0.25$, $\lambda_{0i} = 0.5$ and $\lambda_{0i} = 0.6$ respectively. Clearly, the microstretch property has significant effect on Stoneley wave propagation.

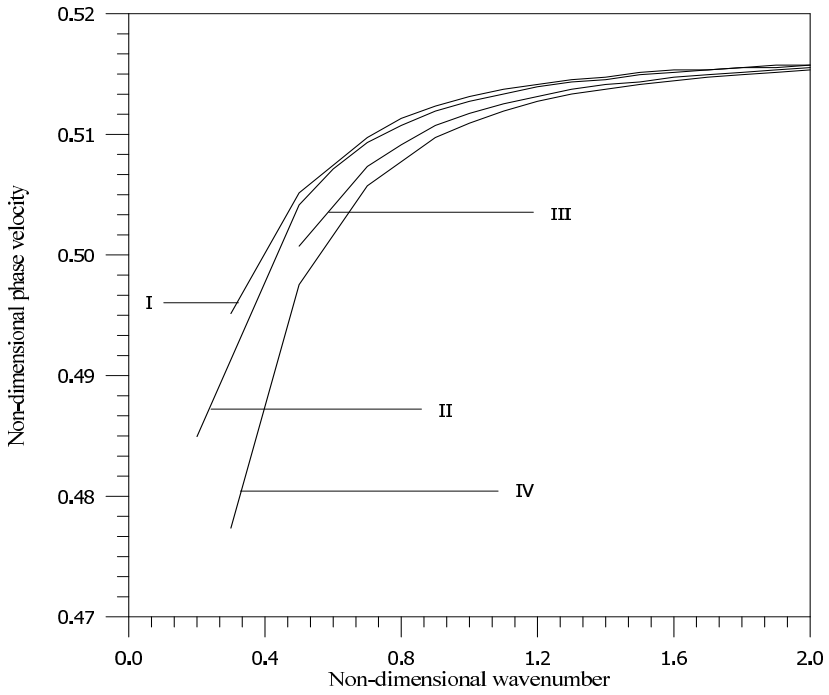

Figure 3.2: Effect of microstretch parameter on dispersion curves of Stoneley wave at unbonded interface between microstretch solid half-spaces (Curve I: $\lambda_{01} = \lambda_{02} = 0.01$, Curve II: $\lambda_{01} = \lambda_{02} = 0.25$, Curve III: $\lambda_{01} = \lambda_{02} = 0.5$, Curve IV: $\lambda_{01} = \lambda_{02} = 0.6$).

3.6 Conclusions

A mathematical treatment is made to study the surface wave propagation at free surface of a microstretch elastic half-space and at an unbonded/bonded interface of two dissimilar microstretch elastic half-spaces. Eringen's theory is employed to derive the frequency equations of Stoneley waves in a linear homogeneous and isotropic microstretch elastic medium. Closed form of frequency equations are derived for Stoneley wave propagation at both unbonded and bonded interface between two microstretch half-spaces when some parameters corresponding to microstretch and micropolarity are very small. We conclude that

(a) Stoneley waves at an unbonded interface and at a bonded interface between two microstretch elastic half-spaces are found to be dispersive.

(b) Likewise, the Rayleigh waves at the free surface of a microstretch elastic solid half-space and also at the free surface of a micropolar elastic solid half-space are found to be dispersive.

(c) Numerical results reveal that the phase velocity of Stoneley waves at an unbonded interface between two micropolar elastic half-spaces is greater than that of

at an unbonded interface between two microstretch half-spaces for certain initial range of wavenumber parameter. This shows that there is significant effect of microstretch property in this range. For higher values of wavenumber parameter, no effect of microstretch is observed on Stoneley waves or on Rayleigh waves.

Chapter 4

Longitudinal waves at a micropolar fluid/solid interface[3]

4.1 Introduction

The theory of micro-fluids (or micromorphic fluids) was introduced by Eringen (1964a), which deals with a class of fluids exhibiting certain microscopic effects arising from the local structure and the micro-motions of the fluid elements. A subclass of these micro-fluids is 'micropolar fluid', which exhibits the microrotational effects and micro-rotational inertia (see Eringen, 1966b). Micropolar fluids can support couple stress and body couples, in addition to asymmetric stress tensor and possess a rotational field, which is independent of the velocity of the fluids. A large class of fluids such as anisotropic fluids, liquid crystals with rigid molecules, magnetic fluids, cloud with dust, muddy fluids, biological fluids, dirty fluids (dusty air, snow) over airfoil can be modelled more realistically as micropolar fluids. The problems of reflection and refraction of elastic waves at an interface between a liquid half-space and a micropolar elastic half-space has been investigated by Tomar and Kumar (1995), Tomar and Kumar (1999b) and Kumar and Tomar (2001). But the corresponding problem at the interface of a micropolar fluid and a micropolar solid has not been considered hitherto. In this Chapter, we have investigated the possibility of plane wave propagation in an infinite micropolar fluid and found that four waves can propagate with differ-

[3] ***International Journal of Solids and Structures*** **45(1)**, 225-244(2008).

ent phase velocities, which are dispersive and attenuated. Reflection and transmission phenomena of a plane longitudinal displacement wave at a plane interface between a micropolar solid half-space and a micropolar fluid half-space has been studied in two cases: (i) when the wave is made incident after propagating through the micropolar solid half-space, (ii) when the wave is made incident after propagating through the micropolar fluid half-space. The formulae of amplitude ratios (reflection and transmission coefficients) and energy ratios of various reflected and transmitted waves are presented and depicted graphically. The frequency equation for Stoneley waves at an interface between a micropolar solid half-space and a micropolar fluid half-space has also been derived.

4.2 Basic equations and problem formulation

The equations of motion in micropolar fluid, in the absence of body force and body couple densities, are given by (Eringen, 1966b)

$$(c_{1f}^2 + c_{3f}^2)\nabla(\nabla \cdot \dot{\mathbf{u}}^f) - (c_{2f}^2 + c_{3f}^2)\nabla \times (\nabla \times \dot{\mathbf{u}}^f) + c_{3f}^2 \nabla \times \dot{\boldsymbol{\phi}}^f = \ddot{\mathbf{u}}^f, \tag{4.1}$$

$$(c_{4f}^2 + c_{5f}^2)\nabla(\nabla \cdot \dot{\boldsymbol{\phi}}^f) - c_{4f}^2 \nabla \times (\nabla \times \dot{\boldsymbol{\phi}}^f) + c_{6f}^2(\nabla \times \dot{\mathbf{u}}^f - 2\dot{\boldsymbol{\phi}}^f) = \ddot{\boldsymbol{\phi}}^f. \tag{4.2}$$

For micropolar solid medium, the equations of motion are given in Chapter-1 through equations (1.123) and (1.124). These equations in the absence of body force and body couple densities, are written as

$$(c_{1s}^2 + c_{3s}^2)\nabla(\nabla \cdot \mathbf{u}^s) - (c_{2s}^2 + c_{3s}^2)\nabla \times (\nabla \times \mathbf{u}^s) + c_{3s}^2 \nabla \times \boldsymbol{\phi}^s = \ddot{\mathbf{u}}^s, \tag{4.3}$$

$$(c_{4s}^2 + c_{5s}^2)\nabla(\nabla \cdot \boldsymbol{\phi}^s) - c_{4s}^2 \nabla \times (\nabla \times \boldsymbol{\phi}^s) + c_{6s}^2(\nabla \times \mathbf{u}^s - 2\boldsymbol{\phi}^s) = \ddot{\boldsymbol{\phi}}^s, \tag{4.4}$$

where $c_{1r}^2 = (\lambda^r + 2\mu^r)/\rho^r$, $c_{2r}^2 = \mu^r/\rho^r$, $c_{3r}^2 = K^r/\rho^r$, $c_{4r}^2 = \gamma^r/\rho^r j^r$, $c_{5r}^2 = (\alpha^r + \beta^r)/\rho^r j^r$, $c_{6r}^2 = c_{3r}^2/j^r$, ρ^r is the density of the medium, j^r is the micro-inertia, $\mathbf{u}^r$ and $\boldsymbol{\phi}^r$ are respectively the displacement and microrotation vectors for the micropolar elastic half-spaces. Here, the quantity having superscript r corresponds to the fluid and solid medium when $r = f$ and $r = s$ respectively. λ^f, μ^f, K^f are the fluid

viscosity coefficients and α^f, β^f and γ^f are the fluid viscosity coefficients responsible for gyrational dissipation of the micropolar fluid, and the symbols λ^s, μ^s, K^s, α^s, β^s and γ^s are defined in Chapter-1 for micropolar elastic solid half-space.
The constitutive relations, for micropolar fluid medium are given by (Eringen 1966b),

$$\tau^f_{kl} = \lambda^f \dot{u}^f_{r,r}\delta_{kl} + \mu^f(\dot{u}^f_{k,l} + \dot{u}^f_{l,k}) + K^f(\dot{u}^f_{l,k} - \varepsilon_{klp}\dot{\phi}^f_p), \tag{4.5}$$

$$m^f_{kl} = \alpha^f \dot{\phi}^f_{r,r}\delta_{kl} + \beta^f \dot{\phi}^f_{k,l} + \gamma^f \dot{\phi}^f_{l,k}, \tag{4.6}$$

and those for micropolar solid medium can be stemmed from relations (1.128) and (1.129) of Chapter-1, which are given by

$$\tau^s_{kl} = \lambda^s u^s_{r,r}\delta_{kl} + \mu^s(u^s_{k,l} + u^s_{l,k}) + K^s(u^s_{l,k} - \varepsilon_{klp}\phi^s_p), \tag{4.7}$$

$$m^s_{kl} = \alpha^s \phi^s_{r,r}\delta_{kl} + \beta^s \phi^s_{k,l} + \gamma^s \phi^s_{l,k}, \tag{4.8}$$

where symbols have their usual meanings and are well defined earlier.
Using Helmholtz representation of vector, we can write

$$\begin{bmatrix} \mathbf{u}^r \\ \boldsymbol{\phi}^r \end{bmatrix} = \nabla \begin{bmatrix} A^r \\ C^r \end{bmatrix} + \nabla \times \begin{bmatrix} \mathbf{B}^r \\ \mathbf{D}^r \end{bmatrix}, \qquad \nabla \cdot \begin{bmatrix} \mathbf{B}^r \\ \mathbf{D}^r \end{bmatrix} = 0. \quad (r = f,\ s), \tag{4.9}$$

where A^r and C^r are the scalar potentials, while $\mathbf{B}^r$ and $\mathbf{D}^r$ are the vector potentials. Plugging (4.9) into equations (4.1) and (4.2), we obtain

$$\Box_1 A^f = 0, \qquad \Box_2 C^f = 0, \tag{4.10}$$

$$(c^2_{2f} + c^2_{3f})\nabla^2 \dot{\mathbf{B}}^f + c^2_{3f}\nabla \times \dot{\mathbf{D}}^f = \ddot{\mathbf{B}}^f, \tag{4.11}$$

$$c^2_{4f}\nabla^2 \dot{\mathbf{D}}^f + c^2_{6f}\nabla \times \dot{\mathbf{B}}^f - 2c^2_{6f}\dot{\mathbf{D}}^f = \ddot{\mathbf{D}}^f, \tag{4.12}$$

where

$$\Box_1 = [(c_{1f}^2 + c_{3f}^2)\nabla^2 - \frac{\partial}{\partial t}]\frac{\partial}{\partial t} \qquad \Box_2 = [(c_{4f}^2 + c_{5f}^2)\nabla^2 - 2c_{6f}^2 - \frac{\partial}{\partial t}]\frac{\partial}{\partial t}.$$

It can be seen that the equations in (4.10) are un-coupled in scalar potentials A^f and C^f, while equations in (4.11) and (4.12) are coupled in vector potentials $\mathbf{B}^f$ and $\mathbf{D}^f$.

4.3 Plane waves in a micropolar fluid

Consider the following form of a plane wave propagating in the positive direction of a unit vector $\mathbf{n}$ as

$$\{A^r,\ C^r,\ \mathbf{B}^r,\ \mathbf{D}^r\} = \{a^r,\ c^r,\ \mathbf{b}^r,\ \mathbf{d}^r\}\exp\{\imath k(\mathbf{n}\cdot\mathbf{r} - Vt)\}, \tag{4.13}$$

where $a^r,\ c^r,\ \mathbf{b}^r$ and $\mathbf{d}^r$ are constants, $\mathbf{r}(= x\hat{i} + y\hat{j} + z\hat{k})$ is the position vector, V is the phase velocity in the direction of $\mathbf{n}$, $k(= \omega/V)$ is the wavenumber, ω being the angular frequency. Substituting (4.13) into equation (4.10), we obtain two wave velocities denoted by V_{f1} and V_{f4}, given by

$$V_{f1}^2 = -\imath\omega(c_{1f}^2 + c_{3f}^2), \qquad V_{f4}^2 = \frac{-\imath\omega^2(c_{4f}^2 + c_{5f}^2)}{(\omega + 2\imath c_{6f}^2)}.$$

Again, Substituting (4.13) into equations (4.11) and (4.12), we obtain two wave velocities given by

$$V_{f2,f3}^2 = \frac{1}{2a'}[-b' \pm \sqrt{b'^2 - 4a'c'}],$$

where

$$a' = \omega + 2\imath c_{6f}^2,$$

$$b' = \omega[\imath\omega c_{4f}^2 + \imath(c_{2f}^2 + c_{3f}^2)(\omega + 2\imath c_{6f}^2) + c_{3f}^2 c_{6f}^2],$$

$$c' = -\omega^3 c_{4f}^2(c_{2f}^2 + c_{3f}^2).$$

It can be seen that these velocities are complex and dispersive in nature. Using (4.13) into (4.9), it can be seen that $\mathbf{u}^f$ and $\boldsymbol{\phi}^f$ are parallel to $\mathbf{n}$, which means that the waves associated with the velocities V_{f1} and V_{f4} are longitudinal in nature. It is easy to see that the waves associated with the velocities V_{f2} and V_{f3} are transverse in nature. Note

that at $\omega = 0$, all these four velocities vanish. Since the vector potentials $\mathbf{B}^f$ and $\mathbf{D}^f$ are coupled to each other, therefore, the waves with velocities V_{f2} and V_{f3} are coupled waves similar to the coupled waves encountered in micropolar elastic solid (see Parfitt and Eringen, 1969). The waves propagating with velocities V_{f1} and V_{f4} respectively are analogous to the longitudinal displacement wave and the longitudinal micro-rotational wave encountered in micropolar elastic solid.

Parfitt and Eringen (1969) have already shown that there exist four waves in an infinite micropolar elastic solid medium propagating with distinct phase velocities. These are (i) an independent longitudinal displacement wave propagating with velocity V_{s1} given by $V_{s1}^2 = c_{1s}^2 + c_{3s}^2$, (ii) two sets of coupled waves, each consists of a transverse displacement wave and a transverse microrotational wave perpendicular to each other, propagating with phase velocities V_{s2} and V_{s3} given by

$$V_{s2,s3}^2 = \frac{1}{2(1-2\omega_0^2/\omega^2)}[\{c_{2s}^2 + c_{3s}^2 + c_{4s}^2 - (2c_{2s}^2 + c_{3s}^2)\omega_0^2/\omega^2\}$$

$$\pm(\{c_{2s}^2 + c_{3s}^2 + c_{4s}^2 - (2c_{2s}^2 + c_{3s}^2)\omega_0^2/\omega^2\}^2 - 4(1-2\omega_0^2/\omega^2)\{c_{4s}^2(c_{2s}^2 + c_{3s}^2)\})^{1/2}],$$

where $\omega_0^2 = c_{6s}^2$ and (iii) an independent longitudinal micro-rotational wave propagating with velocity V_{s4} given by $V_{s4}^2 = (c_{4s}^2 + c_{5s}^2)(1-2\omega_0^2/\omega^2)^{-1}$. They have also shown that the waves propagating with velocities V_{s2} and V_{s4} can propagate in a micropolar elastic solid only if $\omega > \sqrt{2}\omega_0$, otherwise they degenerate into distance decaying sinusoidal vibrations. Note that no such cut-off frequency occur in case of waves propagating with phase velocities V_{f2} and V_{f4}.

4.4 Reflection and transmission of longitudinal waves

Introducing the Cartesian coordinates $x,\ y$ and z such that $x-y$ plane ($z = 0$) lies along the interface between a micropolar solid half-space (M_1) and a micropolar fluid half-space (M_2). The $z-$ axis is taken perpendicular to the interface and pointing downward into the medium M_1. We shall consider a two-dimensional problem in $x - z$ plane, so that the followings are the displacement and microrotational vectors in micropolar elastic solid and in micropolar fluid:

$$\mathbf{u}^r = (u_1^r(x,\ z), 0, u_3^r(x,\ z)), \quad \phi^r = (0, \phi_2^r(x,\ z), 0), \quad (r = f,\ s), \tag{4.14}$$

4.4.1 Case I: Incidence from the solid half-space

Let a plane longitudinal wave with phase velocity V_{s1} propagating through the micropolar solid medium M_1 be striking at the interface $z = 0$ and making an angle θ_0 with the normal. To satisfy the boundary conditions at the interface, we postulate that the incident wave will give rise to the following reflected and refracted waves:
(a) a reflected longitudinal displacement wave in medium M_1 traveling with speed V_{s1} and making an angle θ_1 with the normal;
(b) two sets of reflected coupled waves in medium M_1 traveling with speeds V_{s2} and V_{3s} and making angles θ_2 and θ_3 with the normal, respectively;
(c) a refracted longitudinal displacement wave in medium M_2 traveling with speed V_{f1} and making an angle θ_1' with the normal;
(d) two sets of refracted coupled waves in medium M_2 traveling with speeds V_{f2} and V_{f3} and making angles θ_2' and θ_3' with the normal, respectively.
We take the following form of potentials in the two half-spaces.
In the half-space M_1:

$$A^s = A_0 \exp\{\imath k_1(\sin\theta_0 x - \cos\theta_0 z) - \imath\omega_1 t\}$$

$$+ A_1 \exp\{\imath k_1(\sin\theta_1 x + \cos\theta_1 z) - \imath\omega_1 t\}, \tag{4.15}$$

$${B_2}^s = A_2 \exp\{\imath k_2(\sin\theta_2 x + \cos\theta_2 z) - \imath\omega_2 t\}$$

$$+ A_3 \exp\{\imath k_3(\sin\theta_3 x + \cos\theta_3 z) - \imath\omega_3 t\}, \tag{4.16}$$

$${\phi_2}^s = A_2\eta_2 \exp\{\imath k_2(\sin\theta_2 x + \cos\theta_2 z) - \imath\omega_2 t\}$$

$$+ A_3\eta_3 \exp\{\imath k_3(\sin\theta_3 x + \cos\theta_3 z) - \imath\omega_3 t\}, \tag{4.17}$$

and in the half-space M_2:

$$A^f = A_1' \exp\{\imath k_1'(\sin\theta_1' x - \cos\theta_1' z) - \imath\omega_1' t\}, \tag{4.18}$$

$${B_2}^f = A_2' \exp\{\imath k_2'(\sin\theta_2' x - \cos\theta_2' z) - \imath\omega_2' t\}$$

$$+ A'_3 \exp\{\imath k'_3(\sin\theta'_3 x - \cos\theta'_3 z) - \imath\omega'_3 t\}, \tag{4.19}$$

$$\phi_2{}^f = A'_2\eta'_2 \exp\{\imath k'_2(\sin\theta'_2 x - \cos\theta'_2 z) - \imath\omega'_2 t\}$$

$$+ A'_3\eta'_3 \exp\{\imath k'_3(\sin\theta'_3 x - \cos\theta'_3 z) - \imath\omega'_3 t\}, \tag{4.20}$$

where A_0 - amplitude of the incident longitudinal displacement wave, A_1 - amplitude of the reflected longitudinal displacement wave at an angle θ_1, A_2 - amplitude of the reflected coupled wave at an angle θ_2, A_3 - amplitude of the reflected couple wave at an angle θ_3, A'_1 - amplitude of the refracted longitudinal displacement wave at an angle θ'_1, A'_2 - amplitude of the refracted couple wave at an angle θ'_2 and A'_3 - amplitude of the refracted couple wave at an angle θ'_3. The coupling parameters $\eta_{2,3}$ and $\eta'_{2,3}$ are given by

$$\eta_{2,3} = -c_{6s}^2\left[V_{s2,s3}^2 - 2\frac{c_{6s}^2}{k_{2,3}^2} - c_{4s}^2\right]^{-1}, \quad \eta'_{2,3} = \imath c_{6f}^2\left[\frac{V_{f2,f3}}{k'_{2,3}} + 2\frac{\imath c_{6f}^2}{k_{2,3}^{\prime 2}} + \imath c_{4f}^2\right]^{-1}.$$

The appropriate boundary conditions to be satisfied at the interface $z = 0$, are the continuity of force stress, couple stress, displacement and micro-rotation. Mathematically, these boundary conditions can be written as

$$\tau_{zz}^s = \tau_{zz}^f, \quad \tau_{zx}^s = \tau_{zx}^f, \quad m_{zy}^s = m_{zy}^f, \quad u_1^s = u_1^f, \quad u_3^s = u_3^f, \quad \phi_2^s = \phi_2^f, \quad \text{at} \quad \text{z} = 0. \tag{4.21}$$

Employing the Snell's law given by

$$\frac{\sin\theta_0}{V_{s1}} = \frac{\sin\theta_1}{V_{s1}} = \frac{\sin\theta_2}{V_{s2}} = \frac{\sin\theta_3}{V_{s3}} = \frac{\sin\theta'_1}{V_{f1}} = \frac{\sin\theta'_2}{V_{f2}} = \frac{\sin\theta'_3}{V_{f3}},$$

assuming that all frequencies are equal at the interface and making use of (4.5) - (4.9) and (4.14)-(4.20) into the boundary conditions given in (4.21), we obtain six homogeneous equations as

$$-k_1^2[\lambda^s + (2\mu^s + K^s)\cos^2\theta_0]A_0 - k_1^2[\lambda^s + (2\mu^s + K^s)\cos^2\theta_0]A_1 - (2\mu^s + K^s)k_2^2\frac{V_{s2}}{V_{s1}}\sin\theta_0$$

$$\times\sqrt{1 - \frac{V_{s2}^2}{V_{s1}^2}\sin^2\theta_0}A_2 - (2\mu^s + K^s)k_3^2\frac{V_{s3}}{V_{s1}}\sin\theta_0\sqrt{1 - \frac{V_{s3}^2}{V_{s1}^2}\sin^2\theta_0}A_3$$

$$-\imath\omega k_1'^2\left[\lambda^f+(2\mu^f+K^f)\left(1-\frac{V_{f1}^2}{V_{s1}^2}\sin^2\theta_0\right)\right]A_1'+(2\mu^f+K^f)\imath\omega k_2'^2\frac{V_{f2}}{V_{s1}}\sin\theta_0$$

$$\times\sqrt{1-\frac{V_{f2}^2}{V_{s1}^2}\sin^2\theta_0}A_2'+(2\mu^f+K^f)\imath\omega k_3'^2\frac{V_{f3}}{V_{s1}}\sin\theta_0\sqrt{1-\frac{V_{f3}^2}{V_{s1}^2}\sin^2\theta_0}A_3'=0, \quad (4.22)$$

$$(2\mu^s+K^s)k_1^2\sin\theta_0\cos\theta_0A_0-(2\mu^s+K^s)k_1^2\sin\theta_0\cos\theta_0A_1+[\mu^sk_2^2\left(1-2\frac{V_{s2}^2}{V_{s1}^2}\sin^2\theta_0\right)$$

$$+K^sk_2^2\left(1-\frac{V_{s2}^2}{V_{s1}^2}\sin^2\theta_0\right)-K^s\eta_2]A_2+[\mu^sk_3^2\left(1-2\frac{V_{s3}^2}{V_{s1}^2}\sin^2\theta_0\right)+K^sk_3^2\left(1-\frac{V_{s3}^2}{V_{s1}^2}\sin^2\theta_0\right)$$

$$-K^s\eta_3]A_3+(2\mu^f+K^f)\imath k_1'^2\omega\sin\theta_0\frac{V_{f1}}{V_{s1}}\sqrt{1-\frac{V_{f1}^2}{V_{s1}^2}\sin^2\theta_0}A_1'+[\imath\mu^f\omega k_2'^2(1-2\frac{V_{f2}^2}{V_{s1}^2}\sin^2\theta_0)$$

$$+\imath K^fk_2'^2\omega(1-\frac{V_{f2}^2}{V_{s1}^2}\sin^2\theta_0)-\imath K^f\omega\eta_2']A_2'+[\imath\mu^f\omega k_3'^2(1-2\frac{V_{f3}^2}{V_{s1}^2}\sin^2\theta_0)+\imath K^f\omega k_3'^2$$

$$\times\left(1-\frac{V_{f3}^2}{V_{s1}^2}\sin^2\theta_0\right)-\imath K^f\omega\eta_3']A_3'=0, \quad (4.23)$$

$$\imath\gamma^s\eta_2k_2\cos\theta_2A_2+\imath\gamma^s\eta_3k_3\cos\theta_3A_3+\gamma^f\omega\eta_2'k_2'\cos\theta_2'A_2'+\gamma^f\omega\eta_3'k_3'\cos\theta_3'A_3'=0, \quad (4.24)$$

$$k_1\sin\theta_0A_0+k_1\sin\theta_1A_1-k_2\cos\theta_2A_2-k_3\cos\theta_3A_3-k_1'\sin\theta_1'A_1-k_2'\cos\theta_2'A_2$$

$$-k_3'\cos\theta_3'A_3'=0, \quad (4.25)$$

$$-k_1\cos\theta_0A_0+k_1\cos\theta_1A_1+k_2\sin\theta_2A_2+k_3\sin\theta_3A_3+k_1'\cos\theta_1'A_1'-k_2'\sin\theta_2'A_2'$$

$$-k_3'\sin\theta_3'A_3'=0, \quad (4.26)$$

$$\eta_2A_2+\eta_3A_3-\eta_2'A_2'-\eta_3'A_3'=0. \quad (4.27)$$

These six equations (4.22) - (4.27) can be written in matrix form as

$$PZ=Q, \quad (4.28)$$

where $P = [a_{ij}]_{6\times 6}$, $Z = [Z_1 \;\; Z_2 \;\; Z_3 \;\; Z_1' \;\; Z_2' \;\; Z_3']^t$ and $Q = [1 \;\; -1 \;\; 0 \;\; -1 \;\; 1 \;\; 0]^t$. The entries of the matrix P in non-dimensional form are given by

$$a_{11} = -1, \quad a_{12} = -\frac{V_{s1}}{V_{s2}} \frac{(2\mu^s + K^s)\sin\theta_0 \sqrt{1 - \frac{V_{s2}^2}{V_{s1}^2}\sin^2\theta_0}}{[\lambda^s + (2\mu^s + K^s)\cos^2\theta_0]},$$

$$a_{13} = -\frac{V_{s1}}{V_{s3}} \frac{(2\mu^s + K^s)\sin\theta_0 \sqrt{1 - \frac{V_{s3}^2}{V_{s1}^2}\sin^2\theta_0}}{[\lambda^s + (2\mu^s + K^s)\cos^2\theta_0]},$$

$$a_{14} = -\frac{V_{s1}^2}{V_{f1}^2} \frac{\imath\omega[\lambda^f + (2\mu^f + K^f)(1 - \frac{V_{f1}^2}{V_{s1}^2}\sin^2\theta_0)]}{[\lambda^s + (2\mu^s + K^s)\cos^2\theta_0]},$$

$$a_{15} = \frac{V_{s1}}{V_{f2}} \frac{\imath\omega(2\mu^f + K^f)\sin\theta_0 \sqrt{1 - \frac{V_{f2}^2}{V_{s1}^2}\sin^2\theta_0}}{[\lambda^s + (2\mu^s + K^s)\cos^2\theta_0]},$$

$$a_{16} = \frac{V_{s1}}{V_{f3}} \frac{\imath\omega(2\mu^f + K^f)\sin\theta_0 \sqrt{1 - \frac{V_{f3}^2}{V_{s1}^2}\sin^2\theta_0}}{[\lambda^s + (2\mu^s + K^s)\cos^2\theta_0]},$$

$$a_{21} = -1, \quad a_{22} = \frac{V_{s1}^2}{V_{s2}^2} \frac{[\mu^s(1 - 2\frac{V_{s2}^2}{V_{s1}^2}\sin^2\theta_0) + K^s(1 - \frac{V_{s2}^2}{V_{s1}^2}\sin^2\theta_0) - \frac{K^s\eta_2}{k_2^2}]}{(2\mu^s + K^s)\sin\theta_0\cos\theta_0},$$

$$a_{23} = \frac{V_{s1}^2}{V_{s3}^2} \frac{[\mu^s(1 - 2\frac{V_{s3}^2}{V_{s1}^2}\sin^2\theta_0) + K^s(1 - \frac{V_{s3}^2}{V_{s1}^2}\sin^2\theta_0) - \frac{K^s\eta_3}{k_3^2}]}{(2\mu^s + K^s)\sin\theta_0\cos\theta_0},$$

$$a_{24} = \imath\frac{V_{s1}}{V_{f1}} \frac{\omega(2\mu^f + K^f)\sqrt{1 - \frac{V_{f1}^2}{V_{s1}^2}\sin^2\theta_0}}{(2\mu^s + K^s)\cos\theta_0},$$

$$a_{25} = \imath\omega\frac{V_{s1}^2}{V_{f2}^2} \frac{[\mu^f(1 - 2\frac{V_{f2}^2}{V_{s1}^2}\sin^2\theta_0) + K^f(1 - \frac{V_{f2}^2}{V_{s1}^2}\sin^2\theta_0) - \frac{K^f\eta_2'}{k_2'^2}]}{(2\mu^s + K^s)\sin\theta_0\cos\theta_0},$$

$$a_{26} = \imath\omega\frac{V_{s1}^2}{V_{f3}^2} \frac{[\mu^f(1 - 2\frac{V_{f3}^2}{V_{s1}^2}\sin^2\theta_0) + K^f(1 - \frac{V_{f3}^2}{V_{s1}^2}\sin^2\theta_0) - \frac{K^f\eta_3'}{k_3'^2}]}{(2\mu^s + K^s)\sin\theta_0\cos\theta_0},$$

$$a_{31} = 0, \quad a_{32} = 1, \quad a_{33} = \frac{\eta_3}{\eta_2}\frac{V_{s2}}{V_{s3}} \frac{\sqrt{1 - \frac{V_{s3}^2}{V_{s1}^2}\sin^2\theta_0}}{\sqrt{1 - \frac{V_{s2}^2}{V_{s1}^2}\sin^2\theta_0}}, \quad a_{34} = 0,$$

$$a_{35} = -\imath\omega\frac{\gamma^f}{\gamma^s}\frac{\eta_2'}{\eta_2}\frac{V_{s2}}{V_{f2}}\frac{\sqrt{1-\frac{V_{f2}^2}{V_{s1}^2}\sin^2\theta_0}}{\sqrt{1-\frac{V_{s2}^2}{V_{s1}^2}\sin^2\theta_0}}, \quad a_{36} = -\imath\omega\frac{\gamma^f}{\gamma^s}\frac{\eta_3'}{\eta_2}\frac{V_{s2}}{V_{f3}}\frac{\sqrt{1-\frac{V_{f3}^2}{V_{s1}^2}\sin^2\theta_0}}{\sqrt{1-\frac{V_{s2}^2}{V_{s1}^2}\sin^2\theta_0}},$$

$$a_{41} = 1, \quad a_{42} = -\frac{V_{s1}}{V_{s2}}\frac{\sqrt{1-\frac{V_{s2}^2}{V_{s1}^2}\sin^2\theta_0}}{\sin\theta_0}, \quad a_{43} = -\frac{V_{s1}}{V_{s3}}\frac{\sqrt{1-\frac{V_{s3}^2}{V_{s1}^2}\sin^2\theta_0}}{\sin\theta_0},$$

$$a_{44} = -1, \quad a_{45} = -\frac{V_{s1}}{V_{f2}}\frac{\sqrt{1-\frac{V_{f2}^2}{V_{s1}^2}\sin^2\theta_0}}{\sin\theta_0}, \quad a_{46} = -\frac{V_{s1}}{V_{f3}}\frac{\sqrt{1-\frac{V_{f3}^2}{V_{s1}^2}\sin^2\theta_0}}{\sin\theta_0},$$

$$a_{51} = 1, \quad a_{52} = \tan\theta_0, \quad a_{53} = \tan\theta_0,$$

$$a_{54} = \frac{V_{s1}}{V_{f1}}\frac{\sqrt{1-\frac{V_{f1}^2}{V_{s1}^2}\sin^2\theta_0}}{\cos\theta_0}, \quad a_{55} = a_{56} = -\tan\theta_0, \quad a_{61} = 0, \quad a_{62} = 1,$$

$$a_{63} = \frac{\eta_3}{\eta_2}, \quad a_{64} = 0, \quad a_{65} = \frac{-\eta_2'}{\eta_2}, \quad a_{66} = \frac{-\eta_3'}{\eta_2}$$

and the elements of the matrix Z are given by

$$Z_1 = A_1/A_0, \quad Z_2 = A_2/A_0, \quad Z_3 = A_3/A_0, \quad Z_1' = A_1'/A_0, \quad Z_2' = A_2'/A_0, \quad Z_3' = A_3'/A_0,$$

where Z_1, Z_2 and Z_3 are the amplitude ratios for the reflected longitudinal displacement wave at an angle θ_1, reflected coupled wave at an angle θ_2 and reflected coupled wave at an angle θ_3 respectively, Z_1', Z_2' and Z_3' are the amplitude ratios for the refracted longitudinal displacement wave at an angle θ_1', refracted coupled wave at an angle θ_2' and refracted coupled wave at an angle θ_3' respectively. The matrix equation (4.28) is enable to provide the amplitude ratios of various reflected and refracted waves in the corresponding problem.

4.4.2 Case II: Incidence from the fluid half-space

A similar treatment can be made when a longitudinal displacement wave with amplitude A_0' propagating with phase velocity V_{f1} through the micropolar fluid medium M_2 strikes the interface $z = 0$ making an angle θ_0' with the normal. We take the following form of potentials in the two half-spaces:
In the half-space M_1:

$$A^s = A_1 \exp\{\imath k_1(\sin\theta_1 x + \cos\theta_1 z) - \imath\omega_1 t\}, \tag{4.29}$$

$$B_2{}^s = A_2 \exp\{\imath k_2(\sin\theta_2 x + \cos\theta_2 z) - \imath\omega_2 t\}$$

$$+ A_3 \exp\{\imath k_3(\sin\theta_3 x + \cos\theta_3 z) - \imath\omega_3 t\}, \tag{4.30}$$

$$\phi_2{}^s = A_2\eta_2 \exp\{\imath k_2(\sin\theta_2 x + \cos\theta_2 z) - \imath\omega_2 t\}$$

$$+ A_3\eta_3 \exp\{\imath k_3(\sin\theta_3 x + \cos\theta_3 z) - \imath\omega_3 t\}, \tag{4.31}$$

and in the half-space M_2:

$$A^f = A'_0 \exp\{\imath k'_1(\sin\theta'_0 x + \cos\theta'_0 z) - \imath\omega'_1 t\}$$

$$+ A'_1 \exp\{\imath k'_1(\sin\theta'_1 x - \cos\theta'_1 z) - \imath\omega'_1 t\}, \tag{4.32}$$

$$B_2{}^f = A'_2 \exp\{\imath k'_2(\sin\theta'_2 x - \cos\theta'_2 z) - \imath\omega'_2 t\}$$

$$+ A'_3 \exp\{\imath k'_3(\sin\theta'_3 x - \cos\theta'_3 z) - \imath\omega'_3 t\}, \tag{4.33}$$

$$\phi_2{}^f = A'_2\eta'_2 \exp\{\imath k'_2(\sin\theta'_2 x - \cos\theta'_2 z) - \imath\omega'_2 t\}$$

$$+ A'_3\eta'_3 \exp\{\imath k'_3(\sin\theta'_3 x - \cos\theta'_3 z) - \imath\omega'_3 t\}. \tag{4.34}$$

Using the same boundary conditions given in equation (4.21) and adopting the same procedure, one can arrive at a matrix equation similar to (4.28) given by

$$MR = S, \tag{4.35}$$

where $M = [a_{ij}]_{6\times 6}$. The non dimensional elements of matrix M, in this case, are given by

$$a_{11} = \frac{-\imath V_{f1}^2}{V_{s1}^2} \frac{\left[\lambda^s + (2\mu^s + K^s)\left(1 - \frac{V_{s1}^2}{V_{f1}^2}\sin^2\theta'_0\right)\right]}{\omega[\lambda^f + (2\mu^f + K^f)\cos^2\theta'_0]},$$

$$a_{12} = \frac{-\imath V_{f1}}{V_{s2}} \frac{(2\mu^s + K^s)\sin\theta'_0\sqrt{1 - \frac{V_{s2}^2}{V_{f1}^2}\sin^2\theta'_0}}{\omega[\lambda^f + (2\mu^f + K^f)\cos^2\theta'_0]},$$

$$a_{13} = \frac{-\imath V_{f1}}{V_{s3}} \frac{(2\mu^s + K^s)\sin\theta_0' \sqrt{1 - \frac{V_{s3}^2}{V_{f1}^2}\sin^2\theta_0'}}{\omega[\lambda^f + (2\mu^f + K^f)\cos^2\theta_0']},$$

$$a_{14} = 1, \quad a_{15} = \frac{-V_{f1}(2\mu^f + K^f)\sin\theta_0' \sqrt{1 - \frac{V_{f2}^2}{V_{f1}^2}\sin^2\theta_0'}}{V_{f2}[\lambda^f + (2\mu^f + K^f)\cos^2\theta_0']},$$

$$a_{16} = \frac{-V_{f1}(2\mu^f + K^f)\sin\theta_0' \sqrt{1 - \frac{V_{f3}^2}{V_{f1}^2}\sin^2\theta_0'}}{V_{f3}(\lambda^f + (2\mu^f + K^f)\cos^2\theta_0')},$$

$$a_{21} = \frac{\imath V_{f1}(2\mu^s + K^s)\sqrt{1 - \frac{V_{s1}^2}{V_{f1}^2}\sin^2\theta_0'}}{(2\mu^f + K^f)V_{s1}\omega\cos\theta_0'},$$

$$a_{22} = \frac{-\imath V_{f1}^2}{V_{s2}^2} \frac{[\mu^s(1 - 2\frac{V_{s2}^2}{V_{f1}^2}\sin^2\theta_0') + K^s(1 - \frac{V_{s2}^2}{V_{f1}^2}\sin^2\theta_0') - \frac{K^s\eta_2}{k_2^2}]}{(2\mu^f + K^f)\omega\sin\theta_0'\cos\theta_0'},$$

$$a_{23} = \frac{-\imath V_{f1}^2}{V_{s3}^2} \frac{[\mu^s(1 - 2\frac{V_{s3}^2}{V_{f1}^2}\sin^2\theta_0') + K^s(1 - \frac{V_{s3}^2}{V_{f1}^2}\sin^2\theta_0') - \frac{K^s\eta_3}{k_3^2}]}{(2\mu^f + K^f)\omega\sin\theta_0'\cos\theta_0'},$$

$$a_{24} = 1,$$

$$a_{25} = \frac{V_{f1}^2}{V_{f2}^2} \frac{[\mu^f(1 - 2\frac{V_{f2}^2}{V_{f1}^2}\sin^2\theta_0') + K^f(1 - \frac{V_{f2}^2}{V_{f1}^2}\sin^2\theta_0') - \frac{K^f\eta_2'}{k_2'^2}]}{(2\mu^f + K^f)\sin\theta_0'\cos\theta_0'},$$

$$a_{26} = \frac{V_{f1}^2}{V_{f3}^2} \frac{[\mu^f(1 - 2\frac{V_{f3}^2}{V_{f1}^2}\sin^2\theta_0') + K^f(1 - \frac{V_{f3}^2}{V_{f1}^2}\sin^2\theta_0') - \frac{K^f\eta_3'}{k_3'^2}]}{(2\mu^f + K^f)\sin\theta_0'\cos\theta_0'},$$

$$a_{31} = 0, \quad a_{32} = 1, \quad a_{33} = \frac{\eta_3 V_{s2}\sqrt{1 - \frac{V_{s3}^2}{V_{f1}^2}\sin^2\theta_0'}}{\eta_2 V_{s3}\sqrt{1 - \frac{V_{s2}^2}{V_{f1}^2}\sin^2\theta_0'}}, \quad a_{34} = 0,$$

$$a_{35} = \frac{-V_{s2}\gamma^f\eta_2'\omega\sqrt{1 - \frac{V_{f2}^2}{V_{f1}^2}\sin^2\theta_0'}}{\eta_2 V_{f2}\gamma^s\sqrt{1 - \frac{V_{s2}^2}{V_{f1}^2}\sin^2\theta_0'}}, \quad a_{36} = \frac{-V_{s2}\gamma^f\eta_3'\omega\sqrt{1 - \frac{V_{f3}^2}{V_{f1}^2}\sin^2\theta_0'}}{\eta_2 V_{f3}\gamma^s\sqrt{1 - \frac{V_{s2}^2}{V_{f1}^2}\sin^2\theta_0'}},$$

$$a_{41} = 1, \quad a_{42} = \frac{-V_{f1}\sqrt{1 - \frac{V_{s2}^2}{V_{f1}^2}\sin^2\theta_0'}}{V_{s2}\sin\theta_0'}, \quad a_{43} = \frac{-V_{f1}\sqrt{1 - \frac{V_{s3}^2}{V_{f1}^2}\sin^2\theta_0'}}{V_{s3}\sin\theta_0'},$$

$$a_{44} = -1, \quad a_{45} = \frac{-V_{f1}\sqrt{1 - \frac{V_{f2}^2}{V_{f1}^2}\sin^2\theta_0'}}{V_{f2}\sin\theta_0'}, \quad a_{46} = \frac{-V_{f1}\sqrt{1 - \frac{V_{f3}^2}{V_{f1}^2}\sin^2\theta_0'}}{V_{f3}\sin\theta_0'},$$

$$a_{51} = \frac{V_{f1}\sqrt{1 - \frac{V_{s1}^2}{V_{f1}^2}\sin^2\theta_0'}}{V_{s1}\cos\theta_0'}, \quad a_{52} = \tan\theta_0', \quad a_{53} = \tan\theta_0', \quad a_{54} = 1,$$

$$a_{55} = -\tan\theta_0', \quad a_{56} = -\tan\theta_0', \quad a_{61} = 0, \quad a_{62} = 1, \quad a_{63} = \frac{\eta_3}{\eta_2},$$

$$a_{64} = 0, \quad a_{65} = \frac{-\eta_2'}{\eta_2}, \quad a_{66} = \frac{-\eta_3'}{\eta_2},$$

$S = [-1 \;\; 1 \;\; 0 \;\; 1 \;\; 1 \;\; 0]^t$ and the elements of the matrix R are given by

$$R_1 = A_1/A_0', \quad R_2 = A_2/A_0', \quad R_3 = A_3/A_0', \quad R_1' = A_1'/A_0', \quad R_2' = A_2'/A_0', \quad R_3' = A_3'/A_0'.$$

Here $R_i \;\; (i = 1, 2, 3)$ are the amplitude ratios corresponding to the refracted longitudinal displacement wave at an angle θ_1, refracted coupled waves at angles θ_2 and θ_3, respectively and $R_i' \;\; (i = 1, 2, 3)$ are the amplitude ratios for the reflected longitudinal displacement wave at an angle θ_1', reflected coupled waves at angles θ_2' and θ_3', respectively.

4.5 Energy partitioning

We shall now consider the partitioning of incident energy between different reflected and refracted waves at the surface element of unit area. Following Achenbach (1973), the instantaneous rate of work of surface traction is the scalar product of the surface traction and the particle velocity. This scalar product is called the power per unit area, denoted by P^*, and represents the rate at which the energy is transmitted per unit area of the surface, i.e., the energy flux across the surface element. The time average of P^* over a period, denoted by $< P^* >$, represents the average energy transmission per unit surface area per unit time. For the cases considered above, the rate of energy transmission at the free surface $z = 0$ is given by: In the *Case I*,

$$P^* = \sum_{r=s,f} \tau_{zz}^r \dot{u}_3^r + \tau_{zx}^r \dot{u}_1^r + m_{zy}^r \dot{\phi}_2^r, \tag{4.36}$$

where superposed dot represents the temporal derivative. The real part of $< P^* >$ gives the time averaged intensity vector and imaginary part equal to the amplitude of the reactive intensity. We shall now calculate P^* for the incident and each of the reflected waves using the appropriate potentials and hence obtain the energy ratios giving the time rate of average energy transmission for the respective wave to that of the incident wave. The expressions for these energy ratios $E_i (i = 1, ..., 6)$ for the reflected and refracted waves are given by

$$E_i =< P_i^* > / < P_0^* >, \quad (i = 1, ..., 6) \tag{4.37}$$

where

$$< P_0^* >= \frac{1}{2}(\lambda^s + 2\mu^s + K^s)\cos\theta_0\omega_1 k_1^3 A_0^2 \exp\{\imath k_1 \sin\theta_0 x\},$$

$$< P_1^* >= -\frac{1}{2}(\lambda^s + 2\mu^s + K^s)\cos\theta_1\omega_1 k_1^3 A_1^2 \exp\{\imath k_1 \sin\theta_1 x\},$$

$$< P_2^* >= -\frac{1}{2}[(\mu^s + K^s) - \frac{\eta_2}{k_2^2}(K^s + \gamma^s\eta_2)]\cos\theta_2\omega_2 k_2^3 A_2^2 \exp\{\imath k_2 \sin\theta_2 x\},$$

$$< P_3^* >= -\frac{1}{2}[(\mu^s + K^s) - \frac{\eta_3}{k_3^2}(K^s + \gamma^s\eta_3)]\cos\theta_3\omega_3 k_3^3 A_3^2 \exp\{\imath k_3 \sin\theta_3 x\},$$

$$< P_4^* >= -\frac{\imath}{2}(\lambda^f + 2\mu^f + K^f)\cos\theta_1'\omega_1'^2 k_1'^3 A_1'^2 \exp\{\imath k_1' \sin\theta_1' x\},$$

$$< P_5^* >= -\frac{\imath}{2}[(\mu^f + K^f) - \frac{\eta_2'}{k_2'^2}(K^f + \gamma^f\eta_2')]\cos\theta_2'\omega_2'^2 k_2'^3 A_2'^2 \exp\{\imath k_2' \sin\theta_2' x\},$$

$$< P_6^* >= -\frac{\imath}{2}[(\mu^f + K^f) - \frac{\eta_3'}{k_3'^2}(K^f + \gamma^f\eta_3')]\cos\theta_3'\omega_3'^2 k_3'^3 A_3'^2 \exp\{\imath k_3' \sin\theta_3' x\}.$$

Similarly, for the *Case II*, using equation (4.36), the expressions for $< P_i^* >$ are the same as given above except the expression of $< P_0^* >$, which is given by

$$< P_0^* >= \frac{\imath}{2}(\lambda^f + 2\mu^f + K^f)\omega_1'^2 k_1'^3 \cos\theta_0' A_0'^2 \exp\{\imath k_1' \sin\theta_0' x\}.$$

4.6 Dispersion relation of Stoneley waves

To obtain the dispersion equation for Stoneley waves at the interface between a micropolar solid half-space and a micropolar fluid half-space, we shall take the following potentials satisfying the radiation conditions in the two half spaces. In the lower half-

space M_1,

$$L^s = A\exp(-S^s z)\exp\{\imath(kx-\omega t)\}, \tag{4.38}$$

$$M^s = \{B\exp(-P^s z) + E\exp(-Q^s z)\}\exp\{\imath(kx-\omega t)\}, \tag{4.39}$$

$$\phi_2^s = \{c^s B\exp(-P^s z) + d^s E\exp(-Q^s z)\}\exp\{\imath(kx-\omega t)\}, \tag{4.40}$$

and in the upper half-space M_2,

$$L^f = A'\exp(S^f z)\exp\{\imath(kx-\omega t)\}, \tag{4.41}$$

$$M^f = \{B'\exp(P^f z) + E'\exp(Q^f z)\}\exp\{\imath(kx-\omega t)\}, \tag{4.42}$$

$$\phi_2^f = \{c^f B'\exp(P^f z) + d^f E'\exp(Q^f z)\}\exp\{\imath(kx-\omega t)\}, \tag{4.43}$$

where

$$S^s = \sqrt{k^2 - \frac{\rho^s\omega^2}{\lambda^s+2\mu^s+K^s}}, \quad S^f = \sqrt{k^2 - \frac{\imath\rho^f\omega}{\lambda^f+2\mu^f+K^f}},$$

$$P^{s2},\ Q^{s2} = k^2 - \frac{1}{2}[(\frac{\rho^s j^s\omega^2 - 2K^s}{\gamma^s} + \frac{\gamma^s\rho^s\omega^2+K^{s2}}{\gamma^s(\mu^s+K^s)})$$

$$\pm\sqrt{\{\frac{\rho^s j^s\omega^2-2K^s}{\gamma^s} + \frac{\gamma^s\rho^s\omega^2+K^{s2}}{\gamma^s(\mu^s+K^s)}\}^2 - 4\frac{\rho^s\omega^2(\rho^s j^s\omega^2-2K^s)}{\gamma^s(\mu^s+K^s)}}],$$

$$P^{f2},\ Q^{f2} = k^2 - \frac{1}{2}[(\frac{\imath\rho^f j^f\omega - 2K^f}{\gamma^f} + \frac{\imath\gamma^f\rho^f\omega+K^{f2}}{\gamma^f(\mu^f+K^f)})$$

$$\pm\sqrt{\{\frac{\imath\rho^f j^f\omega-2K^f}{\gamma^f} + \frac{\imath\gamma^f\rho^f\omega+K^{f2}}{\gamma^f(\mu^f+K^f)}\}^2 + 4\frac{\rho^f\omega K^f}{\gamma^f(\mu^f+K^f)}(2\imath + \frac{\omega\rho^f j^f}{K^f})}],$$

$$c^s = \{(\mu^s+K^s)(-k^2+P^{s2}) + \rho^s\omega^2\}/K^s, \quad d^s = \{(\mu^s+K^s)(-k^2+Q^{s2}) + \rho^s\omega^2\}/K^s,$$

$$c^f = \{(\mu^f+K^f)(-k^2+P^{f2}) + \imath\rho^f\omega\}/K^f, \quad d^f = \{(\mu^f+K^f)(-k^2+Q^{f2}) + \imath\rho^f\omega\}/K^f.$$

Using Helmholtz decomposition of a vector, the $x-$ and $z-$ components of displacements denoted by u_1^r and u_3^r in the solid and fluid half-spaces are related to the above potentials, through the following relations

$$u_1^r = \frac{\partial L^r}{\partial x} + \frac{\partial M^r}{\partial z}, \quad u_3^r = \frac{\partial L^r}{\partial z} - \frac{\partial M^r}{\partial x}, \quad (r = s, f).$$

Substituting these values into the boundary conditions for bonded interface given in (4.21), we obtain six homogeneous equations in six unknowns namely A, B, E, A', B' and E'. The condition for non-trivial solutions of these equations would give the dispersion equation for the propagation of Stoneley waves. The required conditions is that the determinant of the coefficient matrix $[b_{ij}]$ (say) must vanish.

$$\begin{vmatrix} b_{11} & b_{12} & b_{13} & b_{14} & b_{15} & b_{16} \\ b_{21} & b_{22} & b_{23} & b_{24} & b_{25} & b_{26} \\ \imath k & -P^s & -Q^s & -\imath k & -P^f & -Q^f \\ -S^s & -\imath k & -\imath k & -S^f & \imath k & \imath k \\ 0 & c^s & d^s & 0 & -c^f & -d^f \\ 0 & -\gamma^s P^s c^s & -\gamma^s Q^s d^s & 0 & \imath\omega\gamma^f P^f c^f & \imath\omega\gamma^f Q^f d^f \end{vmatrix} = 0, \tag{4.44}$$

where

$b_{11} = [-k^2\lambda^s + (\lambda^s + 2\mu^s + K^s)S^{s2}]$, $b_{12} = [\imath kP^s(2\mu^s + K^s)]$, $b_{13} = [\imath k(2\mu^s + K^s)Q^s]$, $b_{14} = \imath\omega[-k^2\lambda^f + (\lambda^f + 2\mu^f + K^f)S^{f2}]$, $b_{15} = [\omega kP^f(2\mu^f + K^f)]$, $b_{16} = [\omega kQ^f(2\mu^f + K^f)]$, $b_{21} = [-\imath kS^s(2\mu^s + K^s)]$, $b_{22} = [\mu^s k^2 + (\mu^s + K^s)P^{s2} - K^s c^s]$, $b_{23} = [\mu^s k^2 + (\mu^s + K^s)Q^{s2} - K^s d^s]$, $b_{24} = -[\omega kS^f(2\mu^f + K^f)]$, $b_{25} = \imath\omega[\mu^f k^2 + (\mu^f + K^f)P^{f2} - K^f c^f]$, $b_{26} = \imath\omega[\mu^f k^2 + (\mu^f + K^f)Q^{f2} - K^f d^f]$.

We note that the frequency equation is an implicit function of the phase velocity and the wavenumber and involves complex quantities. Therefore, it is expected that the Stoneley waves are dispersive and attenuated. This equation also depend on the fluid viscosity coefficients and elastic properties of the solid half-space. The effect of these parameters on the dispersion curves have been noticed numerically.

4.7 Limiting cases

(I) To discuss the reflection and transmission of longitudinal displacement wave when propagating through the micropolar solid half-space is made incident at micropolar

solid/ viscous fluid interface, the formulae for the reflection and transmission coefficients are obtained from equations (4.22)- (4.27) by putting $\eta = \mu^f$ and $K' = (\lambda^f + \frac{2}{3}\mu^f)\frac{\partial}{\partial t}$. We see that the equations (4.24) and (4.27) reduce to a single equation given by

$$\eta_2 k_2 \cos\theta_2 A_2 + \eta_3 k_3 \cos\theta_3 A_3 = 0,$$

and the remaining equations reduce to

$$-k_1^2[\lambda^s + (2\mu^s + K^s)\cos^2\theta_0]A_0 - k_1^2[\lambda^s + (2\mu^s + K^s)\cos^2\theta_0]A_1 - (2\mu^s + K^s)k_2^2\frac{V_{s2}}{V_{s1}}\sin\theta_0$$

$$\times\sqrt{1 - \frac{V_{s2}^2}{V_{s1}^2}\sin^2\theta_0}A_2 - (2\mu^s + K^s)k_3^2\frac{V_{s3}}{V_{s1}}\sin\theta_0\sqrt{1 - \frac{V_{s3}^2}{V_{s1}^2}\sin^2\theta_0}A_3$$

$$-\imath\omega k_1'^2\left[\lambda^f + 2\mu^f\left(1 - \frac{V_{f1}^2}{V_{s1}^2}\sin^2\theta_0\right)\right]A_1' + 2\imath\mu^f\omega k_3'^2\frac{V_{f3}}{V_{s1}}\sin\theta_0\sqrt{1 - \frac{V_{f3}^2}{V_{s1}^2}\sin^2\theta_0}A_3' = 0,$$

$$(2\mu^s + K^s)k_1^2\sin\theta_0\cos\theta_0 A_0 - (2\mu^s + K^s)k_1^2\sin\theta\cos\theta A_1 + [\mu^s k_2^2\left(1 - 2\frac{V_{s2}^2}{V_{s1}^2}\sin^2\theta_0\right)$$

$$+K^s k_2^2(1 - \frac{V_{s2}^2}{V_{s1}^2}\sin^2\theta_0) - K^s\eta_2]A_2 + [\mu^s k_3^2\left(1 - 2\frac{V_{s3}^2}{V_{s1}^2}\sin^2\theta_0\right) + K^s k_3^2\left(1 - \frac{V_{s3}^2}{V_{s1}^2}\sin^2\theta_0\right)$$

$$-K^s\eta_3]A_3 + 2\mu^f\imath k_1'^2\omega\sin\theta_0\frac{V_{f1}}{V_{s1}}\sqrt{1 - \frac{V_{f1}^2}{V_{s1}^2}\sin^2\theta_0}A_1' + \left[\imath\mu^f\omega k_3'^2\left(1 - 2\frac{V_{f3}^2}{V_{s1}^2}\sin^2\theta_0\right)\right]A_3' = 0,$$

$$k_1\sin\theta_0 A_0 + k_1\sin\theta_1 A_1 - k_2\cos\theta_2 A_2 - k_3\cos\theta_3 A_3 - k_1'\sin\theta_1' A_1 - k_3'\cos\theta_3' A_3' = 0,$$

$$-k_1\cos\theta_0 A_0 + k_1\cos\theta_1 A_1 + k_2\sin\theta_3 A_3 + k_1'\cos\theta_1' A_1' - k_3'\sin\theta_3' A_3' = 0,$$

where now $V_{f1}^2 = -\imath\omega c_{1f}^2$, $V_{f2} = 0$ and $V_{f3}^2 = -\imath\omega c_{2f}^2$.
These equations match with those obtained by Kumar and Tomar (2001) for the relevant problem.

(II) To obtain the reflection and transmission coefficients of longitudinal displacement wave at micropolar solid/solid interface, we replace the quantities $-\imath\omega\lambda^f$ by λ', $-\imath\omega\mu^f$ by μ', $-\imath\omega K^f$ by K', $-\imath\omega\gamma^f$ by γ', $-\imath\omega\alpha^f$ by α' and $-\imath\omega\beta^f$ by β'. The six homogeneous equations (4.22) - (4.27) reduce to

$$(\lambda^s + (2\mu^s + K^s)\cos^2\theta_0)k_1^2 A_0 + (\lambda^s + (2\mu^s + K^s)\cos^2\theta_1)k_1^2 A_1 + (2\mu^s + K^s)k_2^2\sin\theta_2\cos\theta_2 A_2$$

$$+(2\mu^s + K^s)k_3^2\sin\theta_3\cos\theta_3 A_3 - (\lambda' + (2\mu' + K')\cos^2\theta_1')k_1'^2 A_1' + (2\mu' + K')k_2'^2\sin\theta_2'\cos\theta_2' A_2'$$

$$+(2\mu' + K')k_3'^2 \sin\theta_3' \cos\theta_3' A_3' = 0,$$

$$(2\mu^s+K^s)\sin\theta_0\cos\theta_0 k_1^2 A_0-(2\mu^s+K^s)\sin\theta_0\cos\theta_0 k_1^2 A_1+[\mu^s\cos 2\theta_2+K^s\cos^2\theta_2-\frac{K^s\eta_2}{k_2^2}]k_2^2 A_2$$

$$+[\mu^s\cos 2\theta_3 + K^s\cos^2\theta_3 - \frac{K^s\eta_3}{k_3^2}]k_3^2 A_3 - (2\mu' + K')\sin\theta_1'\cos\theta_1' k_1'^2 A_1'$$

$$-[\mu\cos 2\theta_2' + K\cos^2\theta_2' - \frac{K'\eta_2'}{k_2'^2}]k_2'^2 A_2' - [\mu'\cos 2\theta_3' + K'\cos^2\theta_3' - \frac{K'\eta_3'}{k_3'^2}]k_3'^2 A_3' = 0,$$

$$\gamma^s\eta_2 k_2\cos\theta_2 A_2 + \gamma^s\eta_3 k_3\cos\theta_3 A_3 + \gamma'\eta_2' k_2'\cos\theta_2' A_2' + \gamma'\eta_3' k_3'\cos\theta_3' A_3' = 0,$$

$$\sin\theta_0 k_1 A_0 + \sin\theta_1 k_1 A_1 - \sum_{2,3}(k_i\cos\theta_i A_i + k_i'\cos\theta_i' A_i') - \sin\theta_1' k_1' A_1 = 0,$$

$$\cos\theta_0 k_1 - k_1\cos\theta_1 A_1 - \sum_{2,3}(k_i\sin\theta_i A_i - k_i'\sin\theta_i' A_i') - k_1'\cos\theta_1' A_1' = 0,$$

$$\eta_2 A_2 + \eta_3 A_3 - \eta_2' A_2' - \eta_3' A_3' = 0.$$

These equations are same as Tomar and Gogna (1995b) after converting the angle of incidence to angle of emergence.

(III) To obtain the dispersion relation of Stoneley waves at the viscous fluid/ elastic solid interface, we shall neglect the parameters corresponding to micropolarity in both the half-spaces. Thus, on neglecting the quantities $K^r, \alpha^r, \beta^r, \gamma^r$ and j^r, equation (4.44) becomes

$$\begin{vmatrix} k^2(2\mu^s-\rho^s c^2) & 2\imath k\mu^s Q^s & \imath k^2 c(2k\mu^f - \imath\rho^f c) & 2ck^2\mu^f Q^f \\ -2\imath k S^s\mu^s & \mu^s(k^2+Q^{s2}) & -2ck^2 S^f\mu^f & \imath\mu^f kc(k^2+Q^{f2}) \\ \imath k & -Q^s & -\imath k & -Q^f \\ -S^s & -\imath k & -S^f & \imath k \end{vmatrix} = 0, \quad (4.45)$$

where $(S^s)^2 = k^2 - \dfrac{\rho^s\omega^2}{\lambda^s+2\mu^s}$, $(S^f)^2 = k^2 - \dfrac{\imath\rho^f\omega}{\lambda^f+2\mu^f}$, $(Q^s)^2 = k^2 - \dfrac{\rho^s\omega^2}{\mu^s}$ and $(Q^f)^2 = k^2 - \dfrac{\imath\rho^f\omega}{\mu^f}$.

Further, if we neglect the fluid viscosity μ^f and taking the bulk modulus in the inviscid liquid as $\lambda' = -\imath\omega\lambda^f$ in the above equation, then the above frequency equation for Stoneley wave matches with the frequency equation of Stoneley wave at inviscid liquid/elastic solid interface given in Ewing et al. (1957).

4.8 Numerical results and discussions

For numerical computations, we take the following values of the relevant parameters for both the half spaces. For micropolar elastic solid-M_1(Polyurethane closed cell foam) [see Hsia and Cheng (2006)]:

Symbol	Value
λ^s	$2.09730 \times 10^{10}\ dyne/cm^2$
μ^s	$0.91822 \times 10^{10}\ dyne/cm^2$
K^s	$0.22956 \times 10^{10}\ dyne/cm^2$
α^s	$-0.0000291 \times 10^{10}\ dyne$
β^s	$0.000045 \times 10^{10}\ dyne$
γ^s	$0.0000423 \times 10^{10}\ dyne$
j^s	$0.037\ cm^2$
ρ^s	$0.0034\ gm/cm^3$

For micropolar viscous fluid medium- M_2:

Symbol	Value
λ^f	$1.5 \times 10^{10}\ dyne\ sec/cm^2$
μ^f	$0.3 \times 10^{10}\ dyne\ sec/cm^2$
K^f	$0.00223 \times 10^{10}\ dyne\ sec/cm^2$
α^f	$0.00111 \times 10^{10}\ dyne\ sec$
β^f	$0.0022 \times 10^{10}\ dyne\ sec$
γ^f	$0.000222 \times 10^{10}\ dyne\ sec$
j^f	$0.0400\ cm^2$
ρ^f	$0.8\ gm/cm^3$

and $\omega/\omega_0 = 100$. The system of equations given in (4.28) and (4.35) are solved by Gauss elimination method. The values of the amplitude and energy ratios have been computed at different angles of incidence.

Figure 4.1 shows the variation of the modulus of amplitude ratios of various reflected and refracted waves with the angle of incidence (θ_0), when a plane longitudinal wave propagating with velocity V_{s1} is made incident from the micropolar elastic half-space. It is found that the variation of the modulus of these amplitude ratios is different for different values of θ_0. It can be noticed from Figure 4.1 that the reflection coefficient Z_1 decreases monotonically from the value 1 to the value 0.0066 at $\theta_0 = 62^o$ angle of

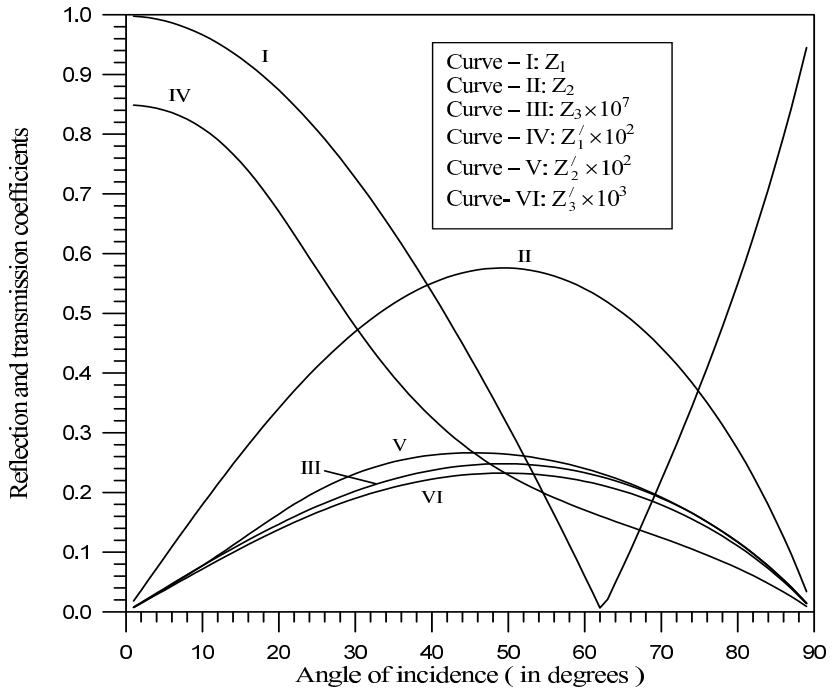

Figure 4.1: Incidence of longitudinal wave with velocity V_{s1}: Variation of reflection and transmission coefficients

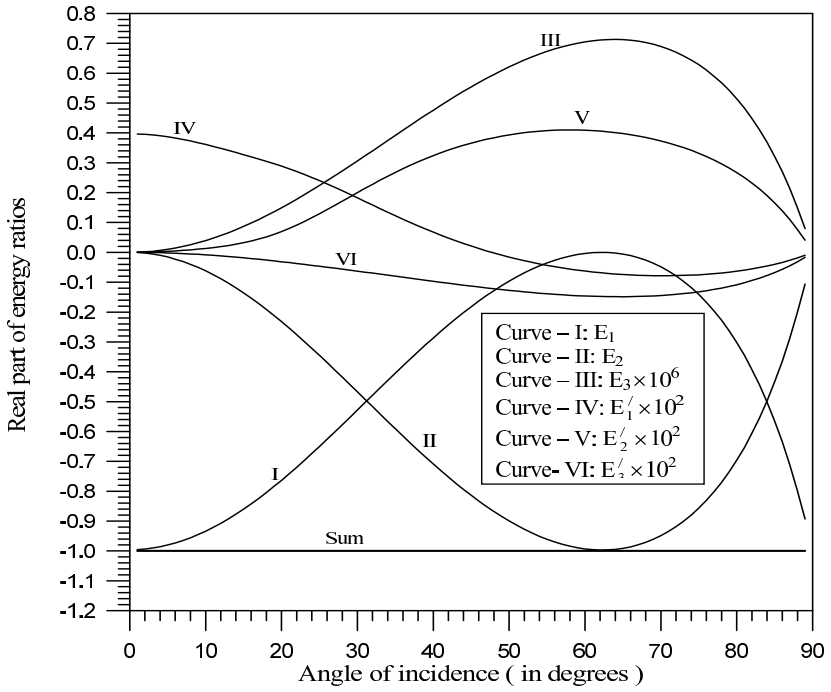

Figure 4.2: Incidence of longitudinal wave with velocity V_{s1}: Variation of real part of energy ratios.

incidence and then it starts increasing attaining its maximum value of equal to 1 at 90^o angle of incidence. The amplitude ratio Z_2 increases monotonically from the value 0 at 0^o angle of incidence, to the value 0.5760 at 49^o angle of incidence and thereafter, it starts decreasing and decreases to the value zero at 90^o angle of incidence. All the other amplitude ratios namely Z_3, Z_1', Z_2' and Z_3' are found to be very small in magnitude and hence they have been depicted after multiplying their original values with the factors 10^7, 10^2, 10^2 and 10^3 respectively. The reason of the amplitude ratios Z_1', Z_2' and Z_3' being too small is due to the big contrast in the densities of the fluid and solid half spaces. It has been found that if we increase the density of the micropolar solid half space to a certain extent, then amplitude ratios increase significantly at each angle of incidence. The amplitude ratios Z_2, Z_3, Z_2' and Z_3' have almost similar behavior with θ_0. Note that at grazing incidence, no reflected or refracted waves appear, except the reflected wave corresponding to the amplitude ratio Z_1. At normal incidence, only the reflected and refracted longitudinal displacement waves are found to appear.

When the longitudinal wave with velocity V_{s1} is made incident, the variations of the real part of the energy ratios of various reflected and refracted waves with respect to the angle of incidence is depicted through Figure 4.2. We see that at normal incidence, the value of the energy ration E_1 is -1. It starts increasing with increase in angle of incidence and reaches its maximum value zero at 62^o angle of incidence, thereafter, it starts decreasing and goes to the value -1 at 90^o angle of incidence. Curve II depicts the energy ratio of the reflected coupled wave with velocity V_{s2}, which is zero at zero degree of incidence and it decreases to the value -1 at 62^o angle of incidence, and after this it starts increasing and increases to the value zero at 90^o angle of incidence. Since the values of the amplitude ratios Z_3, Z_1', Z_2' and Z_3' were found to very small, therefore, the corresponding energy ratios E_3, E_1', A_2' and A_3' are also very very small and these have been shown after multiplying their original values by the factors 10^6, 10^2, 10^2 and 10^2 respectively.

Figure 4.3 depicts the variation of imaginary parts of the energy ratios of various reflected and transmitted waves with the angle of incidence. The imaginary parts of E_3, E_1', E_2' and E_3' are drawn after multiplying their original values by the factors 10^8, 10^2, 10^2 and 10^2 respectively. The sum of these imaginary parts of all the energy ratios is equal to zero as was predicted in law of conservation of energy [see Ainslie and Burns (1995)]. In fact, what we have found is that the algebraic sum of the real

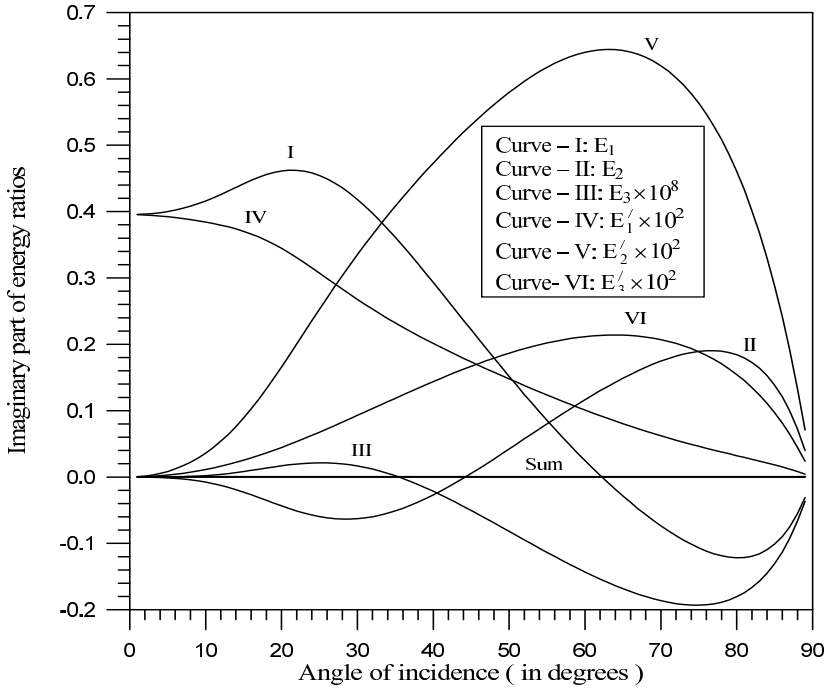

Figure 4.3: Incidence of longitudinal wave with velocity V_{s1}: Variation of imaginary part of energy ratios.

parts of energy ratios is equal to unity and the algebraic sum of the imaginary parts of the energy ratios vanish. Thus, the sum of the energy ratios of all the reflected and transmitted waves comes out to be unity.

Figure 4.4 depicts the variation of the modulus of the amplitude ratios of various reflected and refracted waves with the angle of incidence (θ_0'), when a longitudinal wave propagating with velocity V_{f1} is made incident from the micropolar fluid half-space. The values of the amplitude ratio R_1 decreases from a certain value 0.6598 at 1^0 angle of incidence and it decreases with θ_0' approaches to the value zero as $\theta_0' \rightarrow 90^0$, while the values of the amplitude ratio R_1' has value 0.9979 near normal incidence and then it decreases with θ_0', achieving its minimum value equal to 0.8362 at 59^o angle of incidence. Thereafter, it increases to its maximum value equal to 1 at 90^o angle of incidence. All the other amplitude ratios are found to behave alike with θ_0', but with differently. Note that at grazing incidence, no reflected or refracted wave was found to appear, except the reflected longitudinal displacement wave corresponding to the amplitude ratio R_1'. The amplitude ratios R_3 and R_3' are found to be very very small in comparison to the other amplitudes ratios. Hence, they have been shown on the graph after multiplying their original values by the factors 10^8 and 10^2 respectively.

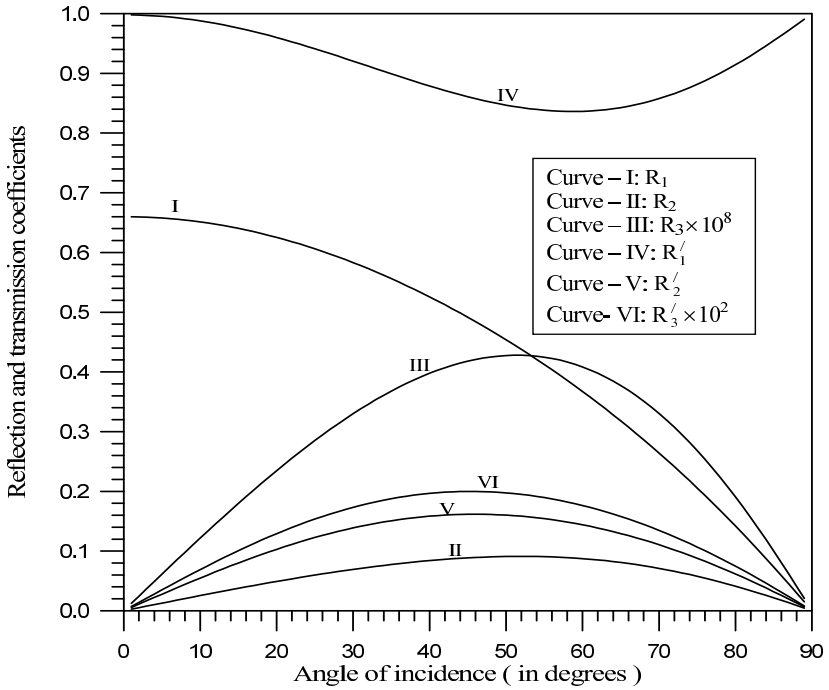

Figure 4.4: Incidence of longitudinal wave with velocity V_{f1}: Variation of reflection and transmission coefficients.

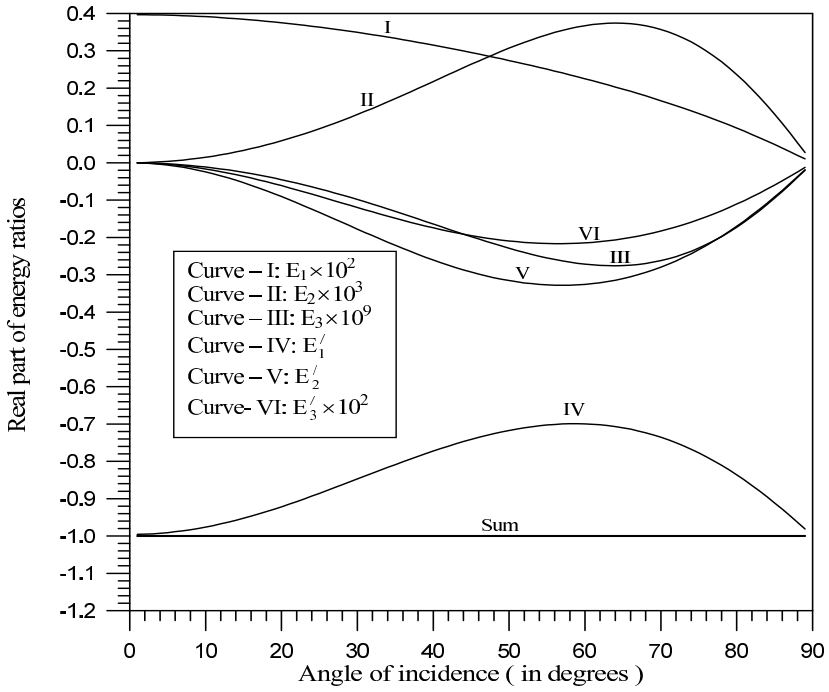

Figure 4.5: Incidence of longitudinal wave with velocity V_{f1}: Variation of real part of energy ratios.

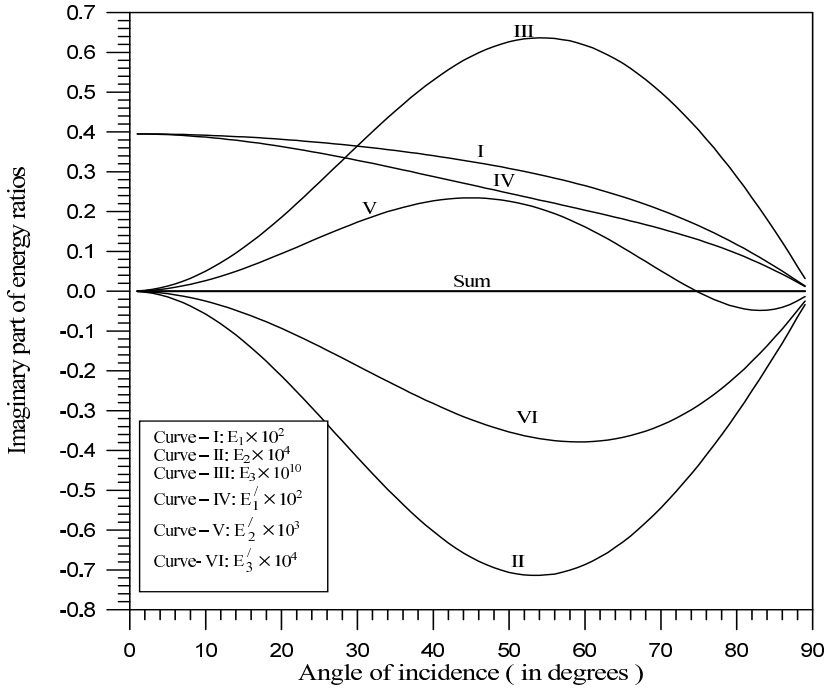

Figure 4.6: Incidence of longitudinal wave with velocity V_{f1}: Variation of imaginary part of energy ratios.

Figure 4.5 depicts the variation of the real parts of the energy ratios of various reflected and transmitted waves with the angle of incidence θ_0'. Since the numerical values of the energy ratios $E_1,\ E_2,\ E_3$ and E_3' are found to be very small in magnitude, therefore, we have depicted them after multiplying their original values by the factors $10^2,\ 10^3,\ 10^9$, and 10^2 respectively. Curve IV depicts the energy ratio of reflected longitudinal displacement wave propagating with velocity V_{f1}. It is seen that its value equal to -1 at 0^o angle of incidence, increases to the value -0.6992 at 59^o angle of incidence and after this, it decreases to the value zero at 90^o angle of incidence. Curve V depicts the variation of real part of energy ratio of reflected coupled wave with velocity V_{f2}. It starts from the value zero and decreases to the value -0.3285 at 57^o of incidence and it again increases to the value 1 at 90^o of incidence. We see that the energy carried by the reflected longitudinal displacement wave with velocity V_{f1} and by the reflected coupled wave with velocity V_{f2} are dominant.

Figure 4.6 shows the variation of the imaginary parts of energy ratios with the angle of incidence, when a longitudinal wave with velocity V_{f1} is made incident. Since all the values of imaginary parts of energy ratios are very small in magnitude, therefore, they have been drawn after multiplying their original values by the factors $10^2,\ 10^4,\ 10^{10},\ 10^2,\ 10^3$

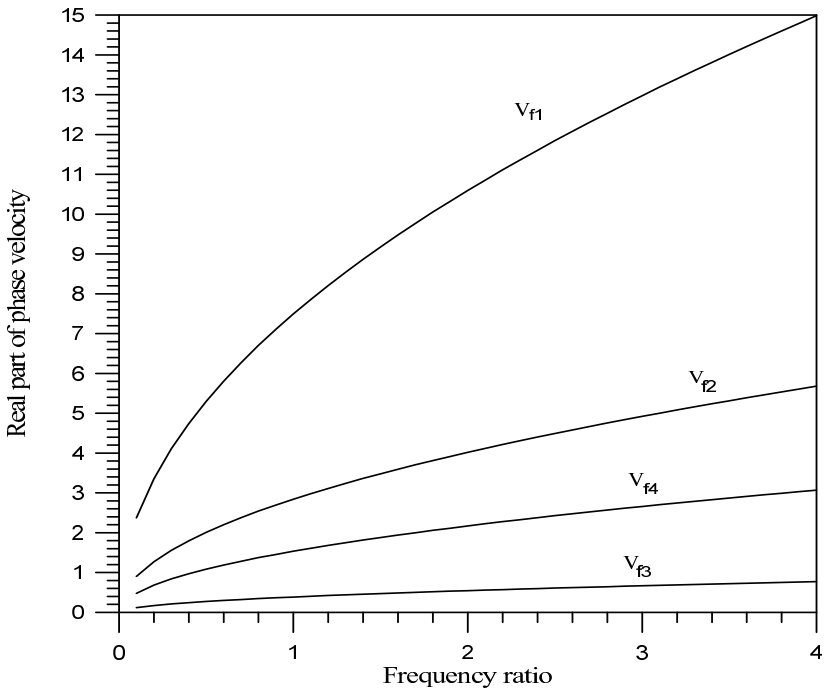

Figure 4.7: Real part of phase velocities of micropolar fluid versus frequency ratio ω/ω_0.

and 10^4 respectively. The algebraic sum of the imaginary parts of energy ratios is found to be equal to zero, while the algebraic sum of the real parts of these energy ratios is found to be equal to unity in magnitude. This verify the energy balance law at the interface.

Figures 4.7 and 4.8 depict the variation of the real and imaginary parts of the velocities of waves in micropolar fluid with respect to the non-dimensional frequency (ω/ω_0). It is clear from figure 4.7 that the velocity V_{f1} of longitudinal displacement wave is more than the velocities of remaining waves. We found that $Re(V_{f1}) > Re(V_{f2}) > Re(V_{f4}) > Re(V_{f3})$. Figure 4.8 shows that all the imaginary parts of the velocities decrease with non-dimensional frequency, but differently. It can be concluded that longitudinal displacement wave is more attenuated than the other waves and the amount of attenuation increase with increase of the frequency.

For a given real value of non-dimensional wavenumber, the value of non-dimensional phase velocity of Stoneley waves is computed from the determinantal equation (4.44). The value of the non-dimensional phase velocity of Stoneley waves is found to be complex, whose imaginary part corresponds to the measures of the attenuation of Stoneley waves.

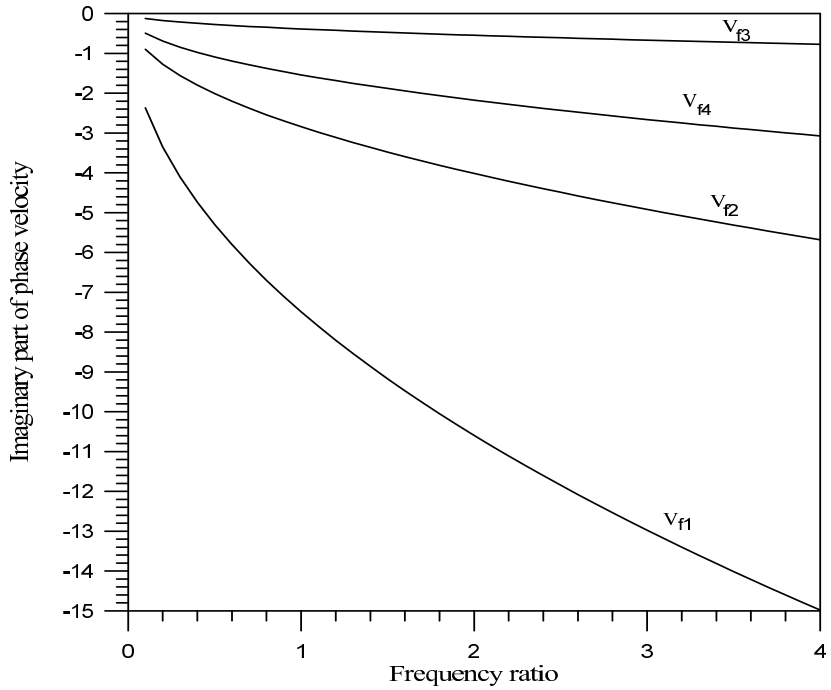

Figure 4.8: Imaginary part of phase velocities of micropolar fluid versus frequency ratio ω/ω_0.

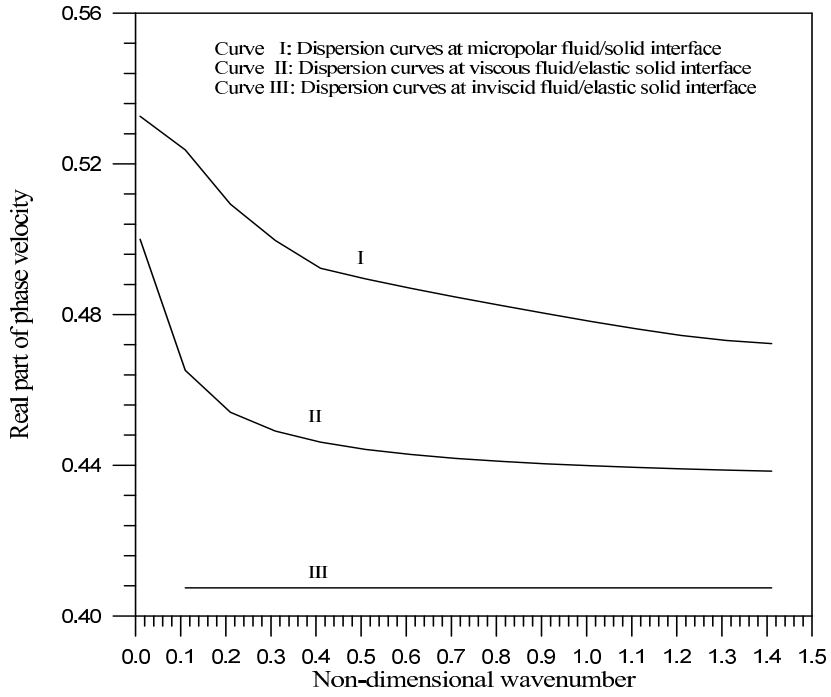

Figure 4.9: Comparison of real part of Stoneley wave velocity.

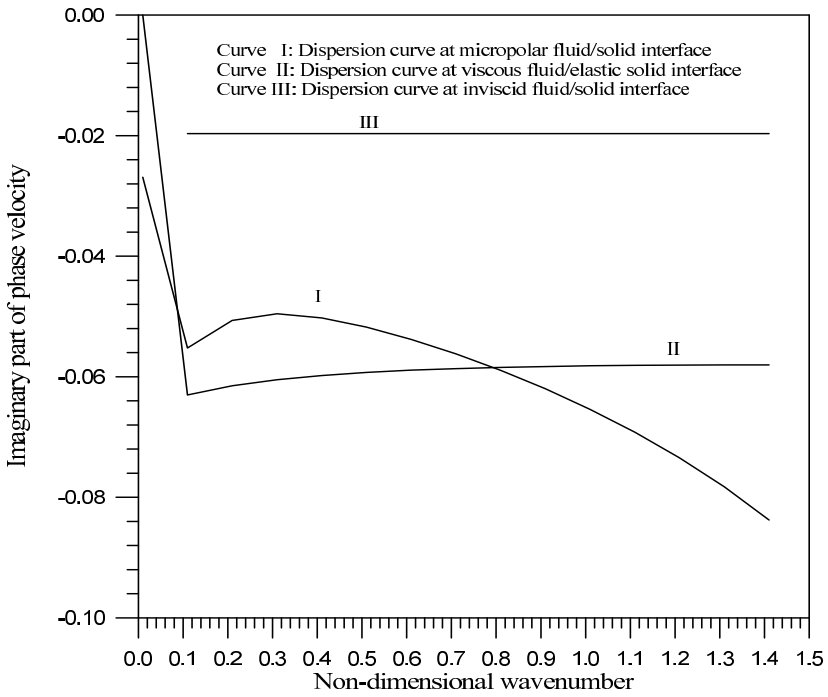

Figure 4.10: Comparison of imaginary part of Stoneley wave velocity.

Figure 4.9 depicts the variation of the real part of the phase velocity of Stoneley waves for different models. Curves I, II and III respectively correspond to the dispersion curves at micropolar fluid/micropolar solid, non-polar viscous fluid/elastic solid and inviscid fluid/elastic solid interface. The effect of micropolarity and viscosity can be clearly noticed on the dispersion curves. We notice that the viscosity of the fluid is responsible to enhance the real part of the phase velocity of Stoneley waves. This is further enhanced due to the micropolar properties of the half-spaces.

Figure 4.10 shows the corresponding variations in the imaginary parts of the phase velocity of Stoneley waves in the models considered. It can be seen from these figures that the Stoneley waves at inviscid liquid/elastic solid interface are attenuated but non-dispersive for the considered model, while at viscous fluid/elastic solid and micropolar fluid/micropolar solid interfaces, the Stoneley waves are attenuated and dispersive also.

4.9 Conclusions

In this chapter, the possibility of plane wave propagation in Eringen's micropolar fluid of infinite extent has been explored. The reflection and transmission phenomena at a

plane interface between a micropolar fluid half-space and a micropolar solid half-space has also been investigated. The frequency equation of surface waves (Stoneley waves) at micropolar fluid/micropolar solid interface has been derived. It may be concluded that

(a) Four plane waves can exist in an infinite micropolar fluid propagating at distinct phase speeds.

(b) All of these waves are found to be dispersive and attenuated in nature.

(c) The reflection and transmission coefficients are found to be the function of the angle of incidence, elastic properties of the half-spaces and the frequency of the incidence wave.

(d) The real part of the Stoneley wave velocity propagating along a micropolar fluid/ micropolar solid interface, is found to be greater than that of propagating along non-polar viscous/nonviscous fluid and an elastic solid interface.

(e) At each angle of incidence, the sum of the real part of the energy ratios of various reflected and transmitted waves is found to be unity, while the sum of the imaginary parts of the energy ratios is found to be zero. This verifies the energy balance law at the interface during transmission phenomena of waves in non-dissipative media.

Chapter 5

Wave propagation in micropolar mixture of porous media[4]

5.1 Introduction

Eringen (2003a) developed a theory of micropolar mixture of porous media (non-reacting mixture of a micropolar elastic solid and a micropolar viscous fluid at a single temperature) to include the rotational degrees of freedom. In his theory, material points of each constituent of porous solid undergoes translation and rotation and hence possessing six degrees of freedom. Rotational degree of freedom is ignored in classical porous theories. Many engineering materials, as well as soils, rocks, granular materials, sand and underground water mixture may be modeled more realistically by means of micropolar continua. In this Chapter, we have explored the possibility of elastic wave propagation in an unbounded micropolar mixture of porous media. We have also studied a problem of reflection of coupled longitudinal waves from a free surface of a micropolar porous half-space. The half-space is taken as a mixture of micropolar elastic solid and a Newtonian liquid. Amplitude ratios and energy ratios of various reflected waves have been obtained in closed form. The expressions of displacements and micro-rotation on the surface of the half-space are also derived. Numerical computations are performed for a specific model and the results obtained are depicted graphically.

[4] ***International Journal of Engineering Science,* 44(18-19)**, 1304-1323(2006).

5.2 Basic equations and formulation of problem

The equations of motion in an isotropic mixture of micropolar elastic solid and a micropolar viscous fluid, in the absence of body force density and body couple density, are given by (Eringen, 2003a)

$$(c_{1s}^2+c_{3s}^2)\nabla(\nabla\cdot\mathbf{u}^s)-(c_{2s}^2+c_{3s}^2)\nabla\times(\nabla\times\mathbf{u}^s)+c_{3s}^2\nabla\times\boldsymbol{\phi}^s$$

$$-c_{4s}^2(\dot{\mathbf{u}}^s-\dot{\mathbf{u}}^f)=\frac{\partial^2\mathbf{u}^s}{\partial t^2}, \tag{5.1}$$

$$(c_{5s}^2+c_{6s}^2)\nabla(\nabla\cdot\boldsymbol{\phi}^s)-c_{6s}^2\nabla\times(\nabla\times\boldsymbol{\phi}^s)+c_{7s}^2(\nabla\times\ \mathbf{u}^s-2\boldsymbol{\phi}^s)$$

$$-c_{8s}^2(\dot{\boldsymbol{\phi}}^s-\dot{\boldsymbol{\phi}}^f)=\frac{\partial^2\boldsymbol{\phi}^s}{\partial t^2}, \tag{5.2}$$

$$(c_{1f}^2+c_{3f}^2)\nabla(\nabla\cdot\dot{\mathbf{u}}^f)-(c_{2f}^2+c_{3f}^2)\nabla\times(\nabla\times\dot{\mathbf{u}}^f)+c_{3f}^2\nabla\times\dot{\boldsymbol{\phi}}^f$$

$$+c_{4f}^2(\dot{\mathbf{u}}^s-\dot{\mathbf{u}}^f)=\frac{\partial^2\mathbf{u}^f}{\partial t^2}, \tag{5.3}$$

$$(c_{5f}^2+c_{6f}^2)\nabla(\nabla\cdot\dot{\boldsymbol{\phi}}^f)-c_{6f}^2\nabla\times(\nabla\times\dot{\boldsymbol{\phi}}^f)+c_{7f}^2(\nabla\times\ \dot{\mathbf{u}}^{\mathbf{f}}-2\dot{\phi}^f)$$

$$+c_{8f}^2(\dot{\boldsymbol{\phi}}^s-\dot{\boldsymbol{\phi}}^f)=\frac{\partial^2\boldsymbol{\phi}^f}{\partial t^2}, \tag{5.4}$$

where

$$c_{1s}^2=(\lambda^s+2\mu^s)/\rho^s,\quad c_{2s}^2=\mu^s/\rho^s,\quad c_{3s}^2=K^s/\rho^s,\quad c_{4s}^2=\xi/\rho^s,$$

$$c_{5s}^2=(\alpha^s+\beta^s)/\rho^s j^s,\quad c_{6s}^2=\gamma^s/\rho^s j^s,\quad c_{7s}^2=K^s/\rho^s j^s,\quad c_{8s}^2=\Omega/\rho^s j^s,$$

$$c_{1f}^2=(\lambda^f+2\mu^f)/\rho^f,\quad c_{2f}^2=\mu^f/\rho^f,\quad c_{3f}^2=K^f/\rho^f,\quad c_{4f}^2=\xi/\rho^f,$$

$$c_{5f}^2=(\alpha^f+\beta^f)/\rho^f j^f,\quad c_{6f}^2=\gamma^f/\rho^f j^f,\quad c_{7f}^2=K^f/\rho^f j^f,\quad c_{8f}^2=\Omega/\rho^f j^f,$$

and the symbols $\lambda^s,\ \mu^s,\ K^s,\ \alpha^s,\ \beta^s,\ \gamma^s,\ \rho^s,\ j^s,\ \lambda^f,\ \mu^f,\ K^f,\ \alpha^f,\ \beta^f,\ \gamma^f,\ \rho^f$ and j^f are defined in Chapter-4. The quantities ξ and Ω are the momentum generation coefficients due to the velocity difference and due to the difference in gyrations, respectively.

The constitutive relations in a linear isotropic micropolar mixture are given by (Eringen, 2003a)

$$\tau^s_{kl} = \lambda^s \nabla \cdot \mathbf{u}^s \delta_{kl} + \mu^s (u^s_{k,l} + u^s_{l,k}) + K^s (u^s_{l,k} + \varepsilon_{lkm} \phi^s_m), \tag{5.5}$$

$$m^s_{kl} = \alpha^s \nabla \cdot \boldsymbol{\phi}^s \delta_{kl} + \beta^s \phi^s_{k,l} + \gamma^s \phi^s_{l,k}, \tag{5.6}$$

$$\tau^f_{kl} = \lambda^f v^f_{m,m} \delta_{kl} + \mu^f (v^f_{k,l} + v^f_{l,k}) + K^f (v^f_{l,k} + \varepsilon_{lkm} \nu^f_m), \tag{5.7}$$

$$m^f_{kl} = \alpha^f \nabla \cdot \boldsymbol{\nu}^f \delta_{kl} + \beta^f \nu^f_{k,l} + \gamma^f \nu^f_{l,k}, \tag{5.8}$$

$$\hat{\mathbf{p}}^s = -\hat{\mathbf{p}}^f = -\xi(\dot{\mathbf{u}}^s - \mathbf{v}^f), \tag{5.9}$$

$$\hat{\mathbf{m}}^s = -\hat{\mathbf{m}}^f = -\Omega(\dot{\boldsymbol{\phi}}^s - \boldsymbol{\nu}^f), \tag{5.10}$$

where $\mathbf{v}^f = \dfrac{\partial \mathbf{u}^f}{\partial t}$ and $\boldsymbol{\nu}^f = \dfrac{\partial \boldsymbol{\phi}^f}{\partial t}$; The second order tensors, τ^s_{kl} and τ^f_{kl} are respectively the force stress tensors in micropolar solid and in micropolar fluid, while m^s_{kl} and m^f_{kl} are respectively the couple stress tensors in micropolar solid and in micropolar fluid, $\hat{\mathbf{p}}^s$ and $\hat{\mathbf{m}}^s$ are respectively, the force and the couple exerted on the solid constituent from the fluid constituent, $\hat{\mathbf{p}}^f$ and $\hat{\mathbf{m}}^f$ are respectively, the force and couple exerted on the fluid constituent from the solid constituent.
Introducing the scalar potentials $A^s,\ A^f,\ C^s$ and C^f, vector potentials $\mathbf{B}^s,\ \mathbf{B}^f,\ \mathbf{D}^s$ and $\mathbf{D}^f$ through Helmholtz representation of vector field, we can write

$$\mathbf{u}^s = \nabla A^s + \nabla \times \mathbf{B}^s, \quad \nabla \cdot \mathbf{B}^s = 0; \quad \mathbf{u}^f = \nabla A^f + \nabla \times \mathbf{B}^f, \quad \nabla \cdot \mathbf{B}^f = 0, \tag{5.11}$$

$$\boldsymbol{\phi}^s = \nabla C^s + \nabla \times \mathbf{D}^s, \quad \nabla \cdot \mathbf{D}^s = 0; \quad \boldsymbol{\phi}^f = \nabla C^f + \nabla \times \mathbf{D}^f, \quad \nabla \cdot \mathbf{D}^f = 0. \tag{5.12}$$

Plugging (5.11) and (5.12) into equations (5.1) to (5.4), we obtain

$$(c^2_{1s} + c^2_{3s}) \nabla^2 A^s - c^2_{4s} (\dot{A}^s - \dot{A}^f) = \ddot{A}^s, \tag{5.13}$$

$$(c_{1f}^2 + c_{3f}^2)\nabla^2 \dot{A}^f + c_{4f}^2(\dot{A}^s - \dot{A}^f) = \ddot{A}^f, \tag{5.14}$$

$$(c_{5s}^2 + c_{6s}^2)\nabla^2 C^s - 2c_{7s}^2 C^s - c_{8s}^2(\dot{C}^s - \dot{C}^f) = \ddot{C}^s, \tag{5.15}$$

$$(c_{5f}^2 + c_{6f}^2)\nabla^2 \dot{C}^f - 2c_{7f}^2 \dot{C}^f + c_{8f}^2(\dot{C}^s - \dot{C}^f) = \ddot{C}^f, \tag{5.16}$$

$$(c_{2f}^2 + c_{3f}^2)\nabla^2 \dot{\mathbf{B}}^f + c_{3f}^2 \nabla \times \dot{\mathbf{D}}^f + c_{4f}^2(\dot{\mathbf{B}}^s - \dot{\mathbf{B}}^f) = \ddot{\mathbf{B}}^f, \tag{5.17}$$

$$c_{6s}^2 \nabla^2 \mathbf{D}^s + c_{7s}^2 \nabla \times \mathbf{B}^s - 2c_{7s}^2 \mathbf{D}^s - c_{8s}^2(\dot{\mathbf{D}}^s - \dot{\mathbf{D}}^f) = \ddot{\mathbf{D}}^s, \tag{5.18}$$

$$(c_{2s}^2 + c_{3s}^2)\nabla^2 \mathbf{B}^s + c_{3s}^2 \nabla \times \mathbf{D}^s - c_{4s}^2(\dot{\mathbf{B}}^s - \dot{\mathbf{B}}^f) = \ddot{\mathbf{B}}^s, \tag{5.19}$$

$$c_{6f}^2 \nabla^2 \dot{\mathbf{D}}^f + c_{7f}^2 \nabla \times \dot{\mathbf{B}}^f - 2c_{7f}^2 \dot{\mathbf{D}}^f + c_{8f}^2(\dot{\mathbf{D}}^s - \dot{\mathbf{D}}^f) = \ddot{\mathbf{D}}^f. \tag{5.20}$$

We see that the equations (5.13) and (5.14) are coupled in scalar potentials A^s and A^f, the equations (5.15) and (5.16) are coupled in scalar potentials C^s and C^f; while the equations (5.17) to (5.20) are coupled in vector potentials $\mathbf{B}^s,\ \mathbf{B}^f,\ \mathbf{D}^s$ and $\mathbf{D}^f$.

5.3 Wave propagation

To discuss the possibility of plane wave propagation in an infinite medium of mixture of micropolar solid and viscous micropolar fluid, we shall first solve the equations (5.13) to (5.20). Consider the following form of plane waves propagating in the positive direction of a unit vector $\mathbf{n}$

$$\{A^s,\ A^f,\ C^s,\ C^f\} = \{a^s,\ a^f, c^s,\ c^f\} \exp\left[\imath k(\mathbf{n} \cdot \mathbf{r} - Vt)\right], \tag{5.21}$$

where $a^s,\ a^f,\ c^s$ and c^f are the constant complex scalar wave amplitudes, $\imath = \sqrt{-1}$, $\mathbf{r}$ is the position vector, V is the phase velocity in the direction of vector $\mathbf{n}$, k is the wavenumber and $\omega(= kV)$ is angular frequency. Inserting the values of potentials A^s and A^f from equation (5.21) into equations (5.13) and (5.14), we obtain a set of two

homogeneous equations in two unknown amplitudes, namely a^s and a^f. Eliminating these unknown constants, we get the following equation

$$a_1 V^4 - b_1 V^2 + c_1 = 0, \tag{5.22}$$

where

$$a_1 = \omega + \imath(c_{4s}^2 + c_{4f}^2),$$

$$b_1 = (c_{1s}^2 + c_{3s}^2)(\omega + \imath c_{4f}^2) + (c_{1f}^2 + c_{3f}^2)(c_{4s}^2\omega - \imath\omega^2),$$

$$c_1 = -\imath\omega^2(c_{1s}^2 + c_{3s}^2)(c_{1f}^2 + c_{3f}^2).$$

Similarly, inserting the values of C^s and C^f from (5.21) in equation (5.15) and (5.16), we obtain

$$a_2 V^4 - b_2 V^2 + c_2 = 0, \tag{5.23}$$

where

$$a_2 = [-2c_{7s}^2(2\imath c_{7f}^2 + \imath c_{8f}^2 + \omega) - 2c_{7f}^2\omega(c_{8f}^2 - \imath\omega) + \omega^2(\imath c_{8s}^2 + \imath c_{8f}^2 + \omega)],$$

$$b_2 = \omega^2[(c_{5s}^2 + c_{6s}^2)(2\imath c_{7f}^2 + \imath c_{8f}^2 + \omega) + (c_{5f}^2 + c_{6f}^2)(2\imath c_{7s}^2 + c_{8s}^2\omega - \imath\omega^2)],$$

$$c_2 = -\imath\omega^4(c_{5s}^2 + c_{6s}^2)(c_{5f}^2 + c_{6f}^2).$$

The roots of equations (5.22) and (5.23) are given by

$$V_{1,\,2}^2 = \frac{1}{2a_1}[b_1 \pm \sqrt{b_1^2 - 4a_1c_1}] \text{ and } V_{3,\,4}^2 = \frac{1}{2a_2}[b_2 \pm \sqrt{b_2^2 - 4a_2c_2}], \tag{5.24}$$

respectively. Here V_1^2 and V_3^2 are taken with 'plus' sign and V_2^2 and V_4^2 are taken with 'minus' sign. Insertion of (5.21) into equations (5.11) and (5.12) will show that the displacement vectors ($\mathbf{u}^s$, $\mathbf{u}^f$) and microrotation vectors ($\boldsymbol{\phi}^s$, $\boldsymbol{\phi}^f$) are parallel to the direction of $\mathbf{n}$. Hence, the waves propagating with phase velocities given by V_i (i=1,2,3,4) are longitudinal in nature. The waves propagating with velocities V_1 and V_2 may be called *coupled longitudinal displacement waves* and the waves propagating with velocities V_3 and V_4 may be called *coupled longitudinal microrotational waves*. These longitudinal waves are analogous to the longitudinal displacement and longitudinal microrotational waves of micropolar elasticity. In the limiting case, when the

presence of liquid is neglected, the velocities V_1 and V_3 reduce to the velocities of longitudinal displacement wave and longitudinal microrotational wave of micropolar theory for elastic solids. The other velocities V_2 and V_4 become zero in this limiting case. It is to be noted here that these coupled longitudinal displacement waves are analogous to the dialatational waves of classical elastic solid and fluid, while there are no classical analogy to the microrotation waves.

To solve equations (5.17) to (5.20), which are coupled in the vector potentials $\mathbf{B}^s,\ \mathbf{B}^f,\ \mathbf{D}^s,\ \mathbf{D}^f$, we take the following form of vector potentials

$$\{\mathbf{B}^s,\ \mathbf{B}^f,\ \mathbf{D}^s, \mathbf{D}^f\} = \{\mathbf{b}^s,\ \mathbf{b}^f\ , \mathbf{d}^s,\ \mathbf{d}^f\} \exp[\imath k(\mathbf{n}\cdot\mathbf{r} - Vt)], \tag{5.25}$$

where $\mathbf{b}^s,\ \mathbf{b}^f,\ \mathbf{d}^s$ and $\mathbf{d}^f$ are constant complex vector wave amplitudes and other symbols are defined earlier.

Plugging (5.25) into equations (5.17)-(5.20), we get four homogeneous vector equations in four unknowns

$$A_1\mathbf{b}^s + A_2\mathbf{b}^f + A_3\mathbf{n}\times\mathbf{d}^s = 0, \tag{5.26}$$

$$B_1\mathbf{n}\times\mathbf{b}^s + B_2\mathbf{d}^s + B_3\mathbf{d}^f = 0, \tag{5.27}$$

$$C_1\mathbf{b}^s + C_2\mathbf{b}^f + C_3\mathbf{n}\times\mathbf{d}^f = 0, \tag{5.28}$$

$$D_1\mathbf{n}\times\mathbf{b}^f + D_2\mathbf{d}^s + D_3\mathbf{d}^f = 0, \tag{5.29}$$

where

$$A_1 = -k^2(c_{2s}^2 + c_{3s}^2) + k^2V^2 + c_{4s}^2\imath kV, \quad A_2 = -c_{4s}^2\imath kV, \quad A_3 = c_{3s}^2\imath k,$$

$$B_1 = c_{7s}^2\imath k, \quad B_2 = -k^2c_{6s}^2 - 2c_{7s}^2 + c_{8s}^2\imath kV + k^2V^2, \quad B_3 = -c_{8s}^2\imath kV,$$

$$C_1 = -c_{4f}^2\imath kV, \quad C_2 = \imath k^3V(c_{2f}^2 + c_{3f}^2) + c_{4f}^2\imath kV + k^2V^2, \quad C_3 = k^2Vc_{3f}^2,$$

$$D_1 = c_{7f}^2k^2V, \quad D_2 = -\imath kVc_{8f}^2, \quad D_3 = c_{6f}^2k^3V\imath + 2c_{7f}^2\imath kV + c_{8f}^2\imath kV + k^2V^2.$$

Eliminating the vectors $\mathbf{b}^s$, $\mathbf{b}^f$, $\mathbf{d}^s$ and $\mathbf{d}^f$, we obtain

$$a_3V^4 + b_3V^2 + c_3 = 0, \tag{5.30}$$

and

$$N_1V^8 + N_2V^6 + N_3V^4 + N_4V^2 + N_5 = 0, \tag{5.31}$$

where

$$a_3 = (\imath c_{4f}^2 + \omega)[\imath(2c_{7f}^2 + c_{8f}^2) + \omega],$$

$$b_3 = \imath\omega^2(c_{2f}^2 + c_{3f}^2)[\imath(2c_{7f}^2 + c_{8f}^2) + \omega] + \imath c_{6f}^2\omega^2(\imath c_{4f}^2 + \omega) + c_{7f}^2c_{3f}^2\omega^2,$$

$$c_3 = -(c_{2f}^2 + c_{3f}^2)c_{6f}^2\omega^4,$$

$$N_1 = (\omega + \imath c_{4s}^2)(-2c_{7s}^2 + \imath c_{8s}^2\omega + \omega^2)(\omega + \imath c_{4f}^2)(2\imath c_{7f}^2 + \imath c_{8f}^2 + \omega) + c_{8s}^2c_{8f}^2\omega(\omega + \imath c_{4s}^2)$$
$$(\omega + \imath c_{4f}^2) + (-2c_{7s}^2 + \imath c_{8s}^2\omega + \omega^2)(2\imath c_{7f}^2 + \imath c_{8f}^2 + \omega)c_{4s}^2c_{4f}^2 + \omega c_{4s}^2c_{4f}^2c_{8s}^2c_{8f}^2,$$

$$N_2 = \omega[(\omega + \imath c_{4f}^2)(2\imath c_{7f}^2 + \imath c_{8f}^2 + \omega)[-(c_{2s}^2 + c_{3s}^2)(-2c_{7s}^2 + \imath c_{8s}^2\omega + \omega^2) - c_{6s}^2\omega(\omega + \imath c_{4s}^2)$$
$$-c_{7s}^2c_{3s}^2] + \omega\{(\omega + \imath c_{4s}^2)(-2c_{7s}^2 + \imath c_{8s}^2\omega + \omega^2)[\imath(c_{2f}^2 + c_{3f}^2)(2\imath c_{7f}^2 + \imath c_{8f}^2 + \omega)$$
$$+\imath c_{6f}^2(\imath c_{4f}^2+\omega)+c_{7f}^2c_{3f}^2]-\imath c_{7s}^2c_{4s}^2c_{8f}^2c_{3f}^2-\imath c_{3s}^2c_{8s}^2c_{4f}^2c_{7f}^2+c_{8s}^2c_{8f}^2[-(c_{2s}^2+c_{3s}^2)(\omega+\imath c_{4f}^2)$$
$$+\imath\omega(\omega+\imath c_{4s}^2)(c_{2f}^2+c_{3f}^2)]+c_{4s}^2c_{4f}^2[-c_{6s}^2(2\imath c_{7f}^2+\imath c_{8f}^2+\omega)+\imath c_{6f}^2(-2c_{7s}^2+c_{8s}^2\imath\omega+\omega^2)]\}],$$

$$N_3 = \omega^3[c_{6s}^2(c_{2s}^2 + c_{3s}^2)(\imath c_{4f}^2 + \omega)(2\imath c_{7f}^2 + \imath c_{8f}^2 + \omega) - [(c_{2s}^2 + c_{3s}^2)(-2c_{7s}^2 + \imath c_{8s}^2\omega + \omega^2)$$
$$+ \omega c_{6s}^2(\omega + \imath c_{4s}^2) + c_{7s}^2c_{3s}^2][\imath(c_{2f}^2 + c_{3f}^2)(2\imath c_{7f}^2 + \imath c_{8f}^2 + \omega) + \imath c_{6f}^2(\imath c_{4f}^2 + \omega) + c_{7f}^2c_{3f}^2]$$
$$- \omega\{[c_{6f}^2(c_{2f}^2 + c_{3f}^2)(\omega + \imath c_{4s}^2)(-2c_{7s}^2 + \imath c_{8s}^2\omega + \omega^2)$$
$$+\imath c_{8s}^2c_{8f}^2(c_{2s}^2 + c_{3s}^2)(c_{2f}^2 + c_{3f}^2) + \imath c_{4s}^2c_{4f}^2c_{6s}^2c_{6f}^2]\}],$$

$$N_4 = \omega^4[c_{6s}^2(c_{2s}^2 + c_{3s}^2)[\imath(c_{2f}^2 + c_{3f}^2)(2\imath c_{7f}^2 + \imath c_{8f}^2 + \omega) + \imath c_{6f}^2(\imath c_{4f}^2 + \omega) + c_{7f}^2c_{3f}^2]$$
$$+c_{6f}^2(c_{2f}^2 + c_{3f}^2)[(c_{2s}^2 + c_{3s}^2)(-2c_{7s}^2 + \imath c_{8s}^2\omega + \omega^2) + c_{6s}^2(\omega + \imath c_{4s}^2) + c_{7s}^2c_{3s}^2]],$$

$$N_5 = -\omega^7c_{6s}^2c_{6f}^2(c_{2s}^2 + c_{3s}^2)(c_{2f}^2 + c_{3f}^2).$$

The roots of equation (5.30) are given by

$$V^2_{5,\ 6} = \frac{1}{2a_3}[-b_3 \pm \sqrt{b_3^2 - 4a_3c_3}], \tag{5.32}$$

where V_5^2 is taken with 'plus' sign and V_6^2 is taken with 'minus' sign. It can be seen from the coefficients of equation (5.32) that the velocities $V_{5,6}^2$ depend purely on micropolar fluid viscosities and they do not depend on the properties of solid constituent. Moreover, if the constant γ^f is put equal to zero then the quantity V_6^2 vanishes. Also, if the constants K^f, ξ and Ω vanish, then the velocity V_5^2 reduces to $V_5^2 = \sqrt{-\imath\omega\mu^f/\rho^f}$, which is the velocity of transverse wave in viscous fluid. Equation (5.31) is not simple to solve analytically and the roots of this equation can be obtained by some numerical procedure. Since equation (5.31) is four degree equation in V^2, therefore it can give four roots, in general. Let these roots be $V_7^2,\ V_8^2,\ V_9^2$ and V_{10}^2. This means that equation (5.31) will represent four waves propagating with these velocities. Using (5.25) into second and fourth equations of (5.11) and (5.12), it becomes apparent that $\mathbf{n}\cdot\mathbf{b}^s = \mathbf{n}\cdot\mathbf{b}^f = \mathbf{n}\cdot\mathbf{d}^s = \mathbf{n}\cdot\mathbf{d}^f = 0$. Hence, all the four vectors $\mathbf{b}^s,\ \mathbf{b}^f,\ \mathbf{d}^s$ and $\mathbf{d}^f$ lie in a common plane whose unit normal is $\mathbf{n}$. This means that the waves propagating with velocities $V_j,\ (j = 5, 6, 7, 8, 9, 10)$ are transverse in nature. It is clear from the expressions of velocities that they depend on frequency. Hence, all waves propagating with these velocities are dispersive.

In a limiting case, when the presence of liquid is ignored, we see that the velocities given by V_5 and V_6 vanish and equation (5.31) reduces to

$$aV^4 + bV^2 + c = 0,$$

where $a = 1 - \frac{2c_{7s}^2}{\omega^2},\quad b = -[c_{2s}^2(1 - \frac{2c_{7s}^2}{\omega^2}) + c_{3s}^2(1 - \frac{c_{7s}^2}{\omega^2}) + c_{6s}^2]$ and $c = c_{6s}^2(c_{2s}^2 + c_{3s}^2)$. This equation is the same equation as obtained by Parfitt and Eringen (1969) and gives the velocities of *coupled transverse waves* in micropolar elastic solid. In another limiting case, when micropolarity of both fluid and solid constituents along with the moment generation coefficients are neglected, then one can verify that the reduced equations (5.30) and (5.31) yield two velocities given by $\sqrt{c_{2s}}$ and $\sqrt{-\imath\omega c_{2f}^2}$. These velocities are the velocities of purely transverse waves in classical elastic solid and viscous fluid, respectively.

Now, let us look at the behavior of these velocities at low and high frequencies.

For higher frequency waves, i.e., when $\omega \to \infty$, we see that the velocities of coupled longitudinal waves reduce to $V_1^2 = c_{1s}^2 + c_{3s}^2$ and $V_2^2 \to \infty$, while the velocities of coupled longitudinal microrotational waves $V_{3,4}^2 \to \infty$. The velocities of two coupled transverse waves reduce to $V_5^2 = V_6^2 = \infty$ and that of the remaining four coupled transverse waves reduce to $V_7^2 = V_8^2 = \infty$ and $V_9^2 = c_{6s}^2,\ V_{10}^2 = c_{2s}^2 + c_{3s}^2$. At low frequency waves, i.e., when $\omega \to 0$, all the velocities vanish except

$$V_1^2 = \frac{(c_{1s}^2 + c_{3s}^2)c_{4f}^2}{c_{4s}^2 + c_{4f}^2}.$$

5.4 Reflection of coupled longitudinal waves

We shall discuss the reflection phenomena of coupled longitudinal waves impinging obliquely at the stress free plane surface of a half-space H composed of mixture of a micropolar elastic solid and an inviscid non-polar simple liquid. Let $x - y$ axes be horizontal and $z-$axis be vertically downward. We shall discuss a two-dimensional problem in $x - z$ plane such that the $x-$ axis is along the free plane boundary of the half-space. The half-space H occupies the region $H = \{-\infty < x, y < \infty, z \geq 0\}$. Since we are considering simple inviscid liquid, therefore, we shall first find the expressions of velocities of existing waves in the mixture considered. For this substituting zero values of the parameters corresponding to micropolarity and viscosity of the fluid constituent, i.e., $c_{2f}^2 = c_{3f}^2 = c_{5f}^2 = c_{6f}^2 = c_{7f}^2 = c_{8f}^2 = c_{8s}^2 = 0$ into the expressions of velocities obtained earlier. From the expression given in (5.22), we obtain

$$V_{1,2}^2 = \frac{1}{2a_1'}[b_1' \pm \sqrt{b_1'^2 - 4a_1'c_1'}], \tag{5.33}$$

where

$$a_1' = \omega + \imath(c_{4s}^2 + c_{4f}^2), \qquad b_1' = (c_{1s}^2 + c_{3s}^2)(\imath c_{4f}^2 + \omega) + c_{1f}^2\omega(c_{4s}^2 - \imath\omega)$$

and

$$c_1' = -\imath(c_{1s}^2 + c_{3s}^2)c_{1f}^2\omega^2.$$

These are the velocities of coupled longitudinal displacement waves in a mixture consisting of micropolar elastic solid constituent and inviscid liquid constituent. From the

expression of velocity given in (5.23), we obtain

$$V_3^2 = [c_{5s}^2 + c_{6s}^2]\left[1 - 2\frac{c_{7s}^2}{\omega^2}\right]^{-1}, \tag{5.34}$$

which is the velocity of longitudinal microrotational wave in micropolar solid constituent. From the expressions of velocities given in (5.31), we obtain

$$V_{9,10}^2 = \frac{1}{2n_1}[n_2 \pm \sqrt{n_2^2 - 4n_1 n_3}], \tag{5.35}$$

where $n_1 = (\omega^2 - 2c_{7s}^2)\{(\omega + \imath c_{4s}^2)(\omega + \imath c_{4f}^2) + c_{4s}^2 c_{4f}^2\},\ n_3 = \omega^3 c_{6s}^2(c_{2s}^2 + c_{3s}^2)(\imath c_{4f}^2 + \omega),$

$$n_2 = \omega(\omega + \imath c_{4f}^2)\{(c_{2s}^2 + c_{3s}^2)(\omega^2 - 2c_{7s}^2) + \omega c_{6s}^2(\omega + \imath c_{4s}^2) + c_{7s}^2 c_{3s}^2\} + c_{4s}^2 c_{4f}^2 c_{6s}^2 \omega^2.$$

These velocities correspond to the waves arising from solid-liquid interactions. It is easy to verify that by neglecting the presence of liquid, these velocities reduce to the same velocities of coupled transverse waves of micropolar elastic solid obtained earlier by Parfitt and Eringen (1969).

Note that for a two dimensional problem in $x - z$ plane, we shall consider

$$\mathbf{u}^s = (u_1^s,\ 0,\ u_3^s), \qquad \mathbf{u}^f = (u_1^f,\ 0,\ u_3^f) \quad \text{and} \quad \phi_2^s = (-\boldsymbol{\phi}^s)_2.$$

5.4.1 Incidence of coupled longitudinal plane wave with velocity V_1

Let a plane coupled longitudinal wave propagating through the half-space H be incident obliquely at the boundary surface $z = 0$. Let the incident wave with amplitude A_0 propagates with velocity V_1 be striking at the boundary surface making an angle θ_0 with z-axis. To satisfy the boundary conditions on stresses at the boundary surface, it is necessary to postulate the existence of reflected wave in four distinct directions. (i) A set of coupled longitudinal wave of amplitude A_1 propagating with speed V_1 and making an angle θ_1 with the $z-$ axis. (ii) A similar set of coupled longitudinal wave of amplitude A_2 propagating with speed V_2 and making an angle θ_2 with the $z-$ axis. (iii) A set of coupled transverse wave of amplitude A_3 propagating with speed V_9 and making an angle θ_3 with the $z-$ axis. (iv) A similar set of coupled transverse wave of amplitude A_4 propagating with speed V_{10} and making an angle θ_4 with the $z-$ axis.

The followings are the relevant potentials in the half-space H

$$A^s = A_0 \exp\{\imath k_1(\sin\theta_0 x - \cos\theta_0 z) - \imath\omega_1 t\}$$

$$+ \sum_{p=1,\ 2} A_p \exp\{\imath k_p(\sin\theta_p x + \cos\theta_p z) - \imath\omega_p t\}, \tag{5.36}$$

$$A^f = \xi_1 A_0 \exp\{\imath k_1(\sin\theta_0 x - \cos\theta_0 z) - \imath\omega_1 t\}$$

$$+ \sum_{p=1,\ 2} \xi_p A_p \exp\{\imath k_p(\sin\theta_p x + \cos\theta_p z) - \imath\omega_p t\}, \tag{5.37}$$

$$B_2^s = \sum_{q=3,\ 4} A_q \exp\{\imath k_q(\sin\theta_q x + \cos\theta_q z) - \imath\omega_q t\}, \tag{5.38}$$

$$\phi_2^s = \sum_{q=3,\ 4} \eta_q A_q \exp\{\imath k_q(\sin\theta_q x + \cos\theta_q z) - \imath\omega_q t\}, \tag{5.39}$$

where $\xi_{1,2}$ are the coupling parameters between the coefficients A^s and A^f, while $\eta_{3,4}$ are the coupling parameters between the coefficients B_2^s and ϕ_2^s. The expressions of these coupling parameters are given by

$$\xi_{1,2} = 1 - \imath\left[\frac{\omega_{1,2}}{c_{4s}^2} - k_{1,\ 2}\frac{(c_{1s}^2 + c_{3s}^2)}{c_{4s}^2 V_{1,2}}\right], \quad \eta_{3,4} = c_{7s}^2\left[V_{9,10}^2 - c_{6s}^2 - 2\frac{c_{7s}^2}{k_{9,10}^2}\right]^{-1}.$$

Since the boundary surface of the half-space H is free from mechanical stresses, therefore, the boundary conditions at the free surface are the vanishing of force stresses, couple stresses in micropolar solid constituent and stresses in liquid constituent. Mathematically, these boundary conditions can be expressed as

$$\tau_{zz}^s = \tau_{zz}^f = \tau_{zx}^s = m_{zy}^s = 0 \quad \text{at} \quad \text{z} = 0. \tag{5.40}$$

The Snell's law describing the relations between various angles of reflected waves and that of the incident wave, is given by

$$\frac{\sin\theta_0}{V_1} = \frac{\sin\theta_1}{V_1} = \frac{\sin\theta_2}{V_2} = \frac{\sin\theta_3}{V_9} = \frac{\sin\theta_4}{V_{10}}. \tag{5.41}$$

Making use of potentials given by equations (5.36)-(5.39), using Snell's law given by equation (5.41) and assuming that $\omega_1 = \omega_2 = \omega_3 = \omega_4 = \omega$ at the boundary surface $z = 0$, the boundary conditions (5.40) are satisfied if

$$\sum_{j=1}^{4} a_{ij} z_j = b_i \quad (i = 1, ..., 4), \tag{5.42}$$

where

$$a_{1i} = [\lambda^s + (2\mu^s + K^s)\cos^2\theta_i]k_i^2, \quad a_{1j} = (2\mu^s + K^s)\sin\theta_j \cos\theta_j k_j^2, \quad a_{2j} = \xi_i k_i^2,$$

$$a_{3i} = -(2\mu^s + K^s)\sin\theta_i \cos\theta_i k_i^2, \quad a_{3j} = \left[\mu^s \cos 2\theta_j + K^s \cos^2\theta_j - \frac{K^s \eta_j}{k_j^2}\right] k_j^2,$$

$$a_{4j} = \eta_j \cos\theta_j k_j, \quad a_{41} = a_{42} = a_{23} = a_{24} = 0, \quad i = 1, 2, \quad j = 3, 4,$$

and $b_1 = -a_{11},\ b_2 = -a_{21},\ b_3 = a_{31},\ b_4 = a_{41}$.
The quantities

$$z_1 = \frac{A_1}{A_0},\ z_2 = \frac{A_2}{A_0},\ z_3 = \frac{A_3}{A_0} \quad \text{and} \quad z_4 = \frac{A_4}{A_0}$$

are the amplitude ratios for the reflected longitudinal displacement wave due to solid and propagating with velocity V_1 at an angle θ_1, reflected coupled longitudinal displacement wave due to liquid and propagating with velocity V_2 at an angle θ_2, reflected coupled transverse displacement wave propagating with velocity V_9 at an angle θ_3, reflected coupled transverse microrotational wave propagating with velocity V_{10} at angle θ_4, respectively. Solving the equations in (5.42), we obtain

$$z_i = \frac{\Delta_i}{\Delta} \quad (i = 1, 2, 3, 4), \tag{5.43}$$

where $\Delta = -a_{14}a_{22}a_{33}a_{41} + a_{12}a_{24}a_{33}a_{41} + a_{13}a_{22}a_{34}a_{41} - a_{12}a_{23}a_{34}a_{41} + a_{14}a_{21}a_{33}a_{42} - a_{11}a_{24}a_{33}a_{42} - a_{13}a_{21}a_{34}a_{42} + a_{11}a_{23}a_{34}a_{42}$,
$\Delta_1 = (a_{14}a_{33} - a_{13}a_{34})(a_{42}b_2 - a_{22}b_4) + a_{24}(-a_{33}a_{42}b_1 + a_{13}a_{42}b_3 + a_{12}a_{33}b_4) + a_{23}(a_{34}a_{42}b_1 - a_{14}a_{42}b_3 - a_{12}a_{34}b_4)$,
$\Delta_2 = a_{41}(a_{24}a_{33}b_1 - a_{23}a_{34}b_1 - a_{14}a_{33}b_2 + a_{13}a_{34}b_2 + a_{14}a_{23}b_3 - a_{13}a_{24}b_3) + (a_{14}a_{21}a_{33} - a_{11}a_{24}a_{33} - a_{13}a_{21}a_{34} + a_{11}a_{23}a_{34})b_4$,
$\Delta_3 = -(a_{12}a_{41} - a_{11}a_{42})(a_{34}b_2 - a_{24}b_3) + a_{22}(a_{34}a_{41}b_1 - a_{14}a_{41}b_3 - a_{11}a_{34}b_4) + a_{21}(-a_{34}a_{42}b_1 + a_{14}a_{42}b_3 + a_{12}a_{34}b_4)$,

$\Delta_4 = (a_{12}a_{41}-a_{11}a_{42})(a_{33}b_2-a_{23}b_3)+a_{22}(-a_{33}a_{41}b_1+a_{13}a_{41}b_3+a_{11}a_{33}b_4)+a_{21}(a_{33}a_{42}b_1-a_{13}a_{42}b_3-a_{12}a_{33}b_4)$.

5.4.2 Surface response

The following responses of the solid and liquid constituents at the surface of the half-space H are calculated.

(i) Solid constituent The expressions for the displacements and microrotation respectively are given by

$$u_1^s = \iota[k_1 \sin\theta_0 + k_1 \sin\theta_1 z_1 + k_2 \sin\theta_2 z_2 - k_3 \cos\theta_3 z_3 - k_4 \cos\theta_4 z_4]A_0, \tag{5.44}$$

$$u_3^s = \iota[-k_1 \cos\theta_0 + k_1 \cos\theta_1 z_1 + k_2 \cos\theta_2 z_2 + k_3 \sin\theta_3 z_3 + k_4 \sin\theta_4 z_4]A_0, \tag{5.45}$$

$$\phi_2^s = [\eta_3 z_3 + \eta_4 z_4]A_0. \tag{5.46}$$

(ii) Liquid constituent The expressions of the displacements of the liquid constituent are given by

$$u_1^f = \iota[\xi_1 k_1 \sin\theta_0 + \xi_1 k_1 \sin\theta_1 z_1 + \xi_2 k_2 \sin\theta_2 z_2]A_0, \tag{5.47}$$

$$u_3^f = \iota[-\xi_1 k_1 \cos\theta_0 + \xi_1 k_1 \cos\theta_1 z_1 + \xi_2 k_2 \cos\theta_2 z_2]A_0, \tag{5.48}$$

where $k_1 \sin\theta_0 = k_1 \sin\theta_1 = k_2 \sin\theta_2 = k_3 \sin\theta_3 = k_4 \sin\theta_4 = k_0$.

In writing the expressions in (5.44) to (5.48), we have dropped a common factor $\exp\{\iota(k_0 x - \omega t)\}$.

5.4.3 Energy partition

We shall now consider the partitioning of incident energy between various reflected waves at the surface element of unit area. Following Achenbach (1973), the rate of energy transmission at the free surface $z = 0$ for the mixture of micropolar solid with

simple liquid, is given by

$$P^* = \tau^s_{zz}\dot{u}^s_3 + \tau^f_{zz}\dot{u}^f_3 + \tau^s_{zx}\dot{u}^s_1 + m^s_{zy}\dot{\phi}^s_2. \tag{5.49}$$

Following Achenbach (1973), for any two complex functions of the forms

$$F = F_0 \exp\{\imath(\omega t - \gamma_1)\}, \qquad f = f_0 \exp\{\imath(\omega t - \gamma_2)\},$$

F_0 and f_0 being the real-valued functions, the time average of a product of the real parts of two complex functions F and f, is given by

$$< R(F) \times R(f) >= R(F\bar{f})/2. \tag{5.50}$$

To obtain the expressions of energy ratios giving the time rate of average energy transmission for the respective wave to that of the incident wave, we shall now calculate the $< P^* >$ for the incident wave and for each of the reflected waves by using the appropriate potentials. The expressions for these energy ratios $E_i (i = 1, ...4)$ corresponding to reflected waves are given by

$$E_i =< P^*_i > / < P^*_0 > \qquad (i = 1, ...4), \tag{5.51}$$

where

$$< P^*_0 >= (\lambda^s + 2\mu^s + K^s - \imath\lambda^f\omega_1\xi^2_1)k^3_1 \cos\theta_0,$$

$$< P^*_\ell >= -(\lambda^s + 2\mu^s + K^s - \imath\lambda^f\omega_\ell\xi^2_\ell)k^3_\ell \cos\theta_\ell z^2_\ell \qquad (\ell = 1, 2)$$

$$< P^*_m >= -\left(\mu^s + K^s - \eta_m \frac{(\gamma^s\eta_m + K^s)}{k^2_m}\right) k^3_m \cos\theta_m z^2_m \quad (m = 3, 4).$$

The quantities E_1, E_2, E_3 and E_4 represent the energy ratios of reflected coupled longitudinal wave with velocity V_1, reflected coupled longitudinal wave with velocity V_2, reflected coupled transverse wave with velocity V_9 and reflected coupled transverse wave with velocity V_{10} respectively.

5.4.4 Incidence of coupled longitudinal plane wave with velocity V_2

We now consider a train of coupled longitudinal wave of amplitude $\bar{A}_0$ propagating with velocity V_2 through the half space and striking at the interface making an angle θ_0 with the z-axis. In this case, to satisfy the boundary conditions at the free surface of the half-space H, we shall postulate the existence of same set of reflected waves as considered above, in the case of incidence of coupled longitudinal wave with velocity V_1. Therefore, the potentials in the half-space due to various reflected waves will be of the form

$$A^s = \bar{A}_0 \exp\{\imath k_2(\sin\theta_0 x - \cos\theta_0 z) - \imath\omega_2 t\}$$

$$+ \sum_{p=1,\ 2} A_p \exp\{\imath k_p(\sin\theta_p x + \cos\theta_p z) - \imath\omega_p t\}, \tag{5.52}$$

$$A^f = \xi_2 \bar{A}_0 \exp\{\imath k_2(\sin\theta_0 x - \cos\theta_0 z) - \imath\omega_2 t\}$$

$$+ \sum_{p=1,\ 2} \xi_p A_p \exp\{\imath k_p(\sin\theta_p x + \cos\theta_p z) - \imath\omega_p t\}. \tag{5.53}$$

The expressions of the potentials B_2^s and ϕ_2^s will remain same as defined earlier in (5.38) and (5.39). The expressions of parameters $\xi_{1,2}$ and $\eta_{3,4}$ are also defined earlier. Making use of potentials given above and the modified Snell's law for the present case given by

$$\frac{\sin\theta_0}{V_2} = \frac{\sin\theta_1}{V_1} = \frac{\sin\theta_2}{V_2} = \frac{\sin\theta_3}{V_9} = \frac{\sin\theta_4}{V_{10}}, \tag{5.54}$$

into the boundary conditions given in (5.40) and assuming $\omega_1 = \omega_2 = \omega_3 = \omega_4 = \omega$ at the boundary surface $z = 0$, we obtain a system of four non-homogeneous equations as follows

$$\sum_{j=1}^{4} a_{ij}\bar{z}_j = \bar{b}_i \quad (i = 1, ...4), \tag{5.55}$$

where a_{ij} are the same as defined earlier and $\bar{b}_1 = -a_{12},\ \bar{b}_2 = -a_{22},\ \bar{b}_3 = a_{32}$ and $\bar{b}_4 = a_{42}$, while the quantities

$$\bar{z}_1 = A_1/\bar{A}_0,\ \bar{z}_2 = A_2/\bar{A}_0,\ \bar{z}_3 = A_3/\bar{A}_0 \quad \text{and} \quad \bar{z}_4 = A_4/\bar{A}_0$$

are the reflection coefficients of various reflected waves. Solving the system of equations in (5.55), we obtain

$$\bar{z}_i = \frac{\bar{\Delta}_i}{\Delta} \quad (i = 1, 2, 3, 4), \tag{5.56}$$

where $\Delta = -a_{14}a_{22}a_{33}a_{41} + a_{12}a_{24}a_{33}a_{41} + a_{13}a_{22}a_{34}a_{41} - a_{12}a_{23}a_{34}a_{41} + a_{14}a_{21}a_{33}a_{42} - a_{11}a_{24}a_{33}a_{42} - a_{13}a_{21}a_{34}a_{42} + a_{11}a_{23}a_{34}a_{42}$,
$\bar{\Delta}_1 = (a_{14}a_{33}-a_{13}a_{34})(a_{42}\bar{b}_2-a_{22}\bar{b}_4)+a_{24}(-a_{33}a_{42}\bar{b}_1+a_{13}a_{42}\bar{b}_3+a_{12}a_{33}\bar{b}_4)+a_{23}(a_{34}a_{42}\bar{b}_1-a_{14}a_{42}\bar{b}_3 - a_{12}a_{34}\bar{b}_4)$,
$\bar{\Delta}_2 = a_{41}(a_{24}a_{33}\bar{b}_1 - a_{23}a_{34}\bar{b}_1 - a_{14}a_{33}\bar{b}_2 + a_{13}a_{34}\bar{b}_2 + a_{14}a_{23}\bar{b}_3 - a_{13}a_{24}\bar{b}_3) + (a_{14}a_{21}a_{33} - a_{11}a_{24}a_{33} - a_{13}a_{21}a_{34} + a_{11}a_{23}a_{34})\bar{b}_4$,
$\bar{\Delta}_3 = -(a_{12}a_{41}-a_{11}a_{42})(a_{34}\bar{b}_2-a_{24}\bar{b}_3)+a_{22}(a_{34}a_{41}\bar{b}_1-a_{14}a_{41}\bar{b}_3-a_{11}a_{34}\bar{b}_4)+a_{21}(-a_{34}a_{42}\bar{b}_1+a_{14}a_{42}\bar{b}_3 + a_{12}a_{34}\bar{b}_4)$,
$\bar{\Delta}_4 = (a_{12}a_{41}-a_{11}a_{42})(a_{33}\bar{b}_2-a_{23}\bar{b}_3)+a_{22}(-a_{33}a_{41}\bar{b}_1+a_{13}a_{41}\bar{b}_3+a_{11}a_{33}\bar{b}_4)+a_{21}(a_{33}a_{42}\bar{b}_1-a_{13}a_{42}\bar{b}_3 - a_{12}a_{33}\bar{b}_4)$.

5.4.5 Surface response

Similarly, as computed in the case of incidence of coupled longitudinal wave with velocity V_1, the expressions of surface response for the displacements and microrotations of solid constituent and displacements of liquid constituent, for the case of incident coupled longitudinal wave with velocity V_2, are given by

$$u_1^s = \iota[k_2 \sin\theta_0 + k_1 \sin\theta_1 z_1 + k_2 \sin\theta_2 z_2 - k_3 \cos\theta_3 z_3 - k_4 \cos\theta_4 z_4]A_0, \tag{5.57}$$

$$u_3^s = \iota[-k_2 \cos\theta_0 + k_1 \cos\theta_1 z_1 + k_2 \cos\theta_2 z_2 + k_3 \sin\theta_3 z_3 + k_4 \sin\theta_4 z_4]A_0, \tag{5.58}$$

$$\phi_2^s = [\eta_3 z_3 + \eta_4 z_4]A_0, \tag{5.59}$$

and

$$u_1^f = \imath[\xi_2 k_2 \sin\theta_0 + \xi_1 k_1 \sin\theta_1 z_1 + \xi_2 k_2 \sin\theta_2 z_2]A_0, \tag{5.60}$$

$$u_3^f = \imath[-\xi_2 k_2 \cos\theta_0 + \xi_1 k_1 \cos\theta_1 z_1 + \xi_2 k_2 \cos\theta_2 z_2]A_0, \tag{5.61}$$

where $k_2 \sin\theta_0 = k_1 \sin\theta_1 = k_2 \sin\theta_2 = k_3 \sin\theta_3 = k_4 \sin\theta_4 = k_0'$.
In writing the expressions in (5.57) to (5.61), we have dropped a common factor $\exp\{\imath(k_0' x - \omega t)$.

5.4.6 Energy partition

In the case of incident coupled longitudinal wave propagating with velocity V_2, the expressions for energy ratios $\bar{E}_i (i = 1, ...4)$ for various reflected waves are given by

$$\bar{E}_i = < P_i^* > / < \bar{P}_0^* > \qquad (i = 1, ...4), \tag{5.62}$$

where the expressions of $< P_i^* >$ are the same as defined earlier, while the expression of $< \bar{P}_0^* >$ is given by

$$< \bar{P}_0^* > = (\lambda^s + 2\mu^s + K^s - \imath\lambda^f \omega_2 \xi_2^2) k_2^3 \cos\theta_0.$$

5.5 Limiting case

If we neglect the micropolar effects from solid and fluid constituents of the mixture, then we shall be left with the mixture of an elastic solid and a liquid. For this, substituting the parameters corresponding to micropolarity in both solid and fluid constituents equal to zero, i.e., $c_{3s}^2 = c_{5s}^2 = c_{6s}^2 = c_{7s}^2 = c_{8s}^2 = c_{3f}^2 = c_{5f}^2 = c_{6f}^2 = c_{7f}^2 = c_{8f}^2 = 0$, then equation (5.24) reduces to

$$V_{1,\,2}^2 = \frac{1}{2a_1'}[b_1' \pm \sqrt{b_1'^2 - 4a_1' c_1'}] \qquad \text{and} \qquad V_{3,4} = 0, \tag{5.63}$$

where $a_1' = \omega + \imath(c_{4s}^2 + c_{4f}^2),\ b_1' = \imath c_{1s}^2 c_{4f}^2 + (c_{1s}^2 + c_{4s}^2 c_{1f}^2 - \imath c_{1f}^2 \omega)\omega,\ c_1' = -\imath c_{1s}^2 c_{1f}^2 \omega^2$.
Thus there are only two longitudinal displacement waves and the longitudinal micro-rotation waves disappear. Also, it can be seen that in the present case, the velocities

of coupled transverse waves given by equation (5.30) vanish and the velocities given by equation (5.31) reduce to

$$V_{9,10}^2 = \frac{1}{2a_2'}[-b_2' \pm \sqrt{b_2'^2 - 4a_2'c_2'}], \tag{5.64}$$

where $a_2' = \omega + \imath(c_{4s}^2 + c_{4f}^2),\ b_2' = -c_{2s}^2(\omega + \imath c_{4f}^2) + \imath\omega c_{2f}^2(\omega + \imath c_{4s}^2),\ c_2' = -\imath\omega^2 c_{2s}^2 c_{2f}^2$. These two transverse waves are coupled through the coupling parameter given by

$$\mathbf{b}^s = \left[\frac{\imath V_{9,10} c_{4s}^2}{k(V_{9,10}^2 - c_{2s}^2) + \imath V_{9,10} c_{4s}^2}\right] \mathbf{b}^f.$$

It is to be noted here that the velocities $V_{1,2}$ given in (5.63) are analogous to two compressional waves of Biot (1956a, b). The velocities $V_{9,10}$ given in (5.64) correspond to two coupled transverse waves, not observed in Biot's theory. When viscosity of fluid constituent is neglected, i.e., when $\mu^f = 0$, then one of the velocities in (5.64) vanishes and the other velocity becomes $V_{10}^2 = \mu^s/\rho^s$ for high frequency waves.

5.6 Numerical results and discussions

In order to seek the behavior of velocities of the existing waves in micropolar mixture with frequency parameter, we shall consider a specific model. The various amplitude and energy ratios at the free boundary of a porous mixture consisting of micropolar solid and inviscid liquid will be computed subsequently. For the purpose of studying the dispersion and attenuation phenomena of waves, we take the following values of relevant elastic parameters. We shall compute the non-dimensional phase velocity at different values of non-dimensional frequency. The expressions of velocities given in equations (5.22), (5.23), (5.30) and (5.31) are computed and found that they are complex. The variations of real and imaginary parts of these velocities are obtained and depicted graphically through Figures 5.1 to 5.5.

Figure 5.1 shows that the real part of the velocity ratio $V1(= V_1/c_{1s})$ is dispersive untill a certain value of frequency parameter ω/c_{7s}, beyond which, it is independent of frequency. However, the real part of velocity ratio $V2(= V_2/c_{1s})$ is found to be increasing with increase of frequency parameter ω/c_{7s}. The real parts of these two velocity ratios are found to be equal at $\omega_e(= \omega/c_{7s}) = 58.41$. It is clear from this figure that $V_1/c_{1s} > V_2/c_{1s}$ in their real parts untill $\omega/c_{7s} < \omega_e$, but when $\omega/c_{7s} > \omega_e$, we found

$V_2/c_{1s} > V_1/c_{1s}$ in their real parts. The imaginary part of the phase velocity V_1/c_{1s} is found to be non-zero for low values of frequency parameter and it approaches to zero when ω/c_{7s} takes larger and larger values. On the other hand, the imaginary part of V_2/c_{1s} is found to decrease with increase of frequency parameter.

Symbol	Value
λ^s	$7.59 \times 10^{10}\ dyne/cm^2$
μ^s	$1.89 \times 10^{10}\ dyne/cm^2$
K^s	$0.0149 \times 10^{10}\ dyne/cm^2$
α^s	$0.029 \times 10^{10}\ dyne$
β^s	$0.027 \times 10^{10}\ dyne$
γ^s	$0.0263 \times 10^{14}\ dyne$
j^s	$0.00196\ cm^2$
ρ^s	$2192\ gm/cm^3$
ξ	$0.75\ gm/cm^3\ sec$
Ω	$0.40\ gm/cm\ sec$
λ^f	$2.14 \times 10^{10}\ dyne\ sec/cm^2$
μ^f	$0.450 \times 10^{10}\ dyne\ sec/cm^2$
K^f	$0.0112 \times 10^{10}\ dyne\ sec/cm^2$
α^f	$0.0178 \times 10^{10} dyne\ sec$
β^f	$0.0160 \times 10^{10}\ dyne\ sec$
γ^f	$0.0198 \times 10^{10}\ dyne\ sec$
j^f	$0.00180\ cm^2$
ρ^f	$1010.0\ gm/cm^3$

Thus, we conclude that at low frequency, one of the longitudinal wave corresponding to phase velocity V_1 propagates with complex phase velocity and hence dispersive and attenuated, while at high frequency, this wave propagates with constant real phase velocity and remains unattenuated. Thus for high frequency range, this wave is independent of frequency. The other longitudinal wave propagating with phase velocity V_2 propagates with complex phase velocity and hence dispersive and attenuated at all non-zero values of frequency parameter. At zero frequency, it is found that V_1 is non-zero. The wave velocity V_2/c_{1s} vanish at $\omega/c_{7s} = 0$, which increases monotonically with ω/c_{7s} and approaches to infinity as $\omega/c_{7s} \to \infty$.

Figure 5.2 shows that the real part of $V_{3,4}/c_{1s}$ vanish at $\omega/c_{7s} = 0$. As frequency pa-

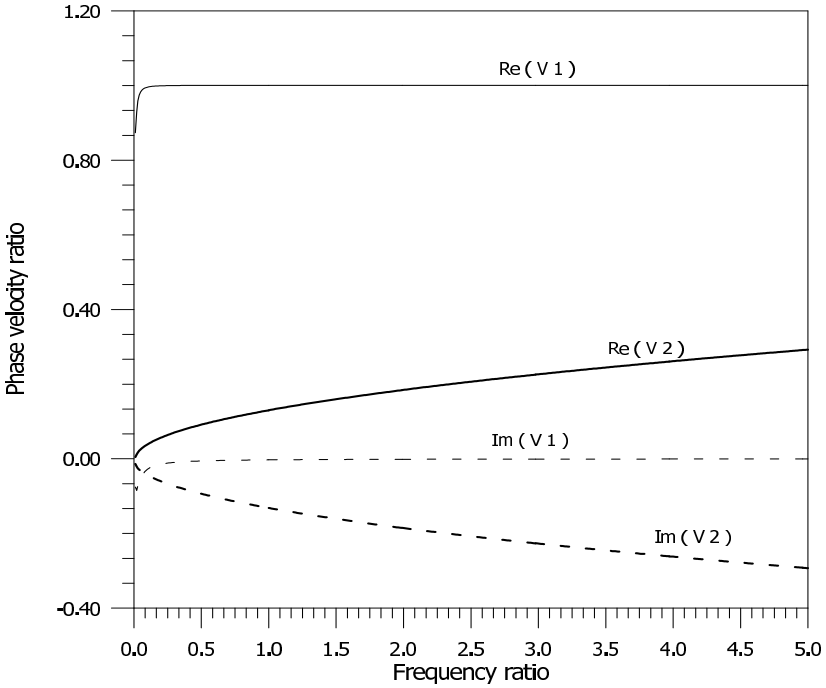

Figure 5.1: Phase velocities V_1 and V_2 versus frequency ratio ω/c_{7s}.

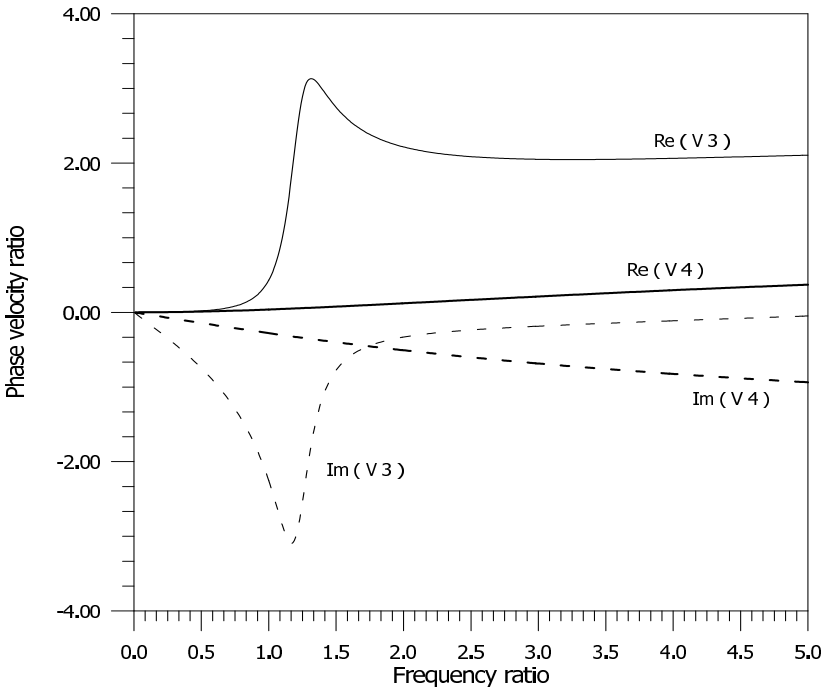

Figure 5.2: Phase velocities V_3 and V_4 versus frequency ratio ω/c_{7s}.

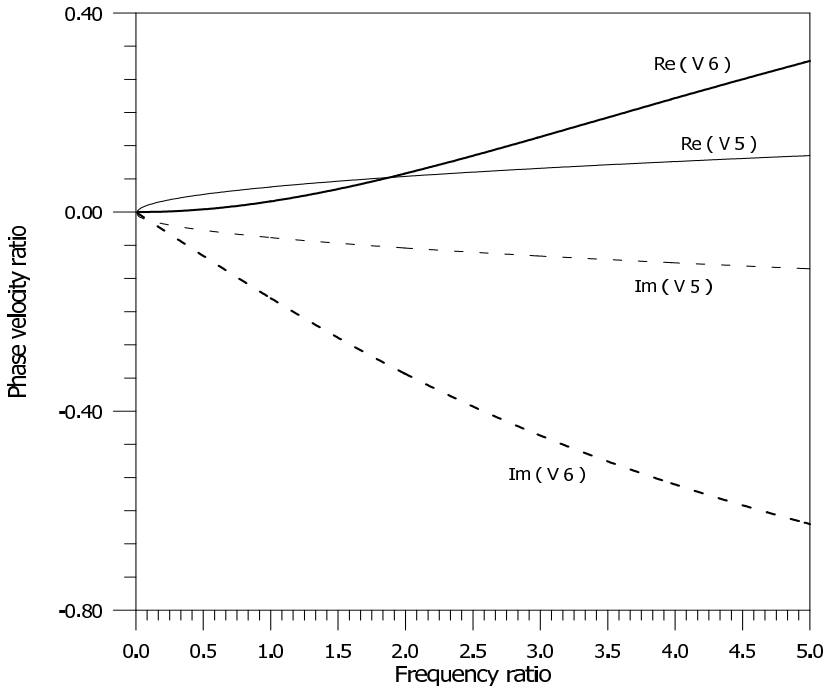

Figure 5.3: Phase velocities V_5 and V_6 versus frequency ratio ω/c_{7s}.

rameter increases, the real part of velocity ratio V_3/c_{1s} increases to the value 3.1319 at $\omega/c_{7s} = 1.32$, thereafter it decreases with further increase of frequency parameter. The real part of velocity ratio V_4/c_{1s} increases with increase of frequency parameter. These velocity ratios are found to approach to infinity as frequency parameter approaches to infinity. The variation of imaginary parts of $V_{3,4}/c_{1s}$ with frequency parameter is also shown in the Figure 5.2. The imaginary part or attenuation of V_3/c_{1s} is maximum in the low frequency range.

Figure 5.3 depicts the variation of real and imaginary parts (attenuation) of $V_{5,6}/V_{1s}$ with frequency parameter. We note that both the parts of these velocities vanish at $\omega/c_{7s} = 0$. Thereafter, their real and imaginary parts increase in positively and negatively with increase of frequency parameter. The real part of V_5/c_{1s} is found to be greater than that of V_6/c_{1s} up to $\omega/c_{7s} = 1.88$ and after that the real part of V_6/c_{1s} becomes greater than the real part of V_5/c_{1s}. These two velocities approaches to ∞ as the frequency parameter tends to ∞. It is also noticed that the imaginary parts of these velocity become more and more negative as ω/c_{7s} approaches to ∞. It is also found that in the absence of γ^f, the velocity V_6 disappears and the velocity V_5 remains unchanged. Thus the velocity V_5 does not depend on γ^f.

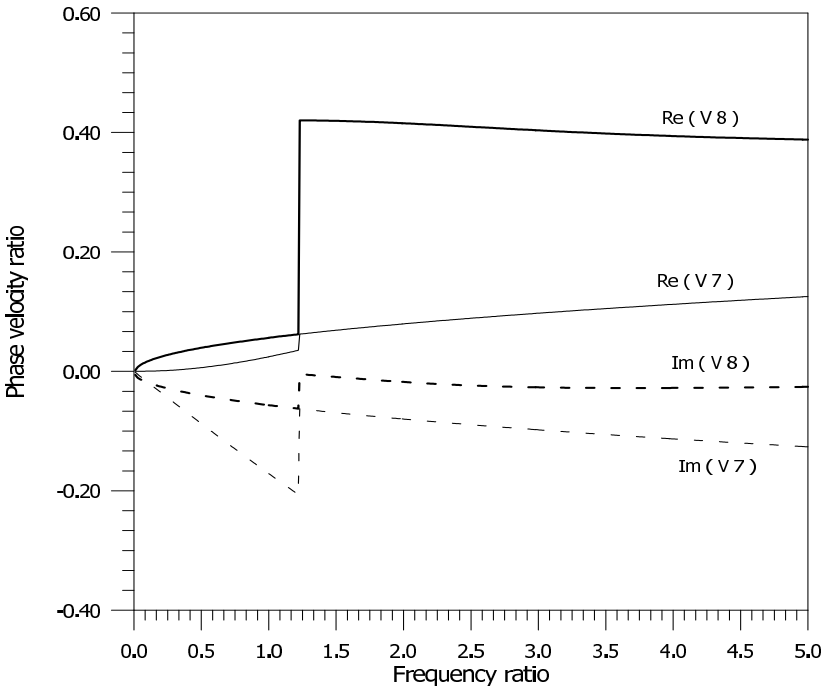

Figure 5.4: Phase velocities V_7 and V_8 versus frequency ratio ω/c_{7s}.

Figure 5.4 shows that the real parts of velocity ratios $V_{7,8}/c_{1s}$ are zero at zero frequency. For $\omega/c_{7s} > 0$, these velocity ratios increase and the real part of V_8/c_{1s} is found to be greater than that of V_7/c_{1s}. We also observe that there is an uplift in both the velocity ratios at $\omega/c_{7s} = 1.23$. The variation of imaginary parts of these velocity ratios with frequency parameter is similar to that of their real parts, but with negative sign. Both the parts of these velocity ratios approaches to ∞ as $\omega/c_{7s} \to \infty$.

In Figure 5.5, we see that the real part of the velocity ratio V_9/c_{1s} starts increasing from zero and goes up to 1.7834 at $\omega/c_{7s} = 1.22$, thereafter decreases to 0.0357 at $\omega/c_{7s} = 1.23$ beyond which it starts increasing. The velocity V_{10} also follows the same pattern, but decreases as continuous function of frequency. We also observe the same trend for attenuation coefficient, however the attenuation for V_9 tends to $-\infty$, while the attenuation of V_{10} tends to zero as the frequency increases.

Figures 5.6-5.11 represent the variation of amplitude ratios, energy ratios and surface responses when the coupled longitudinal waves with velocities V_1 and V_2 are made incident at free surface of a porous half space containing mixture of micropolar elastic solid and inviscid non-polar liquid. These are computed at frequency parameter $\omega/c_{7s} = 10^3$. Figure 5.6 shows that the values of reflection coefficients z_2 and z_3 are

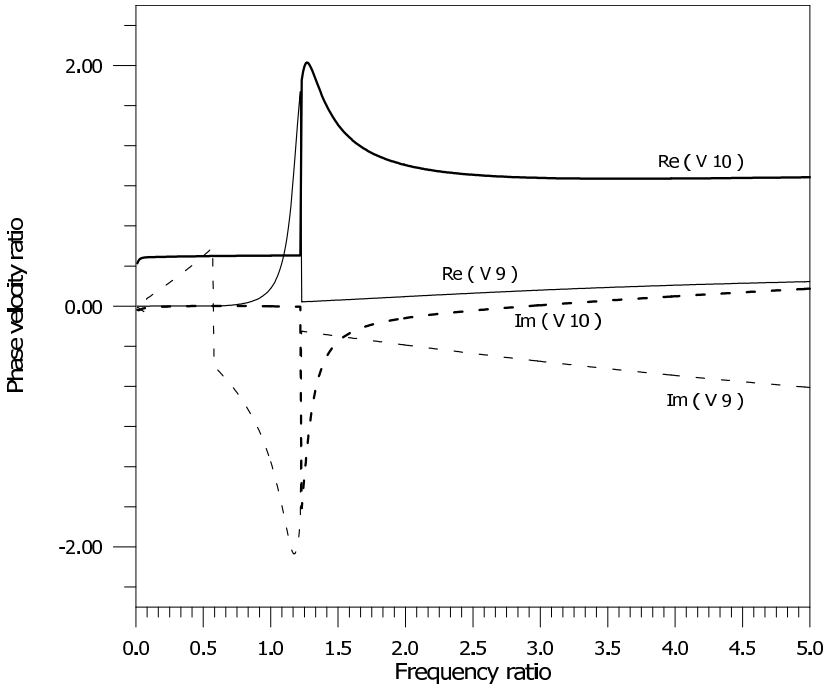

Figure 5.5: Phase velocities V_9 and V_{10} versus frequency ratio ω/c_{7s}.

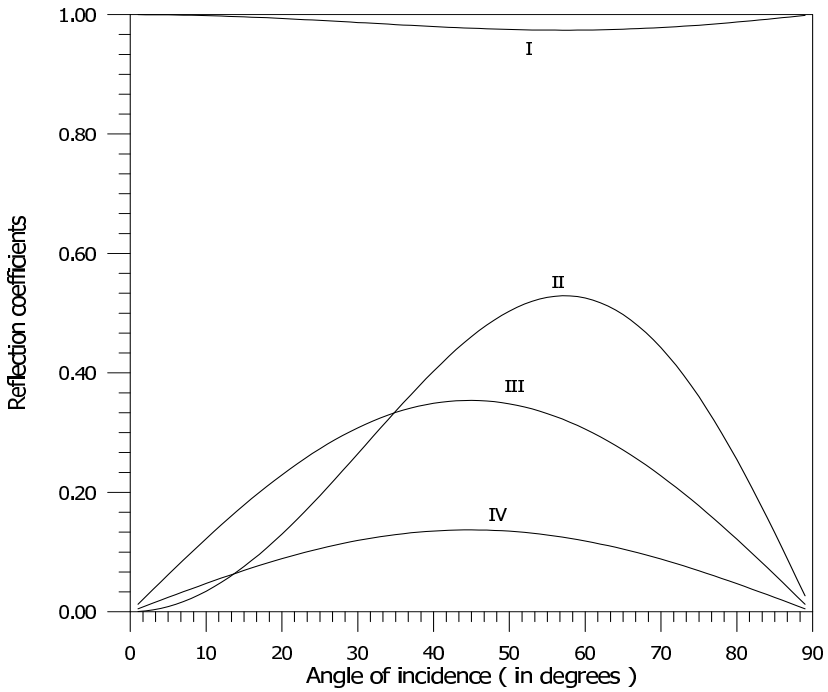

Figure 5.6: Variation of reflection coefficients (Incidence of longitudinal wave with velocity V_1) (Curve - I: z_1, Curve - II: $z_2 \times 10^3$, Curve - III: $z_3 \times 10^6$, Curve - IV: $z_4 \times 10$).

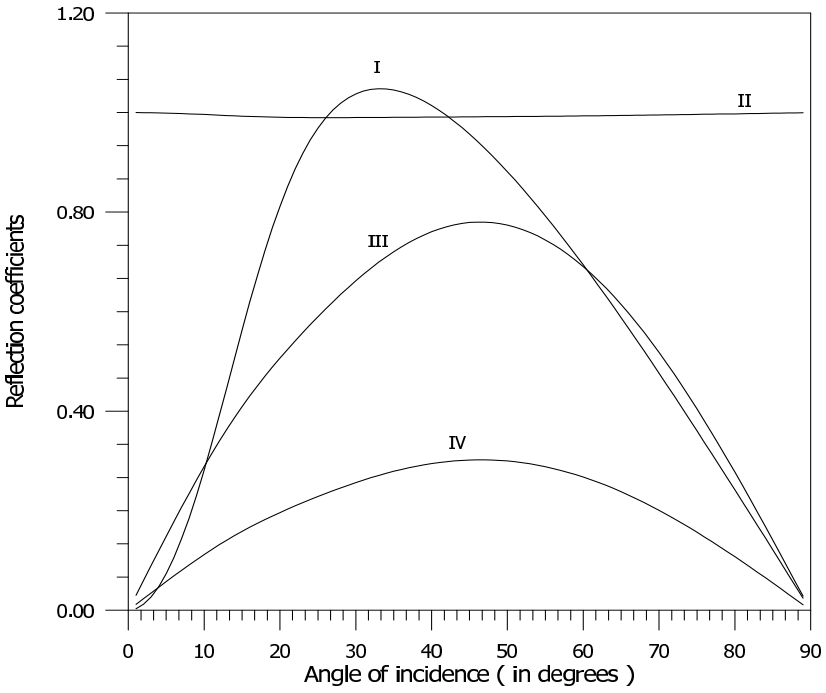

Figure 5.7: Variation of reflection coefficients (Incidence of longitudinal wave with velocity V_2) (Curve - I: z_1, Curve - II: z_2, Curve - III: $z_3 \times 10^5$, Curve - IV: z_4).

very small at each angle of incidence and they have been depicted after magnifying by the factors 10^3 and 10^6 times respectively to their original values. The variation of z_4 is also shown by magnifying its original value with the factor 10. Thus, we conclude that only reflected wave with amplitude z_1 is dominant.

Figure 5.7 shows that the amplitude ratio z_3 is very small as compared to the amplitudes of other reflected waves. The curve corresponding to z_3 is shown after magnifying 10 times its original value. Here, the amplitude ratio z_2 is found to be almost independent of the angle of incidence, while the amplitude ratios z_1 and z_4 behave alike with the angle of incidence. It is also noticed that at normal and grazing incidences, all the reflected waves disappear except the wave corresponding to amplitude ratio z_2.

Figures 5.8 and 5.9 represent the variation of energy ratios with the angle of incidence when coupled longitudinal wave with velocities V_1 and V_2 are made incident, respectively. It is noticed from Figure 5.8 that the maximum amount of energy travels along the reflected wave having amplitude z_1 as was expected. Almost negligible amount of energy is carried by the reflected waves having amplitudes z_3 and z_4.

Similarly, from Figure 5.9, we note that the amount of energy carried by reflected waves having amplitude ratios z_3 and z_4 is negligible and the only reflected wave hav-

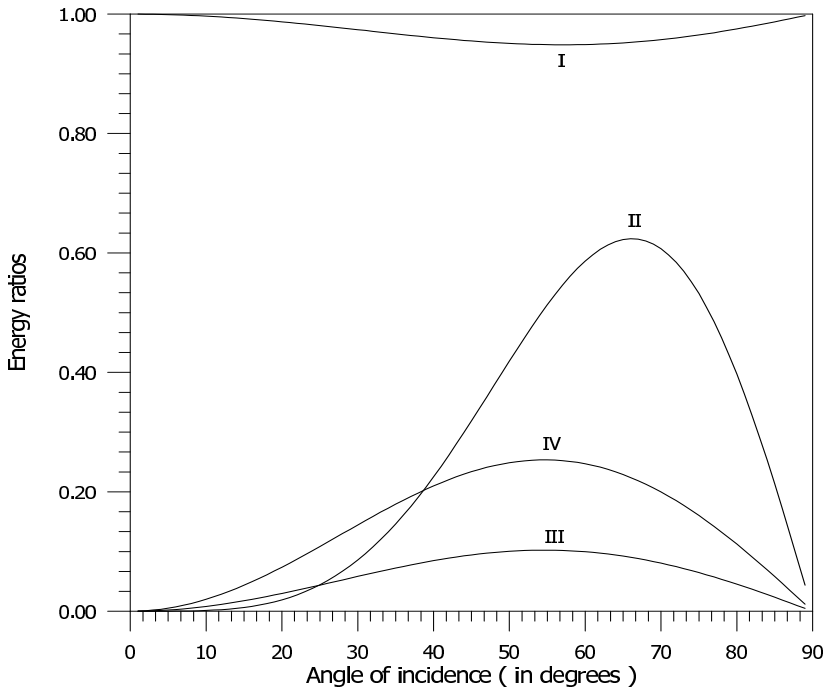

Figure 5.8: Variation of energy ratios with angle of incidence (Incidence of longitudinal wave with velocity V_1). (Curve - I: E_1, Curve - II: $E_2 \times 10^3$, Curve - III: $E_3 \times 10^{20}$, Curve - IV: $E_4 \times 10^{12}$).

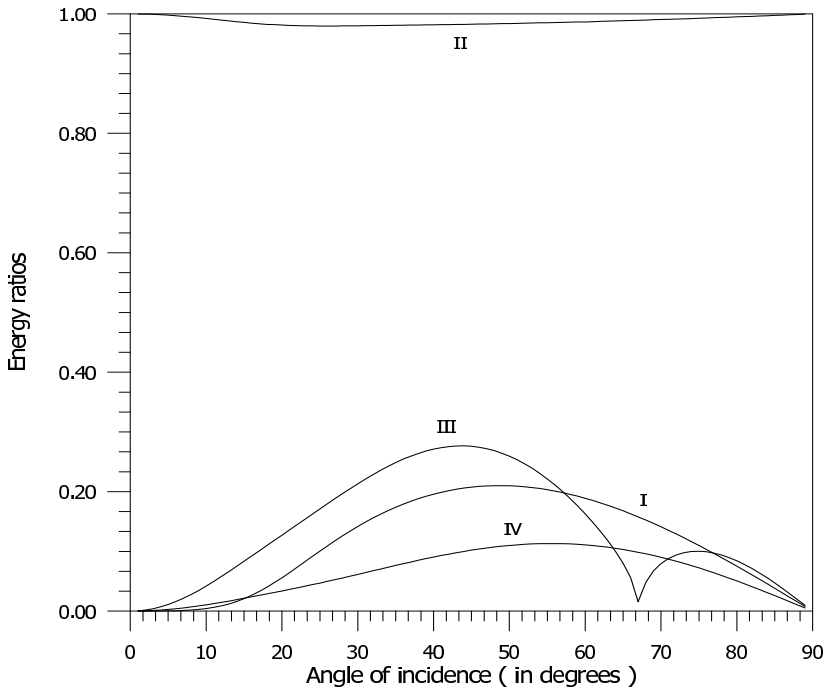

Figure 5.9: Variation of energy ratios with angle of incidence (Incidence of longitudinal wave with velocity V_2). (Curve - I: $E_1 \times 10$, Curve - II: E_2, Curve - III: $E_3 \times 10^{21}$, Curve - IV: $E_4 \times 10^{12}$).

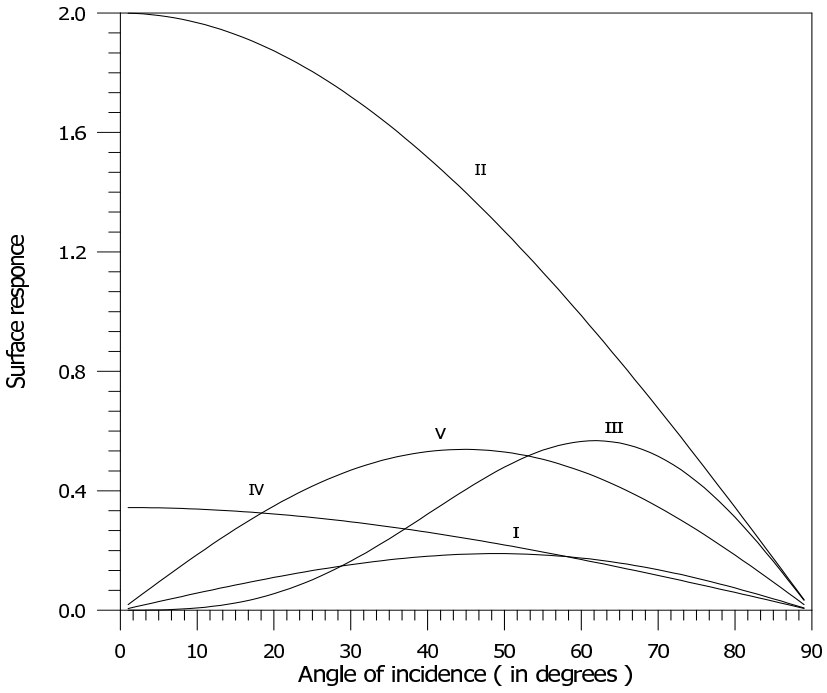

Figure 5.10: Surface response of incidence of longitudinal wave with velocity V_1 (Curve - I: u_1^s, Curve - II: u_3^s, Curve - III: $u_1^f \times 10^{-4}$, Curve - III: $u_3^f \times 10^{-6}$, Curve - IV: $\phi_2^s \times 10^6$).

ing amplitude z_2 carry maximum amount of energy. In both the figures, it has been verified that the sum of the energies carried with reflected waves is equal to the total amount of energy given to the incident wave. Thus, there is no dissipation of energy during reflection, as the medium is considered non-dissipative medium.

Figures 5.10 and 5.11 depict the variation of surface displacement, microrotation in solid and fluid with the angle of incidence in case of incident coupled longitudinal wave with velocity V_1 and V_2 respectively. The displacement components $u_1^s,\ u_3^s$ and $u_1^f,\ u_3^f$ are normalized by a factor of $\imath k_1 A_0 \exp(\imath k_o x - \imath\omega t)$ and $\imath k_2 A_0 \exp(\imath k_o' x - \imath\omega t)$ respectively. The microrotation field for solid ϕ_2^s is normalized by a factor of $A_0 k_1^2 \exp(\imath k_o x - \imath\omega t)$ in the case of incident wave with velocity V_1 and by a factor $A_0 k_2^2 \exp(\imath k_o' x - \imath\omega t)$ in the case of incident wave with velocity V_2. It can be observed from these figures that the surface response of displacement components in fluid constituent is greater than that of in solid constituent.

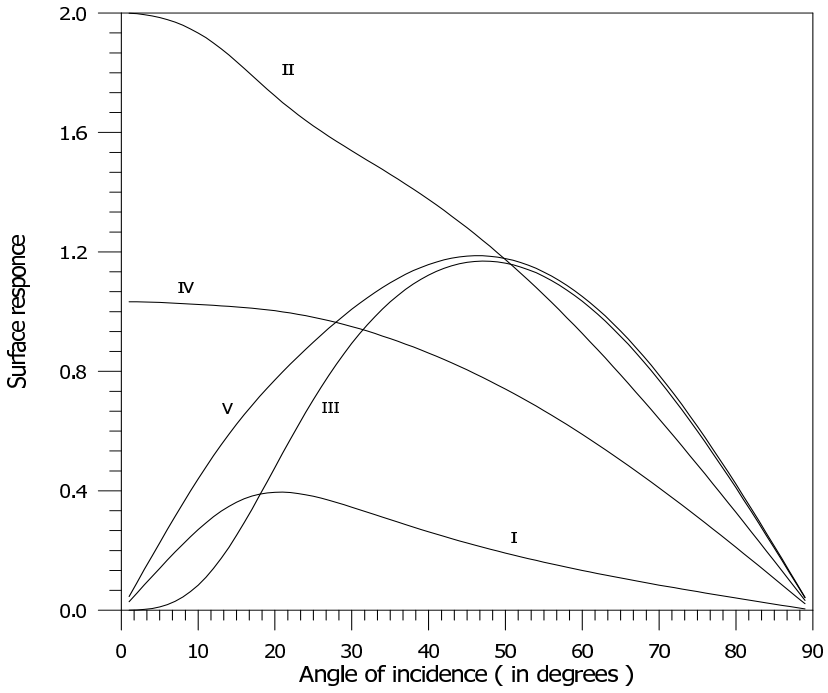

Figure 5.11: Surface response of incidence of longitudinal wave with velocity V_2 (Curve - I: u_1^s, Curve - II: u_3^s, Curve - III: $u_1^f \times 10^{-5}$, Curve - III: $u_3^f \times 10^{-6}$, Curve - IV: $\phi_2^s \times 10^5$).

5.7 Conclusions

The possibility of wave propagation and a problem of reflection of plane longitudinal waves from a free boundary surface of a porous micropolar mixture half-space are investigated. The equations of motion and constitutive relations for micropolar mixture theory of porous media developed by Eringen (2003a) has been employed for mathematical treatment. It is concluded that

(a) There can exist two coupled longitudinal displacement waves, two coupled longitudinal microrotational waves and six coupled transverse waves (two of them purely depend on fluid parameters) in an infinite micropolar mixture of porous media. All the waves are found to be dispersive and attenuated in nature. It has been verified that when the presence of fluid is neglected from the mixture, these waves exactly reduce to the elastic waves of micropolar elastic solid earlier obtained by Parfitt and Eringen (1969).

(b) It is found that there is a significant effect of presence of fluid in the mixture. The longitudinal displacement wave corresponding to solid constituent in micropolar mixture is found to be dispersive at low range of frequency parameter, while it is in-

dependent of the frequency in micropolar elastic solid.

(c) Phase velocities of all the waves corresponding to the micropolar viscous fluid approach to infinity as the frequency approach to infinity.

(d) If the viscosity and micropolarity of the liquid constituent are neglected, then there can exist three longitudinal waves (two corresponding to displacement and one corresponding to microrotational) and two transverse waves (corresponding displacement and microrotation of solid) in a continuum mixture of micropolar solid with Newtonian liquid.

(e) The formulae for reflection coefficients, energy ratios and surface responses have been derived and computed numerically. It is found that the reflection coefficient and energy ratio corresponding to those reflected wave which propagates with same velocity as that of the incident wave, are dominant.

(f) We also concluded that the wave velocity V_1 is greater than the wave velocity V_2 up to certain value of frequency parameter and after that velocity V_2 is found to be more than the velocity V_1. Similarly, the phase velocity V_5 is found to be more than the phase velocity V_6 up to certain value of frequency parameter and thereafter the phase velocity V_6 is found to be more than the phase velocity V_5.

Chapter 6

Waves in a cylindrical borehole filled with micropolar fluid[5]

6.1 Introduction

Biot (1952) studied the propagation of elastic waves in a cylindrical bore filled with and without fluid and embedded in a uniform elastic solid of infinite extent. He studied two-dimensional problems and obtained dispersion relations for the waves propagating along the boundary of such a cylindrical borehole. Since then several problems concerning the cylindrical bore have been attempted by several authors. Some of them are Banerji and Sengupta (1977a, b), Sengupta and Chakrabarti (1980), Sharma and Gogna (1990), Tomar and Kumar (1999a), Deswal et al. (2000), Kumar and Deswal (2002a), Bhujanga Rao and Rama Murthy (2002), Vashishth and Khurana (2005) and Arora and Tomar (2007) including others. Recently, Cheng and Blanch (2008) reviewed the methods of simulating elastic wave propagation in a borehole by considering two different approaches, a quasi-analytic approach known as the discrete wavenumber summation method and a finite difference method. In this Chapter, we have investigated a problem of propagation of surface waves in a cylindrical borehole of infinite length embedded in an infinite micropolar elastic solid and filled with a micropolar viscous fluid. Frequency equation relevant to the propagation of surface waves is derived and then solved numerically for a particular model. The effect of borehole radius, microp-

[5] ***Journal of Applied Physics*** Vol. 104(1), (2008).

olarity and viscosity of the contained fluid column is noticed on the dispersion curves. The present model may be viewed in a situation arising in the field of oil-well exploration. The oil inside the oil-well is generally found in a crude form containing several impurities and therefore can be best modeled with muddy like/dusty viscous fluid of micropolar nature. Thus, the present problem may be of great help to oil companies.

6.2 Formulation of the problem and frequency equation

For micropolar solid and micropolar fluid, we follow the equations of motions and constitutive relations given by equations (4.1)-(4.8) in Chapter-4. We consider a circular cylindrical bore of radius 'a' through a micropolar elastic medium of infinite extent. Taking the cylindrical polar co-ordinates $(r,\ \theta,\ z)$ such that the $z-$ axis is pointing vertically upward along the axis of the cylinder. Our aim is to derive the frequency equation relevant to the propagation of axial symmetric waves, which are harmonic along the axial direction. To discuss the surface waves at micropolar fluid/micropolar solid interface, we consider the following forms of the displacement and microrotation vectors as

$$\mathbf{u}^s = (u_r^s,\ 0,\ u_z^s), \quad \boldsymbol{\phi}^s = (0,\ \phi_2^s, 0),$$

$$\mathbf{u}^f = (u_r^f,\ 0,\ u_z^f), \quad \boldsymbol{\phi}^f = (0,\ \phi_2^f, 0).$$

Since we are considering axially symmetric waves, therefore, the quantities would remain independent of θ. With these considerations, the above equations (4.1) and (4.2) become

$$(\mu^f + K^f)(\nabla^2 - \frac{1}{r^2})\dot{u}_r^f + (\lambda^f + \mu^f)\frac{\partial \dot{e}^f}{\partial r} - K^f \frac{\partial \dot{\phi}_2^f}{\partial z} = \rho^f \frac{\partial^2 u_r^f}{\partial t^2}, \tag{6.1}$$

$$(\mu^f + K^f)\nabla^2 \dot{u}_z^f + (\lambda^f + \mu^f)\frac{\partial \dot{e}^f}{\partial z} + \frac{K^f}{r}\frac{\partial (r\dot{\phi}_2^f)}{\partial r} = \rho^f \frac{\partial^2 u_z^f}{\partial t^2}, \tag{6.2}$$

$$\left[\gamma^f(\nabla^2 - \frac{1}{r^2}) - 2K^f\right]\dot{\phi}_2^f + K^f\left(\frac{\partial \dot{u}_r^f}{\partial z} - \frac{\partial \dot{u}_z^f}{\partial r}\right) = \rho^f j^f \frac{\partial^2 \phi_2^f}{\partial t^2}, \tag{6.3}$$

and equations (4.3) and (4.4) become

$$(\mu^s + K^s)(\nabla^2 - \frac{1}{r^2})u_r^s + (\lambda^s + \mu^s)\frac{\partial e^s}{\partial r} - K^s\frac{\partial \phi_2^s}{\partial z} = \rho^s\frac{\partial^2 u_r^s}{\partial t^2}, \tag{6.4}$$

$$(\mu^s + K^s)\nabla^2 u_z^s + (\lambda^s + \mu^s)\frac{\partial e^s}{\partial z} + \frac{K^s}{r}\frac{\partial (r\phi_2^s)}{\partial r} = \rho^s\frac{\partial^2 u_z^s}{\partial t^2}, \tag{6.5}$$

$$\left[\gamma^s(\nabla^2 - \frac{1}{r^2}) - 2K^s\right]\phi_2^s + K^s\left(\frac{\partial u_r^s}{\partial z} - \frac{\partial u_z^s}{\partial r}\right) = \rho^s j^s\frac{\partial^2 \phi_2^s}{\partial t^2}, \tag{6.6}$$

where $e^R = \dfrac{1}{r}\dfrac{\partial (ru_r^R)}{\partial r} + \dfrac{\partial u_z^R}{\partial z}, \quad \nabla^2 = \dfrac{\partial^2}{\partial r^2} + \dfrac{1}{r}\dfrac{\partial}{\partial r} + \dfrac{\partial^2}{\partial z^2}.$

Introducing the potentials ϕ'^R, ψ^R and Γ^R as follows

$$u_r^R = \frac{\partial \phi'^R}{\partial r} + \frac{\partial^2 \psi^R}{\partial r \partial z}, \quad u_z^R = \frac{\partial \phi'^R}{\partial z} - \left(\nabla^2 - \frac{\partial^2}{\partial z^2}\right)\psi^R, \quad \phi_2^R = -\frac{\partial \Gamma^R}{\partial r}, \tag{6.7}$$

into equations (6.1)-(6.6), we obtain

$$[(c_{1R}^2 + c_{3R}^2)\nabla^2 - \Box_R]\phi'^R = 0, \tag{6.8}$$

$$[(c_{2R}^2 + c_{3R}^2)\nabla^2 - \Box_R]\psi^R + c_{3R}^2\Gamma^R = 0, \tag{6.9}$$

$$[c_{4R}^2\nabla^2 - 2c_{6R}^2 - \Box_R]\Gamma^R - c_{6R}^2\nabla^2\psi^R = 0, \tag{6.10}$$

where

$$\Box_R = \begin{cases} \partial_t^2 & \text{for } R = s\ , \\ \partial_t & \text{for } R = f\ . \end{cases}$$

We note that equation (6.8) is uncoupled in the potential ϕ'^R, while equations (6.9) and (6.10) are coupled in the potentials ψ^R and Γ^R. Next, we shall find the solutions of these equations for time harmonic waves propagating along $z-$ direction. In order to solve the equation (6.8), we take

$$\phi'^R = \chi_1^R(r)\exp\{\imath(kz - \omega t)\},$$

where the symbols ω, k and $c(=\omega/k)$ represent the angular frequency, the wavenumber and the phase velocity, respectively. Inserting it into equation (6.8), we obtain

$$\frac{\partial^2\chi_1^R}{\partial r^2}+\frac{1}{r}\frac{\partial\chi_1^R}{\partial r}-(\lambda_1^R)^2\chi_1^R=0, \tag{6.11}$$

where

$$(\lambda_1^R)^2=k^2-\frac{\omega^2}{V_{R1}^2}.$$

The expressions of quantities V_{s1} and V_{f1} are given by

$$V_{s1}^2=c_{1s}^2+c_{3s}^2,\quad V_{f1}^2=-\imath\omega(c_{1f}^2+c_{3f}^2).$$

From equations (6.9) and (6.10), one can obtain

$$\{A\nabla^4+B\nabla^2+C\}(\psi^R,\Gamma^R)=0, \tag{6.12}$$

where

$$A=c_{4R}^2(c_{2R}^2+c_{3R}^2),\quad B=c_{3R}^2c_{6R}^2-\square_Rc_{4R}^2-(c_{2R}^2+c_{3R}^2)(2c_{6R}^2+\square_R)$$

and

$$C=\square_R(2c_{6R}^2+\square_R).$$

Equation (6.12) can be further written as

$$\{(\nabla^2-\delta_1)(\nabla^2-\delta_2)\}(\psi^R,\ \Gamma^R)=0, \tag{6.13}$$

where $\delta_1=\dfrac{1}{2A}[-B+\sqrt{B^2-4AC}]$ and $\delta_2=\dfrac{1}{2A}[-B-\sqrt{B^2-4AC}]$.
Let us find the solution of equation (6.13) corresponding to ψ^R, by taking

$$\psi^R=\chi_2^R(r)\exp\{\imath(kz-\omega t)\}.$$

Inserting it into equation (6.13), we obtain

$$\frac{\partial^2\chi_2^R}{\partial r^2}+\frac{1}{r}\frac{\partial\chi_2^R}{\partial r}-(\lambda_i^R)^2\chi_2^R=0\qquad(i=2,3), \tag{6.14}$$

where $(\lambda_i^R)^2 = k^2 - \dfrac{\omega^2}{V_{Ri}^2}$.

The expressions of the quantities V_{si} and V_{fi} are given by

$$V^2_{s2,\ s3} = \frac{1}{2a}[b \pm (b^2 - 4ac)^{1/2}],$$

$$V^2_{f2,\ f3} = \frac{1}{2a'}[-b' \pm (b'^2 - 4a'c')^{1/2}],$$

where

$$a = 1 - 2\omega_0^2/\omega^2, \qquad b = c_{2s}^2 + c_{3s}^2 + c_{4s}^2 - (2c_{2s}^2 + c_{3s}^2)\omega_0^2/\omega^2,$$

$$c = c_{4s}^2(c_{2s}^2 + c_{3s}^2), \qquad \omega_0^2 = c_{6s}^2, \qquad a' = \omega + 2\imath c_{6f}^2,$$

$$b' = \omega[\imath\omega c_{4f}^2 + \imath(c_{2f}^2 + c_{3f}^2)(\omega + 2\imath c_{6f}^2) + c_{3f}^2 c_{6f}^2], \qquad c' = -\omega^3 c_{4f}^2(c_{2f}^2 + c_{3f}^2).$$

We note that the equations in (6.11) and (6.14) are the modified Bessel differential equations of order zero. Their solutions are the modified Bessel functions of first and second kind, i.e., $I_0(\lambda_j^R r)$ and $K_0(\lambda_j^R r)$ $(j = 1, 2, 3)$. Note that the function I_0 is bounded as $r \to 0$, the function $K_0 \to 0$ as $|r| \to \infty$ and they represent incoming and outgoing waves in cylindrical coordinates, respectively.

Now, we intend to apply the boundary conditions at the fluid− solid interface. For the type of waves considered in a fluid-filled cylindrical borehole, there are three boundary conditions at the surface of the cylindrical borehole:
(i) the motion (i.e., displacement and micro-rotation) must remain finite at the center of the borehole.
(ii) there are no incoming waves from infinity.
(iii) the displacement, micro-rotation and stresses at the fluid−solid interface should be continuous.
Thus, condition (i) implies that only the function I_0 would work in the inner fluid column, and condition (ii) implies that the function K_0 alone would work in the outer formation. Hence, the general solutions of equations (6.8) - (6.10) satisfying the boundary conditions (i) and (ii) (with a common factor $\exp\{\imath(kz - \omega t)\}$) can be written as

$$\{\phi'^s,\ \phi'^f\} = \{A_1^s K_0(\lambda_1^s r),\ A_1^f I_0(\lambda_1^f r)\}, \tag{6.15}$$

$$\{\psi^s,\ \psi^f\} = \{[A_2^s K_0(\lambda_2^s r) + A_2'^s K_0(\lambda_3^s r)],\quad [A_2^f I_0(\lambda_2^f r) + A_2'^f I_0(\lambda_3^f r)]\}, \tag{6.16}$$

$$\{\Gamma^s,\ \Gamma^f\} = \{[A_3^s K_0(\lambda_2^s r) + A_3'^s K_0(\lambda_3^s r)],\quad [A_3^f I_0(\lambda_2^f r) + A_3'^f I_0(\lambda_3^f r)]\}, \tag{6.17}$$

where the quantities $A_1^s,\ A_1^f,\ A_2^s, A_2'^s, A_2^f, A_2'^f, A_3^s, A_3'^s, A_3^f$ and $A_3'^f$ are arbitrary constants. Note that the solution of coupled equations corresponding to Γ^R can be obtained by plugging the solution of ψ^R from (6.16) into equation (6.9), where the unknown coefficients are given by

$$A_3^s = b_2^s A_2^s, \qquad A_3'^s = b_3^s A_2'^s, \qquad A_3^f = b_2^f A_2^f, \qquad A_3'^f = b_3^f A_2'^f,$$

$$b_{2,3}^s = \frac{c_{2s}^2 + c_{3s}^2}{c_{3s}^2}\left[k^2 - \frac{\omega^2}{c_{2s}^2 + c_{3s}^2} - (\lambda_{2,3}^s)^2\right],$$

and

$$b_{2,3}^f = \frac{c_{2f}^2 + c_{3f}^2}{c_{3f}^2}\left[k^2 - \frac{\imath\omega}{c_{2f}^2 + c_{3f}^2} - (\lambda_{2,3}^f)^2\right].$$

In our present problem, the fluid column inside the micropolar solid formation is micropolar as well as viscous in nature. Since the micropolar viscous fluid can support couple stresses and shear stresses, therefore, both shear and couple stresses must be taken into account while formulating the boundary conditions at the surface of cylindrical borehole. Thus, the boundary condition (iii) implies that the radial displacement, micro-rotation, radial force stress, shear force stress and couple stress across the fluid-solid interface must be continuous. Mathematically, these boundary conditions can be expressed as follows.

At the fluid - solid interface, $r = a$

$$\tau_{rr}^s = \tau_{rr}^f,\quad \tau_{rz}^s = \tau_{rz}^f,\quad m_{r\theta}^s = m_{r\theta}^f,\quad u_r^s = u_r^f,\quad u_z^s = u_z^f,\quad \phi_2^s = \phi_2^f. \tag{6.18}$$

Using (4.5)-(4.8), (6.7) and (6.15) - (6.17) into the above boundary conditions given in (6.18), we obtain a system of six homogeneous equations in six unknowns namely, $A_1^s,\ A_2^s,\ A_2'^s,\ A_1^f,\ A_2^f$ and $A_2^{'f}$, given by

$$\{[(\lambda^s + 2\mu^s + K^s)(\lambda_1^s)^2 - \lambda^s k^2]K_0(\lambda_1^s a) + (2\mu^s + K^s)\frac{\lambda_1^s}{a}K_1(\lambda_1^s a)\}A_1^s$$

$$+\imath k(2\mu^s + K^s)(\lambda_2^s)^2 K_0''(\lambda_2^s a)A_2^s + \imath k(2\mu^s + K^s)(\lambda_3^s)^2 K_0''(\lambda_3^s a)A_2'^s$$

$$+\imath\omega\{[(\lambda^f+2\mu^f+K^f)(\lambda_1^f)^2-\lambda^f k^2]I_0(\lambda_1^f a)-(2\mu^f+K^f)\frac{\lambda_1^f}{a}I_1(\lambda_1^f a)\}A_1^f$$

$$-\omega k(2\mu^f+K^f)(\lambda_2^f)^2 I_0''(\lambda_2^f a)A_2^f-\omega k(2\mu^f+K^f)(\lambda_3^f)^2 I_0''(\lambda_3^f a)A_2^{'f}=0, \tag{6.19}$$

$$-(2\mu^s+K^s)\imath k\lambda_1^s K_1(\lambda_1^s a)A_1^s+\lambda_2^s[(\mu^s+K^s)(\lambda_2^s)^2+\mu^s k^2+K^s b_2^s]K_1(\lambda_2^s a)A_2^s$$
$$+\lambda_3^s[(\mu^s+K^s)(\lambda_3^s)^2+\mu^s k^2+K^s b_3^s]K_1(\lambda_3^s a)A_2^{'s}-\omega k(2\mu^f+K^f)\lambda_1^f I_1(\lambda_1^f a)A_1^f$$
$$-\imath\omega\lambda_2^f[(\mu^f+K^f)(\lambda_2^f)^2+\mu^f k^2+K^f b_2^f]I_1(\lambda_2^f a)A_2^f$$

$$-\imath\omega\lambda_3^f[(\mu^f+K^f)(\lambda_3^f)^2+\mu^f k^2+K^f b_3^f]I_1(\lambda_3^f a)A_2^{'f}=0, \tag{6.20}$$

$$b_2^s\lambda_2^s\left[\frac{-\beta^s}{a}K_1(\lambda_2^s a)+\gamma^s\lambda_2^s K_1'(\lambda_2^s a)\right]A_2^s+b_3^s\lambda_3^s\left[\frac{-\beta^s}{a}K_1(\lambda_3^s a)+\gamma^s\lambda_3^s K_1'(\lambda_3^s a)\right]A_2^{'s}$$
$$+\imath\omega b_2^f\lambda_2^f[\frac{\beta^f}{a}I_1(\lambda_2^f a)-\gamma^f\lambda_2^f I_1'(\lambda_2^f a)]A_2^f$$

$$+\imath\omega b_3^f\lambda_3^f[\frac{\beta^f}{a}I_1(\lambda_3^f a)-\gamma^f\lambda_3^f I_1'(\lambda_3^f a)]A_2^{'f}=0, \tag{6.21}$$

$$\lambda_1^s K_1(\lambda_1^s a)A_1^s+\imath k\lambda_2^s K_1(\lambda_2^s a)A_2^s+\imath k\lambda_3^s K_1(\lambda_3^s a)A_2^{'s}+\lambda_1^f I_1(\lambda_1^f a)A_1^f+\imath k\lambda_2^f I_1(\lambda_2^f a)A_2^f$$

$$+\imath k\lambda_3^f I_1(\lambda_3^f a)A_2^{'f}=0, \tag{6.22}$$

$$\imath k K_0(\lambda_1^s a)A_1^s-(\lambda_2^s)^2 K_0(\lambda_2^s a)A_2^s-(\lambda_3^s)^2 K_0(\lambda_3^s a)A_2^{'s}-\imath k I_0(\lambda_1^f a)A_1^f$$

$$+(\lambda_2^f)^2 I_0(\lambda_2^f a)A_2^f+(\lambda_3^f)^2 I_0(\lambda_3^f a)A_2^{'f}=0, \tag{6.23}$$

$$b_2^s\lambda_2^s K_1(\lambda_2^s a)A_2^s+b_3^s\lambda_3^s K_1(\lambda_3^s a)A_2^{'s}+b_2^f\lambda_2^f I_1(\lambda_2^f a)A_2^f+b_3^f\lambda_3^f I_1(\lambda_3^f a)A_2^{'f}=0. \tag{6.24}$$

For a nontrivial solution of these equations, the determinant of the coefficient matrix must vanish. This will provide us the frequency equation for the propagation of surface waves at the micropolar solid/micropolar fluid interface, given by

$$D(k,c,F)=0, \tag{6.25}$$

where D is the determinant of the coefficient matrix $[a_{mn}]_{6\times 6}$ of the homogeneous linear system of equations (6.19)-(6.24). Here, the parameter F involves the geometrical and material constants. The non-dimensional entries of the matrix a_{mn} in the equation (6.25) are given by

$$a_{11} = (ka)\{[(\frac{\lambda^s + 2\mu^s + K^s}{\lambda^s})(\lambda_1^s a)^2 - (ka)^2]K_0(\lambda_1^s a) + (\frac{2\mu^s + K^s}{\lambda^s})(\lambda_1^s a)K_1(\lambda_1^s a)\},$$

$$a_{14} = \imath(ka)\{[(\frac{\lambda^f\omega + 2\mu^f\omega + K^f\omega}{\lambda^s})(\lambda_1^f a)^2 - \frac{\lambda^f\omega}{\lambda^s}(ka)^2]I_0(\lambda_1^f a)$$

$$-(\frac{2\mu^f\omega + K^f\omega}{\lambda^s})(\lambda_1^f a)I_1(\lambda_1^f a)\},$$

$$a_{1i} = \imath(ka)(\frac{2\mu^s + K^s}{\lambda^s})(\lambda_i^s a)^2 K_0''(\lambda_i^s a),$$

$$a_{1j} = -(ka)(\tfrac{2\mu^f\omega + K^f\omega}{\lambda^s})(\lambda_{j-3}^f a)^2 I_0''(\lambda_{j-3}^f a),$$

$$a_{21} = -\imath(ka)^2(\lambda_1^s a)[\frac{2\mu^s + K^s}{\lambda^s}]K_1(\lambda_1^s a),$$

$$a_{2i} = (\lambda_i^s a)[(\lambda_i^s a)^2(\tfrac{\mu^s + K^s}{\lambda^s}) + (ka)^2\tfrac{\mu^s}{\lambda^s} + (b_i^s a^2)\tfrac{K^s}{\lambda^s}]K_1(\lambda_i^s a),$$

$$a_{24} = -(\lambda_1^f a)(ka)^2(\lambda_1^f a)(\frac{2\mu^f\omega + K^f\omega}{\lambda^s})I_1(\lambda_1^f a),$$

$$a_{2j} = -\imath(\lambda_{j-3}^f a)[(\lambda_{j-3}^f a)^2(\frac{\mu^f\omega + K^f\omega}{\lambda^s}) + (ka)^2\frac{\mu^f\omega}{\lambda^s} + (b_{j-3}^f a^2)\frac{K^f\omega}{\lambda^s}]I_1(\lambda_{j-3}^f a), \quad a_{31} = 0,$$

$$a_{3i} = (b_i^s a^2)(\lambda_i^s a)[\frac{-\beta^s}{\lambda^s a^2}K_1(\lambda_i^s a) + \frac{\gamma^s}{\lambda^s a^2}(\lambda_i^s a)K_1'(\lambda_i^s a)], \quad a_{34} = 0,$$

$$a_{3j} = \imath(b_{j-3}^f a^2)(\lambda_{j-3}^f a)[\frac{\beta^f\omega}{\lambda^s a^2}I_1(\lambda_{j-3}^f a) - \frac{\gamma^f\omega}{\lambda^s a^2}(\lambda_{j-3}^f a)I_1'(\lambda_{j-3}^f a)],$$

$$a_{41} = (ka)(\lambda_1^s a)K_1(\lambda_1^s a), \quad a_{4i} = \imath(ka)(\lambda_i^s a)K_1(\lambda_i^s a), \quad a_{44} = (ka)(\lambda_1^f a)I_1(\lambda_1^f a),$$

$$a_{4j} = \imath(ka)(\lambda_{j-3}^f a)I_1(\lambda_2^f a), \quad a_{51} = \imath(ka)^2 K_0(\lambda_1^s a), \quad a_{5i} = -(\lambda_i^s a)^2 K_0(\lambda_i^s a),$$

$$a_{54} = -\imath(ka)^2 I_0(\lambda_1^f a), \quad a_{5j} = (\lambda_{j-3}^f a)^2 I_0(\lambda_{j-3}^f a), \quad a_{61} = 0, \quad a_{6i} = (b_i^s a^2)(\lambda_i^s a)K_1(\lambda_i^s a),$$

$a_{64} = 0, \quad a_{6j} = (b^f_{j-3}a^2)(\lambda^f_{j-3}a)I_1(\lambda^f_{j-3}a) \;\text{ for } i = 2,\ 3, \;\text{ and } j = 5,\ 6.$

It can be noticed from equation (6.25) that for a fixed value of parameter F, it is an implicit functional relationship between the wavenumber and the phase velocity. Moreover, some of the coefficients are involving complex quantities, therefore, it is expected that the relevant surface waves are dispersive and attenuated.
For the waves of very short wavelengths, i.e., for sufficiently large values of ka, the dispersion equation (6.25) will converge to the dispersion equation of Stoneley-type surface waves at micropolar solid/micropolar fluid interface. For this to achieve, making $ka \to \infty$ and using the asymptotic expansions of the modified Bessel functions given by

$$K_0(u) = K_1(u) = \sqrt{\frac{\pi}{2u}}\exp(-u), \quad I_0(u) = I_1(u) = \frac{1}{\sqrt{2\pi u}}\exp(u), \quad \text{as} \quad u \to \infty,$$

The dispersion relation (6.25) reduces to the equation (4.44) in Chapter-4 for the propagation of Stoneley waves at micropolar solid/micropolar fluid interface.

6.3 Numerical results and discussions

Since some of the entries of the determinantal equation (6.25) are complex, therefore it is not analytically possible to find the roots of this equation for a given value of wavenumber. So, for a given value of wavenumber, equation (6.25) is solved numerically by taking numerical data of the physical parameters. For a specific model, we have investigated the dispersion relation (6.25) numerically. Since this equation is an implicit functional relation of wavenumber and phase velocity of Stoneley waves, therefore one can proceed to find the variation of phase velocity with wavenumber. Once the phase velocity is computed at different wavenumbers, the corresponding group velocity, V_g can be determined from the formula given by

$$V_g = c + k\frac{dc}{dk}.$$

For numerical computations, we take the following values of the relevant parameters for micropolar solid (aluminium epoxy) and micropolar fluid. The radius 'a' of the cylindrical borehole is taken $a = 10\ cm$, whenever not mentioned.

Symbol	Value
λ^s	7.59×10^{10} $dyne/cm^2$
μ^s	1.89×10^{10} $dyne/cm^2$
K^s	0.0149×10^{10} $dyne/cm^2$
β^s	0.0226×10^{10} $dyne$
γ^s	0.0263×10^{10} $dyne$
j^s	0.00196 cm^2
ρ^s	2.192 gm/cm^3
λ^f	1.0×10^{10} $dyne\ sec/cm^2$
μ^f	0.5×10^{10} $dyne\ sec/cm^2$
K^f	0.0110×10^{10} $dyne\ sec/cm^2$
β^f	0.0122×10^{10} $dyne\ sec$
γ^f	0.0126×10^{10} $dyne\ sec$
j^f	0.00140 cm^2
ρ^f	1.0 gm/cm^3

Suppose the roots of equation (6.25) lie along a smooth curve $\mathcal{C}$ in the phase velocity-wavenumber domain, then for a particular value of wavenumber $k = k_0$, $\exists$ some $c = c_0 \in \mathcal{C}$ such that $D(k_0, c_0, F) = 0$. The dispersion relation $c(k, F)$ for this mode, is obtained by tracing the locus of the root in the c domain as k takes values greater than k_0. We require that the dispersion curve $c(k, F) \in \mathcal{C}$, should also be a smooth function of k in order to avoid a mix-up with other modes at possible points of degeneracy where different dispersion curves intersect. This notion of dispersion leads directly to a numerical method for computing modal dispersion curves practically. Starting from c_0, one or two (depending on whether c_0 is an endpoint of $\mathcal{C}$ or not) sequences of sufficiently close phase velocity on $\mathcal{C}$ are computed. Using the initial guess, $c(k_0, F)$ is determined by finding the zero of $D(k, c, F)$ with the help of *MATHEMATICA*. Subsequently, stepping along k away from k_0, all the samples of $c(k, F)$ are computed for each k, using the value of c found at the previous wavenumber as initial guess. Thus the dispersion curve is obtained by this mode tracking procedure. In the present computation, we have computed non-dimensional phase velocity (c/V_{s1}) from equation (6.25) at different real values of non-dimensional wavenumber, ka using *MATHEMATICA*. It is found that the phase velocity is complex in nature, which means that the concerned waves are not only dispersive but possess attenuation too.

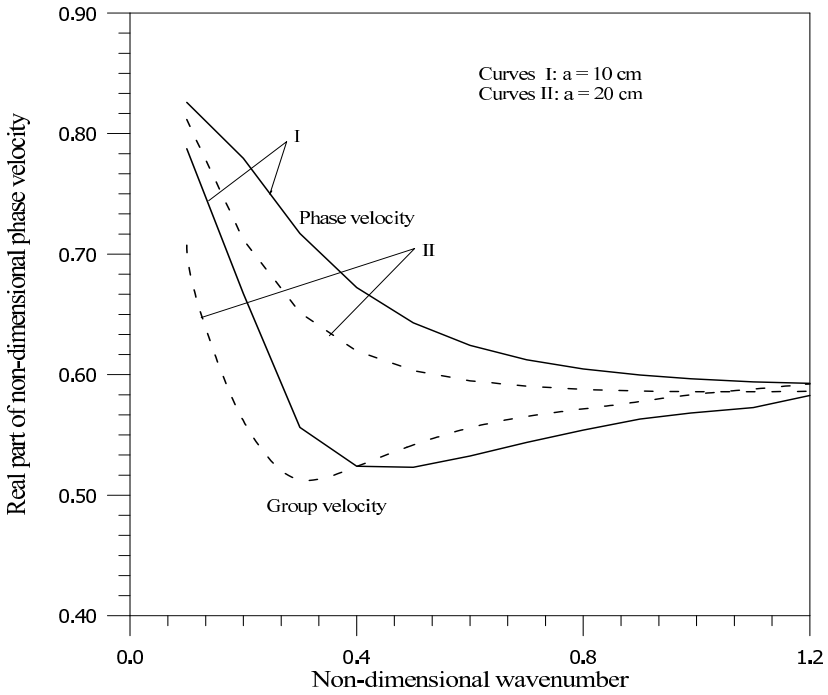

Figure 6.1: Comparison of the real parts of phase velocities and group velocities at different radii of the borehole.

Figure 6.1 depicts the variations of the real parts of the non-dimensional phase and group velocities with the real non-dimensional wavenumber corresponding to two different values of the radii of the borehole. The solid curves correspond to the case when the radius of the borehole is 10 cm, while the dotted curves correspond to the case when the radius of the borehole is 20 cm. We observe that for small values of the non-dimensional wavenumber, there is significant effect of the radius of the borehole. The increase in radius of the borehole results in decrease in the phase velocity of the surface waves. As the value of the non-dimensional wavenumber increases and takes higher and higher values, the non-dimensional phase velocity of the surface waves, for both the radii, tends to the same value and remains constant, which is equal to 0.588676. We also notice that the group velocity is less than the phase velocity for small values of wavenumber for both the radii. However, for higher values of wavenumber, the values of group and phase velocities also tend to the same value.

Figure 6.2 represents the variation of the imaginary parts of the non-dimensional phase velocity versus non-dimensional wavenumber at two different radii of the borehole. We see that at a given value of ka, the value of the imaginary part of the non-dimensional phase velocity corresponding to $a = 10\ cm$ is greater than that of

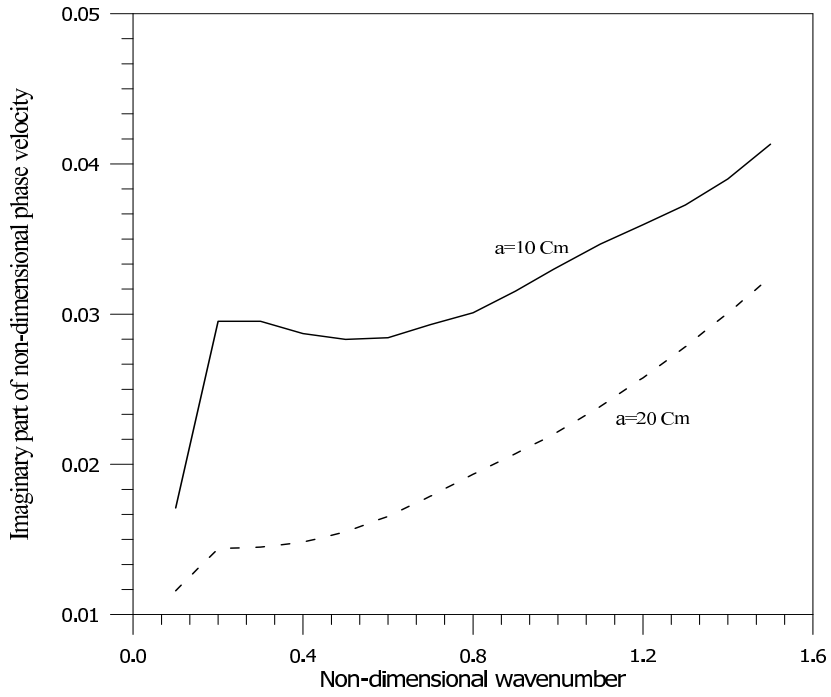

Figure 6.2: Comparison of the imaginary parts of phase velocities at different radii of the borehole.

corresponding to $a = 20\ cm$. However, corresponding to both the radii considered, the values of the imaginary parts of the phase velocity increase with increase of wavenumber. Since the imaginary part of the phase velocity is connected with attenuation of the corresponding waves, therefore, we may conclude that the concerned surface waves are more attenuated when the borehole radius is relatively small.

Figures 6.3 and 6.4 show the effect of fluid viscosity on the dispersion curves corresponding to the real and imaginary parts of the non-dimensional phase velocity. The solid curves in Figure 6.3, correspond to low viscosity fluid and the dotted curves correspond to high viscosity fluid. For limitedly high and low viscous fluids, we have taken the numerical values of the relevant coefficient as $\mu^f = 2.0 \times 10^{10}\ dyne\ sec/cm^2$ and $\mu^f = 0.00001 \times 10^{10}\ dyne\ sec/cm^2$, respectively. However, we have kept the density of the fluid to be fixed for both types of fluids, which may not be the same in general. These numerical values of the coefficient μ^f are taken for computational purposes only. We see that the real part of the phase velocity for highly viscous fluid is greater than that for the low viscous fluid upto certain values of the non-dimensional wavenumber 'ka'. In Figure 6.4, we have depicted the variation of the imaginary part of the phase velocity with the wavenumber at two different values of μ^f, the viscosity of the fluid.

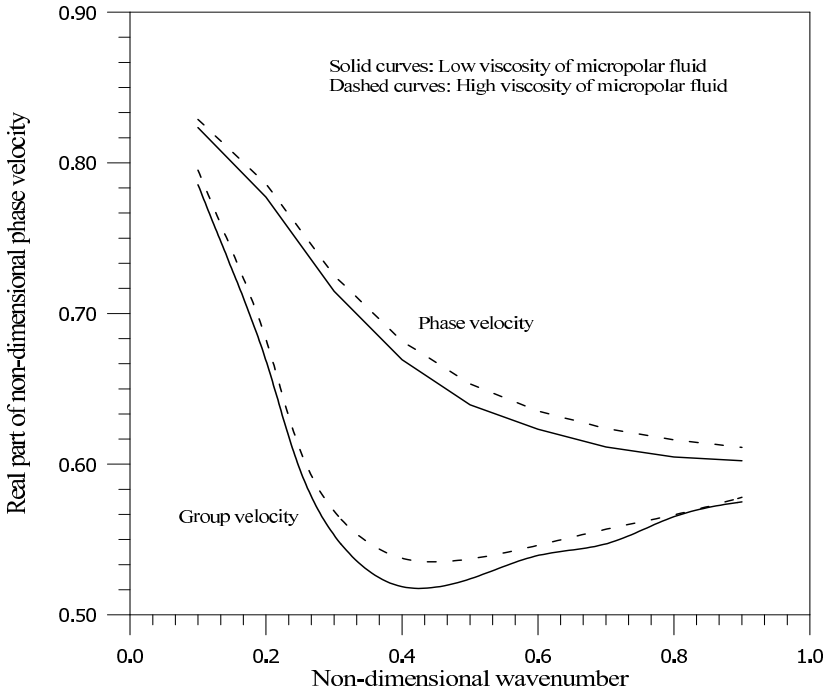

Figure 6.3: Comparison of the real parts of phase velocities and their group velocities at very low and very high viscosity μ^f of micropolar fluid.

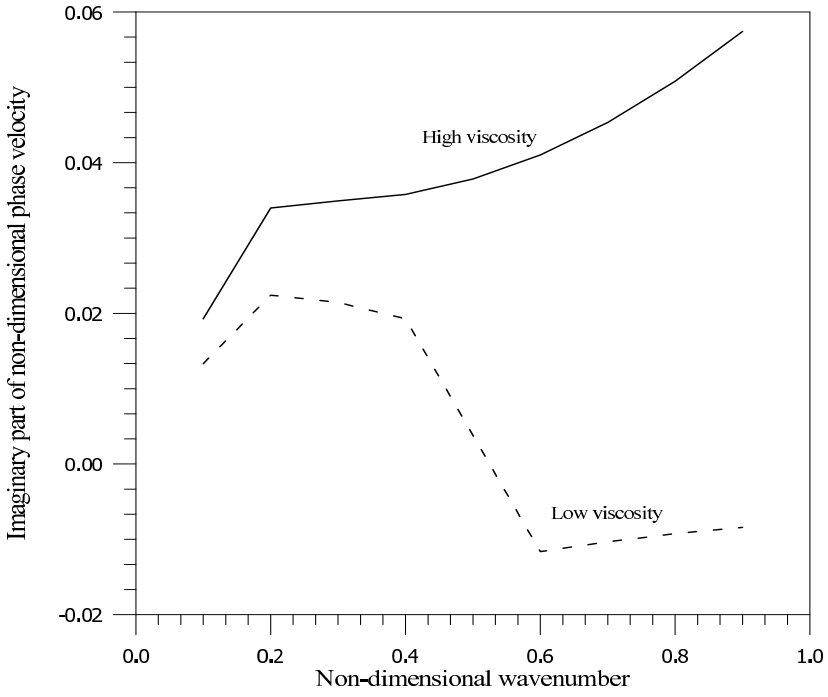

Figure 6.4: Comparison of the imaginary parts of phase velocities at very low and very high fluid viscosity μ^f of the micropolar fluid.

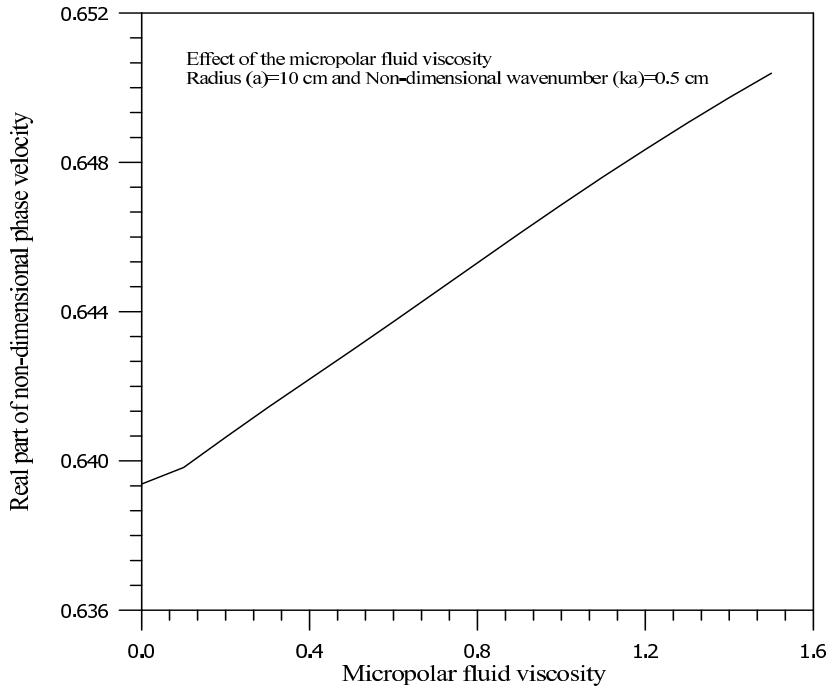

Figure 6.5: Variation of real part of phase velocity versus micropolar fluid viscosity (μ^f).

The solid curve corresponds to highly viscous fluid and dashed curve corresponds to low viscosity. We see that the imaginary part of non-dimensional phase velocity corresponding to highly viscous fluid is greater than that corresponding to low viscous fluid. Hence, we may conclude that the attenuation of the surface waves decrease with decrease of the viscosity of the fluid.

Figures 6.5 and 6.6 depict the variation of the real and imaginary parts of the phase velocity versus viscosity μ^f, when $a = 10\ cm$ and $ka = 5$. we observe that the real and imaginary parts of the non-dimensional phase velocity increase with the increase of μ^f.

Figures 6.7 and 6.8 depict the variation of the real and imaginary parts of the non-dimensional phase velocity versus micropolarity K^f, the micropolarity of the fluid. It is clear from these figures that both the parts of the phase velocity increase very slowly with K^f. Hence, the effect of the micropolar parameter, K^f on the dispersion curve is not appreciable as compared to the effect of viscous parameter, μ^f on the dispersion curve.

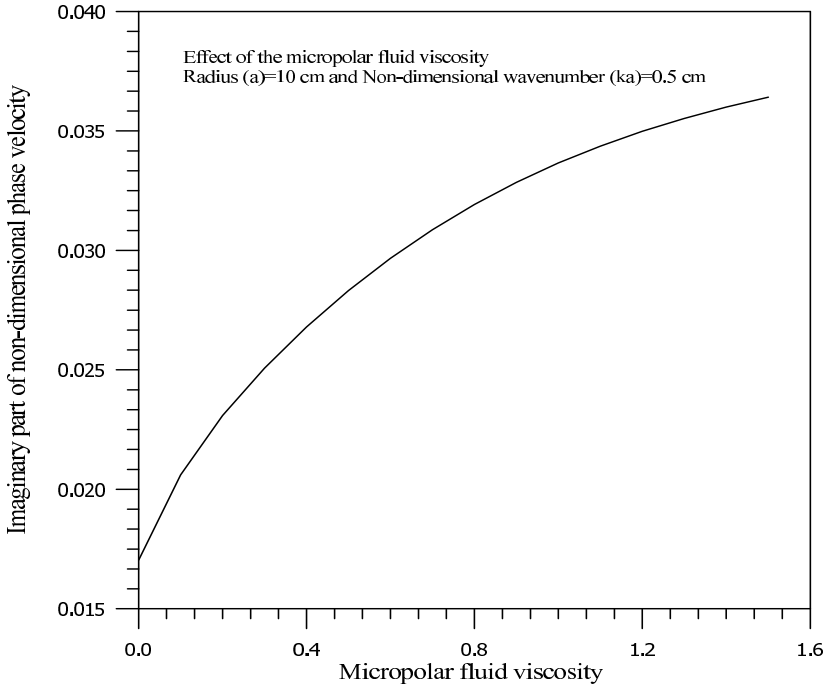

Figure 6.6: Variation of imaginary part of phase velocity versus micropolar fluid viscosity (μ^f).

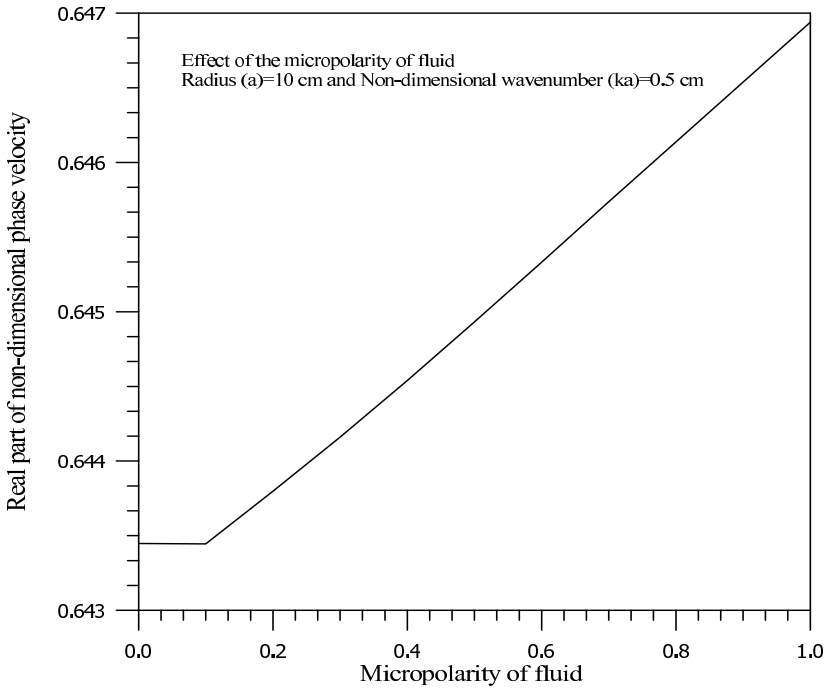

Figure 6.7: Variation of real part of phase velocity versus micropolarity of the fluid K^f.

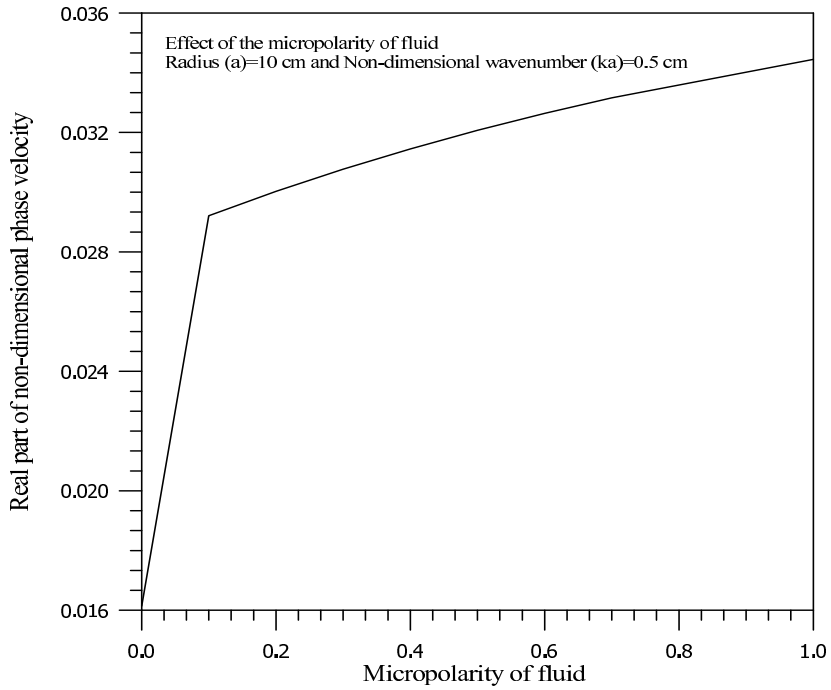

Figure 6.8: Variation of imaginary part of phase velocity versus micropolarity of the fluid K^f.

6.4 Conclusions

A problem of propagation of Stoneley type waves at the surface of a cylindrical borehole situated in an infinite micropolar elastic medium is investigated. The cylindrical borehole is assumed to be vertical and filled with micropolar viscous fluid. Using appropriate boundary conditions, the frequency equation corresponding to the surface wave propagation is derived and solved numerically for a particular model. From the present analysis, it can be concluded that

(a) The frequency equation corresponding to the surface wave propagation is found to be dispersive and attenuated in nature.

(b) The increase in radius of the borehole results in decrease the phase velocity of the surface waves.

(c) On the real part of the phase velocity of the surface waves, the effect of viscosity is found to be more dominant as compared to the effect of micropolarity of the fluid column. It is found that higher is the viscosity of the fluid, slower is the phase velocity of the surface waves.

(d) The phase and the group velocities are found to be affected only at small values

of the wavenumber, while at higher values of the wavenumber, both phase and group velocities are found to be the same and constant. This constant phase velocity corresponds to the wave speed of Stoneley wave at micropolar solid/fluid interface.

(e) For a given value of the wavenumber, the imaginary part of the phase velocity at $a = 10\ cm$ is found to be greater than that of at $a = 20\ cm$.

References

Abbudi, M. and Barnett, D. M., 1990, On the existence of interfacial (Stoneley) waves in a bonded piezoelectric half-spaces, *Proceedings of Royal Society of London*, **A 429**, 587-611.

Abd-Alla, A. M., 1999, Propagation of Rayleigh waves in an elastic half-space of orthotropic material, *Applied Mathematics and Computation*, **99**(1), 61-69.

Abd-Alla, A. M. and Ahmed, S. M., 2003, Stoneley and Rayleigh waves in a non-homogeneous orthotropic elastic medium under the influence of gravity, *Applied Mathematics and Computation*, **135**, 187-200.

Achenbach, J. D., 1973, *Wave propagation in elastic solids*, North Holland, Amsterdam.

Aero, E. L. and Kuvshinskii, E. V., 1960, Fundamental equations of the theory of elastic media with rotationally interacting particles, *Fizika Tverdogo Tela*, **2**, 1399-1409.

Ainslie, M. A. and Burns, P. W., 1995, Energy conserving reflection and transmission coefficients for a solid-solid boundary, *Journal of Acoustical Society of America*, **98**(5), 2836-2840.

Arora, A. and Tomar, S. K., 2007, Elastic waves along a cylindrical borehole in a poroelastic medium saturated by two immiscible fluids, *Journal of Earth System Science*, **116** (3), 225-234.

Ariman, T., 1972, Wave propagation in a micropolar elastic half-space, *Acta Mechanica*, **13**, 11-20.

Ashour, A. S., 1999, Theoretical investigation of Stoneley wave attenuation and dispersion in a fluid filled fracture in transversely isotropic formation, *ARI - An International Journal for Physical and Engineering Sciences*, **51**, 254-257.

Banerji, D. K. and Sengupta, P. R., 1977a, Micropolar elastic waves in a cylindrical bore containing a fluid-I, *Bulletin de l'Acadmie Polonaise des Sciences. Srie des Sci-*

ences Techniques, **25**, 257-262.

Banerji, D. K. and Sengupta, P. R., 1977b, Micropolar elastic waves in a cylindrical bore containing a fluid-II, *Bulletin de l'Acadmie Polonaise des Sciences. Srie des Sciences Techniques*, **25**, 263-270.

Ben-Menahem, A. and Singh, S. J., 1981, *Seismic Waves and Sources*, Springer-Verlag, New York.

Bera, R. K., 1973, Propagation of monochromatic waves in an initially stressed infinite micropolar elastic plate, *Applications of Mathematics*, **18**(1), 9-17.

Biot, M. A., 1952, Propagation of elastic waves in a cylindrical bore containing fluid, *Journal of Applied Physics*, **223**, 997-1005.

Biot, M. A., 1956a, Theory of propagation of elastic waves in a fluid saturated porous solid-I, Low frequency range, *Journal of Acoustical society of America*, **28**, 168-178.

Biot, M. A., 1956b, Theory of propagation of elastic waves in a fluid saturated porous solid-II, Higher frequency range, *Journal of Acoustical society of America*, **28**, 179-191.

Bhujanga Rao, M. and Rama Murthy, D., 2002, Propagation of elastic waves in an infinite micropolar elastic solid with a cylindrical bore, *Journal of Indian Academy of Mathematics*, **24** (2), 253-261.

Brekhoviskikh, L. M., 1960, *Waves in Layered Media*, Academic Press, New York.

Bullen, K. E. and Bolt, B. A., 1985, *Introduction to Seismology*, Cambridge University Press.

Chandrasekharaiah, D. S. and Debnath, L., 1994, *Continuum mechanics*, Academic Press. India.

Cheng, A. C. H. and Blanch, J. O., 2008, Numerical modeling of elastic wave propagation in a fluid filled borehole, *Communications in Computational Physics*, **3**, 33-51.

Cosserat, E. and Cosserat, F., 1909, Theorie des Corps Deformables, *Hermann et Fils*, Paris.

De, S. N. and Sengupta, P. R., 1974, Surface waves in micropolar elastic medium, *Bul-*

letin de l'academie Polonaise des Sciences, serie des Sciences Techniques, **22**, 213-222.

Deswal, S., Tomar, S. K. and Kumar, R., 2000, Effect of fluid viscosity on wave propagation in a cylindrical bore in micropolar elastic medium, *Sadhana*, **25**(5), 439-452.

Eremeyev, V. A., 2005, Acceleration waves in micropolar elastic media, *Doklady Physics*, **50**(4), 204-206.

Eringen, A. C., 1962, *Nonlinear Theory of Continuous Media*, McGraw-Hill, New York.

Eringen, A. C., 1964a, Simple micro-fluids, *International Journal of Engineering Science*, **2**, 205-217.

Eringen, A. C., 1964b, Mechanics of micromorphic materials, in *Proceedings of 11th International Congress of Applied Mecahnics* (Gortler, H., ed.), Springer-Verlag, New York.

Eringen, A. C., 1966a, Linear theory of micropolar elasticity, *Journal of Mathematics and Mechanics*, **15**, 909-924.

Eringen, A. C., 1966b, Theory of micropolar fluids, *Journal of Mathematics and Mechanics*, **16**, 1-18.

Eringen, A. C., 1968, Theory of micropolar Elasticity, *in fracture*, Chapter-7, Vol. II, (ed. H. Liebowitz), Academic Press, New York.

Eringen, A. C., 1980, *Mechanics of Continua*, 2nd ed. Krieger, Melbourne, Florida.

Eringen, A. C., 1990, Theory of thermo-microstretch elastic solids, *International Journal of Engineering Science*, **28**(12), 1291-1301.

Eringen, A. C., 1999, *Microcontinuum Field Theories-I, Foundations and Solids*, Springer-Verlag, New York.

Eringen, A. C., 2003a, Micropolar mixture theory of porous media, *Journal of Applied Physics*, **94**, 4184-4190.

Eringen, A. C., 2003b, Continuum theory of micromorphic electromagnetic thermoelastic solids, *International Journal of engineering Science*, **41** (7), 653-665.

Eringen, A. C., 2004, Electromagnetic theory of microstretch elasticity and bone mod-

eling, *International Journal of Engineering Science*, **42**(3-4), 231-242.

Eringen, A. C. and Suhubi, E. S., 1964, Nonlinear theory of simple microelastic solids-I, *Internatinal Journal of Engineering Science*, **2**, 189-203.

Ewing, W. M., Zardetzky, W. S. and Press, F., 1957, *Elastic Waves in Layered Media*, McGraw-Hill Book Co., New York.

Goda, M. A., 1992, The effect of inhomogeneity and anisotropy on Stoneley waves, *Acta Mechanica*, **93**, 89-98.

Graff, K. F., 1991, *Wave Motion in Elastic Solids*, Dover Publications, New York.

Grioli, G., 1960, Elasticita asimmetrica, *Annali di Matematica Pura ed Applicata. Series IV*, **50**, 389-417.

Grot, R. A., 1969, Thermodynamics of a continuum with microstructure, *International Journal of Engineering Science*, **7**, 801-814.

Gunther, W., 1958, Zurstatik und kinematik des cosseratschen kontinuums, *Abhandlungen der Braunschweigischen Wissenschaftlichen Gesellschaft*, **10**, 195-213.

Hsia, S. Y. and Cheng, J. W., 2006, Longitudinal plane wave propagation in elastic-micropolar porous media, *Japanese Journal of Applied Physics*, **45**(3A), 1743-1748.

Hsia, S. Y., Chiu, S. M. and Cheng, J. W., 2006, Wave propagation at the human muscle-compact bone interface, *Theoretical and Applied Mechanics*, **33** (3), 223-243.

Hsia, S. Y., Chiu, S. M., Su, C. C. and Chen, T. H., 2007, Propagagtion of transverse waves in elastic micropolar porous semispaces, *Japanese Journal of Applied Physics*, **46**, 7399-7405.

Hsieh, T. M., Lindgren, E. A. and Rosen, M., 1991, Effect of interfacial properties on Stoneley wave propagation, *Ultrasonics*, **29**, 38-44.

Iesan, D., 2007, Thermoelasticity of bodies with microstructure and microtempratures, *International Journal of Engineering Science*, **44** (25-26), 8648-8662.

Koiter, W. T., 1964, Couple-stresses in the linear theory of elasticity, *Proceedings Konin Klije Nederlandse Akademie van Wetenshappen*, **67**, 17-29, 30-44.

Kumar, R., 2000, Wave propagation in micropolar viscoelastic generalized thermoelastic solid, *International Journal of Engineering Science*, **38**, 1377-1395.

Kumar, R. and Barak, M., 2007, Wave propagation in liquid-saturated porous solid with micropolar elastic skeleton at boundary surface, *Applied Mathematics and Mechanics*, **28**(3), 337-349.

Kumar, R. and Deswal, S., 2000, Wave propagation in micropolar liquid-saturated porous solid, *Indian journal of Pure and Applied Mathematics*, **31**(10), 1317-1337.

Kumar, R. and Deswal, S., 2002a, Wave propagation through a cylindrical bore contained in a microstretch elastic medium, *Journal of Sound and Vibration*, **250**(4), 711-722.

Kumar, R. and Deswal, S., 2002b, Surface wave propagation in a micropolar thermoelastic medium without energy dissipation, *Journal of Sound and Vibration*, **256**(1), 173-178.

Kumar, R. and Deswal, S., 2006, Some problems of wave propagation in a micropolar elastic medium with voids, *Journal of Vibration and control*, **12**(8), 849-879.

Kumar, R. and Partap, G., 2007, Axisymmetric free vibrations of infinite micropolar thermoelastic plate, *Applied Mathematics and Mechanics*, **28**(3), 369-383.

Kumar, R. and Rupinder, 2008, Reflection and deformation in magneto-thermo-microstretch elastic solid, *International Journal of Pure and Applied Mathematics*, **42**(3), 413-420.

Kumar, R. and Singh, B., 1996, Wave propagation in a micropolar generalized thermoelastic body with stretch, *Proceedings of Indian Academy of Sciences (Math. Sci.)* **106**(2), 183-199.

Kumar, R. and Singh, B., 1997, Reflection and transmission of elastic waves at a loosely bonded interface between an elastic and micropolar elastic solid, *Indian Journal of Pure and Applied Mathematics*, **28** (8), 1133-1153.

Kumar, R. and Singh, B., 2000, Reflection of plane waves at a planar viscoelastic micropolar interface, *Indian Journal of Pure and Applied Mathematics*, **31**(3), 287-303.

Kumar, R. and Tomar, S. K., 2001, Reflection and transmission of elastic waves at viscous liquid/ micropolar elastic solid interface, *International Journal of Mathematics and Mathematical Sciences*, **26**(11), 685-694.

Lamb, H., 1917, On waves in an elastic plate, *Proceedings of Royal Society of London*, Ser. **A93**, 114-128.

Love, A. E. H., 1911, *Some Problems in Geodynamics*, Cambridge University Press, London.

Maugin, G. A., 1974, Acceleration waves in simple and linear viscoelastic micropolar materials, *International Journal of Engineering Science*, **12**, 143-157.

McCarthy, M. and Eringen, A. C., 1969, Micropolar viscoelastic waves, *International Journal of Engineering Science*, **7**, 447-458.

Midya, G. K., 2004, On Love-type surface waves in homogeneous micropolar elastic media, *International Journal of Engineering Science*, **42**(11-12), 1275-1288.

Midya, G. K., Layek, G. C. and De, T. K., 2007, On diffraction of normally incident SH-waves by a line crack in micropolar elastic medium, *International Journal of Solids and structures*, **44**(11-12), 4092-4109.

Midya, G. K., Layek, G. C. and De, T. K., 2008, A note on diffraction of normally incident P-wave by a line crack in micro-polar elastic medium, *International Journal of Solids and structures*, **45**(9), 2706-2722.

Mindlin, R. D., 1964, Micro-structure in linear elasticity, *Archive for Rational Mechanics and Analysis*, **16**, 51-78.

Mindlin, R. D. and Tiersten, H. F., 1962, Effects of couple-stresses in linear elasticity, *Archive for Rational Mechanics and Analysis*, **11**, 415-448.

Murty, G. S., 1975a, A theoretical model for the attenuation and dispersion of Stoneley waves at the loosely bonded interface between two elastic half-spaces, *Physics of the Earth and Planetary Interiors*, **11**, 65-79.

Murty, G. S., 1975b, Wave propagation at an unbonded interface between two elastic

half-spaces, *Journal of Acoustical Society of America*, **58**, 1094-1095.

Murty, G. S., 1976, Reflection, transmission and attenuation of elastic waves at a loosely-bonded interface of two half-spaces, *Geophysical Journal of Royal Astronomical Society*, **44**, 389-404.

Musgrave, M. J. P., 1988, Stress waves in orthorhombic micropolar media, *Proceedings of the Royal Society of London, Series A. Mathematical, Physical and Engineering Sciences*, **415**, 163-183.

Nowacki, W., 1974, *Micropolar Elasticity*, International Center for Mechanical Sciences, Courses and Lectures No. 151, Udine, Springer-Verlag, Wien-New York.

Nowacki, W. and Nowacki, W. K., 1969, Propagation of monochromatic waves in an infinite micropolar elastic plate, *Bulletin de l'Academie Polonaise des Sciences, Sere des Sciences Techniques*, **17**, 45-53.

Othman, M. I. and Song, Y. Q., 2007, Reflection and refraction of thermo-viscoelastic waves at the interface between two micropolar viscoelastic media without energy dissipation, *Canadian Journal of Physics*, **85**(7), 797-812.

Parameshwaran, S. and Koh, S. L., 1973, Wave propagation in a micro-isotropic, micro-elastic solid, *International Journal of Engineering Science*, **11** (11), 95-107.

Palmov, V. A., 1964, Basic equations of the theory of asymmetric elasticity, *Prikladnaya Matematika i Mekhanika*, **28**, 401-408.

Parfitt, V. R. and Eringen, A. C., 1969, Reflection of plane waves from the flat boundary of a micropolar elastic half-space, *Journal of Acoustical Society of America*, **45**, 1258-1272.

Pujol, J., 2003, *Elastic Wave Propagation and Generation in Seismology*, Cambridge University Press.

Rajagopal, E. S., 1960, The existence of interfacial couples in infinitesimal elasticity, *Annalen der Physik*, **6**, 192-201.

Rao, K. M., 1988, Longitudinal wave propagation in a micropolar wave guide, *Inter-*

national Journal of Engineering Science, **26**(2), 135-141.

Rao, K. M. and Reddy, M. P., 1993, Rayleigh-type wave propagation on a micropolar cylindrical surface, *Journal of Applied Mechanics*, **60**, 857-865.

Sengupta, P. R. and Chakrabarti, J., 1980, Propagation of micropolar thermoelastic waves in an infinite elastic space containing a cylindrical bore, *Journal of Thermal Stresses*, **3**, 133-140.

Sharma, M. D. and Gogna, M. L., 1990, Propagation of elastic waves in a cylindrical bore in a liquid saturated porous solid, *Geophysical Journal International*, **103**, 47-54.

Sharma, J. N. and Pal, M., 2004, Rayleigh-Lamb waves in magneto-thermoelastic homogeneous isotropic plates, *International Journal of Engineering Science*, **42**, 137-155.

Sharma, J. N. and Pathania, V., 2003, Thermoelastic waves in a plate bordered with layers of inviscid liquid, *Journal of Thermal Stresses*, **26**, 149-166.

Sharma, J. N. and Pathania, V., 2004, Generalized thermoelastic waves in anisotropic plate sandwiched between liquid layers, *Journal of Sound and vibration*, **278**, 343-371.

Sharma, J. N., Pathania, V. and Gupta, S. K., 2003, Thermoelastic Lamb waves in a transversely isotropic plate bordered with layers of inviscid liquid, *International Journal of Engineering Science*, **41**, 1219-1237.

Sharma, J. N., Pathania, V. and Gupta, S. K., 2004, Circular crested waves in anisotropic thermoelastic plates bordered with inviscid liquid, *International journal of Engineering Science*, **42**, 99-121.

Singh, B., 2000a, Reflection of plane sound wave from a micropolar generalized thermoelastic solid half space, *Journal of Sound and Vibration*, **235**, 685-696.

Singh, B., 2000b, Reflection and transmission of plane harmonic waves at an interface between liquid and micropolar viscoelastic solid with stretch, *Sadhana*, **25**(6), 589-600.

Singh, B., 2001a, Reflection and refraction of plane waves at a liquid/thermo-microstretch elastic solid interface, *International Journal of Engineering Science*, **39**, 583-598.

Singh, B., 2001b, Reflection and refraction of micropolar thermoelastic waves at a

liquid-solid interface, *Indian Journal of Pure and Applied Mathematics*, **32**(8), 1229-1236.

Singh, B., 2002a, Reflection of plane micropolar viscoelastic waves at a loosely bonded solid-solid interface, *Sadhana*, **27** (5), 493-506.

Singh, B., 2002b, Reflection of plane waves from free surface of a microstretch elastic solid, *Proceedings of Indian Academy of Sciences (Earth and Planetary Sciences)*, (Now *Journal of earth System Sciences*), **111**, 29-37.

Singh, B., 2002c, Reflection and refraction of microstretch elastic waves at a liquid-solid interface in the presence of magnetic field, *Proceedings of National Academy of Sciences, India*, **72** (A), 95-108.

Singh, B., 2002d, Reflection of thermo-viscoelastic waves from free surface in the presence of magnetic field, *Proceedings of National Academy of Sciences, India*, **72**, 109-120.

Singh, B., 2007, Wave propagation in an orthotropic micropolar elastic solid, *International Journal of Solids and Structures*, **44**(11-12), 3638-3645.

Singh, B. and Kumar, R., 1998a, Refection and refraction of micropolar elastic waves at a loosely bonded interface between viscoelastic solid and micropolar elastic solid, *International Journal of Engineering Science*, **36**, 101-117.

Singh, B. and Kumar, R., 1998b, Reflection and refraction of plane waves at an interface between micropolar elastic solid and viscoelastic solid, *International Journal of Engineering Science*, **36**, 119-135.

Singh, B. and Kumar, R., 1998c, Reflection of plane waves from a flat boundary of a micropolar generalized thermoelastic half space with stretch, *Indian Journal of Pure and Applied Mathematics*, **29**, 657-669.

Singh, B. and Kumar, R., 1998d, Reflection of plane waves from the flat boundary of a micropolar generalized thermoelastic half-space, *International Journal of Engineering Science*, **36**, 865-890.

Singh, B. and Kumar, R., 1998e, Wave propagation in a generalized thermo-microstretch

elastic solid, *International Journal of Engineering Science*, **36**, 891-912.

Singh, B. and Kumar, R., 2007, Wave reflection at viscoelastic-micropolar elastic interface, *Applied Mathematics and Computation*, **185**(1), 421-431.

Singh, J. and Tomar, S. K., 2007, Plane waves in a rotating micropolar porous elastic solid, *Journal of Applied Physics*, **102**, 074906.

Smith, A. C., 1967, Waves in micropolar elastic solids, *International Journal of Engineering Science*, **5** (10), 741-746.

Smith, A. C., 1970, *Torsion and vibrations of cylinders of a micropolar elastic solid*, in Recent Advances in Engineering Science, 5/11 (ed.- A. C. Eringen) Gordan and Breach, London, 129.

Sokolnikoff, I. S., 1956, *Mathematical Theory of Elasticity*, McGraw-Hill Book Company, Newyork.

Song,Y., Xu, H. and Zhang, Y., 2006a, Reflection and refraction of micropolar magneto-thermoviscoelastic waves at the interface between two micropolar viscoelastic media, *International Journal of Thermophysics*, **27**(3), 970-993.

Song, Y. Q., Zhang, Y. C., Xu, H. Y. and Lu, B. H., 2006b, Magneto-thermoviscoelastic wave propagation at the interface between two micropolar viscoelastic media, *Applied Mathematics and Computation*, **176**, 785-802.

Stoneley, R., 1924, Elastic waves at the surface of separation of two solids, *Proceedings of Royal Society of London*, **106**, 416-428.

Suhubi, E. S. and Eringen, A. C., 1964, Nonlinear theory of simple microelastic solids-II, *Internatinal Journal of Engineering Science*, **2**, 389-404.

Tajuddin, M., 1995, Existence of Stoneley waves at an unbonded interface between two micropolar elastic half-spaces, *Journal of Applied Mechanics*, **62**, 255-257.

Tomar, S. K., 2002, Wave propagation in a micropolar elastic layer, *Proceedings of National Academy of Sciences, India*, **72**(A) IV, 339-350.

Tomar, S. K., 2005, Wave propagation in a micropolar plate with voids, *Journal of*

Vibration and Control, **11**, 849-863.

Tomar, S. K. and Garg, M., 2005, Reflection and transmission of waves from a plane interface between two microstretch solid half-spaces, *International Journal of Engineering Science*, **43**(1-2), 139-169 [Errata, *ibid*, **44**(3-4), (2006), 285-287].

Tomar, S. K. and Gogna, M. L., 1992, Reflection and Refraction of a longitudinal microrotational wave at an interface between two micropolar elastic solids in welded contact, *International Journal of Engineering Science*, **30** (11), 1637-1646.

Tomar, S. K. and Gogna, M. L., 1995a, Reflection and refraction of coupled transverse and micro-rotational waves at an interface between two different micropolar elastic media in welded contact, *International Journal of Engineering Science*, **33** (4), 485-496.

Tomar, S. K. and Gogna, M. L., 1995b, Reflection and refraction of longitudinal wave at an interface between two micropolar elastic solids in welded contact, *Journal of Acoustical Society of America*, **97**(2), 822-830 [Erratum, *ibid*, **102**(4), (1997), 2452].

Tomar, S. K. and Kumar, R., 1995, Reflection and refraction of longitudinal displacement wave at a liquid-micropolar solid interface, *International Journal of Engineering Science*, **33**(10), 1507-1515.

Tomar, S. K. and Kumar, R., 1999a, Elastic wave propagation in a cylindrical bore situated in a micropolar elastic medium with stretch, *Proceedings of Indian Academy of Sciences (Math. Sci.)*, **109**, 425-433.

Tomar, S. K. and Kumar, R., 1999b, Wave propagation at liquid/ micropolar elastic solid interface, *Journal of Sound and Vibration*, **222**(5), 858-869.

Tomar, S. K., Kumar, R. and Kaushik, V. P., 1998, Wave propagation of micropolar elastic medium with stretch, *International Journal of Engineering Science*, **36**(5-6), 683-698.

Tomar, S. K. and Singh, J., 2006, Plane waves in micropolar porous elastic solid, *International Journal of Applied Mathematics and Mechanics*, **2**(3), 52-70.

Toupin, R. A., 1962, Elastic materials with couple stresses, *Archive for Rational Me-*

chanics and Analysis, **11**, 385-414.

Twiss, R. J. and Eringen, A. C., 1971, Theory of mixtures for micromorphic materials-I. Balance laws, *International Journal of Engineering Science*, **9**(10), 1019-1044.

Twiss, R. J. and Eringen, A. C., 1972, Theory of mixtures for micromorphic materials-II. Elastic constitutive equations, *International Journal of Engineering Science*, **10** (5), 437-465.

Udias, A., 1999, *Principles of Seismology*, Cambridge University Press, UK.

Vashishth, A. K. and Khurana, P., 2005, Wave propagation along a cylindrical borehole in an anisotropic poroelastic solid, *Geophysical Journal International*, **161**(2), 295-302.

Voigt, W., 1887, Theoritiscke studien uber die elastizitats verhaltnisse der krystalle, *Abhandlungen der Braunschweigischen Wissenschaftlichen Gesellschaft*, **34**, 3-51.

Willson, A. J., 1972, The micropolar elastic vibrations of a circular cylinder, *International Journal of Engineering Science*, **10**, 17-22.

Wu., J. and Zhu, Z., 1992, The propagation of Lamb waves in a plate bordered with layers of a liquid, *Journal of Acoustical Society of America*, **91**, 861-867.

Yang, S. K. and Hsia, S. Y., 1998, Acoustic wave propagation at a fluid-micropolar boundary, *Japanese Journal of Applied Physics*, **37**, 247-252.

Yerofeyev, V. I. and Soldatov, I. N., 1999, A shear surface wave at the interface of an elastic body and a micropolar liquid, *Journal of Applied Mathematics and Mechanics*, **63**(2), 277-281.

Zhu, Z. and Wu, J., 1995, The propagation of lamb waves in a plate bordered with a viscous liquid, *Journal of Acoustical Society of America*, **98**, 1057-1067.